

Université du Québec  
Institut National de la Recherche Scientifique-  
Institut Armand-Frappier

# **DEVELOPMENT OF CELLULOSE NANOCRYSTAL REINFORCED ANTIMICROBIAL NANOCOMPOSITE FILMS FOR FOOD PACKAGING APPLICATION**

---

Par  
**Avik Khan**

*Thèse présentée pour l'obtention du grade de*  
**Doctorat en Biologie**

Jury d'évaluation

Président du jury et examinateur interne	Dr. Charles Ramassamy, INRS-Institut Armand Frappier
Examineur externe	Dr. Tatjana Stevanovic, Université Laval
Examineur externe	Dr. Philippe Bébin, Centre de Technologie Minérale et de Plasturgie (CTMP)
Directrice de recherche	Dr. Monique Lacroix, INRS-Institut Armand Frappier
Codirecteur de recherche	Dr. Bernard Riedl, Université Laval

**© Droits réservés de Avik Khan October 2014**

## **Acknowledgement**

A PhD is a degree that not only requires and demands research aptitude but also dedication, commitment and patience. There can be times when a PhD student might feel the whole world is against his/her; in these kind of moments, it is the support of the people around him/her that makes all the difference. I take this opportunity to acknowledge all the people who made my PhD, a pleasant journey.

At first, I sincerely thank my PhD director Prof. Monique Lacroix for giving me the opportunity to conduct this research work at INRS-Institut Armand Frappier and help me to realize my research potential. I also thank her for all the advice, support and encouragement throughout my PhD. I would also like to thank my co-director Prof. Bernard Riedl for his valuable suggestions, corrections and comments during my PhD. I would like to thank Dr. Gregory Chauve, Dr. Carole Fraschini and Dr. Jean Bouchard from FPInnovations for their suggestions and corrections to my manuscripts.

I am greatly thankful to Dr. Ruhul A. Khan, Dr. Dominic Dussault, Dr. Khanh Dang Vu, Dr. Le Tien Canh and Stephane Salmieri for their friendship and advice. I would also like to acknowledge the entire current and past student, colleagues and trainees of Labo Resala, those whom I had the pleasure to meet and work with. Special mention must go to Johan Viguier, Hejer Gallah, Coline Philip, Victor Henry and Farah Hossain.

I would like to dedicate my thesis to my loving wife Tanzina, my beloved parents, all my family members and in-laws. I express my profound love and gratitude to Tanzina for her constant inspiration and support. She makes my life complete and fills it with ecstasy. Nothing would have been possible without her.

# Table of Contents

<b>Acknowledgement</b> .....	<b>II</b>
<b>Table of Contents</b> .....	<b>III</b>
<b>Résumé</b> .....	<b>IX</b>
<b>Abstract</b> .....	<b>XII</b>
<b>List of Figures</b> .....	<b>XIV</b>
<b>List of Tables</b> .....	<b>XVII</b>
<b>List of Abbreviations</b> .....	<b>XVIII</b>
<b>CHAPTER 1</b> .....	<b>1</b>
<b>Literature Review</b> .....	<b>1</b>
<b>Cellulose Nanocrystal based composites and bioactive agents for food packaging</b> .....	<b>2</b>
1.1. Contribution of the authors .....	3
1.2. Résumé.....	4
1.3. Abstract.....	5
1.3. Introduction.....	6
1.4. Nanocomposites .....	10
1.4.1. <i>Advantages of Nanocomposites</i> .....	10
1.4.2. <i>Application of Nanocomposites in Food Packaging</i> .....	12
1.5. Cellulose Nanocrystal (CNC) .....	12
1.5.1. <i>Types of CNC</i> .....	13
1.5.2. <i>CNC from Bacteria</i> .....	13
1.5.3. <i>CNC from Wood</i> .....	14
1.5.4. <i>Application of CNC</i> .....	16
1.5.5. <i>CNC Based Composites</i> .....	16
1.6. Classification of Biopolymers.....	22
1.7. Bioactive Packaging.....	23
1.7.1. <i>Bioactive Polymers</i> .....	24
1.7.2. <i>Organic Acids</i> .....	26
1.7.3. <i>Bacteriocins</i> .....	27
1.7.4. <i>Essential Oils and Plant Extracts</i> .....	28
1.8. Conclusion.....	30

1.9. Acknowledgement .....	31
1.10. References.....	31
1.11 Problematic, Hypothesis and Objectives.....	44
1.11.1 Problematic.....	44
1.11.2 Hypothesis.....	45
1.11.3 Objectives.....	45
1.11.4 Simplified Organogram for the PhD Thesis.....	47
<b>CHAPTER 2 .....</b>	<b>48</b>
<b>Publication 1 .....</b>	<b>48</b>
<b>Mechanical and barrier properties of cellulose nanocrystal reinforced chitosan based nanocomposite films .....</b>	<b>49</b>
2.1. Contribution of the authors .....	50
2.2. Specific objectives of the Publication-1 .....	51
2.3. Résumé.....	52
2.4. Abstract.....	53
2.5. Introduction.....	54
2.6. Materials and methods.....	56
2.6.1 Materials.....	56
2.6.2. Film preparation .....	56
2.6.3. Mechanical properties of the films .....	57
2.6.4. Water vapor permeability test .....	57
2.6.5. Gel swelling property.....	58
2.6.7. Thermo gravimetric analysis (TGA).....	58
2.6.8. X-ray diffraction (XRD).....	59
2.6.9. Scanning electron microscopy (SEM).....	59
2.6.10. Statistical analysis.....	59
2.7. Results and discussion.....	60
2.7.1. Mechanical properties of the CNC reinforced chitosan-based films .....	60
2.7.2. Water vapor permeability.....	62
2.7.3. Gel swelling property.....	63
2.7.4. Fourier transform infrared spectroscopy .....	63

2.7.5. Thermal property of the films .....	65
2.7.6. X-ray diffraction (XRD).....	65
2.7.7. Surface morphology of the films .....	66
2.8. Conclusions.....	67
2.9. Acknowledgements .....	68
2.10. References.....	68
2.11. General discussion of the Publication-1 .....	83
<b>CHAPTER 3 .....</b>	<b>84</b>
<b>Publication 2 .....</b>	<b>84</b>
<b>Genipin cross-linked nanocomposite films for the immobilization of antimicrobial agent .</b>	<b>85</b>
3.1. Contribution of the authors .....	86
3.2. Specific objectives of the Publication-2 .....	87
3.3. Résumé .....	88
3.4. Abstract.....	89
3.5. Introduction.....	90
3.6. Materials and Methods.....	92
3.6.1. Preparation of the nanocomposite films.....	92
3.6.2. Preparation of nisin solution .....	93
3.6.3. Adsorption of nisin onto the surface of the films .....	93
3.6.4. In situ evaluation of the antimicrobial activity against <i>L. monocytogenes</i> .....	94
3.6.5. Enumeration of bacteria .....	95
3.6.6. Preparation of genipin-nisin cross-linked films.....	95
3.6.7. Fourier Transform Infrared Spectroscopy (FTIR).....	96
3.6.8. In vitro evaluation of the bioactivity of the cross-linked films .....	96
3.6.9. Swelling ratio and water solubility of the films.....	97
3.6.10. Mechanical properties of the films.....	97
3.6.11. Antimicrobial activity of the cross-linked films against <i>L. monocytogenes</i> .....	98
3.6.12. Bacterial growth rate calculation.....	98
3.6.13. Scanning Electron Microscopy (SEM).....	99
3.6.14. Statistical analysis.....	99

3.7. Results and Discussion.....	99
3.7.1. Antimicrobial activity in situ.....	99
3.7.2. Spectroscopic analysis of the films.....	102
3.7.3. Effect of genipin cross-linking on the bioactivity of nisin during storage .....	105
3.7.4. Swelling ratio and water solubility of the films.....	107
3.7.6. Mechanical properties of the films .....	108
3.7.8. Surface morphology of the films.....	110
3.8. Conclusion.....	110
3.9. Acknowledgements .....	111
3.10. References.....	111
3.11. General discussion of the Publication-2 .....	130
<b>CHAPTER 4 .....</b>	<b>131</b>
<b>Publication 3 .....</b>	<b>131</b>
<b>Optimization of microfluidization for the homogeneous distribution of cellulose nanocrystals (CNCs) in biopolymeric matrix .....</b>	<b>132</b>
4.1. Contribution of the authors .....	133
4.2. Specific objectives of the Publication-3 .....	134
4.3. Résumé.....	135
4.4. Abstract.....	136
4.5. Introduction.....	137
4.6. Materials & Methods .....	139
4.6.1. Preparation of the nanocomposite suspensions .....	139
4.6.2. Experimental design .....	140
4.6.3. Microfluidization of the nanocomposite suspensions .....	141
4.6.4. Preparation of the nanocomposite films.....	141
4.6.5. Measurement of the mechanical properties of the nanocomposite films.....	142
4.6.6. Field emission scanning electron microscopy (FE-SEM).....	142
4.6.7. Atomic force microscopy (AFM) .....	142
4.6.8. Statistical analysis of the design.....	143
4.7. Results & Discussions .....	143
4.7.1. Regression analysis of the design.....	143
4.7.2. Surface morphology of the nanocomposite films.....	145

4.7.3. Response surface plots.....	147
4.8. Conclusion.....	150
4.9. Acknowledgements.....	151
4.10. References.....	151
4.11. General discussion of the Publication-3.....	166
<b>CHAPTER 5 .....</b>	<b>167</b>
<b>Publication 4 .....</b>	<b>167</b>
5.1. Contribution of the authors.....	169
5.2. Specific objectives of the Publication-4.....	170
5.3. Résumé.....	171
5.4. Abstract.....	172
5.5. Introduction.....	173
5.6. Materials & Methods.....	175
5.6.1. Bacterial strains.....	175
5.6.2. Preparation of antimicrobial formulations.....	176
5.6.3. Agar diffusion assay.....	176
5.6.4. Central composite design (CCD).....	177
5.6.5. Statistical analysis of the design.....	177
5.7. Results.....	178
5.7.1. Regression analysis of the design.....	178
5.7.2. Response surface plots.....	179
5.8. Discussions.....	181
5.9. Conclusion.....	183
5.10. Acknowledgements.....	183
5.11. References.....	183
5.12. General discussion of the Publication-4.....	194
<b>CHAPTER 6 .....</b>	<b>195</b>
<b>Publication 5 .....</b>	<b>195</b>
<b>Genipin cross-linked antimicrobial nanocomposite films to prevent the surface growth of bacteria in fresh meats .....</b>	<b>196</b>
6.1. Contribution of the authors.....	197
6.2. Specific objectives of the Publication-5.....	198
6.3. Résumé.....	199
6.4. Abstract.....	200
6.5. Introduction.....	201
6.6. Materials and methods.....	203
6.6.1. Bacterial strains.....	203

6.6.2. Preparation of nisin-EDTA antimicrobial formulation .....	203
6.6.3. Preparation of the nanocomposite films.....	204
6.6.4. Preparation of the antimicrobial nanocomposite films.....	205
6.6.5. In vitro analysis .....	205
6.6.6. In situ analysis.....	206
6.6.7. Microbiological and chemical analysis.....	206
6.6.8. Statistical analysis .....	207
6.7. Results and Discussions .....	207
6.7.1. Antimicrobial activity of the films in vitro.....	207
6.8. Conclusion.....	214
6.9. Acknowledgements .....	214
6.10. References.....	214
6.11. General discussion of the Publication-5 .....	225
<b>CHAPTER 7 .....</b>	<b>226</b>
<b>General Discussion, Conclusions and Future Perspectives.....</b>	<b>226</b>
<b>ANNEXE A .....</b>	<b>233</b>
<b>Modification of cellulose nanocrystal (CNC) for the attachment of antioxidant molecules</b> .....	<b>234</b>
Synthesis of CNC-antioxidant conjugates.....	234
Antiradical Test.....	235
Determination of grafting efficiency.....	236
Preparation of chitosan based nanocomposite films .....	236
Results.....	237
References: .....	239
<b>ANNEXE B .....</b>	<b>241</b>
<b>ANNEXE C .....</b>	<b>246</b>
<b>ANNEXE D .....</b>	<b>250</b>

## Résumé

Au cours des dernières années, il y a eu une formidable expansion de l'évolution de la recherche et de la technologie dans le domaine de la nanotechnologie, ce qui a entraîné des développements significatifs et des applications dans les domaines de l'alimentation et de l'agriculture. En particulier, le domaine de l'emballage alimentaire représente un domaine prometteur et excitant pour l'utilisation de la nanotechnologie. La cellulose nanocrystalline (CNC), qui est produite à partir du bois, représente une occasion en or pour les vastes ressources forestières du Canada. Des essais toxicologiques ont également montré que la CNC est moins dommageable pour l'environnement que les autres nanomatériaux et sans effets toxiques. Cette thèse porte sur l'utilisation de la CNC pour le développement de nouveaux matériaux, respectueux de l'environnement, tels des films bionanocomposites antimicrobiens pour l'application dans l'emballage alimentaire. Le chitosane, un polymère naturel, non toxique, biocompatible et biodégradable, a été choisi comme matrice pour la fabrication de films bionanocomposites. Des films de chitosane bionanocomposite renforcés par la CNC ont été fabriqués par un procédé à partir de solutions et on a constaté que la CNC a agi comme un bon agent de renforcement dans le chitosane. L'incorporation de CNC a amélioré la résistance mécanique, la transmission de la vapeur d'eau, la perméabilité et les propriétés de gonflement des films de chitosane. La concentration optimale CNC est de 5% pds/ pds de chitosane.

Après la mise au point d'une formulation de chitosane /CNC optimisée, l'attention a été déplacée vers le développement de films bionanocomposite capables d'inhiber la croissance, à la surface, de bactéries pathogènes dans les produits carnés. La nisine, un agent antimicrobien naturel, a été immobilisé à la surface des films de chitosane/CNC à l'aide de la génipine. Les films antimicrobiens développés ont inhibé avec succès la croissance de *L. monocytogenes* dans des

échantillons de viande prête-à-manger (PAM). Une faible concentration de réticulation de genipin (0,05% pds/v) a protégé de l'activité antimicrobienne des films dans un état de stockage extrême. La résistance à l'eau et la résistance mécanique des films ont également augmenté en raison de la réticulation de la génipine. La spectroscopie à transformée de Fourier (FTIR) a été effectuée pour étudier les changements dans les bandes infrarouges liés à la réticulation du film par la génipine. La microfluidization, qui est une technique d'homogénéisation à haute pression, a été utilisée pour distribuer de manière homogène au sein de la matrice de chitosane la CNC et de développer des films bionanocomposites de résistance élevée. Une méthodologie statistique, dite de 'surface de réponse' (RSM), a été adoptée pour optimiser systématiquement le contenu en CNC, la pression de la microfluidisation et le nombre de cycles de microfluidisation pour optimiser la résistance mécanique des films de chitosane/CNC. La microscopie électronique à balayage (MEB) des films microfluidisées chitosane/CNC a révélé une réduction de 10 à 15 fois dans la taille des agrégats par rapport aux films de chitosane/CNC non microfluidisé. La RSM a également été utilisée pour optimiser une nouvelle formulation capable d'inhiber les bactéries gramme-négatives (*E. coli* et *S. typhimurium*) et les bactéries à Gramme-positives (*L. monocytogenes*). Une concentration de nisine de 125 à 150 µg/mL avec un éthylènediaminetétraacétate disodique (Na<sup>-</sup>EDTA) concentration de 20 à 30 mM et un pH de 5-6 a inhibé l'ensemble des trois bactéries. La formulation antimicrobienne développée a été immobilisée sur la surface des films de chitosane /CNC microfluidisées par la génipine par réticulation. L'irradiation gamma à faible dose a été appliquée sur les films. On a constaté chez les films préparés par la combinaison de la réticulation de génipine et l'irradiation gamma (1,5 kGy), la plus haute activité antimicrobienne in vitro contre *E. coli* et *Listeria monocytogenes* à la fin de 35 jours de stockage. Les films ont augmenté la durée de vie de la viande de porc frais de

plus de 5 semaines et ont aussi inhibé la croissance de bactéries pathogènes dans des échantillons de viande.

**Avik Khan**  
Candidat PhD

**Prof. Monique Lacroix**  
Directrice de Recherche

## **Abstract**

In recent years there is a tremendous expansion of research and technology developments in the field of nanotechnology, which resulted in significant application developments in the food and agriculture areas. Particularly, the field of food packaging represents a promising and exciting field for the use of nanotechnology. Cellulose nanocrystals (CNC), which are produced from wood, represent a glorious opportunity for Canada's vast forest resources. Toxicological experiments have also shown CNC to be far more environmentally benign than other nanomaterials. This thesis examines the use of CNC for the development of novel, environment friendly, antimicrobial bionanocomposite films for food packaging application. Chitosan, a natural, non-toxic, biodegradable, biocompatible polymer was chosen as the matrix for the fabrication of bionanocomposite films. CNC reinforced chitosan based bionanocomposite films were fabricated by solution casting method and it was found that CNC acted as a good reinforcing agent in chitosan. CNC incorporation improved the mechanical strength, water vapor permeability and swelling property of the chitosan films. The optimum CNC concentration was found to be 5% w/w of chitosan.

After the development of an optimized chitosan/CNC formulation, the focus was shifted to the development of bionanocomposite films capable of inhibiting surface growth of pathogenic bacteria in meat products. Nisin, a natural antimicrobial agent, was immobilized on the surface of the CNC/chitosan films by using genipin as a cross-linking agent. The developed antimicrobial films successfully inhibited the growth of *L. monocytogenes* in ready-to-eat (RTE) meat samples. Low concentration of genipin cross-linking (0.05% w/v) protected the antimicrobial activity of the films in extreme storage condition. Water resistance and mechanical strength of the films also increased due to genipin cross-linking. Fourier transform infrared

spectroscopy (FTIR) was performed to investigate the changes in the infrared bands related to the genipin cross-linking of the film. Microfluidization, which is a high-pressure homogenization technique, was used to homogeneously distributed CNC within the chitosan matrix and develop high strength bionanocomposite films. Response surface methodology (RSM) was adopted to systematically optimize the CNC content, the microfluidization pressure and the number of microfluidization cycles by measuring the mechanical strength of the chitosan/CNC films. Scanning electron microscopy (SEM) analysis of the microfluidized CNC/chitosan films revealed a 10 to 15 times reduction in the size of the aggregates compared to the non-microfluidized CNC/chitosan films. RSM was also used to develop a novel optimize formulation capable of inhibiting both gram-negative (*E. coli* and *Salmonella* spp.) and gram-positive (*Listeria monocytogenes*) bacteria. A nisin concentration of 125-150 µg/mL with a disodium ethylenediaminetetraacetate (Na-EDTA) concentration of 20-30 mM and a pH of 5-6 inhibited all the three bacteria. The developed antimicrobial formulation was immobilized on the surface of the microfluidized CNC/chitosan films by genipin cross-linking. Low dose gamma irradiation was applied on the films. It was found that films prepared by the combination of genipin cross-linking and gamma irradiation (1.5 kGy) the highest antimicrobial activity *in vitro* against *E. coli* and *Listeria monocytogenes* at the end of 35 days of storage. The films increased the microbiological shelf life of fresh pork meats by more than 5 weeks and also inhibited the growth of pathogenic bacteria in meat samples.

**Avik Khan**  
PhD Candidate

**Prof. Monique Lacroix**  
Director of Research

## List of Figures

<i>Figure-1.1: Classification of biodegradable polymer (adopted from John &amp; Thomas, 2008)</i> .....	43
<i>Figure 2.1(a): Effect of CNC content in the tensile strength of the chitosan films</i> .....	76
<i>Figure 2.1(b): Effect of CNC content in the tensile modulus and elongation at break (%) of the chitosan films</i> .....	76
<i>Figure 2.2: Effect of CNC content in the water vapor permeability of the chitosan films</i> .....	77
<i>Figure 2.3: Effect of CNC content in the swelling property of the chitosan films</i> .....	77
<i>Figure 2.4: FT-IR spectra of films based on (a) Chitosan (b) CNC and (c) Chitosan + 5% CNC</i> .....	78
<i>Figure 2.5: TGA curves for CNC, chitosan, chitosan with 5 and 10% CNC films</i> .....	79
<i>Figure 2.6: X-ray Diffractograms of films based on a) CNC b) chitosan and c) chitosan+5%CNC</i> .....	80
<i>Figure 2.7: SEM image of the surface of a) CNC, b) chitosan, c) chitosan+5% CNC and d) chitosan+10% CNC films</i> .....	81
<i>Figure 2.8: SEM image of the cross-section of a) CNC, b) chitosan, c) chitosan+5% CNC and d) chitosan+10% CNC films</i> .....	82
<i>Figure-3.1: Chemical structure (a) and (b) genipin (drawn using MarvinSketch 6.2.0, 2014).. The secondary structure of (c) nisin was generated from the nisin peptide sequence using I-TASSER server (Zhang, 2008; Roy et al., 2010 and 2012)</i> .....	121
<i>Figure-3.3: Antimicrobial activity of nisin films in situ against L. monocytogenes during storage at 4 °C</i> .....	122
<i>Figure 3.4: FT-IR spectra of the (a) control nanocomposite (no nisin) films, nanocomposite films containing (b) 2.33 and (c) 18.65 <math>\mu\text{g}/\text{cm}^2</math> nisin</i> .....	123
<i>Figure 3.5: FT-IR spectra of the (a) uncross-linked, (b) 0.05, (c) 0.1, (d) 0.2 and (e) 0.4% genipin cross-linked films</i> .....	123
<i>Figure-3.6 (a): The in vitro bioactivity of the films during storage at 4°C and 90-100% RH</i> .....	124

<i>Figure-3.6 (b): A 4<sup>th</sup> order polynomial “standard curve” of inhibition area (cm<sup>2</sup>) versus nisin concentration (µg/cm<sup>2</sup>).....</i>	<i>124</i>
<i>Figure-3.6 (c): Available nisin content of the films during storage at 4°C and 90-100% RH. ....</i>	<i>125</i>
<i>Figure-3.7: Schematic representation of the immobilization of nisin on the surface of the chitosan/CNC films due to genipin cross-linking. Black lines indicate possible linkage between nisin and genipin; red lines indicate possible linkage between genipin and chitosan. ....</i>	<i>125</i>
<i>Figure-3.8 (a): The effect of the genipin concentration on the swelling ratio of the films.....</i>	<i>126</i>
<i>Figure-3.8 (b): Water solubility of the films. ....</i>	<i>126</i>
<i>Figure-3.9: The effect of the genipin cross-linking on the growth rate of L. monocytogenes.....</i>	<i>127</i>
<i>Figure-3.10: SEM micrographs of the surface of the a) control nanocomposite (no nisin), b) 2.33 µg/cm<sup>2</sup> nisin c) 18.65 µg/cm<sup>2</sup> nisin and d) 18.65 µg/cm<sup>2</sup> nisin films cross-linked with 0.05% genipin at two different magnification (4000x and 16000x).....</i>	<i>129</i>
<i>Figure 4.1: Basic principle of a microfluidizer. ....</i>	<i>157</i>
<i>Figure 4.2: Digital images of a) non-microfluidized and b) microfluidized CNC/chitosan suspensions. ....</i>	<i>158</i>
<i>Figure 4.3: Digital images of a) non-microfluidized and b) microfluidized CNC/chitosan films. ....</i>	<i>158</i>
<i>Figure 4.4: FE-SEM micrographs of a) non-microfluidized and b) microfluidized CNC/chitosan films at magnification level of 400x and 2000x.....</i>	<i>162</i>
<i>Figure 4.5: The AFM height images of a) non- microfluidized and b) microfluidized nanocomposite films. ....</i>	<i>163</i>
<i>Figure 4.6: 3D Response surface plot of TS values obtained by varying CNC concentration (X<sub>1</sub>) and microfluidization cycles (X<sub>3</sub>) while keeping microfluidization pressure (X<sub>2</sub>) constant at 7,000 psi.....</i>	<i>164</i>
<i>Figure 4.7: 3D Response surface plot of TM values obtained by varying CNC concentration (X<sub>1</sub>) and microfluidization cycles (X<sub>3</sub>) while keeping microfluidization pressure (X<sub>2</sub>) constant at 7,000 psi.....</i>	<i>164</i>
<i>Figure 4.8(a): 3D Response surface plot of Eb% obtained by varying CNC concentration (X<sub>1</sub>) and microfluidization cycles (X<sub>3</sub>) while keeping microfluidization pressure (X<sub>2</sub>) constant at 7,000 psi.....</i>	<i>165</i>

<i>Figure 4.8(b): 3D Response surface plot of Eb% obtained by varying microfluidization pressure (<math>X_2</math>) and microfluidization cycles (<math>X_3</math>) while keeping CNC concentration (<math>X_1</math>) constant at 8%.</i>	165
<i>Figure 5.1(a): 3D response surface plot for <math>D_E</math> as a function of pH (<math>X_3</math>) and Na-EDTA (<math>X_2</math>), while keeping the nisin (<math>X_1</math>) constant at 125 (<math>\mu\text{g}/\text{mL}</math>).</i>	191
<i>Figure 5.1(b): 3D response surface plot for <math>D_E</math> as a function of pH (<math>X_3</math>) and nisin (<math>X_1</math>), while keeping the Na-EDTA (<math>X_2</math>) constant at 20 mM.</i>	191
<i>Figure 5.2(a): 3D response surface plot for <math>D_S</math> as a function of pH (<math>X_3</math>) and Na-EDTA (<math>X_2</math>), while keeping the nisin (<math>X_1</math>) constant at 125 (<math>\mu\text{g}/\text{mL}</math>).</i>	192
<i>Figure 5.2(b): 3D response surface plot for <math>D_S</math> as a function of pH (<math>X_3</math>) and nisin (<math>X_1</math>), while keeping the Na-EDTA (<math>X_2</math>) constant at 20 mM.</i>	192
<i>Figure 5.3(a): 3D response surface plot for <math>D_L</math> as a function of pH (<math>X_3</math>) and Na-EDTA (<math>X_2</math>), while keeping the nisin (<math>X_1</math>) constant at 125 (<math>\mu\text{g}/\text{mL}</math>).</i>	193
<i>Figure 5.3(b): 3D response surface plot for <math>D_L</math> as a function of pH (<math>X_3</math>) and nisin (<math>X_1</math>), while keeping the Na-EDTA (<math>X_2</math>) constant at 20 mM.</i>	193
<i>Figure 6.1: Antimicrobial activity of the films in vitro against E. coli during storage at 4 °C.</i>	221
<i>Figure 6.2: Antimicrobial activity of the films in vitro against L. monocytogenes during storage at 4 °C.</i>	221
<i>Figure 6.3: Total count of psychrotrophic bacteria in fresh pork during storage at 4 °C.</i>	222
<i>Figure 6.4: Total count of mesophilic bacteria in fresh pork during storage at 4 °C.</i>	222
<i>Figure 6.5: Total count of LAB in fresh pork during storage at 4 °C.</i>	223
<i>Figure 6.6: pH of the fresh pork during storage at 4 °C.</i>	223
<i>Figure 6.7(a): Antimicrobial activity of the films in situ against E. coli during storage at 4 °C.</i>	223
<i>Figure 6.7(b): Antimicrobial activity of the films in situ against L. monocytogenes during storage at 4 °C.</i>	224

## List of Tables

<i>Table-3.1: Effect of genipin concentration on the mechanical properties of films *</i> .....	127
<i>Table-4.1: Levels of the factor tested in the CCD</i> .....	159
<i>Table-4.2: Results of the mechanical properties of the CNC/chitosan films from CCD</i> .....	160
<i>Table-4.3: Response surface regression analyses for the mechanical properties of the CNC/chitosan films</i> .....	161
<i>Table-5.1: Levels of the factor tested in the CCD</i> .....	188
<i>Table-5.2: Results of the inhibition zones of the formulations from CCD.</i> .....	189
<i>Table-5.3: Response surface regression analyses for the inhibition zones of the formulations.</i> .....	190

## List of Abbreviations

---

---

### *A*

Analysis of Variance (ANOVA)

Atomic Force Microscopy (AFM)

Attenuated Total Reflectance (ATR)

---

### *B*

Bacterial cellulose (BC)

Brain Heart Infusion (BHI)

---

### *C*

Cellulose Nanocrystal (CNC)

Colony Forming Units (CFU)

Central Composite Design (CCD)

Coefficient of Thermal Expansion (CTE)

---

### *D*

Degree of Polymerization (DP)

De-Man Rogosa, Sharp (MRS)

Differential scanning calorimetry (DSC)

Disodium ethylenediaminetetraacetate (Na-EDTA)

Dynamic Mechanical Analysis (DMA)

---

### *E*

Elongation at Break (Eb)

Emulsion Droplet Size (EDS)

Ethylene Vinyl Alcohol (EVA)

---

### *F*

Field Emission Scanning Electron Microscopy (FE-SEM)

Food and Drug Administration (FDA)

Fourier Transform Infrared Spectroscopy (FTIR)

---

### *G*

GRAS (generally considered as safe)

---

### *H*

Hydroxypropylmethylcellulose (HPMC)

---

*L*

Lactic Acid Bacteria (LAB)

Linear Low Density Polyethylene (LLDPE)

Lipopolysaccharide (LPS)

---

*M*

Micro Fibrillated Cellulose (MFC)

Molecular Weight (Mw)

Montmorillonite (MMT)

---

*O*

Outer Membrane (OM)

---

*P*

Polycaprolactone (PCL)

Polyelectrolyte complexes (PECs)

Polyethylene (PE) · 25

Polyethylene-co-methacrylic acid (PEMA)

Polylactic acid (PLA)

Polypropylene (PP)

Polyurethane (PU)

Polyvinyl Alcohol (PVOH)

Prêt-À-Manger (PAM)

Puncture Deformation (PD)

Puncture Strength (PS)

---

*R*

Ready-To-Eat (RTE)

Response Surface Methodology (RMS)

Ring-opening Polymerization (ROP)

---

*S*

Scanning electron microscopy (SEM)

Swelling ratio (SR)

---

*T*

Tensile Modulus (TM)

Tensile Strength (TS)

Thermo-gravimetric Analysis (TGA)

Thermoplastic starch (TPS)

Three-dimensional (3D)

Tryptic Soy Agar (TSA)

---

*W*

Water Solubility (WS)

Water Vapor Permeability (WVP)

World Health Organization (WHO)

---

*X*

X-ray Diffraction (XRD)

X-ray photoelectron spectroscopy (XPS)

---

*Y*

Young's Modulus (YM)

**CHAPTER 1**  
**Literature Review**

# Cellulose Nanocrystal based composites and bioactive agents for food packaging

Avik Khan<sup>1</sup>, Tanzina Huq<sup>1</sup>, Ruhul A. Khan<sup>1</sup>,  
Bernard Riedl<sup>2</sup> and Monique Lacroix<sup>1\*</sup>

<sup>1</sup>Research Laboratories in Sciences Applied to Food, Canadian Irradiation Centre (CIC),  
INRS-Institut Armand-Frappier, Université du Québec, 531 Boulevard des Prairies,  
Laval, Québec, H7V 1B7, Canada

<sup>2</sup>Département des sciences du bois et de la forêt, Faculté de foresterie, géographie et géomatique,  
Université Laval, Québec-city, Québec, G1V 0A6, Canada

**Keywords:** Packaging materials; Nanocellulose; Biodegradable films; Nanocomposites;  
Bioactive polymers; Biopolymers; Essential oils.

\* **Corresponding Author:** Prof. Monique Lacroix.

Telephone: +1-450-687-5010; Fax: +1-450-686-5501.

**E-mail:** [monique.lacroix@iaf.inrs.ca](mailto:monique.lacroix@iaf.inrs.ca)

This article has been published in *Critical Reviews in Food Science and Nutrition* (2012), 54(2),  
163–174.

### **1.1. Contribution of the authors**

The review was written by Avik Khan. The framework of the review was planned with guidance from Prof. Monique Lacroix. Both Prof. Monique Lacroix and Prof. Bernard Riedl corrected the main draft. Tanzina Huq helped in writing the part of bioactive agents. Dr. Ruhul A. Khan corrected the main draft. Both Avik Khan and Prof. Monique Lacroix replied to the reviewers' comments and corrected the review.

## **1.2. Résumé**

Le souci environnemental global concernant l'utilisation de matériaux d'emballage issus de la chimie du pétrole ou du gaz naturel, encourage les chercheurs et les industries dans la recherche de matériaux d'emballage issus de biopolymères naturels et de la biomasse. Les emballages bioactifs gagnent de plus en plus d'intérêt non seulement en raison de leur origine qui peut être bio-sourcée, mais aussi en raison de leur potentiel d'améliorer la qualité des aliments et la sécurité alimentaire. Certains défauts des biopolymères, tels que de faibles propriétés mécaniques et barrières peuvent être considérablement améliorées par l'utilisation de nanomatériaux tels que la nanocellulose (CNC). L'utilisation de CNC peut prolonger la durée de conservation des aliments et peut également améliorer la qualité de la nourriture, car ils peuvent servir de supports pour certaines substances actives, telles que des antioxydants et des agents antimicrobiens. Les composites à base de fibres CNC ont un grand potentiel dans la préparation de nanocomposites bon marché, légers et très solides pour l'emballage alimentaire. Cette recherche met en évidence l'utilisation potentielle et l'application de nanocomposites CNC à base de fibres et aussi l'incorporation d'agents bioactifs dans les emballages alimentaires.

### **1.3. Abstract**

Global environmental concern, regarding the use of petroleum-based packaging materials, is encouraging researchers and industries in the search for packaging materials from natural biopolymers. Bioactive packaging is gaining more and more interest not only due to its environment friendly nature but also due to its potential to improve food quality and safety during packaging. Some of the shortcomings of biopolymers, such as weak mechanical and barrier properties can be significantly enhanced by the use of nanomaterials such as cellulose nanocrystal (CNC). The use of CNC can extend the food shelf life and can also improve the food quality as they can serve as carriers of some active substances, such as antioxidants and antimicrobials. The CNC fiber-based composites have great potential in the preparation of cheap, lightweight, and very strong nanocomposites for food packaging. This review highlights the potential use and application of CNC fiber-based nanocomposites and also the incorporation of bioactive agents in food packaging.

### **1.3. Introduction**

The purpose of food packaging is to preserve the quality and safety of the food it contains, from the time of manufacture to the time it is used by the consumer. An equally important function of packaging is to protect the product from physical, chemical, or biological damages. The packaging also has a secondary function, i.e., reduction of loss, damage and waste for distributor and customer, and facilitates its storage, handling and other commercial operations. About 50% of agricultural products are destroyed because of the absence of packaging. The causes of this loss are bad weather, physical, chemical and microbiological deteriorations. Progress in the packaging of foodstuffs will prove crucial over the next few years mainly because of new consumer patterns and demands creation, as the world population growth is estimated at 15 billion by 2025. The most well-known packaging materials that meet these criteria are polyethylene- or co-polymer based materials, which have been in use by the food industry for over 50 years. These materials are not only safe, inexpensive, versatile, but also flexible. However, one of the limitations with plastic food packaging materials is that these are meant to be discarded, with very little being recycled (Villanueva *et al.*, 2006; Cha & Chinnan, 2004). Currently, almost all the plastics that are widely used in the various sectors are produced from petrochemical products. With rising petroleum costs, there is concern with finding cost-effective ways to manufacture packaging materials. In addition to the above environmental issues, food packaging has been impacted by notable changes in food distribution, including globalization of the food supply, consumer trends for more fresh and convenient foods, as well as desire for safer and better quality foods. Given these and previously mentioned issues, consumers are demanding that food packaging materials be more natural, disposable, potentially biodegradable, as well as recyclable (Chandra and Rustgi, 1998; Fischer *et al.*, 1999).

Biobased packaging is defined as packaging containing raw materials originating from agricultural sources, i.e., produced from renewable, biological raw materials such as starch, cellulose and bioderived monomers. To date, biodegradable packaging has commanded great attention, and numerous projects are under way in this field. One important reason for this attention is the marketing of environmentally friendly packaging materials. Furthermore, use of biodegradable packaging materials has the greatest potential in countries where landfill is the main waste management tool. Biobased packaging materials include both edible films and edible coatings along with primary and secondary packaging materials (Siro and Plackett, 2010; Khan *et al.*, 2010a). Unfortunately, so far the use of biodegradable films for food packaging has been strongly limited because of the poor barrier properties and weak mechanical properties shown by natural polymers. For this reason natural polymers were frequently blended with other synthetic polymers or, less frequently, chemically modified with the aim of extending their applications in more special or severe circumstances (Weber *et al.*, 2002; Khan *et al.*, 2010b).

Cellulose is one of the most abundant biopolymers on earth, occurring in wood, cotton, hemp and other plant-based materials and serving as the dominant reinforcing phase in plant structures. Plant fibers are mainly composed of cellulose, hemicellulose and lignin. Cellulose, which awards the mechanical properties of the complete natural fiber, is ordered in micro-fibrils enclosed by the other two main components: hemicellulose and lignin (Bledzki, & Gassan, 1999). Cellulose microfibrils can be found as intertwined microfibrils in the cell wall (2–20 nm diameter and 100–40,000 nm long depending on its source). As well as these microfibrils, there exist nanofibers (also composed by cellulose) with diameters of 5–50 nm and lengths of several millimetres conformed by nanocrystalline domains and amorphous regions (Darder *et al.*, 2007). Cellulose is a linear carbohydrate polymer chain consisting of D-glucofuranose units joined together by  $\beta$ -

1,4-glycosidic linkages. In the unit cell of cellulose, two chains are joined by hydrogen bonding to each other in a parallel conformation, which is called cellulose. These units are packed side-by-side to form microfibrils of cellulose, which also contain disordered or amorphous regions. There are several polymorphs of crystalline cellulose such as, cellulose I, II, III and IV. Cellulose I is the crystalline cellulose that is naturally produced by a variety of organisms (trees, plants, tunicates, algae, and bacteria). It is sometimes referred to as “natural” cellulose. Its structure is thermodynamically metastable and can be converted to either cellulose II or III. Cellulose I has two polymorphs, a triclinic structure ( $I\alpha$ ) and a monoclinic structure ( $I\beta$ ), which coexist in various proportions depending on the cellulose source (Moon *et al.*, 2011). The arrangement of the cellulose microfibrils in the primary wall is random. Secondary cell walls of plants contain cellulose (40–80%), hemicellulose (10–40%), and lignin (5–25%), where cellulose microfibrils are embedded in lignin. Hemicellulose is a highly branched polymer compared to linear cellulose. Its structure contains a variety of sugar units, whereas cellulose contains only 1,4- $\beta$ -D-glucopyranose units and its degree of polymerization is 10–100 times lower than that of cellulose. Finally, lignin is a complex hydrocarbon polymer with both aliphatic and aromatic constituents (Soykeabkaew *et al.*, 2008).

The cellulose molecules are always biosynthesized in the form of nanosized fibrils, which are in turn assembled into fibers, films, walls, etc. The cellulose nanofibers are called cellulose nanocrystal (CNC). The molecular arrangements of these fibrillar bundles are so small that the average diameter of the bundle is about 10 nm. These cellulose nanofibers are with diameters of 5–50 nm and lengths of thousands of nanometers. CNC is a cellulose derivative composed of a nano-sized fiber network that determines the product properties and its functionality. CNC fibers are very interesting nanomaterials for production of cheap, lightweight, and very strong

nanocomposites. Generally, CNC is produced by the bio-formation of cellulose via bacteria and also by the disintegration of plant celluloses using shear forces in refiner techniques. Wood-derived CNC can also be prepared by electro-spinning from pulp solutions (Dufresne, 1997) or by controlled acid hydrolysis of bleached chemical pulp (Beck-Candanedo, *et al.*, 2005). Cellulose nanofibers are recognized as being more effective than their micro sized counterparts to reinforce polymers due to interactions between the nano-sized elements that form a percolated network connected by hydrogen bonds, provided there is a good dispersion of the nanofibers in the matrix and their very high specific area in the orders of several 100 m<sup>2</sup>/g. It is predicted that CNC reinforcements in the polymer matrix may provide value-added materials with superior performance and extensive applications for the next generation of biodegradable materials. CNC is expected to show high stiffness since the Young's modulus (YM) of the cellulose crystal is as high as 134 GPa. The tensile strength of the crystal structure was assessed to be approximately 0.8 up to 10 GPa (Dieter-Klemm *et al.*, 2009; Azeredo *et al.*, 2010; Cao *et al.*, 2008).

Polymer composites are mixtures of polymers with inorganic or organic additives having certain geometries (fibres, flakes, spheres, particulates). The use of nanoscale fillers is leading to the development of polymer nanocomposites and represents a radical alternative to the conventional polymer composites ((Dieter-Klemm *et al.*, 2006). Polymer nanocomposites have generated enormous interest since Toyota<sup>®</sup> researchers in the late 1980s showed that as little as 5% addition of nano-sized clays to nylons greatly increased their modulus and heat distortion temperature (Kojima *et al.*, 1993). The use of nanocomposites serve a number of important functions, such as extending the food shelf life, enhancing food quality because they can serve not only as barriers to moisture, water vapor, gases, and solutes, but also serve as carriers of some active substances, such as antioxidants and antimicrobials (Rhim and Hong, 2006). These

nanocomposites are significant due to their nanoscale dispersion with size less than 1,000 nm (Sanguansri & Augustin, 2006). Addition of relatively low levels of nanoparticles (less than 5%) have been shown to substantially improve the properties of the finished plastic, increasing the deformability and strength, and reducing the electrical conductivity and gas permeability (Sorrentino & Gorrasi, 2007).

This review discusses potential use, application and advantages of nanocomposites, especially nanocellulose, in the field of food packaging. It highlights the potential of biopolymers (alginate, chitosan etc.) for food packaging and also the incorporation of bioactive agents or antimicrobials (organic acids, bacteriocins, essential oils etc.) into packaging to improve the quality and safety of food products during storage.

## **1.4. Nanocomposites**

Nanocomposites are mixture of polymers with nanosized inorganic or organic fillers with particular size, geometry, and surface chemistry properties. The polymers used are normally hydrocolloids, such as proteins, starches, pectins, and other polysaccharides. Various inorganic nano-particles have been recognized as possible additives to enhance the polymer performance (John and Thomas, 2008). Nanofillers include solid layered clays, synthetic polymer nanofibers, cellulose nanofibers, and carbon nano-tubes. Up to now only the layered inorganic solids like layered silicate have attracted the attention of the packaging industry. This is due to their ready availability and low cost, and also their significant enhancement of finished product properties and relative simple processing (Sorrentino and Gorrasi, 2007).

### **1.4.1. Advantages of Nanocomposites**

When polymers are combined with nanofillers, the resulting nanocomposites exhibit significant improvements in mechanical properties, dimensional stability, and solvent or gas resistance with

respect to the pristine polymer. Owing to the nano size particles obtained by dispersion, these nanocomposites can exhibit many advantages such as, biodegradability, enhanced organoleptic characteristics of food, such as appearance, odor, and flavor; reduced packaging volume, weight, and waste; extended shelf life and improved quality of usually non-packaged items; individual packaging of small particulate foods, such as nuts and raisins; function as carriers for antimicrobial and antioxidant agents; controlled release of active ingredients; annually renewable resources (Rhim, 2007; Hitzky, *et al.*, 2005).

Nanocomposites also offer extra benefits like low density, transparency, good flow, better surface properties, and recyclability. The enhancement of many properties resides in the fundamental length scales dominating the morphology and properties of these materials. The nanofiller particles have at least one dimension in the nanometer (from 1 to 100 nm) range. It means that a uniform dispersion of these particles can lead to ultra-large interfacial area between the constituents. The very large organic or inorganic interface alters the molecular mobility and the relaxation behavior, improves the mechanical properties of nanocomposites both in solid and melt states, and the thermal stability and melt viscosity of renewable polymers also increase after nanocomposite preparation. However, increased aggregation and problems related to the dispersion of nanofillers can occur due to their large surface area (Sorrentino and Gorrasi, 2007; Han and Floros, 1997; Penner and Lagaly, 2001). Manias *et al.* (2001), reported that small additions—typically less than 6 wt % of nanoscale inorganic fillers could promote concurrently several of the polypropylene material properties, including improved tensile characteristics, higher heat deflection temperature, retained optical clarity, high barrier properties, better scratch resistance, and increased flame retardancy. Strawhecker and Manias, (2000) suggested that for a 5% montmorillonite (MMT) exfoliated composite, the softening temperature of nanocomposites

increased by 25°C, the water permeability reduced by 60% and the nanocomposites could retain their optical clarity. For these reasons, these are far lighter in weight than conventional biodegradable composites and make them competitive with other materials for specific applications, especially food packaging (Petersen, *et al.*, 1999). Another advantage of nanocomposite is that it can be biodegraded efficiently. Degradation of a polymer may result from the action of microbes, macro organisms, photo degradation or chemical degradation (Avella *et al.*, 2005).

#### **1.4.2. Application of Nanocomposites in Food Packaging**

The use of proper packaging materials and methods to minimize food losses and provide safe and wholesome food products have always been the focus of food packaging. In addition, consumer trends for better quality, fresh-like, and convenient food products have intensified during the last decades. Therefore, a variety of active packaging technologies have been developed to provide better quality, wholesome, and safe foods and also to limit package related environmental pollution and disposal problems. The application of nanocomposites may open a new possibility to solve these problems. Nanocomposite packaging materials have great potential for enhanced food quality, safety, and stability as an innovative packaging and processing technology. The unique advantage of the natural biopolymer packaging may lead to new product development in food industry, such as individual packaging of particulate foods, carriers for functionally active substances, and nutritional supplements (Ozdemir and Floros, 2004; Ruiz-Hickey *et al.*, 2005).

#### **1.5. Cellulose Nanocrystal (CNC)**

Nanocelluloses (CNCs) are described as celluloses composed of nanosized fibers and the nanofiber structuring which determines the product properties. The similar term *nanosized*

*cellulose* is used in case of isolated crystallites and whiskers formed by acid-catalyzed degradation of celluloses. This field and the application of that nanosized cellulose, e.g. in composites, have been intensively investigated. Typical examples have been reported (Ljungberg *et al.*, 2005; Masa *et al.*, 2005).

### **1.5.1. Types of CNC**

As described before, one type of CNC is formed directly as the result of biosynthesis of special bacteria and these types of CNCs are called bacterial cellulose. A very pure product with subsequently reported significant properties is formed that necessitates challenging biosynthesis / biotechnological handling and the development of large-scale production. Another kind of CNC can be prepared from the nearly inexhaustible source of feedstock wood using controlled mechanical disintegration steps to produce the favoured product properties (Masa *et al.*, 2005).

### **1.5.2. CNC from Bacteria**

In 1886, A. J. Brown discovered bacterial cellulose (BC) as a biosynthetic product of *Gluconacetobacter xylinus* strains (Klemm *et al.*, 1998). He identified a gelatinous mass, formed on the solution during the vinegar fermentation as cellulose. It is mentioned that, in the middle of the 20th century a special culture medium was developed for *Gluconacetobacter xylinus* to optimize cellulose formation on the laboratory scale. As a result of systematic and comprehensive research over the last decade, broad knowledge of the formation and structure of BC has been acquired. This work is an important part of the integration of biotechnological methods into polysaccharide chemistry and the development of cellulose products with new properties and application potential (Tischer *et al.*, 2011).

### 1.5.3. CNC from Wood

In contrast to BC, cellulose from wood is composed of fibers that are about one hundred times thicker. Because of the complex and expensive cultivation of BC (sophisticated medium and long cultivation time), it is also a challenge to produce nano-fibrillated celluloses from wood. The substructures of wood are only accessible by chemical treatment (Klemm *et al.*, 1998) and mechanical disintegration procedures. In the last 25 years, there have been efforts to reduce wood fibers in size. As a first step, in the early 1980s, Turbak *et al.* (1983) developed micro fibrillated cellulose (MFC). Today, there are different ways to produce materials with controlled fiber diameters. At first, a water suspension of bleached chemical pulp has to go through a mechanical treatment that consists of a spring-loaded valve assembly (refiner), where the slurry is pumped at high pressure. The formed MFC is moderately degraded and extremely expanded in surface area. In recent years, cellulose with a nanoscale web-like structure has been made. The fiber diameters are in the range 10–100 nm (Nakagaito & Yano, 2004 & 2005). The degree of fibrillation depends on the number of passes through the refiner. Another technique to prepare wood MFC/NC is described by Takahashi *et al.* (2005). The aim was the creation of strong composites in tension using hot-pressed fibers without synthetic polymers but with the original wood components hemicelluloses and lignin as binders. The starting material was bamboo because of its high cellulose content. Bamboo fiber bundles and monofilaments were ground under high-speed conditions using stone disks. A combination of thermal and alkali pre-treatments, given the appropriate ratio of cellulose, hemicelluloses and lignin in the monofilaments, led to strong adhesion between the fibers under the hot-press conditions. Suzuki and Hattori, (2004) treated a bleached chemical pulp with a solid concentration of 1–6% with a disk refiner more than 10 times. The fibers obtained had a length of less than 0.2 mm. There

have also been some investigations into the properties of CNC from wood, which has an amazing water-storage capacity, similar to BC. A dispersion of these cellulose fibers in water with a solid content of only 2% leads to a mechanically stable transparent gel. The wood CNC fibers are suitable for solidification of emulsion paints and filter aids, useful for both primary rough filtration and precision filtration. Furthermore, NC from wood is used in paper-making as a coating and dye carrier in paper tinting. Moreover, it can be utilized in the food industry as a thickening agent, a gas-barrier and in moisture resistant paper laminate for packaging. In cosmetics, wood CNC is suitable as an additive in skin-cleansing cloths, and as part of disposal diapers, sanitary napkins and incontinence pads. Possible medical applications are directed to excipients such as binders, fillers, and/or disintegrants in the development of solid dosage forms (Kyomori, 2005; Fukuda, 2001; Kumar, 2002)

Besides application in its pure form, it is possible to use CNC from wood in polymer composites. In embedding tests, the tensile strength of such composites was five times higher than that of the original polymers. This result, as well as its natural origin, makes this CNC attractive for combination with different biopolymers. Possible applications for such reinforced biopolymers could arise in areas such as medicine, the food industry, and gardening (Nakagaito and Yano, 2004 and 2005). In these sectors, properties such as biodegradability, high mechanical strength, and, where required, optical transparency, are important. It should also be mentioned that the application of wood CNC prepared by the described techniques where the cell wall is further disintegrated by mechanical treatment leads to lower-strength cellulose fiber reinforced composites than in the corresponding BC materials (Gindl and Keckes, 2004).

#### **1.5.4. Application of CNC**

In recent years due to the exceptional properties of these innovative CNC polymers, there are many widespread utilization. Membranes and composites from cellulose and cellulose esters are important domains in the development and application of these polymeric materials. The most important segment by volume in the chemical processing of cellulose contains regenerated cellulose fibers, films, and membranes. In the case of the cellulose esters, mainly cellulose nitrate and cellulose acetate as well as novel high-performance materials have been created which are widely used as laminates, composites, optical/photographic films and membranes, or as other separation media. The direct formation of stable and manageable BC fleeces as the result of bacterial biosynthesis in the common static culture is significant. This and their exciting properties have led to increasing use of BC as a membrane material and composite component. Contaminations incorporated from the culture medium and bacterial cells can be removed from the BC by smooth purification methods depending on the application area. One recent example of the formation and application of foils/membranes of unmodified bacterial CNC is described by George and co-workers (George *et al.*, 2005). The processed membrane seems to be of great relevance as a packaging material in the food industry, where continuous moisture removal and minimal-oxygen-transmission properties play a vital role. The purity, controllable water capacity, good mechanical stability, and gas-barrier properties of bacterial CNC are important parameters for this application

#### **1.5.5. CNC Based Composites**

There have been several researches on the use of CNC as a reinforcing agent in polymer matrices. Nanocomposites based on nanocellulosic materials have been prepared with petroleum-derived non-biodegradable polymers such as polyethylene (PE) or polypropylene (PP) and also

with biodegradable polymers such as polylactic acid (PLA), polyvinyl alcohol (PVOH), starch, polycaprolactone (PCL), methylcellulose, and chitosan.

Bruce *et al.* (2005) prepared composites based on Swede root MFC and different resins including four types of acrylic and two types of epoxy resins. All the composites were significantly stiffer and stronger than the unmodified resins. The main merit of the study was that it demonstrated the potential for fabricating nanocomposites with good mechanical properties from vegetable pulp in combination with a range of resins. Aside from good mechanical properties, high composite transparency can be important for some applications (e.g., in the optoelectronics industry). Iwamoto *et al.* (2005, 2007) reported that because of the size of nanofibers reinforced acrylic resin retains the transparency of the matrix resin even at fiber contents as high as 70 wt%. The BC with nanofiber widths of 10 nm also has potential as a reinforcing material for transparent composites. As for example, Nogi *et al.* (2005, 2006a, b) obtained transparent composites by reinforcing various acrylic resins with BC at loadings up to 70 wt% by reducing the average fiber size (diameter 15 nm). Abe *et al.* (2007) fabricated a CNC (from wood) containing acrylic resin nanocomposite with transmittance higher than that of BC nanocomposite in the visible wavelength range and at the same thickness and filler content. This finding indicated that nanofibers obtained from wood were more uniform and thinner than BC nanofibers.

Another remarkable and potentially useful feature of CNC is their low coefficient of thermal expansion (CTE), which can be as low as  $0.1 \text{ ppm K}^{-1}$  and comparable with that of quartz glass (Nishino *et al.*, 2004). This low CTE combined with high strength and modulus could make CNC a potential reinforcing material for fabricating flexible displays, solar cells, electronic paper, panel sensors and actuators, etc. As an example, Nogi and Yano (2008) prepared a foldable and ductile transparent nanocomposite film by combining low-YM transparent acrylic

resin with 5 wt% of low CTE and high-YM of BC. The same researchers reported that transparent NC sheets prepared from CNC and coated with acrylic resin have low CTEs of 8.5–14.9 ppm K<sup>-1</sup> and a modulus of 7.2–13 GPa (Nogi and Yano, 2009). Polyurethane (PU), which is a polar polymer, has the potential to interact with the polar groups of cellulose molecules leading to enhanced mechanical and interfacial properties of the composites. PU-MFC composite materials were prepared recently using a film stacking method in which the PU films and non-woven cellulose fibril mats were stacked and compression moulded (Seydibeyoglu and Oksman, 2008). The thermal stability and mechanical properties of the pure PU were improved by MFC reinforcement. Nanocomposites with 16.5 wt% fibril content had tensile strength and YM values nearly 5 and 30 times higher, respectively than that of the corresponding values for the matrix polymer.

Polyvinyl alcohol (PVOH) is a water soluble alcohol which is biocompatible, biodegradable and also has excellent chemical resistance. Therefore PVOH has a wide range of practical applications. In particular, PVOH is an ideal candidate for biomedical applications including tissue reconstruction and replacement; cell entrapment and drug delivery, soft contact lens materials and wound covering bandages for burn victims (Ding *et al.*, 2004). Sun-Young Lee *et al.* (2009) reported the fabrication of PVOH-NC composites by the reinforcement of CNC into a PVOH matrix at different filler loading levels and subsequent film casting. The CNC was prepared by acid hydrolysis of MCC at different hydrobromic acid (HBr) concentration. Chemical characterization of NC was performed for the analysis of crystallinity (X<sub>c</sub>), degree of polymerization (DP), and molecular weight (M<sub>w</sub>). The acid hydrolysis decreased steadily the DP and M<sub>w</sub> of MCC. The crystallinity of MCC with 1.5 M and 2.5 M HBr showed a significant increase due to the degradation of amorphous domains in cellulose. The mechanical and thermal

properties of the CNC reinforced PVOH films were also measured for tensile strength and thermo-gravimetric analysis (TGA). The tensile strength (TS) of pure PVOH film was 49 MPa. The TS of CNC reinforced PVOH films after 1.5 M HBr hydrolysis showed the highest value (73 MPa) at the loading of 1 wt%. This value was 49% higher than pure PVOH film. However, the NC loading of 3 and 5 wt% to PVOH matrix gradually decreased the values of TS. The TS of PVOH films with 3 and 5 wt% NC were 3.0 and 55.3 % lower, respectively, compared to those with 1 wt% NC. The TGA of NC reinforced PVOH films revealed three main weight loss regions. The first region at a temperature of 80°C to 140°C is due to the evaporation of physically weak and chemically strong bound water, and the weight loss of the film in those ranges is about 10 wt%. The second transition region at around 230-370°C is due to the structural degradation of PVOH composite films and the total weight loss in those range was about 70 %. The third stage weight loss occurred above 370°C, due to the cleavage backbone of PVOH composite films or the decomposition of carbonaceous matter. Millon and Wan, (2006) tested BC as a potential reinforcing material in PVOH for medical device applications. These authors developed a PVOH-BC nanocomposite with mechanical properties tuneable over a broad range, thus making it appropriate for replacing different tissues. A number of applications using MFC for reinforcing PVOH have been reported. For example, Zimmermann *et al.* (2004) dispersed MFC into PVOH and generated fibril-reinforced PVOH nanocomposites (fibril content 20 wt%) with up to three times higher YM and up to five times higher TS when compared to the reference polymer. A blend containing 10% NC obtained from various sources, such as flax bast fibers, hemp fibers, kraft pulp or rutabaga and 90% PVOH was used for making nano fiber reinforced composite material by a solution casting procedure (Bhatnagar and Sain, 2005). Both TS and YM were improved compared to neat PVOH film, with a pronounced four- to five-fold

increase in YM observed. Poly(caprolactone) (PCL), a biodegradable polymer, is suitable as a polymer matrix in biocomposites. Lönnberg *et al.* (2008) prepared MFC grafted PCL composites via ring-opening polymerization (ROP). This changes the surface characteristics of MFC due to grafting made it possible to obtain a stable dispersion of MFC in a nonpolar solvent. It also improved the compatibility of MFC's with PCL. The thermal behavior of MFC grafted with different amount of PCL has been investigated using thermal gravimetric analysis (TGA) and differential scanning calorimetry (DSC). The crystallization and melting behaviour of free PCL and MFC-PCL composites were studied with DSC, and a significant difference was observed regarding melting points, crystallization temperature (T<sub>g</sub>), degree of crystallinity, as well as the time required for crystallization.

Khan *et al.* (2010c) prepared methylcellulose (MC)-based films casted from its 1% aqueous solution containing 0.5% vegetable oil, 0.25% glycerol, and 0.025% Tween80<sup>®</sup>. Puncture strength (PS), puncture deformation (PD), viscoelasticity coefficient, and water vapor permeability (WVP) were found to be 147 N/mm, 3.46 mm, 41%, and 6.34 g.mm/m<sup>2</sup>.day.kPa, respectively. Aqueous NC solution (0.1-1%) was incorporated into the MC-based formulation, and it was found that both PS and WVP values were improved by 117 and 26% respectively. Films containing 0.25% NC were found to be the optimum. Khan *et al.* (2010) also reported the effect of gamma radiation on the NC containing MC-based composites. The films were irradiated from 0.5-50 kGy doses, and it was revealed that mechanical properties of the films were slightly increased at low doses because of NC fibers reorientation, whereas barrier properties were further improved to 29% at 50 kGy.

Dufresne and Vignon (1998 and 2000) prepared potato starch-based nanocomposites, while preserving the biodegradability of the material through addition of MFC. The cellulose filler and

glycerol plasticizer content were varied between 0–50 wt% and 0–30 wt% respectively. MFC significantly reinforced the starch matrix, regardless of the plasticizer content, and the increase in YM as a function of filler content was almost linear. The YM was found to be about 7 GPa at 50 wt% MFC content compared to about 2 GPa for unreinforced samples (0% MFC). However, it was noted that when the samples were conditioned at high relative humidity (75% RH), the reinforcing effect of the cellulose filler was strongly diminished. Since starch is more hydrophilic than cellulose, in moist conditions it absorbs most of the water and is then plasticized. The cellulosic network is surrounded by a soft phase and the interactions between the filler and the matrix are strongly reduced. Besides improving mechanical properties of starch, addition of MFC to the matrix resulted in a decrease of both water uptake at equilibrium and the water diffusion coefficient. Nanocomposites from wheat straw nanofibers and thermoplastic starch from modified potato starch were prepared by the solution casting method (Alemdar and Sain, 2008). Thermal and mechanical performance of the composites was compared with the pure thermoplastic starch (TPS) using TGA, dynamic mechanical analysis (DMA) and tensile testing. The TS and YM were significantly enhanced in the nanocomposite films, which could be explained by the uniform dispersion of nanofibers in the polymer matrix. The YM of the TPS increased from 111 to 271 MPa with maximum (10 wt%) nanofiber filling. In addition, the glass transition ( $T_g$ ) of the nanocomposites was shifted to higher temperatures with respect to the pure TPS. Azeredo *et al.* (2010) developed CNC reinforced chitosan films with different CNC and glycerol (plasticizer) content. They evaluated the effect of different concentration of CNC and glycerol on the TS, YM,  $T_g$ , elongation at break ( $E_b$ ), and WVP of the chitosan based composite films. They have an optimum condition of 18% glycerol and 15% CNC, based on the maximization of TS, YM,  $T_g$  and decreasing WVP values while maintaining a acceptable  $E_b$  of

10%. Pereda, *et al.* (2010) developed sodium caseinate films with CNC by dispersing the fibrils into film forming solutions, casting and drying. Composite films have been reported to be less transparent and had a more hydrophilic surface than neat sodium caseinate films. However, the global moisture uptake was almost not affected by the CNC concentration. Addition of CNC to the neat sodium caseinate films produced an initial increase in the WVP and then decreased as filler content increased. The TS and TM of the composite films has been reported to increase significantly with a more than 2 times increase in TS and TM, than the native films at 3% CNC content.

### **1.6. Classification of Biopolymers**

A vast number of biopolymers or biodegradable polymers are chemically synthesized or biosynthesized during the growth cycles of all organisms. Some micro-organisms and enzymes capable of degrading them have been identified (Averous & Boquillon, 2004). **Fig.1.1**, proposes a classification with four different categories, depending on the synthesis:

- (a) Polymers from biomass such as the agro-polymers from agro-resources, e.g., starch, cellulose.
- (b) Polymers obtained by microbial production e.g. poly(hydroxyalkanoates).
- (c) Polymers chemically synthesized using monomers obtained from agro-resources e.g. poly(lactic acid).
- (d) Polymers whose monomers and polymers are both obtained by chemical synthesis from fossil resources e.g. poly(caprolactone), polyester amide etc.

Except the fourth family, which is of fossil origin, most polymers of family (a)–(c) are obtained from renewable resources (biomass). The first family is agro-polymers (e.g. polysaccharides)

obtained from biomass by fractionation. The second and third families are polyesters, obtained, respectively by fermentation from biomass or from genetically modified plants (e.g. polyhydroxyalkanoate) and by synthesis from monomers obtained from biomass (e.g. polylactic acid). The fourth family is polyesters, totally synthesized by the petrochemical process (e.g. polycaprolactone; polyester amide; aliphatic or aromatic copolyesters). A large number of these biopolymers are commercially available. They show a large range of properties and they can compete with non-biodegradable polymers in different industrial fields (John and Thomas, 2008).

### **1.7. Bioactive Packaging**

Bioactive packaging is gaining interest from researchers and industries due to its potential to provide quality and safety benefits. The reason for incorporating bioactive agents into the packaging is to prevent surface growth of micro organisms in foods where a large portion of spoilage and contamination occurs (Coma, 2008; Appendini and Hotchkiss, 2002). This approach can reduce the addition of larger quantities of antimicrobials that are usually incorporated into the bulk of the food. A controlled release from packaging film to the food surface has numerous advantages over dipping and spraying. In the latter processes, in fact, antimicrobial activity may be rapidly lost due to inactivation of the antimicrobials by food components or dilution below active concentration due to migration into the bulk food matrix (Janjarasskul, and Krochta, 2010). Numerous researchers have demonstrated that bioactive polymers such as, alginate, chitosan, gelatine etc. and antimicrobial compounds such as organic acids (acetic, propionic, benzoic, sorbic, lactic, lauric), potassium sorbate, bacteriocins (nisin, lactacin), grape seed extracts, spice extracts (thymol, p-cymene, cinnamaldehyde), thiosulfates

(allicin), enzymes (peroxidase, lysozyme), proteins (conalbumin), isothiocyanates (allylisothiocyanate), antibiotics (imazalil), fungicides (benomyl), chelating agents (ethylenediaminetetraacetic acid-EDTA), metals (silver), or parabens (heptylparaben) could be added to edible films to reduce bacteria in solution, on culture media, or on a variety of muscle foods (Cutter, 2002 and 2006). A short discussion on some of the bioactive polymers and bioactive agents is given here:

### **1.7.1. Bioactive Polymers**

Bioactive polymers such as, alginate, chitosan, gelatin etc. can be used for the packaging of food products. Alginates are linear copolymers of  $\beta$ -(1-4)-linked D-mannuronic acid and  $\alpha$ -(1-4)-linked L-guluronic acid units, which exist widely in many species of brown seaweeds. Since Stanford discovered it in 1881, alginate has been used in a wide range of industries, such as food, textile printing, paper and pharmaceuticals, and for many other novel end-uses (Khan *et al.*, 2010a). Study found that alginate coatings retarded oxidative off-flavors, improved flavor and juiciness in re-heated pork patties (Earl, 1976). Other researchers have extended the shelf life of shrimp, fish, and sausage with alginate coatings (Cutter and Samner, 2002). Sodium alginate coatings extended the shelf life of salted and dried mackerel (Jo, 2001). Chitosan is a natural hetero-polysaccharide composed of 2-amino-deoxy- $\beta$ -D-glucopyranose and 2-acetamido-deoxy- $\beta$ -D-glucopyranose (chitin) residues. It is a partially deacetylated derivative of chitin, which is the second most abundant natural polysaccharide in nature after cellulose. Chitosan has been found to be non-toxic, biodegradable, biofunctional, biocompatible and was reported by several researchers to have strong antimicrobial and antifungal activities. Chitosan has been compared with other biomolecule-based active films used as packaging materials and the reported results showed that chitosan has more advantages because of its antibacterial activity (Chen *et al.*,

2010). Chitosan films have been successfully used as a packaging material for the quality preservation of a variety of foods (Ouattara *et al.*, 2000). Antimicrobial films have been prepared by including various organic acids and essential oils in a chitosan matrix, and the ability of these bio-based films to inhibit the growth of indigenous (*Lactic acid bacteria* and *Enterobacteriaceae*) or inoculated bacteria (*Lactobacillus sakei* and *Serratia liquefaciens*) onto the surfaces of vacuum-packed cured meat products have been investigated. Release of organic acids (acetic and propionic) was found to be initially fast, when the gradient of ion concentration between the inside of the polymer matrix and the outside environment was high, then decreased as the release of acids progressed. At the same time, it was shown that the antimicrobial activity of the bio-based films under study did not affect growth and activity of lactic acid bacteria, whereas the growth of *Enterobacteriaceae* and *S. liquefaciens* was delayed or completely inhibited after storage during 21 days at 4°C (Quintavalla and Vicini, 2002). Recently, a chitosan–starch film has been prepared using microwave treatment, which may find potential application in the food packaging technology (Dutta *et al.*, 2009; Aider, 2010). Chitosan films have been made via treatments with various acids and incorporated into packaging films for processed meats and seafood, as well as combined with nisin and coated onto the surfaces of paper for inhibiting microorganisms (Vartiainen *et al.*, 2004). Durango *et al.* (2006) also developed and evaluated an edible film made from 3% or 5% chitosan and starch against *S. enteritidis* in suspensions. When applied directly to cell suspensions, 1% chitosan reduced the pathogen  $>4\log_{10}$  CFU/ml (or 99.99%). Subsequent experiments demonstrated that chitosan-treated films made with 3% or 5% chitosan reduced populations of *S. enteritidis*  $> 1\log_{10}$  CFU/ml (or 90%). The authors demonstrated that chitosan-treated films made with 5% chitosan were the most efficient treatment for inhibiting *S. enteritidis* in solution and that the application

of these films to foodstuffs was in progress. In another study, Cooksey (2005) incorporated nisin into chitosan to inhibit *L. monocytogenes*. In solution and in agar diffusion assays, the antimicrobial film inhibited the pathogen, but no further studies were conducted in meat systems (Cha and Chinnan, 2004).

### **1.7.2. Organic Acids**

Organic acids, such as acetic, benzoic, lactic, citric, nalidixic, maleic, tartaric, propionic, fumaric, sorbic, etc. are one of the most common ingredients used for bioactive packaging. Yamanaka *et al.* (2002), described the influence of bioactive organic agents such as nalidixic acid as additives to the bacterial cellulose (BC) culture medium. In that case, not only the crystallization of the fibers and the material properties were influenced but the *Gluconacetobacter* cells were also changed. Using antibiotics in a concentration of 0.1mM, a 2–5 times elongation of the cell length was observed due to inhibition of cell division. The fibers became 1–2 times wider compared to common BC. Ghosh *et al.* (1997), developed fungistatic wrappers with sorbic acid and applied them to bread. This wrapper necessitated heating the wrapped bread at 95–100°C for a period of 30 to 60 min. The incorporation of an antioxidant in the treated wrapper and also the use of an odor adsorbent inside the bread packs minimized off-flavor development. Sliced bread, based on sensory evaluation, was found acceptable up to 1 month and as a sandwich, up to 3 months. The fungistatic wrappers were made by coating grease-proof paper with an aqueous dispersion of sorbic acid in 2% carboxymethyl cellulose solution. Using this sorbic acid-treated paper and then enclosing the food in a polyethylen bag could preserve foods that are generally amenable to spoilage by mold for minimum of 10 days. Han and Flores, (1997) studied the incorporation of 1.0% w/w potassium sorbate in low density polyethylene films. A 0.1 mm thick film was used for physical measurements. It was found that

potassium sorbate lowered the growth rate and maximum growth of yeast, and lengthened the lag period before mold growth became apparent. Weng *et al.* (1999) developed the technique of combining polyethylene-co-methacrylic acid (PEMA) with benzoic and sorbic acid to form antimicrobial food packaging material. Devlieghere *et al.* (2000) studied the antimicrobial activity of ethylene vinyl alcohol (EVA)/linear low density polyethylene (LLDPE) containing potassium sorbate. Because of the limited migration of *K*-sorbate from LLDPE film, the inhibition effect of this film against *Candida* spp., *Pichia* spp., *Trichosporon* spp. and *Penicillium* spp. appeared very weak. Moreover, no significant differences could be observed for yeast and mold growth on the cheese cubes compared to a reference film during storage of cheese packaged in a *K*-sorbate film. Benzoic anhydride-incorporated antimicrobial polyethylene films and minimal microwave heating were used to control the microbial growth of Tilapia fish fillets.

### **1.7.3. Bacteriocins**

The bacteriocin such as nisin, which is produced by the lactic acid bacterium, *Lactococcus lactis*, is one of the most effective agents when it comes to antimicrobial packaging. It is the most effective against lactic acid bacteria and other gram-positive organisms, notably the *Clostridia* species (Jin and Zhang, 2008). El-Fahmy *et al.* (2010) developed hydroxypropyl methylcellulose films with nisin and evaluated the antimicrobial activity of the films against *Listeria*, *Staphylococcus*, *Enterococcus*, and *Bacillus* strains. It has been reported that film bioactivity demonstrated efficacy against *Listeria* > *Enterococcus* > *Staphylococcus* > *Bacillus* spp. Scannell *et al.* (2000) developed bioactive food packaging materials using immobilized nisin and lactacin 3147. The antimicrobial packaging reduced the lactic acid bacteria counts in sliced cheese and ham at refrigeration temperatures, thus, extending the shelf life. Nisin adsorbed

bioactive inserts reduced levels of *Listeria innocua* by below 2 log units in cheese and ham and *Staphylococcus aureus* in cheese (~1.5 log units) and ham (~2.8 log units). Ming *et al.* (1997) applied nisin and pediocin to cellulose casings to reduce *L. monocytogenes* in meats and poultry. Pediocin-coated bags completely inhibited the growth of inoculated *L. monocytogenes* through 12 weeks storage at 4°C. Pediocin is another bacteriocin, which was found to be effective against *L. monocytogenes*. Wilhoit (1996 and 1997) has received a patent for the method of employing pediocin-coated cellulose casings on meat for inhibiting the growth of *L. monocytogenes*. Cutter and Siragusa (1997) reported that immobilization of the bacteriocin nisin in calcium alginate gels not only resulted in greater reductions of bacterial populations on lean and adipose beef surfaces, but also resulted in greater and sustained bacteriocin activity when the tissues were ground and stored under refrigerated conditions for up to 7 days, as compared to nisin-only controls.

#### **1.7.4. Essential Oils and Plant Extracts**

The antimicrobial activity of essential oils and plant extracts has been recognized for many years. Ouattara *et al.* (2001) evaluated the combined effect of low-dose gamma irradiation and protein-based coatings with thyme oil and trans-cinnamaldehyde to extend the shelf life of pre-cooked shrimp. The product shelf life was significantly extended without altering the appearance and taste of shrimp for thymol treatment concentrations of up to 0.9%. Oussalah *et al.* (2007) developed alginate-based edible films with 1% (w/v) essential oils of Spanish oregano (O; *Corydothymus capitatus*), Chinese cinnamon (C; *Cinnamomum cassia*), or winter savory (S; *Satureja montana*); to control pathogen growth on bologna and ham slices. The bologna and ham slices were inoculated with *S. typhimurium* or *L. monocytogenes* at  $10^3$  CFU/cm<sup>2</sup>. On bologna,

C-based films were the most effective against the growth of *S. typhimurium* and *L. monocytogenes*. *L. monocytogenes* was the more sensitive bacterium to O-, C-, and S-based films. *L. monocytogenes* concentrations were found to be below the detection level (<10 CFU/ml) after 5 days of storage on bologna coated with O-, C-, or S-based films. On ham, a 1.85 log CFU/cm<sup>2</sup> reduction of *S. typhimurium* ( $P \leq 0.05$ ) have been reported after 5 days of storage with C-based films. *L. monocytogenes* was highly resistant in ham, even in the presence of O-, C-, or S-based films. However, C-based films were the most effective against the growth of *L. monocytogenes*. Oussalah *et al.* (2004) also developed milk protein-based edible films containing 1.0% (w/v) oregano, 1.0% (w/v) pimento, or 1.0% oregano-pimento (1:1) essential oils mix were applied on beef muscle slices. The application of bioactive films on meat surfaces containing 10<sup>3</sup> CFU/cm<sup>2</sup> of *E. coli* O157:H7 or *Pseudomonas* spp. showed that film containing oregano was the most effective against both the bacteria, whereas film containing pimento oils was reported to have least effect against these two bacteria. A 0.95 log reduction of *Pseudomonas* spp. level, as compared to samples without film, was observed at the end of storage in the presence of films containing oregano extracts. A 1.12 log reduction of *E. coli* O157:H7 level was reported in samples coated with oregano-based films. Hammer *et al.* (1999) investigated 52 plant oils and extracts for activity against *Acinetobacter baumannii*, *Aeromonas veronii* biogroup *sobria*, *Candida albicans*, *Enterococcus faecalis*, *E. coli*, *Klebsiella pneumoniae*, *Pseudomonas aeruginosa*, *Serratia marcescens* and *Staphylococcus aureus*, using an agar dilution method. Lemongrass, oregano and bay inhibited all organisms at concentrations of  $\leq 2.0\%$  (v/v). Six oils did not inhibit any organisms at the highest concentration, which was 2.0% (v/v) oil for apricot kernel, evening primrose, macadamia, pumpkin, sage and sweet almond. Variable activity was recorded for the remaining oils. Twenty of the plant oils and extracts were investigated, using a

broth microdilution method, for activity against *C. albicans*, *S. aureus* and *E. coli*. The lowest minimum inhibitory concentrations were 0.03% (v/v) thyme oil against *C. albicans* and *E. coli* and 0.008% (v/v) vetiver oil against *S. aureus*. Smith- Plamer *et al.* (1999) investigated antimicrobial properties of 21 plant essential oils and two essences were investigated against five important food-borne pathogens, *Campylobacter jejuni*, *S. enteritidis*, *E. coli*, *S. aureus* and *L. monocytogenes*. The oils of bay, cinnamon, clove and thyme were the most inhibitory, each having a bacteriostatic concentration of 0.075% or less against all five pathogens. In general, gram-positive bacteria were more sensitive to inhibition by plant essential oils than the gram-negative bacteria. *Campylobacter jejuni* was the most resistant of the bacteria investigated to plant essential oils, with only the oils of bay and thyme having a bacteriocidal concentration of less than 1%. At 35°C, *L. monocytogenes* was extremely sensitive to the oil of nutmeg. A concentration of less than 0.01% was bacteriostatic and 0.05% was bacteriocidal, but when the temperature was reduced to 4°C, the bacteriostatic concentration was increased to 0.5% and the bacteriocidal concentration to greater than 1%.

## **1.8. Conclusion**

Among the many different materials that mankind is currently dependent on; non-biodegradable polymers are arguably still one of the most important considering their widespread usage in food packaging industries. Currently, almost all the non-biodegradable polymers that are widely used in various sectors are produced from petrochemical products. Due to concerns for the global environment and the increasing difficulty in managing solid wastes, biodegradable polymeric materials, bio nanocomposites and bioactive packaging may be among the most suitable alternatives for many applications. Addition of bioactive polymers (alginate, chitosan etc.) or bioactive agents such as, organic acids, essential oils and plant extracts, bacteriocins; can

significantly enhance the quality and safety of food products during storage and can also prevent the growth of microorganism in food. Similarly, CNC based composites due to their excellent mechanical and barrier properties and their role as the carrier of bioactive substances; have great potential in food packaging industries. The field of food packaging represents a promising and exciting field for the use of nanotechnology. Use of nanotechnology in food packaging can not only increase the mechanical and barrier properties of the films but can also increase the safety and shelf life of the packaged food products by allowing a controlled or sustained release of antimicrobials or bioactive agents. However, there has been little study on the combination of NC with bioactive agents to have composite films that will fulfill both the mechanical and antimicrobial properties required for food packaging. So, composites films with both CNC and bioactive agents, represents a promising field of research and should have an enormous impact in food packaging over the coming years.

### **1.9. Acknowledgement**

We thank the Natural Sciences and Engineering Research Council of Canada (NSERC) and FPIInnovation (Pointe-Claire, Canada) for their research support and funding.

### **1.10. References**

- Abe, K., Iwamoto, S., Yano, H. (2007). Obtaining cellulose nanofibers with a uniform width of 15 nm from wood. *Biomacromolecules* **8**:3276–3278.
- Aider, M., (2010). Chitosan application for active bio-based films production and potential in the food industry: Review. *LWT - Food Sci. Technol.* **43**: 837–842.
- Alemdar A, and Sain, M., (2008). Biocomposites from wheat straw nanofibers: morphology, thermal and mechanical properties. *Compos. Sci. Technol.* **68**:557–565.

- Appendini, P., and Hotchkiss, J. H. (2002). Review of antimicrobial food packaging. *Innovative Food Sci. Emerging. Technol.* **3**: 113-126.
- Avella, M., Vlieger, J. J. D., Errico, M. E., Fischer, S., Vacca, P., and Volpe, M. G., (2005). Biodegradable starch/clay nanocomposite films for food packaging applications. *Food Chem.* **93**:467–474.
- Averous L, Boquillon N (2004). Biocomposites based on plasticized starch: thermal and mechanical behaviors. *Carbohydr. Polym.* **56**:111–122.
- Azeredo, H. M.; Mattoso, L. H.; Avena-Bustillos, R. J. A.; Filho, G. C.; Munford, M. L.; Wood, D.; Mchugh, T. H (2010). Nanocellulose reinforced chitosan composite films as affected by nanofiller loading and plasticizer content. *J. Food Sci.* **75**: Nr. 1.
- Beck-Candanedo, S., M. Roman, Gray, D. G., (2005). Effect of reaction conditions on the properties and behavior of wood cellulose nanocrystal suspensions. *Biomacromolecules*, **6**(2): 1048-1054.
- Bhatnagar, A., and Sain, M. (2005). Processing of cellulose nano fiber reinforced composites. *J. Reinf. Plast. Comp.* **24**:1259–1268.
- Bledzki, A.K., Gassan, J. (1999). Composites reinforced with cellulose based fibres. *Prog. Polym. Sci.*, **24**:221–74.
- Bruce, D. M., Hobson, R.N., Farrent, J. W., Hepworth, D. G., (2005). High-performance composites from low-cost plant primary cell walls. *Compos. Part A- Appl. Sci. Manufact.* **36**:1486–1493.
- Cao, X.; Chen, Y.; Chang, P. R.; Muir, A. D.; Falk, G (2008). Starch-based nanocomposites reinforced with flax cellulose nanocrystals. *Polym. Lett.* **2** (7):502–510.

- Cha, D., and Chinnan, M. (2004). Biopolymer-based antimicrobial packaging: a review. *Crit. Rev. Food Sci.* **44**(4):223-237.
- Chandra, R., and Rustgi, R. (1998). Biodegradable polymers. *Prog. Polym. Sci.* **23**: 1273-1335.
- Chen, X. G., Zheng, L., Wang, Z., Lee, C. Y., & Park, H. J., (2002). Molecular affinity and permeability of different molecular weight chitosan membranes. *J. Agric. Food Chem.* **50**(21):5915–5918.
- Coma, V. (2008). Bioactive packaging technologies for extended shelf life of meat-based products. *Meat Sci.* **78**: 90–103.
- Cooksey, K. (2005). Effectiveness of antimicrobial food packaging materials. *Food Addit. Contam.* **22**:980–987.
- Cutter, C. N. (2002). Microbial control by packaging: a review. *Crit. Rev. Food Sci.* **42**:151–161.
- Cutter, C. N. (2006). Opportunities for bio-based packaging technologies to improve the quality and safety of fresh and further processed muscle foods. *Meat Sci.* **74**: 131–142.
- Cutter, C. N., and Siragusa, G. R. (1997). Growth of *Brochothrix thermosphacta* in ground beef following treatments with nisin in calcium alginate gels. *Food Microbiol.* **14**:425–430.
- Cutter, C. N., and Sumner, S. S. (2002). Application of edible coatings on muscle foods. In A. Gennadios (Ed.), *Protein-based films and coatings* (pp. 467–484). Boca Raton, FL: CRC Press.
- Darder, M., Aranda, P., Ruiz-Hitzky, E. (2007). Bionanocomposites: a new concept of ecological, bioinspired, and functional hybrid materials. *Adv Mater.* **19**:1309–1319.

- Devlieghere, F., Vermeiren, L., Bockstal, A., and Debevere, J. (2000). Study on antimicrobial activity of a food packaging material containing potassium sorbate. *Acta Alimentaria* **29**:137–146.
- Dieter-Klemm, D.; Schumann, D.; Kramer, F.; Hessler, N.; Hornung, M.; Schmauder, H. P.; Marsch, S. (2006). Nanocelluloses as innovative polymers in research and application. *Adv. Polym. Sci.* **205**:49–96.
- Dieter-Klemm, D.; Schumann, D.; Kramer, F.; Hessler, N.; Koth, D.; Sultanova, B. (2009). Nanocellulose materials: different cellulose, different functionality. *Macromol. Symp.* **280**: 60–71.
- Ding, B., Kimura, E., Sato, T., Fujita, S., Shiratori, S., (2004). Fabrication of blend biodegradable nanofibrous nonwoven mats via multi-jet electrospinning. *Polym.* **45**:1895–1902.
- Dufresne, A. (1997). Mechanical Behavior of Films Prepared from Sugar Beet Cellulose Microfibrils, *J. Appl. Poly. Sci.* **64**(6): 1185–1194.
- Dufresne, A., Dupeyre, D., Vignon, M.R., (2000). Cellulose microfibrils from potato tuber cells: processing and characterization of starch-cellulose microfibril composites. *J Appl. Polym. Sci.* **76**:2080–2092.
- Dufresne, A., Vignon, M.R., (1998).Improvement of starch film performances using cellulose microfibrils. *Macromolecules* **31**:2693–2696.
- Durango, A. M., Soarres, N. F. F., Benevides, S., Teixeira, J., Carvalho, M., Wobeto, C., and Andrade, N. J. (2006). Development and evaluation of an edible antimicrobial films based on yam starch and chitosan. *Packag. Technol. Sci.* **19**:55–59.

- Dutta, P. K., Tripathi, S., Mehrotra, G. K., and Dutta, J. (2009). Perspectives for chitosan based antimicrobial films in food applications. *Food Chem.* **114**(4):1173–1182.
- Earle, R. D. and McKee, D. H. (1976). US Patent 3,991,218, November 9.
- Fischer, H. R., Gielgens, L. H., and Koster, T. P. M. (1999). Nanocomposites from polymers and layered minerals., *Acta Polymerica* **50**:122-126.
- Fukuda S, Takahashi M, Yuyama M, Oka N (2001) JP Patent 2001293033.
- George, j, Ramana KV, Sabapathy SN, Bawa AS (2005) Physicomechanical properties of chemically treated bacterial (*Acetobacter xylinum*) cellulose membrane. *World J Microb. Biot.* **21**:1323–1327.
- Ghosh, K.G., Srivatsava, A.N., Nirmala, N., and Sharma, T.R. (1977). Development and application of fungistatic wrappers in food preservation. Part II. Wrappers made by coating process. *J. Food Sci. Technol.* **14**:261–264.
- Giannelis, E. P. (1996). Polymer layered silicate nanocomposites. *Adv. Mat.*, **8**(1):29-35.
- Gindl, W., and Keckes, J., (2004). Tensile properties of cellulose acetate butyrate composites reinforced with bacterial cellulose. *Comp. Sci. Technol.* **64**(15): 2407-2413.
- Hammer, K. A., Carson, C.F., and Riley, T.V., (1999). Antimicrobial activity of essential oils and other plant extracts. *J. Appl. Microb.* **86**:985–990.
- Han, J. H., & Floros, J. D. (1997). Casting antimicrobial packaging films and measuring their physical properties and antimicrobial activity. *J. Plast. Film Sheeting*, **13**:287-298.
- Hitzky E.R., Darder, M., Pilar, A., (2005). Functional biopolymer nanocomposites based on layered solids. *J. Mater. Chem.* **15**:3650-3662.
- Imran, M., El-Fahmy, S., Revol-Junelles, A.M., Desobry, S., (2010). Cellulose derivative based active coatings: Effects of nisin and plasticizer on physico-chemical and

- antimicrobial properties of hydroxypropyl methylcellulose films. *Carbohydr. Polym.* **81**(2): 219-225.
- Iwamoto, S., Abe, K., Yano, H., (2008). The effect of hemicelluloses on wood pulp nanofibrillation and nanofiber network characteristics. *Biomacromolecules* **9**:1022–1026.
- Iwamoto, S., Nakagaito, A. N., Yano, H., Nogi, M., (2005). Optically transparent composites reinforced with plant fiber-based nanofibers. *Appl. Phys. A-Mater. Sci. Process.* **81**:1109–1112.
- Janjarasskul, T. and Krochta, J. M., (2010). Edible Packaging Materials. *Annual Rev. Food Sci. Technol.* **1**:415-448.
- Jin, T., and Zhang, H.,(2008). Biodegradable polylactic acid polymer with nisin for use in antimicrobial food packaging. *J. Food Sci.* **73**(3): M127-M134.
- Jo, C., Lee, J. W., Lee, K. H., & Byun, M. W. (2001). Quality properties of pork sausage prepared with water-soluble chitosan oligomer. *Meat Sci.* **59**(4):369–375.
- John, M.J. and Thomas, S., (2008). Biofibres and biocomposites. *Carbohydr. Polym.* **71**: 343–364.
- Khan, A., Huq, T., Saha, M., Khan, R. A., and Khan, M. A., (2010b). Surface modification of calcium alginate fibers with silane and methyl methacrylate monomers. *J. Reinf. Plast. Comp.* **29**(20):3125–3132.
- Khan, A., Huq, T., Saha, M., Khan, R. A., Khan, M. A., and Gofur, M. A. (2010a). Effect silane treatment on the mechanical and interfacial properties of calcium alginate fiber reinforced polypropylene composite. *J. Comp. Mater.*, **24**:2875-2886.

- Khan, R. A., Salmieri, S., Dussault, D., Calderon, J.U., Kamal, M.R., Safrany, A., and Lacroix, M. (2010c). Production and Properties of Nanocellulose Reinforced Methylcellulose-Based Biodegradable Films. *J. Agric. Food Chem.* **58**(13):7878–7885.
- Klemm, D., Philipp, B., Heinze, T., Heinze, U., Wagenknecht, W. (1998). Comprehensive Cellulose Chemistry: Functionalization of Cellulose, Vol. 2; Wiley–VCH Verlag: Weinheim, Germany, 1998; Chapter 4, p.29.
- Kojima, Y., Usuki, A., Kawasumi, M., Okada, A., Fukushima, Y., Kurauchi, T., Kamigaito, O., (1993). Mechanical properties of Nylon 6-clay hybrid. *J. Mater. Res.* **8**(5):1185-1189.
- Kumar, V., (2002). WO Patent 2002022172.
- Kyomori, K., Tadokoro, I., Matsumura, T., (2005). JP Patent 2005126867.
- Lee, S.Y., D. Mohan, D.J., Kang, I.A., Doh, G.H., Lee, S., and Han, S.O., (2009). Nanocellulose Reinforced PVA Composite Films: Effects of Acid Treatment and Filler Loading. *Fibers. Polym.* **10**(1): 77-82.
- Ljungberg, N., Bonini, C., Bortolussi, F., Boisson, C., Heux, L., Cavaille, J. Y. (2005). New Nanocomposite Materials Reinforced with Cellulose Whiskers in Atactic Polypropylene: Effect of Surface and Dispersion Characteristics. *Biomacromolecules* **6** :2732-2739.
- Lönnberg, H., Fogelström, L., Said, M.A., Samir, A., Berglund, L., Malmström, E., Anders Hult, A. (2008). Surface grafting of microfibrillated cellulose with poly( $\epsilon$ -caprolactone) – synthesis and characterization. *European Polym. J.* **44**, 2991–2997.
- Manias, E., Touny, A., Wu, L., Strawhecker, K., Lu, B., and Chung, T.C. (2001). Polypropylene/montmorillonite nanocomposites. Review of the synthetic routes and materials properties. *Chem. Mater.* **13**:3516-3523.

- Masa, S., Alloin, F., Dufresne, A., (2005). Review of recent research into cellulosic whisker, their properties and their application in nanocomposite filed. *Biomacromolecules* **6**: 612-626.
- Ming, X., Weber, G.H., Ayres, J.W., and Sandine, W.E. (1997). Bacteriocins applied to Food packaging materials to inhibit *Listeria monocytogenes* on meats. *J. Food Sci.* **62**(2):413–415.
- Moon, R. J., Martini, A., Nairn, J., Simonsen, J., & Youngblood, J. (2011). Cellulose nanomaterials review: structure, properties and nanocomposites. *Chemical Society Reviews*, *40*, 3941-94.
- Nakagaito, A.N., Yano, H. (2004). The effect of morphological changes from pulp fiber towards nano-scale fibrillated cellulose on the mechanical properties of high-strength plant fiber based composites. *Appl. Phys. A.* **78**:547–552.
- Nakagaito, A.N., Yano, H., (2005) Novel high-strength biocomposites based on microfibrillated cellulose having nanoorder-unit web-like network structure. *Appl. Phys. A.* **80**:155–159.
- Nishino, T., Matsuda, I., Hirao, K., (2004). All-cellulose composite. *Macromolecules* **37**:7683-7687.
- Nogi, M., Abe, K., Handa, K., Nakatsubo, F., Ifuku, S., Yano, H., (2006a). Property enhancement of optically transparent bionanofiber composites by acetylation. *Appl. Phys. Lett.* **89**(23):1–3.

- Nogi, M., Handa, K., Nakagaito, A. N., Yano, H., (2005). Optically transparent bionanofiber composites with low sensitivity to refractive index of the polymer matrix. *Appl. Phys. Lett.* **87**(24):1–3.
- Nogi, M., Ifuku, S., Abe, K., Handa, K., Nakagaito, A.N., Yano, H., (2006b). Fiber-content dependency of the optical transparency and thermal expansion of bacterial nano fiber reinforced composites. *Appl. Phys. Lett.* **88**(13):1–3.
- Nogi, M., Yano, H., (2008). Transparent nanocomposites based on cellulose produced by bacteria offer potential innovation in the electronics device industry. *Adv. Mater.* **20**:1849–1852.
- Nogi, M., Yano, H., (2009). Optically transparent nanofiber sheets by deposition of transparent materials: a concept for rollto- roll processing. *Appl. Phys. Lett.* **94**(23):1–3.
- Ouattara, B., Sabato, S.F., and Lacroix, M. 2001. Combined effect of antimicrobial coating and gamma irradiation on shelf life extension of pre-cooked shrimp (*Penaeus* spp.). *Int. J. Food Microbiol.* **68**:1–9.
- Ouattara, B., Simard, R. E., Piette, G., Begin, A., and Holley, R. A. (2000). Diffusion of acetic and propionic acids from chitosan-based antimicrobial packaging films. *J. Food Sci.* **65**(5):768–773.
- Oussalah, M., Caillet, S., Salmieri, S., Saucier, L. and Lacroix, M. (2007). Antimicrobial effects of alginate-based films containing essential oils on *Listeria monocytogenes* and *Salmonella typhimurium* present in bologna and ham. *J. Food Protec.* **70**(4): 901-908.
- Oussalah, M., Caillet, S., Salmieri, S., Saucier, L. and Lacroix, M. (2004). Antimicrobial and antioxidant effects of milk protein-based film containing essential oils for the preservation of whole beef muscle. *J. Agric. Food Chem.* **52**(18): 5598-5605.

- Ozdemir, M.; Floros, J. D.; (2004). Active Food Packaging Technologies. *Crit. Rev. Food Sci.* 44:185–193.
- Penner, D., and Lagaly, G. (2001). Influence of anions on the rheological properties of clay mineral dispersions. *Appl. Clay Sci.* **19**(1-6):131-142.
- Pereda, M., Amica, G., Rácz, L., Norma E. Marcovich, N.E., (2010). Structure and properties of nanocomposite films based on sodium caseinate and nanocellulose fibers. *J. Food Eng.* **103**(1), 76-83.
- Petersen, K., Nielsen, P. V., Bertelsen, G., Lawther, M., Olsen, M. B., Nilsson, N. H., Mortensen, G. (1999). Potential of biobased materials for food packaging. *Trends Food Sci. Tech.* 10:52-68.
- Quintavalla, S., and Vicini, L. (2002). Antimicrobial food packaging in meat industry. *Meat Sci.* **62**(3) :373–380.
- Ray, S. S.; Okamoto, M.; (2003). Polymer/layered silicate nanocomposites: a review from reinforced with bacterial cellulose. *Comp. Sci. Technol.* **64**:2407-2413.
- Rhim, J.W. (2007). Natural Biopolymer-Based Nanocomposite Films for Packaging Applications. *Crit. Rev. Food Sci. Nutr.* **47**(4):411-433.
- Rhim, J.W., Hong, S.I. (2006). Preparation and characterization of chitosan nanocomposite films with antimicrobial activity. *J. Agric. Food Chem.* **54**(16):5814-5822.
- Sanguansri, P., Augustin, M. A. (2006). Nanoscale Materials Development-A Food Industry Perspective. *Trends Food Sci. Tech.* **17**(10):547-556.
- Scannell, A.G.M., Hill, C., Ross, R.P., Marx, S., Hartmeier, W., and Arendt, K.E. (2000). Development of bioactive food packaging materials using immobilized bacteriocins Lacticin 3147 and Nisaplin. *Int. J. Food Microbiol.* **60**:241–249.

- Seydibeyoglu, M. O., Oksman, K., (2008). Novel nanocomposites based on polyurethane and microfibrillated cellulose. *Compos. Sci. Technol.* **68**:908–914.
- Siro, I., and Plackett, D., (2010). Microfibrillated cellulose and new nanocomposite materials: a review. *Cellulose*, **17**, 459-494.
- Smith-Palmer, A., Stewart, J., and Fyfe, L., (1998). Antimicrobial properties of plant essential oils and essences against five important food-borne pathogens. *Letters in Appl. Microbiol.* **26**:118–122.
- Sorrentino, A., Gorrasi, G., (2007). Potential perspectives of bio-nanocomposites for food packaging applications. *Trends Food Sci. Tech.* **18**(2):84-95.
- Soykeabkaew, N., Arimoto, N., Nishino, T., Peijs, T., (2008). All-cellulose composites by surface selective dissolution of aligned ligno-cellulosic fibres. *Compos. Sci. Technol.* **68**:2201–2207.
- Strawhecker K. E., Manias; E.(2000). Structure and Properties of Poly(vinyl alcohol)/Na<sup>+</sup>Montmorillonite Nanocomposites. *Chem. Mater.* **12**:2943-2949.
- Suzuki, M., Hattori, Y., (2004) WO Patent 2004009902.
- Takahashi, N., Okubo, K. and Fujii, T. (2005). Development of Green Composite using Microfibrillated Cellulose Extracted from Bamboo. *Bamboo J.* **22**: 81–92.
- Tischer, P.C.S.F., Sierakowski, M.R., Westfahl, H.Jr., and Cesar Augusto Tischer, C.A., (2011). Nanostructural Reorganization of Bacterial Cellulose by Ultrasonic Treatment. *Biomacromolecules*, **11**, 1217–1224.
- Turbak, A. F., Snyder, F. W., Sandberg, K. R., (1983). *J. Appl. Polym. Sci. Appl. Polym. Symp.* **37**:815-827.

- Vartiainen, J., Motion, R., Kulonen, K., Ratto, M., Skytta, E., and Advenainen, R. (2004). Chitosan-coated paper: effects of nisin and different acids on the antimicrobial activity. *J. Appl. Polym. Sci.* **94**:986–993.
- Villanueva, M. P., Cabedo, L., Feijoo, J. L., Lagaron, J. M., and Gimenez, E., (2006). Optimization of biodegradable nanocomposites based on a PLA/PCL blends for food packaging applications. *Macromolecular Sympos.* **233**: 191-197.
- Wan W.K., Hutter, J.L., Millon, L.E., Guhados, G., (2006). Bacterial cellulose and its nanocomposites for biomedical applications. In: Oksman K, Sain M (eds) Cellulose nanocomposites. Processing Characterization, and Properties. American Chemical Society, Washington DC.
- Weber, C. J., Haugaard, V., Festersen, R., & Bertelsen, G. (2002). Production and applications of biobased packaging materials for the food industry. *Food Addit. Contam.* **19**:172–177.
- Weng, Y.M., Chen, M.J., and Chen, W., (1999). Antimicrobial Food Packaging Materials from Poly(ethylene-co-methacrylic acid). *Food Sci. Technol.* **32**(4), 191-195.
- Wilhoit, D.L. (1996). Film and method for surface treatment of foodstuffs with antimicrobial compositions. US Patent No. 5,573,79.
- Wilhoit, D.L. (1997). Antimicrobial compositions, film and method for surface treatment of foodstuffs. EU Patent No. EP0 750 853 A2.
- Yamanaka, S., Ishihara, M., and Sugiyama, J., (2000). Structural modification of bacterial cellulose. *Cellulose* **7**:213–225.
- Zimmermann, T., Pohler, E., Geiger, T., (2004). Cellulose fibrils for polymer reinforcement. *Adv. Eng. Mater.* **6**:754–761.

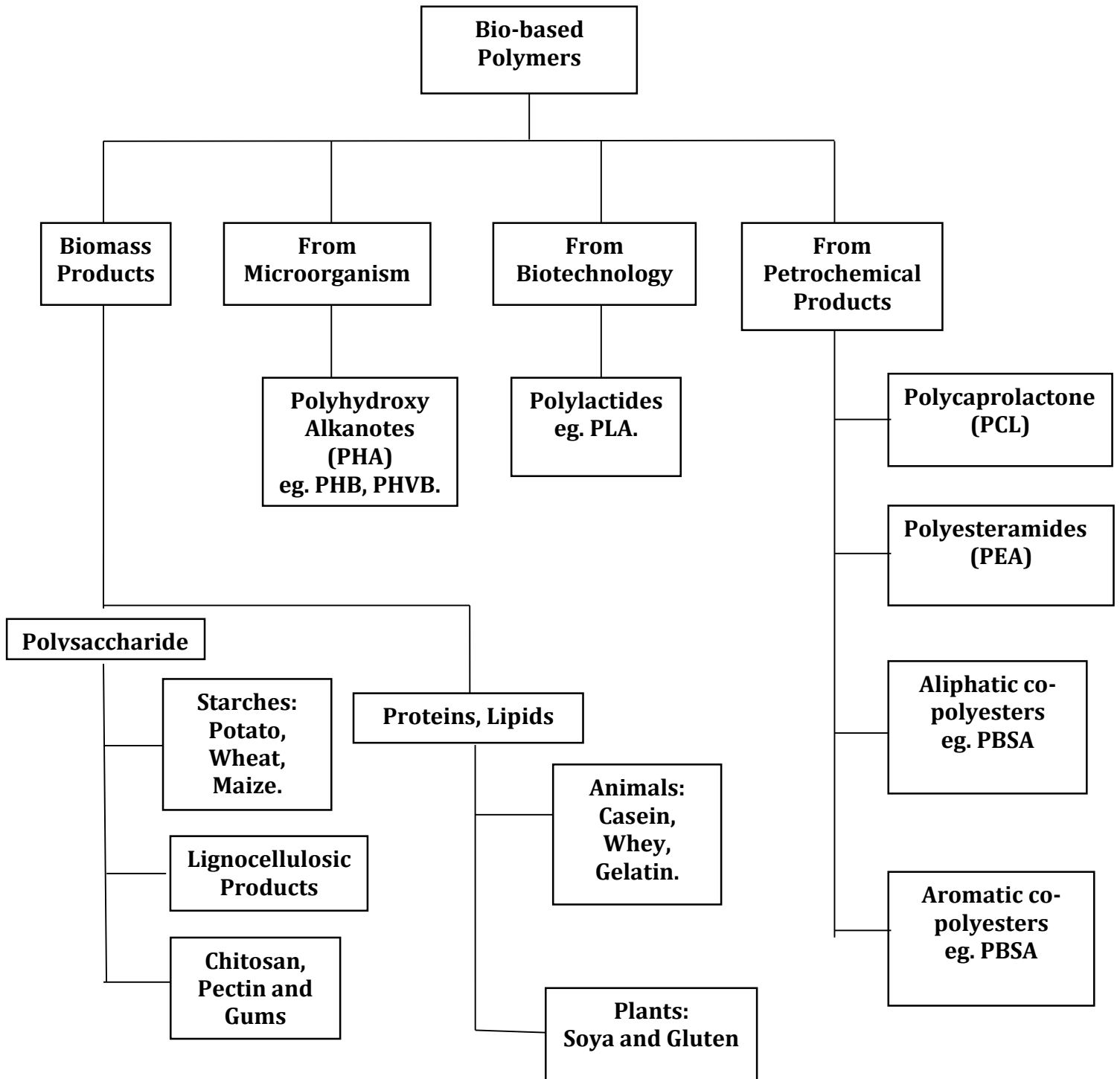


**Figure-1.1:** Classification of biodegradable polymer (adopted from John & Thomas, 2008)

## 1.11 Problematic, Hypothesis and Objectives

### 1.11.1 Problematic

- The packaging materials currently used in food packaging applications are petroleum based synthetic polymers, which are non-biodegradable and harmful to environment. However, the use of bio-based films for food packaging has been strongly limited because of the weak mechanical, poor barrier and water resistance exhibited by natural polymers.
- Direct incorporation of nisin onto meat surface may provide limited efficacy due to the migration of nisin into the bulk food matrix. Also, the activity of nisin may be lost in fresh and RTE meat products due to an interaction and/or inactivation by food components.
- One of the major challenges in the area of nanocomposite is the compatibilization of the nanofiber with the polymer matrix to achieve acceptable dispersion levels of the nanofiber within the polymeric matrix. The electrostatic interactions between CNC and chitosan can lead to aggregation, which would negatively affect the mechanical properties of the nanocomposite films.
- The antimicrobial activity of nisin is generally limited to gram-positive bacteria.

### 1.11.2 Hypothesis

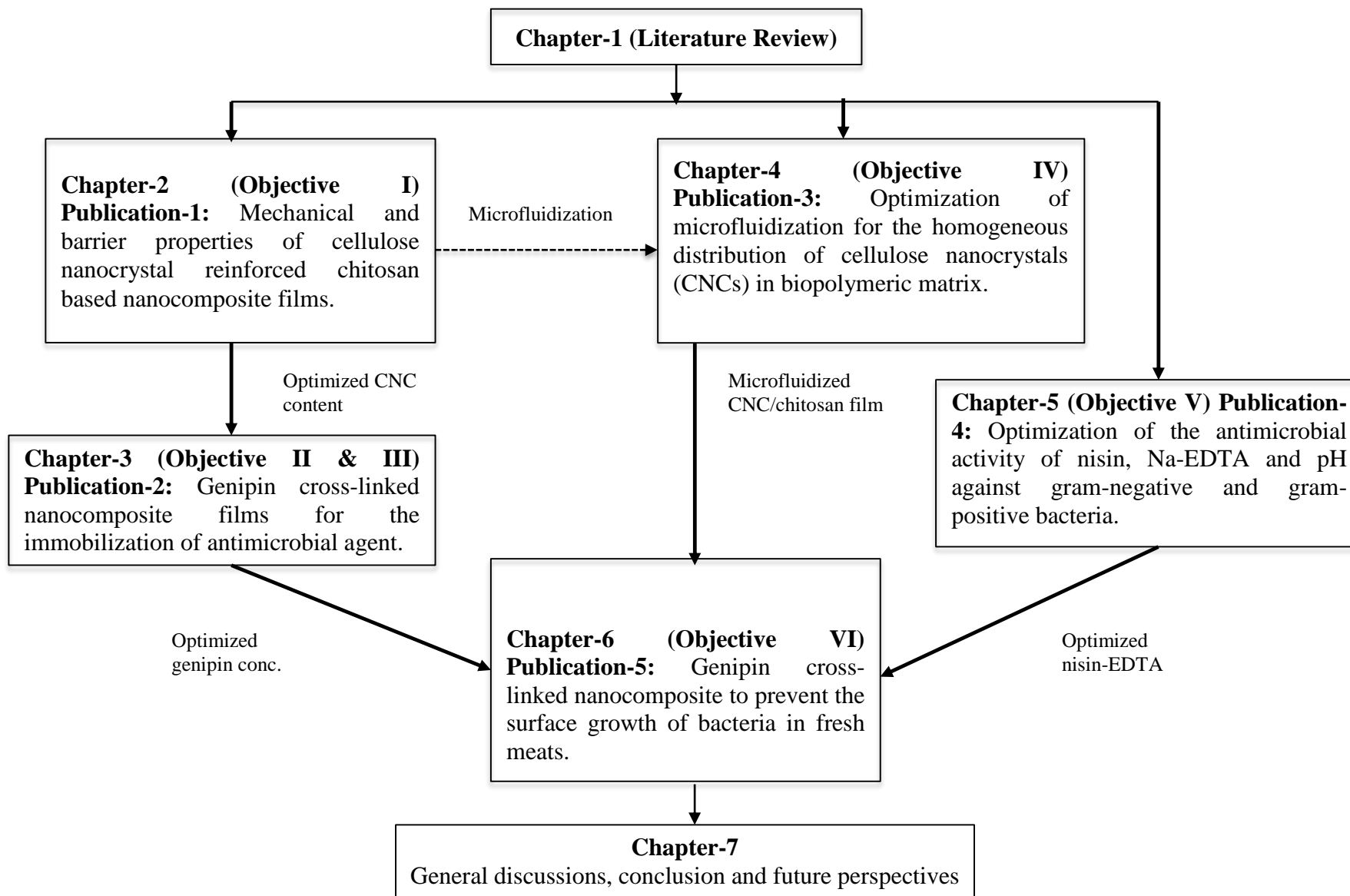
- Incorporation of CNC into the chitosan will produce bio-based nanocomposite films with enhanced mechanical, thermal and barrier properties.
- Immobilization of nisin onto the surface of the developed nanocomposite films will inhibit the growth of pathogenic bacteria in meat products. Genipin cross-linking will protect the antimicrobial activity of nisin during storage and improve the water resistance of the films.
- Microfluidization will lead to the fabrication of high strength nanocomposite films by homogeneously distributing CNC into chitosan matrix.
- Combination of nisin with a chelating agent such as, ethylenediaminetetraacetate (Disodium EDTA) will improve the antimicrobial activity of nisin against a broad spectrum of bacteria.

### 1.11.3 Objectives

- I. To verify the impact of CNC on the physico-chemical properties of the chitosan films by measuring the mechanical properties (tensile strength, tensile modulus and elongation at break%) and barrier properties (water vapour permeability, swelling) of the films. Spectroscopic analysis (FTIR), thermal analysis (TGA) and morphological characterization (scanning electron microscopy, SEM) of the films were also performed.
- II. To develop antimicrobial nanocomposite films by introducing nisin as an antimicrobial agent and evaluate the antimicrobial activity of the films *in situ* in a Ready-To-Eat (RTE) meat (ham) system against *L. monocytogenes*.

- III. To cross-link the nanocomposite films by adding a cross-linking agent genipin and to evaluate the effect of cross-linking through measurement of mechanical properties, water resistance, FT-IR spectral analysis, *in vitro* analysis (disk diffusion assay) and *in situ* (RTE ham against *L. monocytogenes*) analysis.
- IV. To develop microfluidization process for the homogeneous distribution of CNC by adopting Response surface methodology (RSM) and measuring the mechanical properties; investigating the surface morphology (SEM; atomic force microscopy, AFM) of the films.
- V. To develop novel antimicrobial formulation by testing different nisin; disodium ethylenediaminetetraacetate ratio in a broad pH range against selected gram-negative (*E. coli* and *S. typhimurium*) and gram-positive (*L. monocytogenes*) bacteria by agar diffusion assay.
- VI. To examine the possible synergy between cross-linked antimicrobial nanocomposite films with a cold pasteurization (gamma irradiation) to eliminate the growth of pathogenic and non-pathogenic bacteria on raw meat.

### 1.11.4 Simplified Organogram for the PhD Thesis



## **CHAPTER 2**

### **Publication 1**

# Mechanical and barrier properties of cellulose nanocrystal reinforced chitosan based nanocomposite films

Avik Khan<sup>1</sup>, Ruhul A. Khan<sup>1</sup>, Stephane Salmieri<sup>1</sup>, Canh Le Tien<sup>1</sup>,  
Bernard Riedl<sup>2</sup>, Jean Bouchard<sup>3</sup>, Gregory Chauve<sup>3</sup>, Victor Tan<sup>4</sup>, Musa R. Kamal<sup>4</sup> and Monique  
Lacroix<sup>1\*</sup>

<sup>1</sup>Research Laboratories in Sciences Applied to Food, Canadian Irradiation Centre (CIC),  
INRS-Institut Armand-Frappier, Université du Québec, 531 Boulevard des Prairies,  
Laval, Québec, H7V 1B7, Canada

<sup>2</sup>Département des sciences du bois et de la forêt, Faculté de foresterie, géographie et géomatique,  
Université Laval, Québec-city, Québec, G1V 0A6, Canada

<sup>3</sup>FPIinnovations, 570 Boulevard St. Jean, Pointe-Claire, Québec, H9R 3J9, Canada

<sup>4</sup>Department of Chemical Engineering, McGill University, 3610 University Street, Montreal, QC  
H3A 2B2, Canada

**KEYWORDS:** Chitosan, Cellulose Nanocrystal, Biodegradable, Nanocomposite films,  
Mechanical properties, Barrier Properties

\* **Corresponding Author:** Prof. Monique Lacroix.

Telephone: +1-450-687-5010; Fax: +1-450-686-5501.

**E-mail:** [monique.lacroix@iaf.inrs.ca](mailto:monique.lacroix@iaf.inrs.ca)

This article has been published in *Carbohydrate Polymers* (2012) 90:1601– 1608.

## **2.1. Contribution of the authors**

Most of the experimental works were planned, performed and analyzed by Avik Khan with guidance from Prof. Monique Lacroix. The manuscript was written by Avik Khan. Prof. Monique Lacroix and Prof. Bernard Riedl corrected the main draft. Stephane Salmieri helped to improve the discussion for FTIR analysis. Dr. Gregory Chauve corrected the main draft and gave valuable suggestions to improve the discussion. Dr. Ruhul A. Khan, Dr. Jean Bouchard and Dr. Le Tien Canh also corrected the main draft. Dr. Victor Tan performed the thermal and XRD analysis with supervision from Prof. Musa Kamal. Both Avik Khan and Prof. Monique Lacroix replied to the reviewers' comments and corrected the manuscript.

## **2.2. Specific objectives of the Publication-1**

It was necessary to optimize the CNC concentration for the current study, as the optimum CNC concentration reported in the literature seems to vary from one study to another. Chitosan was chosen as the polymer matrix. CNC reinforced chitosan films, containing 0 to 10% w/w of CNC were fabricated by casting method. The mechanical and barrier properties of the films were measured in order to optimize the CNC concentration in the films. The films were also characterized by FTIR, TGA, XRD and SEM analysis.

### **2.3. Résumé**

Des films biodégradables à base de chitosan, renforcés de nanocellulose cristalline (CNC) ont été préparés à partir de solutions. Le contenu en CNC dans les films a été varié de 1-10% (en poids sec). Il a été constaté que la résistance à la traction (TS) des films nanocomposites avec 5% w/w teneur CNC était optimale avec une amélioration de 26% par rapport aux films de chitosane de base. L'incorporation de CNC a aussi considérablement amélioré les propriétés barrière, alors que la perméabilité à la vapeur d'eau (PVE) des films de chitosan /CNC a été diminuée de 27% pour un contenu de CNC de 5 % pds/pds. L'étude a révélé une diminution de l'absorption d'eau des films de chitosane renforcés de CNC. Les analyses des propriétés thermiques n'ont montré aucun effet significatif de la CNC alors que les études de diffraction des rayons X ont confirmé l'apparition de pics cristallins dans les films nanocomposites. La morphologie de surface des films a été étudiée par microscopie électronique à balayage et il a été démontré que la CNC a été dispersée de façon homogène dans la matrice de chitosane.

## **2.4. Abstract**

Cellulose nanocrystal (CNC) reinforced chitosan-based biodegradable films were prepared by solution casting. The CNC content in the films was varied from 1-10% (dry wt. basis). It was found that the tensile strength (TS) of the nanocomposite films with 5% w/w CNC content was optimum with an improvement of 26% compared to the control chitosan films. Incorporation of CNC also significantly improved barrier properties. Water vapor permeability (WVP) of the chitosan/CNC films was decreased by 27% for the optimum 5% w/w CNC content. Swelling study revealed a decrease in water uptake of the CNC-reinforced chitosan films. Analyses of thermal properties showed no significant effect of CNC whereas X-ray diffraction studies confirmed the appearance of crystalline peaks in the nanocomposite films. Surface morphology of the films was investigated by scanning electron microscopy and it was found that CNC was dispersed homogenously into chitosan matrix.

## 2.5. Introduction

Global environmental concern, regarding the use of non-biodegradable petroleum-based packaging materials, has been encouraging researchers, industries and governments in the quest for alternative materials made from natural biopolymers. Bio-based packaging is made from raw materials originating from natural sources, such as starch, cellulose, chitin or biodegradable synthetic polymers such as, polycaprolactone, polylactic acid (Arumugam *et al.*, 1989; Le Tien *et al.*, 2000; Ciesla *et al.*, 2006; Chandra and Rustgi, 1998). Despite great improvements, the use of natural polymers made biodegradable films for food packaging has been strongly limited because of the poor barrier properties and weak mechanical properties (Rhim and Perry, 2007). For these reasons natural polymers were either blended with other synthetic polymers or chemically modified to enhance these features (Giannelis, 1996; Weber *et al.*, 2002; Khan *et al.*, 2010a). Some of the limited mechanical and barrier properties (water vapor and oxygen permeability, etc.) of biopolymers can be significantly enhanced by the use of reinforcing fillers to create nanocomposite films. Nanocomposite films extend the food shelf-life, and also improve food quality as they can serve as carriers of some active substances, such as antioxidants and antimicrobials (Sorrentino and Gorrasi, 2007).

Chitosan, a natural linear polysaccharide consisting of 1,4-linked 2-amino-deoxy- $\beta$ -D-glucan, is a partially deacetylated derivative of chitin, the second most abundant natural polysaccharide after cellulose. Chitosan is non-toxic, biodegradable, biofunctional, biocompatible and was reported by several researchers to have strong antimicrobial and antifungal activities (Darmadji, and Izumim, 1994; Kim *et al.*, 2011; No *et al.*, 2007; Rabea *et al.*, 2003). Chitosan films have been successfully used as a packaging material for the quality of preservation of foods (Jo *et al.*, 2001).

Cellulose, another natural linear carbohydrate polymer chain consisting of D-glucopyranose units joined together by  $\beta$ -1,4-glycosidic linkages, is the most abundant biopolymer and can be found in wood, cotton, hemp among other sources. From cellulosic sources can be extracted cellulose nanocrystals, also called cellulose nanocrystal (CNC) after the cellulose fibers are digested by a controlled acid hydrolysis process. CNC is a highly crystalline nanometer sized rod-like particle that is obtained as a stable aqueous colloidal suspension. This CNC was extracted from softwood bleached kraft pulp with an acid hydrolysis process inspired from the literature (Beck-Candanedo *et al.*, 2005). This type of CNC was found to exhibit an average length of 110 nm long for a 5-10 nm width (Revol *et al.*, 1992). The use of sulfuric acid in the hydrolysis process, leads to a more stable dispersion than the one using hydrochloric acid due to the grafting of sulfate groups on the surface of the CNC that stabilizes the CNC suspensions by electrostatic repulsion (Beck-Candanedo *et al.*, 2005). CNC was evidenced to reinforce polymers due to the formation of a percolation network that connects the well-dispersed CNC by hydrogen bonds (Favier *et al.*, 1995). It was evidenced that the presence of CNC reinforcing fillers in the polymer matrix provides superior performances such as mechanical properties, barrier properties to the next generation of biodegradable materials (Dieter-Klemm *et al.*, 2009; Azeredo *et al.*, 2010; Cao *et al.*, 2008).

The objective of the present research was to evaluate the effect of CNC incorporation on the mechanical, barrier, thermal and structural properties of chitosan-based biodegradable films. The mechanical properties of the films were measured to evaluate the films tensile strength (TS), tensile modulus (TM), and elongation at break (Eb). The barrier properties of the films were investigated by carrying out water vapor permeability tests and swelling properties were monitored by the water uptake of the nanocomposite films. Fourier Transform Infrared

Spectroscopy (FTIR) was used to analyze the interaction between chitosan and CNC. Surface morphology of the CNC reinforced chitosan films was investigated by scanning electron microscopy (SEM).

## **2.6. Materials and methods**

### **2.6.1 Materials**

Chitosan (High mol. weight, degree of deacetylation: 88-89%) was purchased from Kitomer Biotech (Rivière-au-Renard, QC, Canada). CNC (prepared as a dry redispersible powder in water) was produced in the FPInnovations pilot plant CNC reactor (Pointe-Claire, QC, Canada) from a commercial bleached softwood kraft pulp according to a procedure modified from the literature (Dong et al., 1998).

### **2.6.2. Film preparation**

Chitosan (1%, w/v) was dissolved in 2% aqueous acetic acid solution. Dilute aqueous CNC suspension (0.1%, w/w) was prepared by dispersing the CNC powder in distilled water for 3h, under vigorous magnetic stirring at room temperature, followed by ultra-sonication in a water bath for 30 min. The CNC suspension (1-10% w/w in the dry chitosan-based nanocomposite film) was mixed to the chitosan solution and homogenized at 23,000 rpm for 2 min with a high shear mixer (IKA T25 digital Ultra-Turrax disperser, IKA Works Inc., Wilmington, NC, USA). Films were then cast by applying 10 mL of the CNC/chitosan suspension onto Petri dishes (100mm×15mm) and air-dried for 24 h, at room temperature at 35% relative humidity (RH). Dried nanocomposite films were peeled off from the Petri dishes and stored in polyethylene bags at 35% RH prior to characterization. The thickness of the films was ~20 µm. Pure CNC films were prepared by casting from a 1% CNC suspension.

### **2.6.3. Mechanical properties of the films**

Tensile strength (TS), tensile modulus (TM) and elongation at break (Eb) of the films were measured by using Universal Testing Machine (model H5KT, with a 1KN load cell, Tinius-Olsen, Horsham, USA). The samples were cut using ASTM procedure D 638-99 and the film thickness was measured using a Mitutoyo Digimatic Indicator (Type ID-110E; Mitutoyo Manufacturing Co. Ltd., Tokyo, Japan) at five random positions around the film.

### **2.6.4. Water vapor permeability test**

The WVP test was conducted gravimetrically using ASTM procedure 15.09:E96. Films were mechanically sealed onto Vapometer cells (No. 68-1, Twining-Albert Instrument Co., West Berlin, NJ, USA) containing 30 g of anhydrous calcium chloride to create a 0% RH storage condition. The cells were initially weighed and placed in a Shellab 9010 L controlled humidity chamber (Sheldon Manufacturing Inc., Cornelius, OR, USA) maintained at 25°C and 60% RH for 24 h, then the amount of water vapor transferred through the film and absorbed by the desiccant was determined from the weight gain of the cell. The assemblies were weighed initially and after 24 h for all samples. WVP is calculated according to the combined Fick and Henry's laws for gas diffusion through films as follows:

$$\text{WVP (g.mm/m}^2\text{.day.kPa)} = x\Delta w/A\Delta P$$

where  $\Delta w$  is the weight gain of the cell (g) after 24 h,  $x$  is the film thickness (mm),  $A$  is the area of exposed film ( $31.67 \times 10^{-4} \text{ m}^2$ ), and  $\Delta P$  is the differential vapor pressure of water through the film ( $\Delta P = 3.282 \text{ kPa}$  at 25°C). WVP is expressed in g. mm/m<sup>2</sup>.day.kPa.

### **2.6.5. Gel swelling property**

The test samples were first dried at 37°C for 12hr in an incubator and then accurately weighed. The dried films were then immersed in distilled water for 1-8 h. The wet weight of the films was measured by taking out the films from the water and blotting with a filter paper to remove the surface adsorbed water followed by immediately weighing the films (Jin et al., 2004). The water uptake or swelling property of the films was calculated by the following equation:

$$S = [(W_s - W_d) / W_d] \times 100$$

where, S is the percentage of water absorption of the films at equilibrium;  $W_s$  and  $W_d$  are the weights (in g) of the samples in the dry and swollen states, respectively.

### **2.6.6. Fourier transform infrared spectroscopy (FTIR)**

The FTIR spectra of the films were recorded using a Spectrum One spectrophotometer (Perkin-Elmer, Woodbridge, ON, Canada) equipped with an attenuated total reflectance (ATR) device for solids analysis and a high-linearity lithium tantalate detector. Spectra were analyzed using Spectrum 6.3.5 software. Films were stored at room temperature for 72 h in a desiccator containing saturated NaBr solution to ensure a stabilized atmosphere of 59% RH at 23°C. Films were then placed onto a zinc selenide crystal, and the analysis was performed within the spectral region of 650-4000  $\text{cm}^{-1}$  with 64 scans recorded at a 4  $\text{cm}^{-1}$  resolution. After attenuation of total reflectance and baseline correction, spectra were normalized with a limit ordinate of 1.5 absorbance units.

### **2.6.7. Thermo gravimetric analysis (TGA)**

Thermogravimetric analysis of the films was carried out using a TGA 7 (Perkin Elmer, CA, USA) analyser. Experiments were carried out under nitrogen atmosphere (40  $\text{cmL}\cdot\text{min}^{-1}$ ). The

weight of the film samples varied from 6-8 mg, scanning range was maintained to 50–600° C and the heating rate was 10° C.min<sup>-1</sup>.

#### **2.6.8. X-ray diffraction (XRD)**

For XRD analysis, film samples were folded several times to increase the sample thickness. Samples were analyzed between  $2\theta = 5^\circ$  and  $30^\circ$  with step increment  $2\theta = 0.02^\circ$  in a D8 Discover X-ray Diffractometer (Bruker AXS Inc., Madison, MI, USA) using a Cu K $\alpha$  (40 kV/35 mA).

#### **2.6.9. Scanning electron microscopy (SEM)**

Film samples were prepared by dropping in liquid nitrogen a 5×5 mm<sup>2</sup> sample piece that was previously cut from the center of the sample film. The sample piece was allowed to equilibrate in the liquid nitrogen prior to being fractured with a prechilled razor blade held in a vice grip. The samples were deposited on an aluminum holder and sputtered with gold/palladium alloy (deposition rate of 30 s equivalent to coating thickness of approximately 50 Å) in a Hummer IV sputter coater (Anatech Ltd, Alexandria, VA). SEM photographs were taken with a Hitachi S-4700 FEG-SEM (Hitachi Canada Ltd., Mississauga, ON, Canada) at a magnification of 40000×, at room temperature. The microscope was equipped with an X-ray detector model 7200 (Oxford Instruments) with a resolution of 1.36 eV at 5.9 keV.

#### **2.6.10. Statistical analysis**

An analysis of variance (ANOVA) and multiple comparison tests of Duncan's were used to compare all the results. Differences between means were considered significant when the confidence interval is smaller than 5% ( $P \leq 0.05$ ). The analysis was performed by the PASW Statistics 18 software (SPSS Inc., Chicago, IL, USA).

## 2.7. Results and discussion

### 2.7.1. Mechanical properties of the CNC reinforced chitosan-based films

The effect on the tensile strength of CNC incorporated in chitosan-based films was observed as a function of the CNC loading ranging between 1 to 10% w/w of the final dry weight of the film (**Figure 2.1a**). The TS of pure chitosan films was found to be 79 MPa and the reinforced films with addition of 1, 3, 5 and 10% w/w CNC increased the TS values up to 86, 92, 99 and 98 MPa respectively ( $P \leq 0.05$ ). The increase corresponds to a gain in TS of 8.8, 16.5, 25.3 and 24% compared to the control sample respectively. It turns out that the optimum CNC loading to get the best TS value ranges between 3-5 % w/w after which the TS value tends to plateau. The increase in the TS values of the CNC-reinforced chitosan films can be attributed to two factors such as, 1) the favorable nanocrystal-polymer interactions and 2) the reinforcing effect occurred through effective stress transfer at the nanocrystal-polymer interface. The interaction between the anionic sulfate groups of CNC to the cationic amine groups of chitosan might favor a good interface between the matrix and the filler. This may lead to high TS values of the nanocomposite films (De Mesquita *et al.*, 2010). On the other hand, a mean field mechanical model may be adopted to explain the reinforcing effect of CNC observed in the current study. The mean-field model is based on the concept that the nanocrystals are homogeneously dispersed in the polymer matrix, but there is no interaction between the nanocrystals (Favier *et al.*, 1995). The high mechanical strength of the nanocomposite films may result from efficient load transfer to the nanocrystal network, leading to more uniform stress distribution and minimization of the stress concentration area (Kanagaraj *et al.*, 2007). Beyond 5% w/w CNC, the TS values plateau suggesting that the addition of more CNC above this threshold concentration does not help to improve the TS. The reason for the value to plateau may be due to the potential aggregation of CNC particles after a certain concentration is reached, which results in no further improvement

of mechanical properties. Li *et al.* (2009) reported excellent reinforcing properties of the cellulose nanocrystals and obtained almost a 41% increase in the TS of the chitosan films due to the incorporation of 15-20% w/w nanocrystals. The cellulose nanocrystal length and width reported in this manuscript was 400 nm in length and 24 nm in width, which is almost 4 times longer than the CNC used in the current study. This could be the reason why such a high nanocrystal loading (15-20% w/w) was required to reach the percolation threshold and reinforce chitosan. Jalal Uddin *et al.* (2011) reported the fabrication of polyvinyl alcohol (PVOH) nanocomposites reinforced with varying concentrations of cellulosic nanocrystals (0-30% w/w) and have found that 5% w/w nanocrystal concentration is the optimum in terms of mechanical strength. Incorporation of cellulose nanocrystals also improved the mechanical strength of alginate nanocomposite fibers (Ureña-Benavides *et al.*, 2010). **Figure 2.1b** shows the effect of the CNC content on the TM and Eb (%) of CNC-reinforced chitosan films. The TM value of the pure chitosan film was found to be 1590 MPa. The incorporation of 1% CNC caused a significant ( $P \leq 0.05$ ) increase of TM (2264 MPa), which is an increase of more than 43% than the control chitosan films. At 5% CNC content, the TM value was found to be 2971 MPa, which corresponds to an increase of 87% compared to pure chitosan films. After 5%, the TM values of the films reach a plateau similar to the TS values as reported above. Filler-reinforced films usually tend to become more brittle as the concentration of the reinforcing particles increases (Lee *et al.*, 2004; Rhim, 2011; Cyrs *et al.*, 2008). This behavior is also common for nanocomposite films. The increased TM values of the CNC reinforced chitosan films may be attributed to the increased stiffness of the films by the addition of CNC. Ureña-Benavides *et al.* (2010) reported 123% increase in the TM of the calcium alginate fibers due to the incorporation of 10% (w/w) cellulose nanocrystals. Azeredo *et al.* (2009) and Jalal Uddin *et al.* (2011) have

also reported an increase of TM values due to the addition of cellulose nanocrystals. Thus, CNC particles acted as a good reinforcing agent in chitosan films. The Eb value was found to be 8.58% for the pure chitosan film and 6.28, 4.87, 3.98 and 3.95 for 1, 3, 5 and 10% (w/w) of CNC addition respectively. After 5% CNC incorporation, the Eb values tend to a plateau, which follows the similar trend as the TM values. Li *et al.* (2009) also observed a decrease in the Eb values of chitosan films from 20 to 6% due to the incorporation of cellulose nanocrystals. Such a decreased in Eb values indicated that the incorporation of CNC into the chitosan matrix could result in strong interactions between filler and matrix, which restricted the motion of the matrix and hence decreased Eb (Azeredo *et al.*, 2010; Aziz Samir *et al.*, 2004).

### **2.7.2. Water vapor permeability**

The effect of CNC concentration on the WVP of the chitosan films is illustrated in **Figure 2.2**. The values of WVP decreased with the increase in CNC content, from 3.31 g·mm/m<sup>2</sup>·day·kPa for the pure chitosan film down to 2.23 g·mm/m<sup>2</sup>·day·kPa for the 10% loading of CNC. It is clearly observed that CNC had a great impact on the reduction of WVP values of chitosan-based films. The presence of cellulose nanocrystals is thought to increase the tortuosity in the chitosan films leading to slower water vapor diffusion processes and hence, to a lower permeability (Azeredo *et al.*, 2010). Water vapor more favorably diffuses through the amorphous areas of the polymer matrix, so the degree of crystallinity is also of importance in the permeability behavior of the nanocomposite (Rhim *et al.*, 2006). Azeredo *et al.* (2009) reported that the WVP of mango puree films improved significantly with the addition of cellulose nanocrystals. Paralikar *et al.* (2006) have also reported reduction in the WVP of PVOH films due to the addition of 10% (w/w) cellulose nanocrystals

### 2.7.3. Gel swelling property

**Figure 2.3** illustrates the effect of CNC incorporation on the swelling percentages that corresponds to the water uptake of chitosan films. Presence of CNC significantly reduced the swelling percentage (S), of chitosan films. After 1 h, the S value of the pure chitosan films increased to 195%, whereas the S values of the nanocomposite films were only 123 and 108%, for 5 and 10% CNC, respectively. It was also observed that the S values of the CNC reinforced nanocomposite films (10% CNC) decreased again by 20% after 8 h of immersion in water as compared to the control chitosan film. In the above paragraph, it is reported that WVP of chitosan films were reduced because of the addition of CNC in chitosan films, which is in agreement with a decrease in the water uptake of CNC-containing chitosan films. Water uptake of the nanocomposite films depends on the nature of the matrix and filler. This phenomenon of decreased water uptake at equilibrium can be ascribed to the fact that highly crystalline CNC is less hydrophilic than chitosan and the formation of strong filler-matrix interactions (Li *et al.*, 2009, Dufresne *et al.*, 2000). In the current study, the cellulose nanocrystals acted as an interpenetrated network within the matrix and prevented the swelling of the chitosan films when exposed to water. Dufresne *et al.* (2000) and Svagan *et al.* (2009) have also reported similar decrease in water uptake of the nanocomposite films due to the addition of cellulose nanocrystals.

### 2.7.4. Fourier transform infrared spectroscopy

FTIR analysis attempted to characterize the effect of CNC incorporation on the chitosan films and to determine the infrared bands and shifts related to CNC-chitosan interactions. The position of the peaks of chitosan film spectrum is similar to those described by different authors (Chen *et al.*, 2003; Sionkowska *et al.*, 2004; Wu *et al.*, 2005; Cao *et al.*, 2007). The absorption peaks of the chitosan films (**Figure 2.4a**) are mainly assignable to the stretching of intra- and

intermolecular O–H and –CH<sub>2</sub>OH vibrations at 3500-3250, overlapped with stretching –NH<sub>2</sub> (3500-3400 cm<sup>-1</sup>) and –NH secondary amides vibrations (3300-3280 cm<sup>-1</sup>). Also 2960-2870 cm<sup>-1</sup> corresponds to symmetric and asymmetric C–H vibrations. Amide I vibrational mode at 1633 cm<sup>-1</sup> and Amide II at 1538 cm<sup>-1</sup> have also been observed. In the FTIR spectra of pure CNC films the broad absorption band between 3600-3200 cm<sup>-1</sup> was related to the O-H stretching vibrations (**Figure 2.4b**). The sharp peak recorded at 3337 cm<sup>-1</sup> might be attributed to the O-H vibrations due to intramolecular hydrogen bonding (Li and Rennekar, 2011). The absorption bands between 3000-2800 cm<sup>-1</sup> and 1500-1250 cm<sup>-1</sup> originated from the C-H and C-H<sub>2</sub> stretching and bending vibrations, respectively (Wang and Roman, 2011; Nikonenko *et al.*, 2000). The absorption band at 1160 is related to C-O-C stretching motion. The strongest bands across CNC spectra at 1054 and 1032 cm<sup>-1</sup> are assigned to C-O stretching at C-3 position. Other bands between 800-650 cm<sup>-1</sup> originated from O-H out of plane bending vibrations (Nikonenko *et al.*, 2005; Kondo and Sawatari, 1996). Now due to the incorporation of 5% CNC to the chitosan matrix, some differences can be observed in the FTIR spectra of chitosan films (**Figure 2.4c**). A sharp peak appeared at 3342 cm<sup>-1</sup>, which was not present in the control chitosan films. Also the intensity of the band 3342 cm<sup>-1</sup> increased suggesting occurrence of hydrogen bonding between chitosan and CNC (Khan *et al.*, 2010b). Other bands at 1538 and 1340 cm<sup>-1</sup> had their intensity increased after CNC addition. Moreover, there was a drastic increase in the intensity of the absorption bands at 1054 and 1032 cm<sup>-1</sup> due to CNC incorporation. However, other changes introduced by the addition of CNC are minor, as expected from the low amount of CNC incorporated (5% w/w) to make the composite films.

### 2.7.5. Thermal property of the films

TGA curves for the films were represented in **Figure 2.5**. CNC films were very stable during the heating range 50 to 275°C, losing only 4.2% of its initial weight. The weight loss for the chitosan, chitosan with 5 and 10% CNC were 26.7, 27.6 and 27.8%, respectively. For all the films a major weight loss was found at around 280°C which is associated to fast volatilization of polymer segments due to thermal scission of the polymer backbone. All chitosan samples (control, chitosan with 5% and 10% CNC films) displayed a similar thermal behaviour at the temperature range 280-460°C and the influence of CNC on the thermal stability was found to be negligible. So, apart from a small increase in the heat flow, the effect of CNC addition in the thermal property of the chitosan films was not significant.

### 2.7.6. X-ray diffraction (XRD)

Structural analysis of chitosan films and CNC containing chitosan films was investigated by XRD. **Figure 2.6** represents the diffractograms of the pure chitosan film and the CNC reinforced chitosan films. The diffractogram of CNC films exhibited crystalline peaks at  $2\theta = 16.8^\circ$  and  $20-22.4^\circ$ . The observed peaks may be due to the 110 and 220 planes of cellulose I, respectively. Shin *et al.* (2007) also reported that characteristic peaks for cellulose I were in the range of  $2\theta = 14.50, 16.65$  and  $22.80^\circ$ . Chitosan films showed characteristics sharp peak at around  $2\theta = 13^\circ$  and a broad halo at  $2\theta = 20-23^\circ$ . The sharp peak at  $2\theta = 13^\circ$  indicated a hydrated crystalline structure, whereas the broad halo indicated an amorphous structure of chitosan (Ogawa *et al.*, 1994; Wang *et al.*, 2005). Due to the incorporation of CNC into chitosan, an increase in peak intensity at  $2\theta = 13^\circ$  was observed. Also, the characteristic broad halo of amorphous chitosan at  $2\theta = 20-23^\circ$  super-positioned with the sharp peak of CNC at  $2\theta = 22^\circ$ . A sharp peak at  $2\theta = 25^\circ$  was observed for the chitosan samples with 5% CNC content sample. This diffractograms suggested that CNC reinforced chitosan films exhibited a combination of amorphous and

crystalline peaks (Bodin *et al.*, 2007). The increase of peak intensity of the chitosan films may result from the transcrystallization effect. Transcrystallization can be defined as orientation of crystals of a semicrystalline matrix perpendicularly to the cellulose nanocrystals (Helbert and Chanzy, 1994). Gray (2008) reported crystallization of polymer matrix preferentially nucleated by cellulose nanocrystals, leading to a transcrystalline layer around the nanocrystals. The improvement of barrier properties of CNC-reinforced chitosan films might be attributed to the presence of crystalline regions in the films. The higher the degree of crystallinity, the lower the permeability of the films (Rhim *et al.*, 2006). Finally, XRD supported both the mechanical and barrier properties improvement of chitosan films due to the addition of CNC.

#### **2.7.7. Surface morphology of the films**

Scanning electron microscopy (SEM) was employed for morphological inspection of the films. SEM reveals the homogeneity of the composite, the presence of voids, the dispersion level of the nanoparticles within the continuous matrix, the presence of aggregates and the possible orientation of nanoparticles. **Figure 2.7** represents SEM micrographs of the fractured surface of the a) CNC, b) chitosan, c) chitosan with 5% and d) 10% CNC films. The surface of the chitosan films (**Fig. 2.7b**) was found quite smooth which indicated better film homogenization of chitosan in aqueous media. By comparing the micrographs of chitosan (control) to that of the nanocomposite films, cellulose nanocrystals appeared like white dots in the chitosan with 5% and 10% CNC films. These shiny dots could correspond to the transversal sections of the cellulose nanocrystals (Azizi Samir *et al.*, 2005). Nanocomposite films with 5% CNC content (**Figure 2.7c**) exhibited a homogeneous and dense structure, indicating a proper dispersion of CNC into chitosan matrix. The improved mechanical properties of the nanocomposite films with 5% CNC content can be attributed to this homogeneous structure of the films. However, the surface became rougher with the increase in CNC content (**Figure 2.7d**) and aggregation of CNC

can be observed. An increase in the concentration of white dots was also observed. Azizi Samir *et al.* (2005) also reported the concentration of the white dots is a direct function of the cellulose nanocrystal composition in the composite. **Figure 2.8** represents SEM micrographs of the fractured cross-section of a) CNC, b) chitosan, c) chitosan with 5% and d) 10% CNC films. It is clear that addition of CNC caused changes in the film microstructure, since the non-reinforced films (**Figure 2.8b**) exhibited a smooth surface with few cracks, as expected for a homogeneous material. Addition of 5% CNC did not affect the microstructure of the chitosan films adversely (**Figure 2.8c**) and no bubbles or roughness appeared due to the addition of CNC. On the contrary, addition of 10% CNC (**Figure 2.8d**) led to a rough surface, with increasing density of crack deflection sites that resulted in increasing amount of ripples and ridges as CNC concentration increased. Also, formation of some pores or bubbles (probably formed during the drying process) due to trapped air was noticed. Finally, the SEM clarifications have allowed supporting the enhanced mechanical and barrier properties of chitosan films due to the addition of CNC.

## **2.8. Conclusions**

It was observed that CNC acted as a good reinforcing agent in chitosan and only 3-5% of CNC loading gave the best TS values. Improvement of the mechanical properties was due to the formation of a percolating network and strong filler-matrix interaction. Incorporation of only 5% CNC increased the TM of the chitosan films by 87%. CNC also improved the barrier properties of the chitosan by reducing the WVP and swelling property. A 27% reduction of WVP was obtained due to only 5% CNC incorporation. Surface morphology of the nanocomposite films revealed a homogeneous structure indicating proper dispersion of the CNC into the chitosan matrix. Overall, CNC reinforced nanocomposite films due to their excellent mechanical and barrier properties should have a promising impact in food packaging over the coming years.

## **2.9. Acknowledgements**

This research was supported by the Natural Sciences and Engineering Research Council of Canada (NSERC) and by FPInnovations (Pointe-Claire, Canada) through the RDC program. The authors highly appreciate SEM support from Mrs. Line Mongeon, Technician of the Biomedical Engineering Department and the Facility Electron Microscopy Research (FEMR) at McGill University.

## **2.10. References**

- Arumugam, N., Tamareselvy, K., Venkata Rao, K., & Rajalingam, P. (1989). Coconut-fiber reinforced rubber composites. *Journal of Applied Polymer Science*, *37*, 2645–2659.
- ASTM, Standard Test Method for Tensile Strength of Plastics. Annual Book of ASTM Standards, ASTM International, 1999, Method D 638-99.
- ASTM, Standard Test Method for Water Vapor Transmission of Materials; American Society for Testing & Materials, 1983, Philadelphia, PA, Method 15.09:E96.
- Azeredo, H. M. C., Mattoso, L. H. C., Wood, D., Williams, T. G., Bustillos, R. J. A., & McHugh, T. H. (2009). Nanocomposite edible films from mango puree reinforced with cellulose nanofibers. *Journal of Food Science*, *74*(5), 31-35.
- Azeredo, H. M., Mattoso, L. H., Avena-Bustillos, R. J. A., Filho, G. C., Munford, M. L., Wood, D., & Mchugh, T. H. (2010). Nanocellulose reinforced chitosan composite films as affected by nanofiller loading & plasticizer content. *Journal of Food Science*, *75*, 19-28.
- Azizi Samir, M. A. S., Alloin, F., & Dufresne, A. (2005). Review of recent research into cellulosic whiskers, their properties and their application in nanocomposite field. *Biomacromolecules*, *6*(2), 612-26.

- Azizi Samir, M. A. S., Alloin, F., Sanchez, J. Y., & Dufresne, A. (2004). Cellulose nanocrystals reinforced poly(oxyethylene). *Polymer*, *45*, 4149–57.
- Beck-Candanedo, S., Roman, M., & Gray, D. G. (2005). Effect of reaction conditions on the properties and behavior of wood cellulose nanocrystal suspensions. *Biomacromolecules*, *6*(2), 1048-1054
- Bodin, A., Ahrenstedt, L., Fink, H., Brumer, H., Risberg, B., & Gatenholm, P. (2007). Modification of nanocellulose with a xyloglucan-RGD conjugate enhances adhesion and proliferation of endothelial cells: Implications for tissue engineering. Modification of nanocellulose with a xyloglucan-RGD conjugate enhances adhesion and proliferation of endothelial cells: Implications for tissue engineering. *Biomacromolecules*, *8* (12), 3697-3704.
- Cao, X., Chen, Y., Chang, P. R., Muir, A. D., Falk, G. (2008). Starch-based nanocomposites reinforced with flax cellulose nanocrystals. *Polymer Letters*, *2*(7), 502–510.
- Cao, X., Dong, H., & Li, C. M. (2007). New nanocomposite materials reinforced with flax cellulose nanocrystals in waterborne polyurethane. *Biomacromolecules*, *8*, 899-904.
- Chandra, R., & Rustgi, R. (1998). Biodegradable polymers. *Progress in Polymer Science*, *23*, 1273–1335.
- Chen, M., Deng, J., Yang, F., Gong, Y., Zhao, N., & Zhang, X. (2003). Study on physical properties and nerve cell affinity of composite films from chitosan and gelatin solutions. *Biomaterials*, *24*, 2871–2880.
- Ciesla, K., Salmieri, S., & Lacroix, M. (2006).  $\gamma$ -Irradiation influence on the structure and properties of calcium caseinate-whey protein isolate based films. Part 2, Influence of polysaccharide addition and radiation treatment on the structure and functional properties of the films. *Journal of Agricultural and Food Chemistry*, *54*, 8899–8908.

- Cyras, V. P., Manfredi, L. B., Ton-That, M.-T., & Vázquez, A. (2008). Physical and mechanical properties of thermoplastic starch/montmorillonite nanocomposite films. *Carbohydrate Polymers*, 73(1), 55-63.
- Darmadji, P., & Izumimoto, M. (1994). Effect of chitosan in meat preservation. *Meat Science*, 38(2), 243–254.
- De Mesquita, J. P., Donnici, C. L., & Pereira, F. V. (2010). Biobased nanocomposites from layer-by-layer assembly of cellulose nanowhiskers with chitosan. *Biomacromolecules*, 11(2), 473-80.
- Dieter-Klemm, D., Schumann, D., Kramer, F., Hessler, N., Koth, D., & Sultanova, B. (2009). Nanocellulose materials: different cellulose, different functionality. *Macromolecular Symposia*, 280, 60–71.
- Dong, X. M., Revol, J. F., & Gray, D. G. (1998). Effect of microcrystallite preparation conditions on the formation of colloid crystals of cellulose. *Cellulose*, 5, 19-32.
- Dufresne, A., Dupeyre, D., & Vignon, M. R. (2000). Cellulose Microfibrils from Potato Tuber Cells : Processing and Characterization of Starch–Cellulose Microfibril Composites. *Journal of Applied polymer science*, 76, 2080-2092.
- Favier, V., Chanzy, H., & Cavaille., J. Y. (1996). Polymer nanocomposites reinforced by cellulose whiskers. *Macromolecules*, 28, 6365-6367.
- Giannelis, E. P. (1996). Polymer layered silicate nanocomposites. *Advanced Materials*, 8(1), 29-35.

- Gray, D. G. (2007). Transcrystallization of polypropylene at cellulose nanocrystal surfaces. *Cellulose*, 15(2), 297-301.
- Helbert, W., & Chanzy, H. (1994). Oriented growth of V amylase n-butanol crystals on cellulose. *Carbohydrate Polymers*, 24, 119–122.
- Helbert, W., Cavaille, J. Y., & Dufrense, A. (1996). Thermoplastic nanocomposites filled with wheat straw cellulose whiskers. Part I: processing and mechanical behavior. *Polymer composites*, 17(4), 604-611.
- Jalal Uddin, A., Araki, J., & Yasuo Gotoh, Y. (2011). Toward “strong” green nanocomposites: polyvinyl alcohol reinforced with extremely oriented cellulose whiskers. *Biomacromolecules*, 12, 617–624.
- Jin, J., Song, M., & Hourston, D. J. (2004). Novel chitosan-based films cross-linked by genipin with improved physical properties. *Biomacromolecules*, 5(1), 162-8.
- Jo, C., Lee, J. W., Lee, K. H., & Byun, M. W. (2001). Quality properties of pork sausage prepared with water-soluble chitosan oligomer. *Meat Science*, 59(4), 369–375.
- Kanagaraj, S., Varanda, F. R., Zhil'tsova, T. V., Oliveira, M. S. a., & Simões, J. A. O. (2007). Mechanical properties of high density polyethylene/carbon nanotube composites. *Composites Science and Technology*, 67(15-16), 3071-3077.
- Khan, A., Huq, T., Saha, M., Khan, R. A., Khan, M. A., & Gofur, M. A. (2010a). Effect silane treatment on the mechanical and interfacial properties of calcium alginate fiber reinforced polypropylene composite. *Journal of Composite Materials*, 24, 2875-2886.

- Khan, R. A., Salmieri, S., Dussault, D., Calderon, J.U., Kamal, M.R., Safrany, A., & Lacroix, M. (2010b). Production and properties of nanocellulose reinforced methylcellulose-based biodegradable films. *Journal of Agricultural and Food Chemistry*, *58*(13), 7878–7885.
- Kim, K. W., Min, B. J., Kim, Y.-T., Kimmel, R. M., Cooksey, K., & Park, S. I. (2011). Antimicrobial activity against foodborne pathogens of chitosan biopolymer films of different molecular weights. *LWT - Food Science and Technology*, *44*(2), 565-569.
- Kondo, T., & Sawatari, C. (1996). The assignment of IR absorption bands due to free hydroxyl groups in cellulose *Polymer*, *37*, 393–399.
- Le Tien, C., Letendre, M., Ispas-Szabo, P., Mateescu, M. A., Delmas-Patterson, G., Yu, H. L., Lacroix, M. (2000). Development of biodegradable films from whey proteins by cross-linking and entrapment in cellulose. *Journal of Agricultural and Food Chemistry*, *48*, 5566–5575.
- Lee, S. Y., Yang, H. S., Kim, H. J., Jeong, C. S., Lim, B. S., Lee, J. L. (2004). Creep behavior and manufacturing parameters of wood flour filled polypropylene composites, *Composite Structures*, *65*, 459–469.
- Li, Q., & Rennecker, S. (2011). Supramolecular structure characterization of molecularly thin cellulose I nanoparticles. *Biomacromolecules*, *12*, 650–659.
- Nikonenko, N. A., Buslov, D. K., Sushko, N. I., & Zhbankov, R. G. (2000). Investigation of stretching vibrations of glycosidic linkages in disaccharides and polysaccharides with use of IR spectra deconvolution. *Biopolymers*, *57*, 257–262.
- Nikonenko, N. A., Buslov, D. K., Sushko, N. I., & Zhbankov, R. G. (2005). Spectroscopic manifestation of stretching vibrations of glycosidic linkage in polysaccharides. *Journal of Molecular Structure*, *752*, 20–24.

- No, H. K., Meyers, S. P., Prinyawiwatkul, W., & Xu, Z. (2007). Applications of chitosan for improvement of quality and shelf life of foods: a review. *Journal of Food Science*, 72(5), R87-100.
- Ogawa, K., Hirano, S., Miyanishi, T., Yui, T., & Watanabe, T. A. (1994). New polymorph of chitosan. *Macromolecules*, 17, 973-975.
- Rabea, E. I., Badawy, M. E.-T., Stevens, C. V., Smagghe, G., & Steurbaut, W. (2003). Chitosan as antimicrobial agent: applications and mode of action. *Biomacromolecules*, 4(6), 1457-65.
- Revol, J.-F., Bradford, H., Giasson, J., Marchessault, R. H., & Gray, D. G. (1992). Helicoidal self-ordering of cellulose microfibrils in aqueous suspension. *International Journal of Biological Macromolecules*, 14, 170-172.
- Rhim, J.-W. (2011). Effect of clay contents on mechanical and water vapor barrier properties of agar-based nanocomposite films. *Carbohydrate Polymers*, 86(2), 691-699.
- Rhim, J.-W., Hong, S.-I., Park, H.-M., & Ng, P. K. W. (2006). Preparation and characterization of chitosan-based nanocomposite films with antimicrobial activity. *Journal of Agricultural and Food Chemistry*, 54(16), 5814-22.
- Rhim, J.-W., Perry, K.W. NG. (2007). Natural Biopolymer-Based Nanocomposite Films for Packaging Applications. *Critical Reviews in Food Science and Nutrition*, 47,411–433
- Shin, Y., Gregory, J., & Exarhos, G. J. (2007). Template synthesis of porous titania using cellulose nanocrystals. *Materials Letters*, 61, 2594–2597.

- Sionkowska, A., Wisniewski, J., Skopinska, J., Kennedy, C. J., & Wess, T.J. (2004). Molecular interactions in collagen and chitosan blends, *Biomaterials*, *25*, 795–801.
- Sorrentino, A., & Gorrasi, G. (2007). Potential perspectives of bio-nanocomposites for food packaging applications. *Trends in Food Science & Technology*, *18*(2), 84-95.
- Svagan, A. J., Hedenqvist, M. S., & Berglund, L. (2009). Reduced water vapour sorption in cellulose nanocomposites with starch matrix. *Composites Science and Technology*, *69*(3-4), 500-506.
- Ureña-Benavides, E. E., Brown, P. J., & Kitchens, C. L. (2010). Effect of jet stretch and particle load on cellulose nanocrystal-alginate nanocomposite fibers. *Langmuir*, *26*(17), 14263-70.
- Wang, H., & Roman, M. (2011). Formation and properties of chitosan cellulose nanocrystal polyelectrolyte macroion complexes for drug delivery applications. *Biomacromolecules*, *12*, 1585–1593
- Wang, S.-F., Shen, L., Zhang, W.-D., & Tong, Y.-J. (2005). Preparation and mechanical properties of chitosan/carbon nanotubes composites. *Biomacromolecules*, *6*(6), 3067-72.
- Weber, C. J., Haugaard, V., Festersen, R., & Bertelsen, G. (2002). Production and applications of biobased packaging materials for the food industry. *Food Additives & Contaminants*, *19*, 172–177.
- Wu, T., Zivanovic, S., Draughon, F. A., Conway, W. S., & Sams, C. E. (2005). Physicochemical properties and bioactivity of fungal chitin and chitosan. *Journal of Agricultural and Food Chemistry*, *53*, 3888–3894.

Zawadzki, J., & Kaczmarek, H. (2010). Thermal treatment of chitosan in various conditions.  
*Carbohydrate Polymers*, 80(2), 394-400.

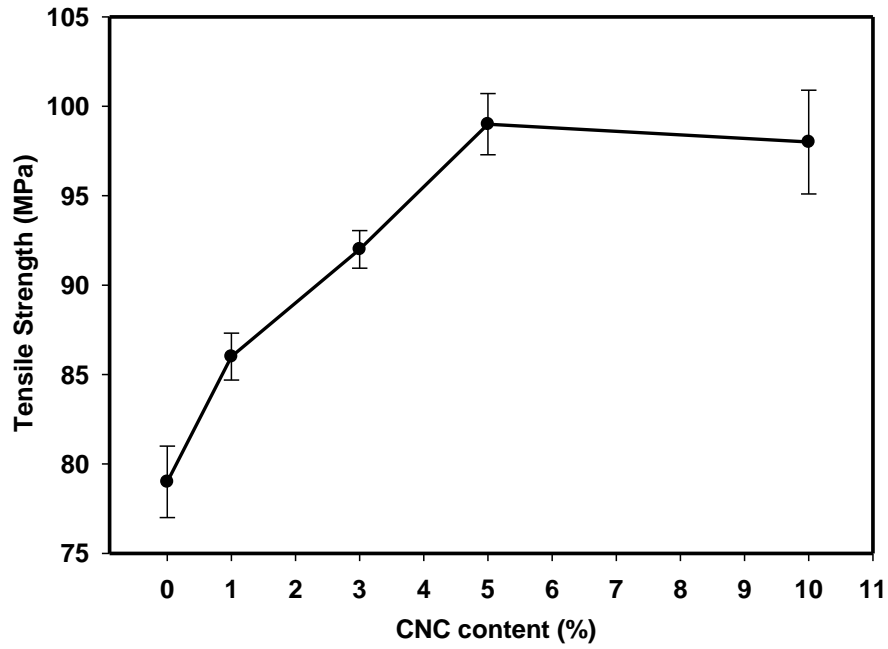


**Figure 2.1(a):** Effect of CNC content in the tensile strength of the chitosan films.

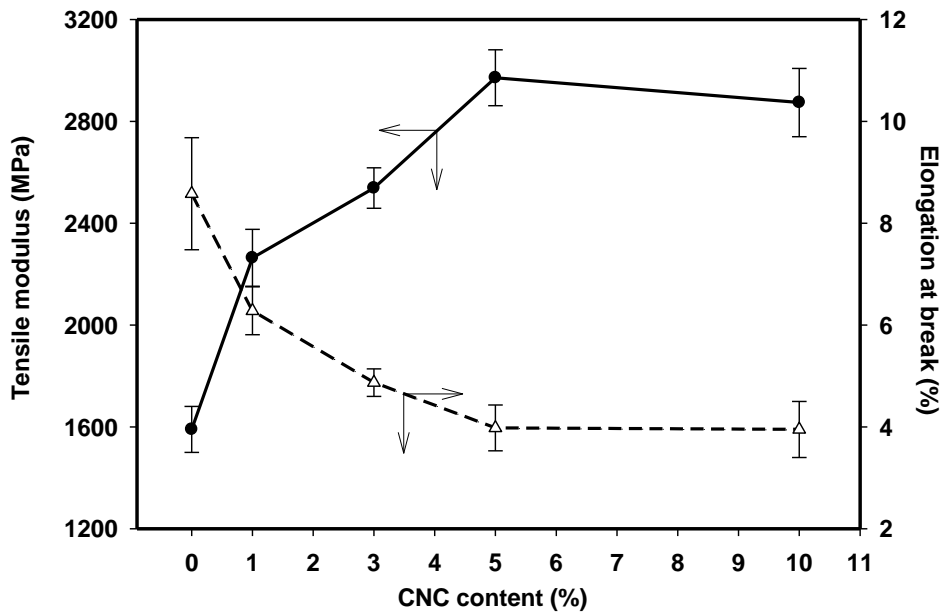


**Figure 2.1(b):** Effect of CNC content in the tensile modulus and elongation at break (%) of the chitosan films.

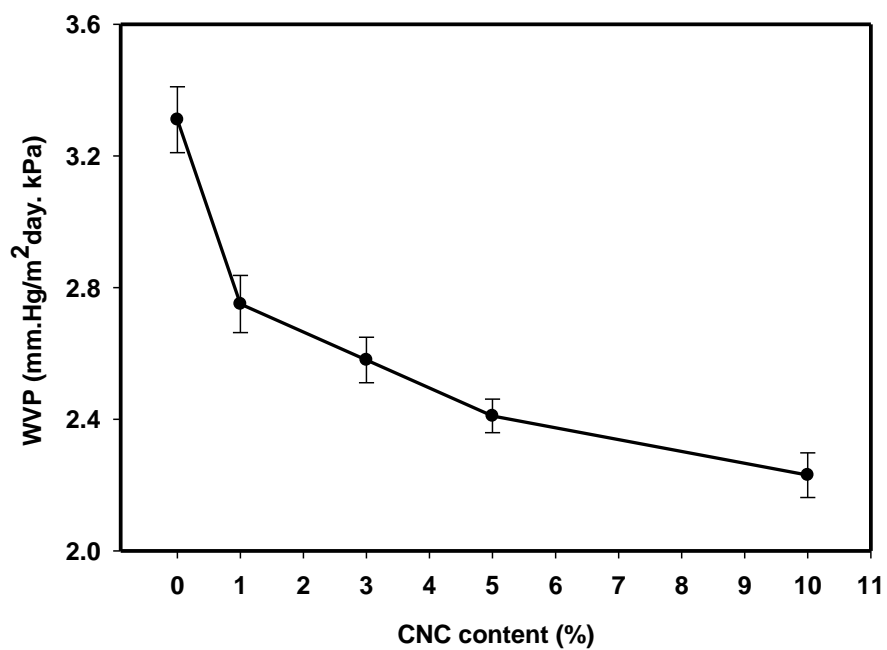


**Figure 2.2:** *Effect of CNC content in the water vapor permeability of the chitosan films.*

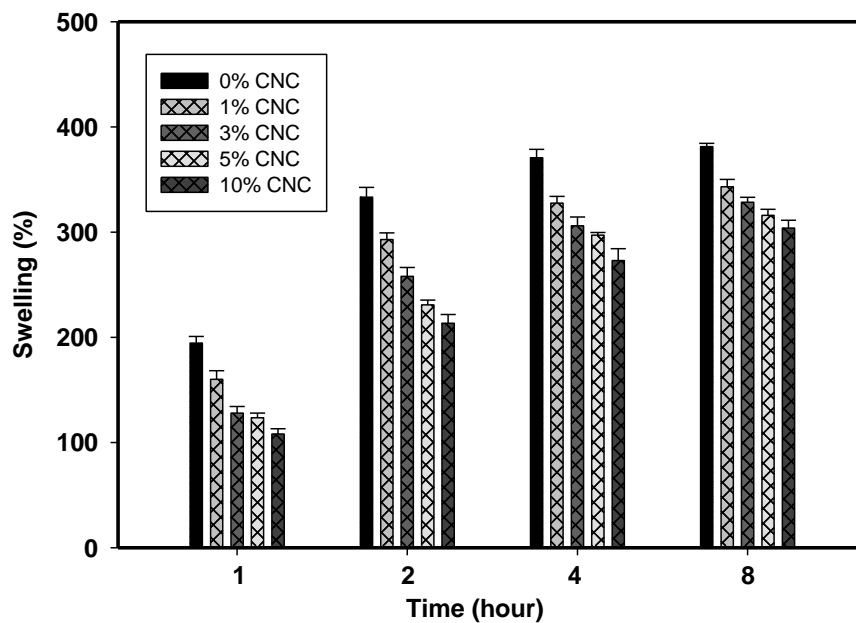


**Figure 2.3:** *Effect of CNC content in the swelling property of the chitosan films.*

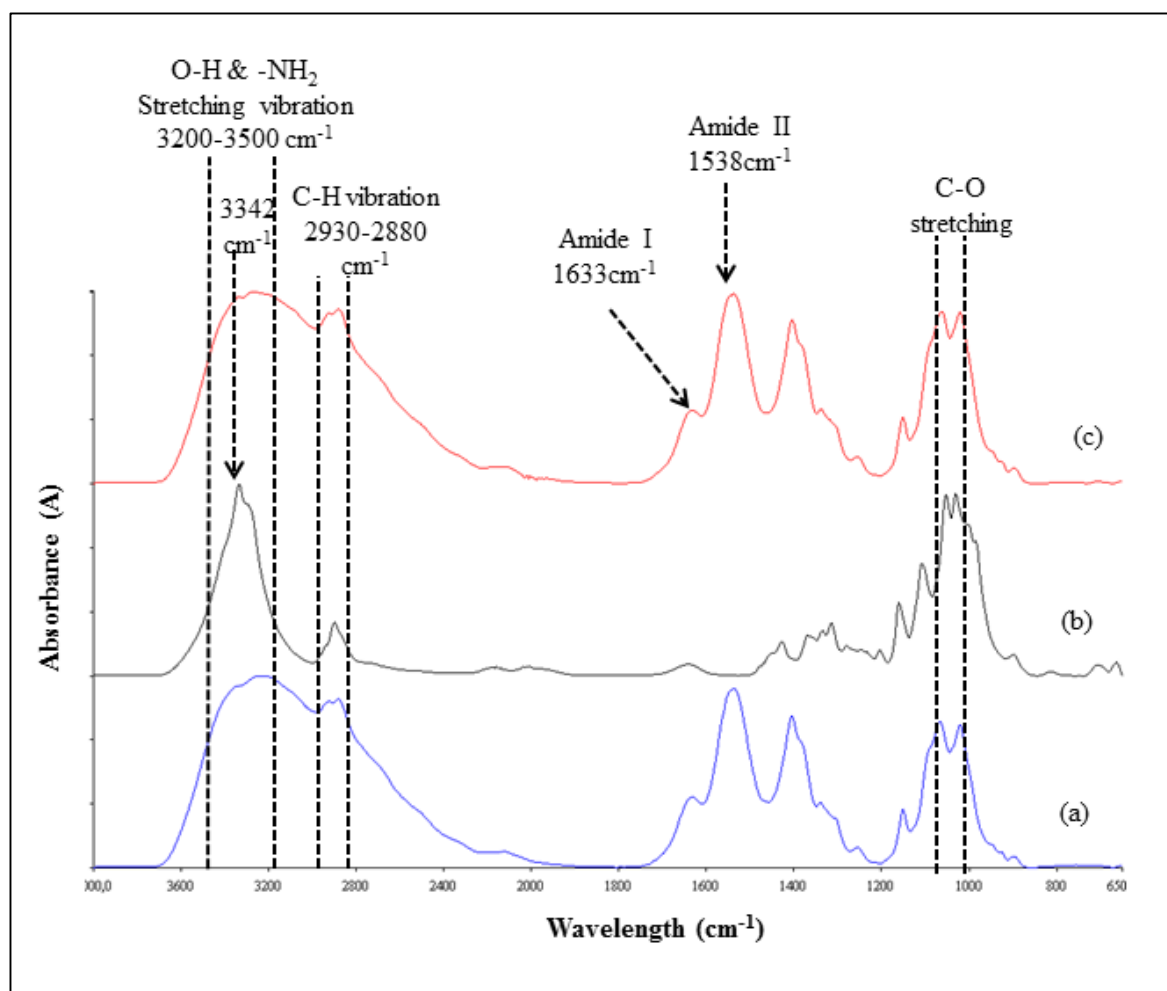


**Figure 2.4:** FT-IR spectra of films based on (a) Chitosan (b) CNC and (c) Chitosan + 5% CNC

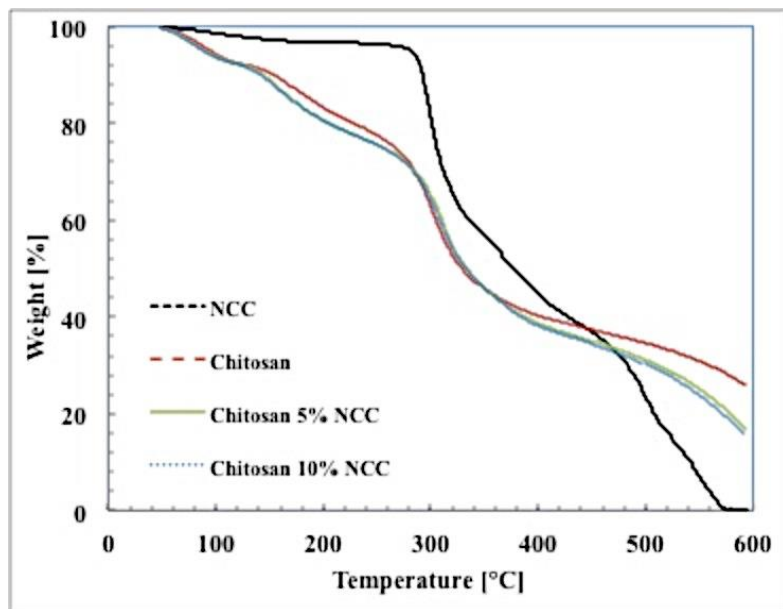


**Figure 2.5:** TGA curves for CNC, chitosan, chitosan with 5 and 10% CNC films.

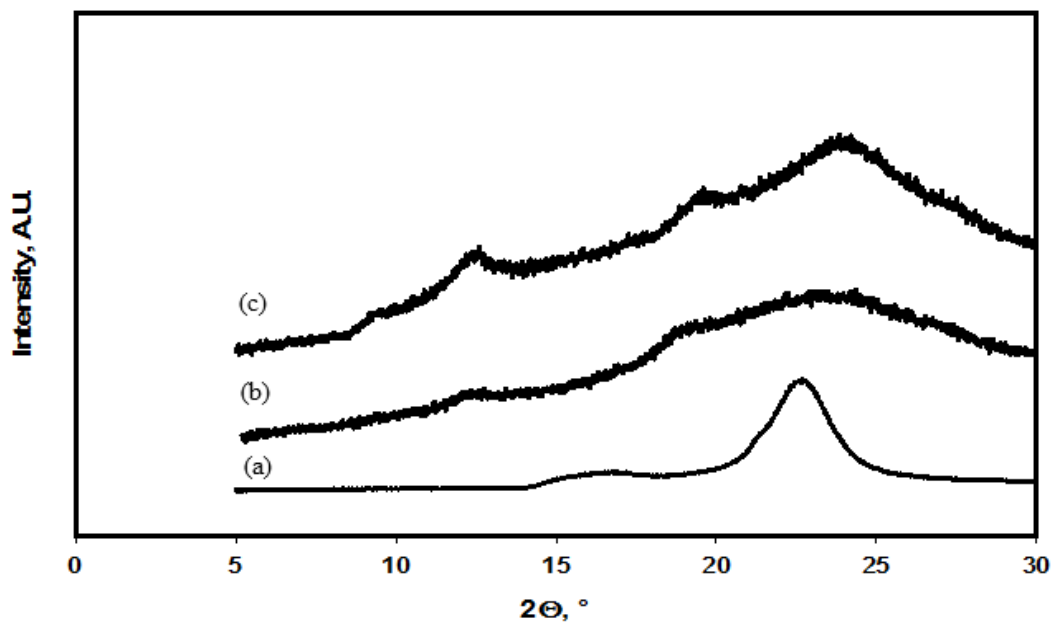


**Figure 2.6:** X-ray Diffractograms of films based on a) CNC b) chitosan and c) chitosan+5%CNC.

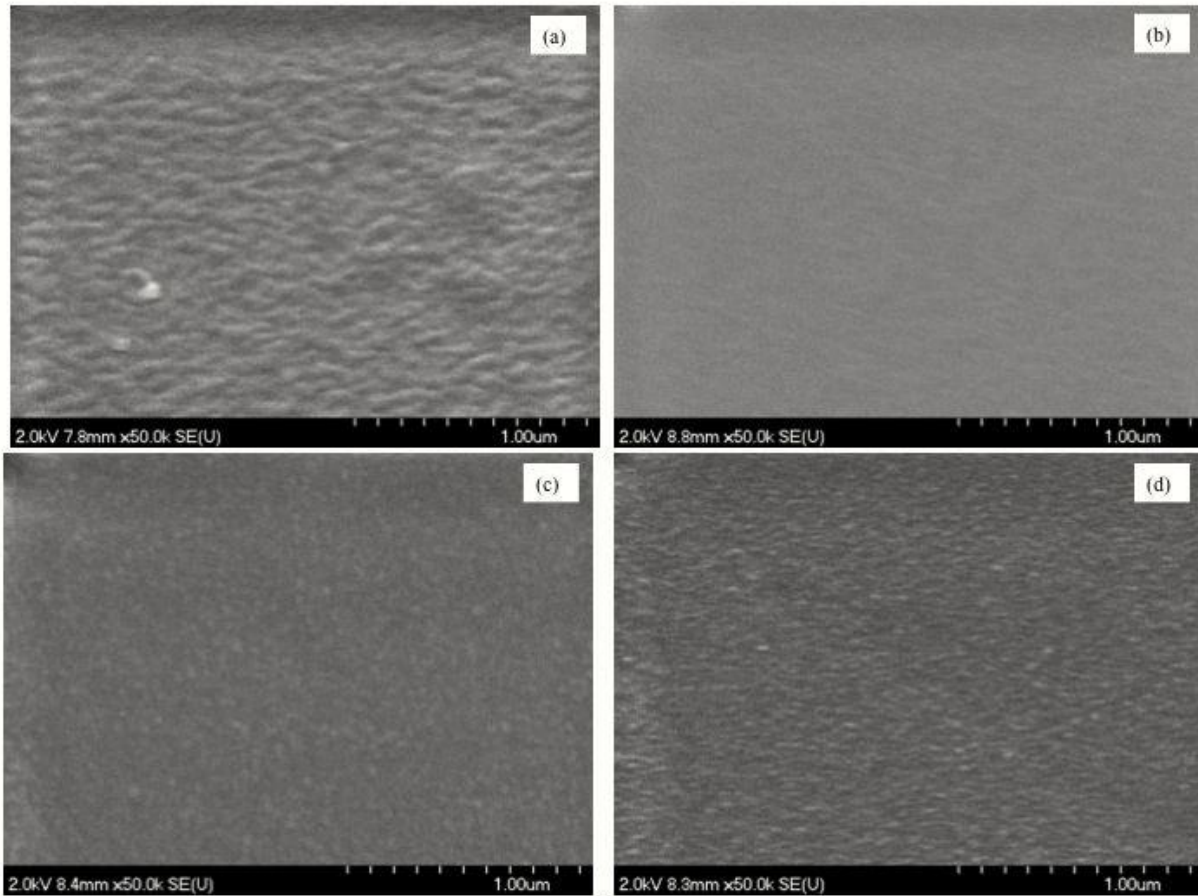


**Figure 2.7:** SEM image of the surface of a) CNC, b) chitosan, c) chitosan+5% CNC and d) chitosan+10% CNC films

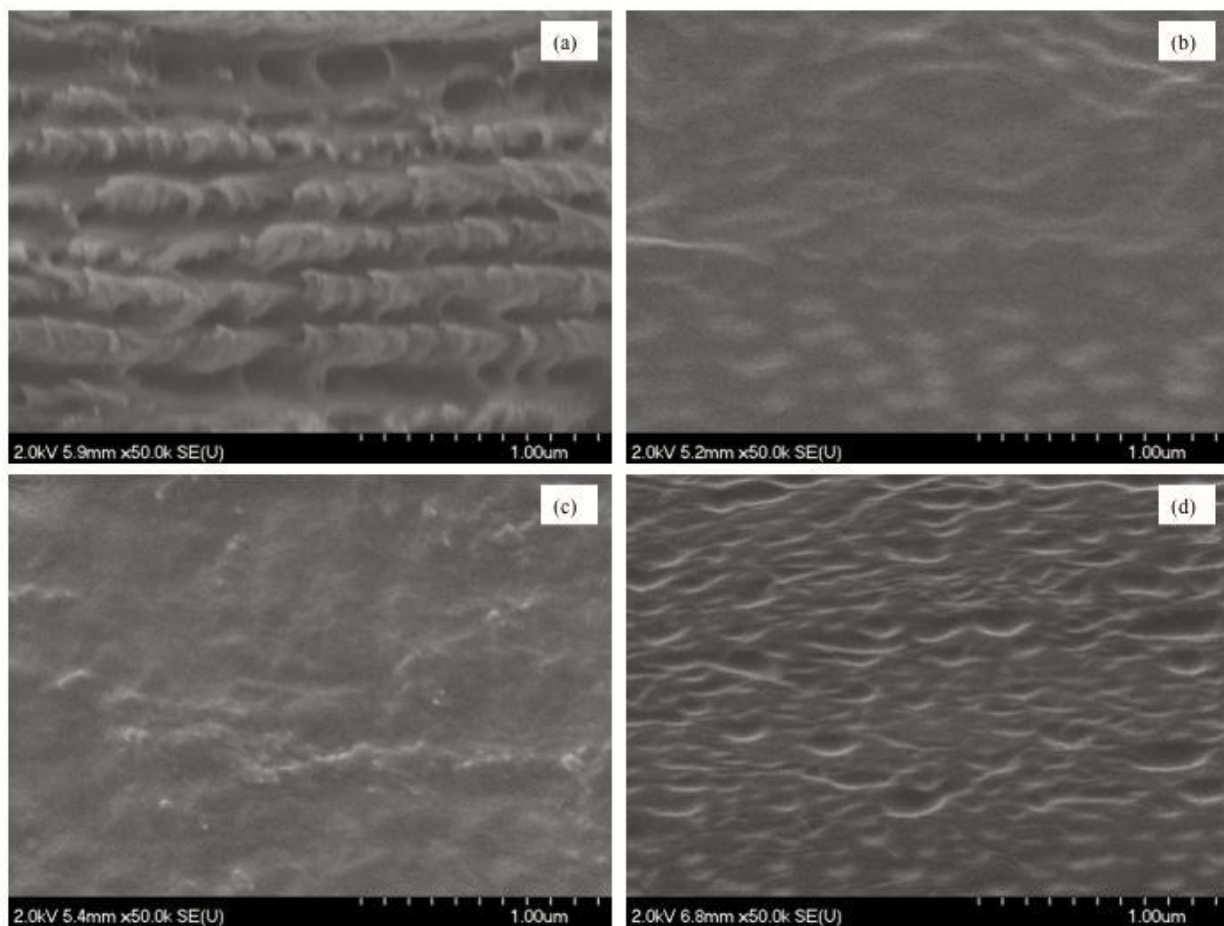


**Figure 2.8:** SEM image of the cross-section of a) CNC, b) chitosan, c) chitosan+5% CNC and d) chitosan+10% CNC films

## **2.11. General discussion of the Publication-1**

The CNC/chitosan films prepared with 0.1% CNC suspension exhibited better mechanical and barrier properties compared to that of chitosan. The optimum CNC concentration was found to be 5% w/w in chitosan. However, dispersion of a concentrated CNC suspension (1-2%) was found to be problematic and further work is required. The mechanical and barrier properties of the films did not improve further at higher CNC loading (10%). This could be due to the aggregation of CNC in the chitosan matrix. The changes in the FT-IR spectra due to the addition of CNC were minor. The TGA analysis also did not reveal any significant changes. This could be due to the low amount of CNC incorporated (5% w/w) to make the composite films. So, There is scope for further studies in order to elucidate the mechanism of CNC-chitosan interaction. However, the XRD analysis revealed increase in the peak intensity of chitosan in the crystalline region and supported improvement of the mechanical and barrier properties of chitosan films due to the addition of CNC. SEM analysis revealed possible aggregation of CNC at 10% loading.

## **CHAPTER 3**

### **Publication 2**

# Genipin cross-linked nanocomposite films for the immobilization of antimicrobial agent

Avik Khan<sup>1</sup>, Stephane Salmieri<sup>1</sup>, Carole Fraschini<sup>3</sup>, Jean Bouchard<sup>3</sup>, Bernard Riedl<sup>2</sup> and Monique Lacroix<sup>1\*</sup>

<sup>1</sup>Research Laboratories in Sciences Applied to Food, Canadian Irradiation Centre (CIC),  
INRS-Institut Armand-Frappier, Université du Québec, 531 Boulevard des Prairies,  
Laval, Québec, H7V 1B7, Canada

<sup>2</sup>Département des sciences du bois et de la forêt, Faculté de foresterie, géographie et géomatique,  
Université Laval, Québec-city, Québec, G1V 0A6, Canada

<sup>3</sup>FPIInnovations, 570 Boulevard St. Jean, Pointe-Claire, Québec, H9R 3J9, Canada

**KEYWORDS:** Chitosan, Nisin, Cellulose nanocrystal, Surface modification, *Listeria monocytogenes*, Antimicrobial films.

\* **Corresponding Author:** Prof. Monique Lacroix.

Telephone: +1-450-687-5010; Fax: +1-450-686-5501.

**E-mail:** [monique.lacroix@iaf.inrs.ca](mailto:monique.lacroix@iaf.inrs.ca)

This article is published in *ACS-Applied Materials & Interfaces*, 2014, 6, 15232-15242.

### **3.1. Contribution of the authors**

The experimental works were planned, performed and analyzed by Avik Khan with guidance from Prof. Monique Lacroix. The manuscript was written by Avik Khan. Prof. Monique Lacroix and Prof. Bernard Riedl corrected the main draft. Stephane Salmieri corrected the discussion for FTIR analysis and helped to improve the discussion. Dr. Carole Fraschini and Dr. Jean Bouchard corrected the main draft.

### **3.2. Specific objectives of the Publication-2**

The objective of the project was to develop novel nanocomposite films to inhibit the growth of pathogenic bacteria in meat products. After development of an optimized CNC/chitosan films (Publication-1), the focus shifted towards its application side. RTE ham was chosen as a model meat product. Nisin was selected as an antimicrobial agent in order to make the films antimicrobial. In the current publication, genipin was used to cross-link the antimicrobial films. At first, the nisin concentration was optimized by evaluating the antimicrobial activity of the films *in situ* against *L. monocytogenes*. Then the film with optimized nisin concentration was cross-linked with different concentration (0 to 0.2% w/v) of genipin. The effect of genipin cross-linking was investigated by measuring the mechanical properties, water resistance, FT-IR spectral analysis, *in vitro* and *in situ* analysis of the films.

### 3.3. Résumé

Des films antimicrobiens de chitosane renforcés de cellulose nanocrystalline (CNC) ont été préparés par immobilisation de la nisine sur la surface des films. Ces films nanocomposites contenant  $18,65\mu\text{g}/\text{cm}^2$  de nisine ont réduit le nombre de *L. monocytogenes* par  $6,73 \log \text{UFC}/\text{g}$ , par rapport à des échantillons de contrôle à base de viande ( $8,54 \log \text{UFC}/\text{g}$ ) suite à un stockage à  $4^\circ\text{C}$  dans un système de viande Prêt-à-Manger (PAM). Les formulations de tels films contenant  $9,33 \mu\text{g}/\text{cm}^2$  de nisine ont augmenté la phase de latence de *L. monocytogenes* sur la viande de plus de 21 jours, alors que les formulations avec  $18.65 \mu\text{g}/\text{cm}^2$  ont complètement inhibé la croissance de *L. monocytogenes* durant le stockage. La génipine a été utilisée pour réticuler et protéger l'activité de la nisine pendant le stockage. Des films nanocomposites réticulés à l'aide de  $0,05 \%$  pds/v de genipine ont présenté la plus forte activité ( $10,89 \mu\text{g}/\text{cm}^2$ ) au cours de l'expérience de stockage, en comparaison avec celle des films non réticulés ( $7,23 \mu\text{g}/\text{cm}^2$ ). Les films réticulés à l'aide de la génipine ont permis de réduire le taux de croissance de *L. monocytogenes* sur des échantillons de jambon de  $21\%$  par rapport aux films non réticulés. L'analyse spectroscopique a confirmé la formation d'un réseau réticulé hétérocyclique génipine-nisine-chitosane. Les films réticulés à la génipine ont également présenté des meilleures propriétés de gonflement, de solubilité dans l'eau et de meilleures propriétés mécaniques.

### 3.4. Abstract

Cellulose nanocrystal (CNC) reinforced chitosan based antimicrobial films were prepared by immobilizing nisin on the surface of the films. Nanocomposite films containing  $18.65 \mu\text{g}/\text{cm}^2$  of nisin reduced the count of *L. monocytogenes* by 6.73 log CFU/g, compared to the control meat samples (8.54 log CFU/g) during storage at  $4^\circ \text{C}$  in a Ready-To-Eat (RTE) meat system. Film formulations containing  $9.33 \mu\text{g}/\text{cm}^2$  of nisin increased the lag phase of *L. monocytogenes* on meat by more than 21 days, whereas formulations with  $18.65 \mu\text{g}/\text{cm}^2$  completely inhibited the growth of *L. monocytogenes* during storage. Genipin was used to cross-link and protect the activity of nisin during storage. Nanocomposite films cross-linked with 0.05% w/v genipin exhibited the highest activity ( $10.89 \mu\text{g}/\text{cm}^2$ ) during storage experiment, as compared to that of the uncross-linked films ( $7.23 \mu\text{g}/\text{cm}^2$ ). Genipin cross-linked films were able to reduce the growth rate of *L. monocytogenes* on ham samples by 21% as compared to the uncross-linked films. Spectroscopic analysis confirmed the formation of genipin-nisin-chitosan heterocyclic cross-linked network. Genipin cross-linked films also improved the swelling, water solubility and mechanical properties of the nanocomposite films.

### **3.5. Introduction**

The purpose of food packaging is to preserve the quality and safety of the packaged food. In the context of a constantly growing population and globalization of markets, prevention of food contamination by microorganisms or pathogens, is becoming increasingly important. In the United States, foodborne diseases cause 9.4 million illnesses, 55,961 hospitalizations and 1,391 deaths each year (Scallan *et al.*, 2011). Antimicrobial packaging is gaining interest from researchers and industries due to its potential to prevent the growth of pathogenic bacteria in food products (Coma, 2008). Antimicrobial packaging can be defined as the incorporation of antimicrobial agent into packaging in order to prevent surface growth of micro-organisms and pathogenic bacteria in foods, thus ensure the quality and safety of food products during storage (Khan *et al.*, 2014). Direct incorporation of antimicrobials into food may lead to drastic loss of antimicrobial efficacy due to the inactivation of the antimicrobials by food components or dilution below active concentration due to migration into the bulk food matrix. Antimicrobial films provide an innovative alternative and can reduce the addition of larger quantities of antimicrobials that are usually incorporated directly into the food bulk (Cooksey, 2005). These films can also allow a better efficiency, stability and controlled release of the antimicrobials to the food surface (Guiga *et al.*, 2010).

Cellulose nanocrystal (CNC), which is also known as nanocrystalline cellulose or cellulose nanowhisker, is made up of highly crystalline, nano-sized, rod like particles that are extracted from softwood bleached kraft pulp by a controlled acid hydrolysis process (Dong *et al.*, 1998). CNC extracted from wood was found to exhibit an average length of 110 nm long for a 5-10 nm width (Revol *et al.*, 1992). Natural nano-fillers such as CNC has been used in great effects to enhance the mechanical and barrier properties of chitosan films (Khan *et al.*, 2012; Li *et al.*, 2009). Chitosan is a natural linear polysaccharide made up with of 1,4-linked 2-amino deoxy- $\beta$ -

D-glucan. Chitosan has been found non-toxic, biodegradable, biofunctional, and biocompatible (Prashanth and Tharanatha, 2007). While several researchers have reported strong antimicrobial and antifungal activities of chitosan suspension (Darmadji and Izumim, 1994; Kim *et al.*, 2011; No *et al.*, 2007; Rabea *et al.*, 2003), films made from chitosan only did not demonstrate any antimicrobial efficacy (Foster and Butt, 2011). The use of natural antimicrobials such as, bacteriocins in combination with natural biopolymeric films represent an interesting and highly potential field in the development of environment friendly active packaging materials.

Nisin is a bacteriocin (**Figure-3.1 a, c**) produced by the lactic acid bacterium, *Lactococcus lactis* subsp. *lactis*, is one of the most effective antimicrobial agents when it comes to food packaging (Jin *et al.*, 2009). It is mostly effective against lactic acid bacteria and other gram-positive organisms (Millette *et al.*, 2007). Nisin is the only bacteriocin that has GRAS (generally considered as safe) status by both the Food and Drug Administration (FDA) and World Health Organization (WHO) (Delves-Broughton, 1990). The activity of nisin may be lost during storage in food products due to enzymatic degradation and interaction with food components such as, protein and fats (Benech and Kheadr, 2002). Genipin, which is a naturally occurring crosslinking agent, can be used to protect the activity of nisin during storage. Genipin (**Figure-3.2 b**) is derived from the fruits *Genipa americana* and *Gardenia jasminoides Ellis* (Chiono *et al.*, 2008). It has the ability to covalently cross-link with amino acids or proteins and has been reported to be 5000-10000 times less cytotoxic than other commonly used cross-linking agent such as glutaraldehyde (Sung *et al.*, 1999). Due to its biocompatibility and low toxicity, genipin is recently being used in biomedical applications (Chiono *et al.*, 2008; Bigi *et al.*, 2002; Butler *et al.*, 2006) and for controlled drug release (Mi and Sung, 2002; Harris *et al.*, 2010; Song *et al.*,

2009). Genipin cross-linked biopolymeric films have high potential for the protection bioactive agents.

The objective of this study was to develop an antimicrobial nanocomposite film by immobilizing nisin onto the polymer surface. The antimicrobial efficacy of the nanocomposite films were evaluated *in situ* on Ready-To-Eat (RTE) ham samples during storage. Then the optimal concentration of nisin was used to be cross-linked with different concentration of genipin and the bioactivity of the films was tested *in vitro*. Spectroscopic analysis was performed in order to characterize and explain the mechanism of genipin as cross-linking agent. Also the effect of genipin cross-linking on the mechanical properties, water resistance and surface morphology of the films was evaluated.

### **3.6. Materials and Methods**

#### **3.6.1. Preparation of the nanocomposite films**

In our previous study, CNC improved the mechanical strength of chitosan based films and 5% (in the dry of chitosan-based films) of CNC was the optimum CNC concentration (Khan *et al.*, 2012). The nanocomposite films, in the current study, were prepared following a modified method as described in Khan *et al.*, 2012. At first a dilute (0.1% w/v) CNC suspension was prepared by dispersing spray dried CNC powder (FPIinnovations, Pointe-Claire, QC, Canada) in deionized water under magnetic stirring. Then a 2% (w/v) of aqueous acetic acid (Laboratoire Mat, Beauport, Quebec, Canada) solution was incorporated into the CNC suspension. The CNC suspension was then subjected to ultra-sonication (QSonica Q-500, Misonix, Qsonica, LLC, Newtown, CT, USA) at 1000 J/g of CNC. Then a 0.5% ethylene glycol (Laboratoire Mat, Beauport, Quebec, Canada) and 2% w/v high mol. wt. chitosan (DD: 85-90%, 85/2500 Heppemedical GmbH, Germany) were incorporated in the suspension. The suspension was then magnetically stirred overnight followed by homogenization with IKA RW-20 mechanical

homogenizer at 1,500 rpm for 3 h. After homogenization, a paraffin film was wrapped on top of the beaker and kept overnight at 4°C. The films were made by casting a 15 mL of the chitosan/CNC nanocomposite suspension on Petri dishes which were allowed to dry at room temperature and 30-35% RH. Films were then treated with 1M NaOH (Laboratoire Mat, Beauport, Quebec, Canada) for 2 min, washed several times with deionized water and allowed to dry.

### **3.6.2. Preparation of nisin solution**

A stock solution of nisin (Niprosin™, purity 2.5%, 77.5% salt and 20% vegetable protein, Profood, IL, USA) was prepared by dispersing 1g of the Niprosin™ powder in 100 mL of deionized water under magnetic stirring. The pH of the suspension was adjusted to 3.0 with dil. lactic acid (3% w/w in water, Laboratoire Mat, Beauport, Quebec, Canada). It has been reported that nisin is most stable and efficient at pH 3 (Davies *et al.*, 1998, Rollema *et al.*, 1995). The suspension was stirred for 5 hours and kept overnight at 4°C. Then the suspension was centrifuged for 15 min at 2500 rpm at 4 °C to remove the insoluble fractions, the supernatant was collected and stored at 4°C.

### **3.6.3. Adsorption of nisin onto the surface of the films**

From the stock solution five different concentrations of nisin solution were prepared by dilution with deionized water and pH of each solution was again adjusted to 3 with lactic acid. A 15 mL of nisin solution from each different concentration was applied on the surface of the insoluble chitosan films and allowed to dry for 2 days. The surface area of the films were 50.26 cm<sup>2</sup> (8 cm diameter). The nisin content on each film was calculated according to the amount of pure nisin (in µg) per surface area of the films (in cm<sup>2</sup>). The nisin content on the five different formulations was calculated to be 37.30, 18.65, 9.33, 4.66 and 2.33 µg/cm<sup>2</sup>, which corresponds to 1,874.8 937.45, 468.72, 234.36, 117.18 and 58.6 IU of nisin in each film formulation, respectively. The

nisin content on each film was calculated according to the amount of pure nisin (in  $\mu\text{g}$ ) per surface area of the films (in  $\text{cm}^2$ ). The nisin content on the five different formulations was calculated to be 37.30, 18.65, 9.33, 4.66 and 2.33  $\mu\text{g}/\text{cm}^2$ . The films containing 37.30  $\mu\text{g}/\text{cm}^2$  of nisin were found to be very brittle and inhomogeneous and were not used for any further experiments.

#### **3.6.4. *In situ* evaluation of the antimicrobial activity against *L. monocytogenes***

RTE ham was chosen as a food model to test the antimicrobial activity of the films *in situ* and to optimize the nisin concentration in the films. The *L. monocytogenes* five strains (HPB 2569 1/2a, 2558 1/2b, 2371 1/2b, 2812 1/2ba and 1043 1/2a) used in this experiment were obtained from Health products and Foods Branch of Health Canada (Ottawa, ON, Canada). The microorganisms were kept frozen at  $-80\text{ }^\circ\text{C}$  in tryptic soy broth (Alpha Biosciences, ML, USA) containing glycerol (10% v/v). Before use, the stock cultures were propagated through 2 consecutive 24 h growth in TSB at  $37\text{ }^\circ\text{C}$  to obtain the working cultures containing approximately  $10^9$  CFU/mL. Lean ground pork was purchased from a local grocery store (IGA, Laval, Quebec, Canada). Ground pork was cooked with a salt mixture containing sodium chloride (1.5%), tripolyphosphate (0.43%), sodium erythorbate (750 ppm), and sodium nitrite (100 ppm) (BSA Food Ingredients, St-Leonard, Quebec, Canada) for about 1 h at  $162\pm 3\text{ }^\circ\text{C}$  in a cooking oven. Following cooking the ham was removed from the oven and placed at  $4\text{ }^\circ\text{C}$  for 24 hr. Then the ham was sliced to 10 g portions. A 1 mL of each culture of five strains of *L. monocytogenes* was mixed together to prepare a cocktail mixture. Appropriate dilutions were made in peptone water (0.1%; BD, Sparks, MD, USA) to obtain an inoculation solution containing approximately  $10^4$  to  $10^5$  CFU/mL of *L. monocytogenes*. After that, a volume of 500  $\mu\text{L}$  of the inoculation solution was spread on the surface of the ham samples to achieve

approximately  $10^3$  CFU/g of ham. Then the ham samples were sandwiched between two films, vacuum packaged and stored at 4 °C up to 35 days.

### **3.6.5. Enumeration of bacteria**

The meat samples were analyzed for the growth of *L. monocytogenes* after 1, 7, 14, 21, 28 and 35 days of storage. On each day of analysis, the nanocomposite films were removed and 3 meat samples from each formulation were put in a sterile filter sample bag (Whirl-Pak; Nasco, Fort Atkinson, WI, USA), diluted 5 fold with peptone water (0.1%; BD) and homogenized in a Lab-blender 400 stomacher (Seward Medical, London, UK) for 1 min at 200 rpm. From this homogenate, appropriate serial dilutions were then plated on PALCAM agar plates (Alpha Biosciences, ML, USA), for the selective enumeration of *L. monocytogenes*. The plates were incubated for 48 h at 37 °C. Following incubation the colony forming units (CFU) were counted using a magnifier and the bacterial counts were expressed as log CFU/g of meat.

### **3.6.6. Preparation of genipin-nisin cross-linked films**

Following the *in situ* experiment, the concentration of nisin ( $18.65 \mu\text{g}/\text{cm}^2$ ) providing the complete inhibition of *L. monocytogenes* was chosen to be cross-linked with genipin (Challenge Bio-products, Yun-Lin Hsien, Taiwan). Different concentrations of genipin (0.05, 0.1, 0.2, and 0.4% w/v) were mixed with the optimized nisin solution at pH 3 and the reaction was carried out for 24 h at room temperature. Then 15 mL of the genipin cross-linked nisin solution was applied on the surface of the insoluble chitosan films and allowed to dry for 2 days. The films with nisin only (no cross-linking) were termed as G0 whereas the films with 0.05, 0.1, 0.2, and 0.4% of genipin were termed as G0.05, G0.1, G0.2 and G0.4, respectively. All the films were stored at 4 °C in a desiccator filled with deionized water to obtain 90-100% RH.

### **3.6.7. Fourier Transform Infrared Spectroscopy (FTIR)**

The FTIR spectra of the films were recorded using a Spectrum One spectrophotometer (Perkin-Elmer, Woodbridge, ON, Canada) equipped with an attenuated total reflectance (ATR) device for solids analysis and a high-linearity lithium tantalate detector. Spectra were analyzed using Spectrum 6.3.5 software. Films were stored at 4 °C in a desiccator containing distilled water to ensure a stabilized atmosphere of 90-100% RH. Films were then placed onto a zinc selenide crystal, and the analysis was performed within the spectral region of 850-1750  $\text{cm}^{-1}$  with 64 scans recorded at a 4  $\text{cm}^{-1}$  resolution. After attenuation of total reflectance and baseline correction, spectra were normalized with a limit ordinate of 1.5 absorbance units.

### **3.6.8. *In vitro* evaluation of the bioactivity of the cross-linked films**

The bioactivity of the films was tested *in vitro* according to a modified agar diffusion assay against the bacterium *Lactobacillus sakei* ATCC 15521 (American Type Culture Collection, Rockville, MD, USA) in order to optimize the concentration of genipin. *L. sakei* is used as an indicator strain or a standard micro-organism to quantify the activity of nisin (Millette *et al.*, 2007). All the films (uncross-linked nisin and genipin cross-linked nisin) were cut into square shapes (1.44  $\text{cm}^2$ ) and were sterilized using  $\gamma$ -irradiation at 2.5 kGy at the Canadian Irradiation Centre (CIC, Laval, Quebec, Canada) at room temperature. A 20 mL of De-Man Rogosa, Sharp (MRS, Alpha Biosciences, Maryland, USA) agar plates were inoculated with bacterial cultures to obtain colony count of approximately  $10^8$  CFU/mL. The films were then put onto the inoculated MRS agar plates and were incubated at 37 °C for 72 hours. The plates were examined for the ‘zone of inhibition’ and the diameter of the zone was measured with a caliper (mm). From the inhibition diameter the area of the whole zone was calculated and reported as the surface area of inhibition. A standard curve was generated by plotting the inhibition area ( $\text{cm}^2$ ) of the different concentrations of uncross-linked nisin films in the X-axis against the nisin concentration

( $\mu\text{g}/\text{cm}^2$ ) in the films (Y-axis). Regression analysis was performed to determine the standard equation. The inhibition areas of the films (at 4 °C and 90-100% RH) were measured (as described before) during 1, 7, 14, 21, 28 and 35 days of storage.

### **3.6.9. Swelling ratio and water solubility of the films**

Swelling ratio (SR) of the films was determined gravimetrically according to a modified procedure as described by Jin *et al.* 2004. Pre-weighed films ( $1.44 \text{ cm}^2$ ) were immersed in a beaker containing 100 mL of distilled water at room temperature. Films were then removed at specified time intervals (1, 2, 4, 8 and 24 h) and weighed immediately after removing the surface adsorbed water with a filter paper. The SR was calculated according to the following equation:

$$\text{SR} = [(W_t - W_0) / W_0] \times 100 \quad \text{(Eq. 3.1)}$$

Where,  $W_0$  and  $W_t$  are the weight of the films before and after immersion, respectively.

Water solubility (WS) of the films was tested in order to determine the resistance of the films in water (Rhim, 2011). At first films ( $1.44 \text{ cm}^2$ ) were dried at 105 °C for 24 h to determine initial dry matter. Then they were immersed in 100 mL of distilled water in a beaker at room temperature, covered with paraffin film and kept for 24 h. Then films were removed from the beaker and dried again at 105 °C for 24 h to determine final dry matter. The WS was calculated by the following equation:

$$\text{WS} = [(W_i - W_f) / W_f] \times 100 \quad \text{(Eq. 3.2)}$$

Where,  $W_i$  and  $W_f$  are the weight of the initial and final dry matter of the films, respectively.

### **3.6.10. Mechanical properties of the films**

Tensile strength (TS), tensile modulus (TM) and elongation at break (Eb) of the films were measured by using a universal testing machine (model H5KT, with a 1kN load cell, Tinius-Olsen, Horsham, USA). The samples were cut using ASTM procedure D638-99 and the film

thickness was measured using a Mitutoyo Digimatic Indicator (Type ID-110E; Mitutoyo Manufacturing Co. Ltd., Tokyo, Japan) at five random positions around the film. All the films were equilibrated at 4 °C and 90-100% RH prior to mechanical analysis.

### **3.6.11. Antimicrobial activity of the cross-linked films against *L. monocytogenes***

Following the *in vitro* and physico-chemical experiment, the concentration of genipin (0.05%) providing the maximum bioactivity at the end of the storage and mechanical properties, was used to prepare films with the previously presented nisin concentrations (18.65 to 2.33µg/cm<sup>2</sup>). The films were tested *in situ* (as described before) during storage of ham against *L. monocytogenes*.

### **3.4.12. Bacterial growth rate calculation**

The growth rate (B) of *L. monocytogenes* on ham samples can be described according to the Gompertz equation (Zwietering *et al.*, 1990), over duration of 35 days.

$$N_t = A + C \cdot \exp[-\exp\{-B(t-M)\}] \quad (\text{Eq. 3.3})$$

Where,

N<sub>t</sub>= microbial count (Log CFU/g at t)

A= lower asymptotic line of the growth curve (initial bacterial count).

C= Difference between upper asymptotic line (N<sub>max</sub>= maximum population level) and lower asymptotic line.

B= Relative maximum growth rate at time M

M= Time at which maximum growth rate is obtained

The bacterial growth data were analyzed using the program DMFit 3.0 for Microsoft Excel based on Baranyi & Roberts, (1994). The B of *L. monocytogenes* in control ham, ham covered with uncross-linked films (no genipin) and ham covered with cross-linked films in presence of 0.05% genipin were presented as B-ham, B-nisin and B-genipin, respectively.

### **3.6.13. Scanning Electron Microscopy (SEM)**

The SEM investigation of the film samples (5×5 mm<sup>2</sup>) were performed on an Environmental SEM (ESEM, Quanta 200 FEG, FEI Company Hillsboro, OR, USA) under low vacuum mode with an accelerating voltage of 20.0 kV and at 0°C temperature. ESEM eliminates the need for any conducting coating thus preventing any potential damage of the samples due to coating. The microscope was equipped with an energy dispersive X-ray (EDX) spectrometer (Genesis 2000, XMS System 60 with a Sapphire Si/Li detector from EDAX Inc. Mahwah, NJ, USA).

### **3.6.14. Statistical analysis**

All the *in situ* analysis was performed with three different meat samples (per day) for each film specimens and plated in three different Petri dishes. The swelling ratio, water solubility and *in vitro* assay were performed with three different film specimens and the average value was reported. The mechanical analysis was performed with six different film specimens and the average value was reported. An analysis of variance (ANOVA) and multiple comparison tests of Turkey's-b were used to compare all the results for each analysis together. Differences between means were considered significant when the confidence interval is smaller than 5% ( $P \leq 0.05$ ). The analysis was performed by the PASW Statistics 18 software (SPSS Inc., Chicago, IL, USA).

## **3.7. Results and Discussion**

### **3.7.1. Antimicrobial activity *in situ***

This experiment was designed to evaluate the antimicrobial efficacy of the films in a RTE ham system during storage. The growth of *L. monocytogenes* was exponential up to 21 days in the ham samples wrapped with control films (no nisin) and then the bacterial growth reached the

stationary phase with limited growth rate. After 35 days of storage there was no significant ( $P>0.05$ ) difference in the bacterial count between the control ham (ham without film) (8.42 log CFU/g) and control film (film without nisin) (8.54 log CFU/g) samples (**Figure-3.3**). The films containing 2.33  $\mu\text{g}/\text{cm}^2$  of nisin reduced the count of *L. monocytogenes* by 1.2 log CFU/g at day 1 but this film was not able to prevent the growth of the *L. monocytogenes* during storage. After 35 days of storage the level of *L. monocytogenes* on ham covered with the films containing 2.33, 4.65, 9.33, and 18.65  $\mu\text{g}/\text{cm}^2$  was 8.7, 7.47, 3.32 and 1.7 log CFU/g, respectively. As a result, the count of *L. monocytogenes* was reduced by almost 0.95, 5.10, 6.72 log CFU/g respectively by the films containing 4.65, 9.33 and 18.65  $\mu\text{g}/\text{cm}^2$  of nisin after 35 days of storage, compared to the control meat samples. Also the films containing 18.65  $\mu\text{g}/\text{cm}^2$  completely inhibited the growth of *L. monocytogenes* during storage and the bacterial count was below the detection limit (1.7 log CFU/g). The antimicrobial films also increased the lag phase of *L. monocytogenes* on ham surface. According to Robinson *et al.* 1998, the lag phase of bacterial growth can be defined as the time interval between the inoculation of a bacterial culture and the time its growth rate is maximum. The lag phase can be measured as the point (days) at which the slope of the exponential phase of growth intercepts a horizontal line drawn from the initial cell concentration. The lag phase of *L. monocytogenes* increased from 7 to more than 35 days with the increase of nisin concentration from 2.33 to 18.65  $\mu\text{g}/\text{cm}^2$ . Other researchers have also reported antimicrobial activity of nisin against *L. monocytogenes* (Pawar *et al.*, 2000; Mangalassary *et al.*, 2008; Jin *et al.*, 2009). Nguyen *et al.* (2008) prepared bacterial cellulose films with 2500 IU/mL of absorbed nisin and tested the efficacy of the films on sausage meat against *L. monocytogenes*. The authors reported that the antimicrobial films reduced the population of *L. monocytogenes* by 2 log CFU/g, under refrigerated condition after 14 days of storage. Marcos *et al.* (2007) reported

the antimicrobial activity of alginate films containing 2000 AU/cm<sup>2</sup> of enteriocin (a bacteriocin) against *L. monocytogenes* on vacuum packed RTE ham samples. The antimicrobial films initially (up to day 15) inhibited the growth of *L. monocytogenes* but could not prevent the growth during long term storage. After 29 days of storage, the count of *L. monocytogenes* on RTE ham samples was 1.7 log CFU/g lower with antimicrobial films than that with the control films without nisin. Chitosan based films are also believed to have antimicrobial activity but, in this experiment, the control films could not prevent the growth of *L. monocytogenes*. The antimicrobial activity of chitosan is related to its molecular weight, degree of deacetylation, viscosity, pH, concentration of the solution, etc. and the activity varies against different microorganisms (Aider, 2010; Kim *et al.*, 2011; Rabea *et al.*, 2003). Also, the cationic amines of chitosan play an important role in its antimicrobial activity. The positively charged amines interact with the negatively charged bacterial cell membrane, causing a leakage of intracellular constituents (Kenawy *et al.*, 2007). However, in this experiment the chitosan-based nanocomposite films were treated with NaOH in order to make them insoluble. As a result, the positively charged amines were neutralized, thus diminishing their antimicrobial activity. Ouattara *et al.* (2004) also reported that neutralized chitosan films could not prevent bacterial growth when applied on the surface of processed meats. The authors suggested that dispersion of the chitosan molecules within the meat matrix is a prerequisite for the antimicrobial activity of chitosan. Foster & Butt, (2011) reported strong bactericidal activity of chitosan solution against *Staphylococcus aureus*, *Staphylococcus epidermidis* and *E. coli*; on the contrary the chitosan films made from the same solution did not exhibit any antimicrobial activity. The authors postulated that the antimicrobial activity of chitosan is due to surface-surface interaction between the chitosan chains and microbial cell walls.

The antimicrobial efficacy of the films containing nisin, observed in this study can be in part explained by the mechanism of nisin's surface adsorption. Nisin is an amphiphilic molecule containing hydrophobic and hydrophilic residues. The N-terminal part of nisin contains a large number of hydrophobic residues and the C-terminal part is considered to be hydrophilic due to the presence of positively charged lysine and histidine residues (Van de Ven *et al.*, 1991). During adsorption of nisin onto a hydrophilic surface like chitosan films, the hydrophilic part of nisin is oriented towards the film surface thus establishing enhanced surface-protein hydrophilic association and the hydrophobic part is oriented outwards (Bower *et al.*, 1995). Considering the orientation of nisin on the surface of the chitosan films, the “Barrel-stave” mechanism can be used to describe antimicrobial activity of nisin against *L. monocytogenes* (Li *et al.*, 2002). The “Barrel-stave” mechanism describes the bactericidal activity of individual peptide molecules oriented in such a way so that the hydrophilic amino acid residues are on the inside and their hydrophobic residues are facing outward. According to this mechanism, the N-terminal (hydrophobic) residues of nisin disrupt the cytoplasmic membrane of susceptible bacteria through the formation of pores in the membrane (Demel *et al.*, 1996; Moll *et al.*, 1996; Shai, 1999; Yeaman & Yount, 2003). So, the orientation of nisin on the surface of chitosan films plays a major role in the antimicrobial activity of the films and the “Barrel-stave” model helps to explain the mechanism of bactericidal action.

### **3.7.2. Spectroscopic analysis of the films**

ATR-FTIR analysis was performed to characterize and determine changes in the infrared bands related to the nisin immobilization and genipin cross-linking of the film. The FTIR spectra of the nanocomposite films with surface immobilized nisin (uncross-linked) are presented in **Figure-3.4**. The spectra revealed characteristic changes in the region of 1750-850  $\text{cm}^{-1}$  due to the incorporation of nisin, as compared to the chitosan based control (no nisin) films. The spectra of

the control film (**Figure-3.4a**) revealed characteristics band at  $1640\text{ cm}^{-1}$  (correspond to Amide I, C=O stretch combined with N-H deformation in amides),  $1560\text{ cm}^{-1}$  (correspond to Amide II, N-H deformation in amides combined with  $-\text{NH}_3^+$  deformation),  $1402\text{ cm}^{-1}$  (correspond to Amide III band, C-N stretch in primary amides combined with  $\text{COO}^-$  symmetric stretch in carboxylic acid salts),  $1335\text{ cm}^{-1}$  (correspond to  $-\text{CH}_3$  symmetric deformation),  $1150\text{ cm}^{-1}$  (correspond to anti-symmetric CH-O-H stretch in secondary alcohols),  $1060\text{ cm}^{-1}$  (correspond to C-O stretch in primary and cyclic alcohols), and at  $1030\text{ cm}^{-1}$  (correspond to carbon ring in cyclic compounds) (Wu *et al.*, 2013; Khan *et al.*, 2012; Le Tien *et al.*, 2003). The absorbance of the Amide I, II and III band increased with increase in nisin concentration (**Figure-3.4b and c**), indicating immobilization of nisin onto film surface (Sebti *et al.*, 2003). A shift of the Amide II band towards lower wavenumber ( $1560$  to  $1535\text{ cm}^{-1}$ ) was also observed. This shift suggested possible hydrogen bonding-induced stabilization of the films in the presence of nisin (Mathew *et al.*, 2006). The appearance of a new band at  $1442\text{ cm}^{-1}$  (correspond to  $-\text{CH}_2$  scissors deformation) for the films with  $18.65\text{ }\mu\text{g}/\text{cm}^2$  of nisin (**Figure-3.4c**), could be due to the amino acid residues in nisin. The decrease in the absorbance of the characteristic saccharide bands (such as,  $1150$ ,  $1060$ ,  $1025\text{ cm}^{-1}$ ) at high nisin concentration ( $18.65\text{ }\mu\text{g}/\text{cm}^2$ ), possibly due to the masking of the resonance, provide further evidence of surface immobilization of nisin.

The spectra of the genipin-nisin cross-linked films were compared with those of the uncross-linked films (**Figure-3.5**) and revealed some interesting changes that were used to explain the reaction mechanism of genipin cross-linking. The absorbance of the Amide II ( $1535\text{ cm}^{-1}$ ) and III ( $1402\text{ cm}^{-1}$ ) band decreased with the increase in genipin concentration, whereas the absorbance of the Amide I band ( $1640\text{ cm}^{-1}$ ) remained constant for all samples. As a result, the ratio of Amide I/Amide II band absorbance increased with the increase in genipin concentration. The

absorbance of the  $\text{-CH}_2$  band ( $1442\text{ cm}^{-1}$ ) decreased whereas, the absorbance of bands at  $1060$  and  $1025\text{ cm}^{-1}$  increased with genipin cross-linking. According to literature (Mi *et al.*, 2000; Mi & Sung, 2002), genipin undergoes two different cross-linking reaction involving two different sites on its structure. One of the reaction mechanisms is the nucleophilic substitution of the ester group of genipin by primary amine group leading to the formation of secondary amide linkage (mechanism I). The decrease in the absorbance of the Amide II band suggested formation of secondary amide linkage between genipin and surface immobilized nisin (Mi *et al.*, 2000). While the other reaction mechanism is the ring opening reaction of the genipin molecule at C-3 position leading to the formation of a heterocyclic cross-linked compound (mechanism II). The ring opening reaction begins with a nucleophilic attack by the amino group on the C-3 carbon atom of genipin and formation of an intermediate aldehyde group. It proceeds further through the opening of the dehydropyran ring of genipin, followed by attack on the intermediate aldehyde group by the secondary amine group leading to the formation of a bifunctional heterocyclic compound (Butler *et al.*, 2003). The increase in the absorbance ratio of Amide I/Amide II band indicated formation of tertiary amide (heterocyclic pyridine derivative) linkage between genipin and the surface immobilized nisin (Chiono *et al.*, 2008). The decrease of Amide III band correlated with genipin cross-linking could be due to a decrease of primary amides into secondary amides and tertiary amides. The increase in absorbance at  $1060$  and  $1025\text{ cm}^{-1}$  could be related to the presence of genipin functional groups. Thus the decrease in Amide II and III band coupled by the increase in the absorbance of Amide I/Amide II band allowed confirming the cross-linking of genipin via primary amino groups of surface immobilized nisin to form secondary amide linkage and the formation of bifunctional heterocyclic compounds after ring opening reaction.

### 3.7.3. Effect of genipin cross-linking on the bioactivity of nisin during storage

The nanocomposite films containing  $18.65 \mu\text{g}/\text{cm}^2$  was considered as optimized nisin concentration as it completely inhibited the growth of *L. monocytogenes* during storage and was chosen for the characterization of genipin cross-linked films. The *in vitro* bioactivity of the films is presented in **Figure-3.6a**. At day 1, the inhibition area of the film formulations G, G0.05, G0.1, G0.3 and G0.4 were 11.43, 4.89, 5.08, 5.17 and  $2.35 \text{ cm}^2$ , respectively. Initially, the bioactivity of the genipin cross-linked films was significantly lower ( $P \leq 0.05$ ), compared to the uncross-linked films regardless of the genipin concentration. The bioactivity of the films (uncross-linked and cross-linked) revealed an intriguing outcome during further storage days. The bioactivity of the uncross-linked films was stable up to 7 days but it started to decline after that and continued to decline in later days. At day 35, the inhibition area obtained from the uncross-linked films was  $8.04 \text{ cm}^2$ , which was significantly lower ( $P \leq 0.05$ ) than that of the films cross-linked with 0.05% genipin ( $10.84 \text{ cm}^2$ ). The inhibition area of the films was correlated with the standard curve (**Figure-3.6b**) to calculate the available nisin remaining in all the films formulation (G0, G0.5, G0.1, and G0.4). The standard curve fitted the experimental data well, as the regression coefficient ( $R^2$ ) of the curve was found to be 0.99. The estimated available nisin content in the films during storage was calculated from the standard equation (Eq. 3.4) and is presented in **Figure-3.6c**.

$$Y = 0.0009X^4 - 0.0264X^3 + 0.2956X^2 - 0.243X + 0.0335 \quad (\text{Eq. 3.4})$$

Where, Y is the available nisin content in the films and X is the inhibition area.

Similar to the inhibition zones, the initial nisin content in the cross-linked films seemed to be lower than that of the uncross-linked films. At day 1, the nisin content of the uncross-linked films was  $11.81 \mu\text{g}/\text{cm}^2$  whereas the nisin of the films cross-linked with 0.05, 0.1, 0.2 and 0.4% of genipin were 3.34, 3.57, 3.68 and  $0.78 \mu\text{g}/\text{cm}^2$ , respectively. However, the nisin content of the

uncross-linked films decreased during storage and after 35 days of storage the nisin content was  $7.23 \mu\text{g}/\text{cm}^2$ . So, the nisin content, after 35 days, was almost 40% lower than its initial content. Bi *et al.* (2011) have also reported depletion of nisin activity during storage. It is very interesting to note that contrary to the uncross-linked films, the bioactivity of the films cross-linked with 0.05, 0.1, and 0.2% of genipin increased during storage. Despite having low initial bioactivity, films cross-linked with 0.05% genipin exhibited the highest bioactivity ( $10.89 \mu\text{g}/\text{cm}^2$ ) at the end of the storage experiment. At day 35, the nisin content of the 0.05% genipin films were significantly higher ( $P < 0.05$ ) than both the uncross-linked and 0.1% genipin cross-linked films. The reason behind the initial low activity of the cross-linked films could be due to the immobilization of the nisin on to the surface of the films as a result of cross-linking. Sebti *et al.* (2003) also reported low activity of the cross-linked nisin-hydroxypropylmethylcellulose (HPMC) films compared to the uncross-linked nisin-HPMC films. Genipin undergoes pH dependent cross-linking reaction with primary amine groups. At pH 3, genipin will have weak interaction with the protonated lysine and histidine residues present at the C-terminal position of nisin. When the genipin-nisin formulation was applied on the surface of the chitosan films, the neutralized chitosan surface favored the ring opening polymerization reaction of genipin (Mi *et al.*, 2005; Buonocore *et al.*, 2003). So, it can be hypothesized that one of the sites of genipin reacted with the chitosan backbone, while the other sites reacted with the nisin thus immobilizing nisin on the surface of the films (**Figure-3.7**). FTIR spectra also confirmed the formation of heterocyclic genipin-surface immobilized nisin cross-linked network. The increase in the activity of the films cross-linked with low genipin concentration can be attributed to the storage condition (in 90-100% RH) of the films. The high RH caused chain-relaxation of the genipin-chitosan cross-linked network as a result more nisin was available on the surface of the films

((Mi *et al.*, 2000). Balaguer *et al.* (2013) have also reported that RH induced release of nisin from cross-linked gelatin films. Films cross-linked with 0.4% genipin showed very negligible bioactivity throughout experiment. The reason could be due to the use of high concentration of cross-linking agent. With the increase of cross-linking agent, more active sites are available to link with the chitosan surface and nisin, as a result nisin was irreversibly immobilized by the cross-linked network. From this study, it could be suggested that low concentration of genipin can be used to cross-link and protect the activity of nisin during storage. Thus, films prepared or cross-linked with a natural cross-linking agent like genipin can offer effective inhibition of micro-organism in food by slow diffusion of the antimicrobial agents

#### **3.7.4. Swelling ratio and water solubility of the films**

The swelling behavior of the films as a function of time is presented in **Figure-3.8(a)**. The swelling ratio (SR) of the films uncross-linked films increased up to 8h and reached equilibrium thereafter. Genipin cross-linking decreased the SR of the surface films and there were significant difference ( $P \leq 0.05$ ) in the SR between the uncross-linked and films cross-linked with 0.1 to 0.4% genipin. After 24 h the SR of the uncross-linked films was 114%, whereas the SR of the 0.1, 0.2 and 0.4% genipin cross-linked films were 54, 64 and 64% ( $P \leq 0.05$ ), respectively. These results showed that incorporation of 0.1% genipin was enough to reduce the SR of films by more than half of its original value. The decrease in the SR of the genipin cross-linked films could be due to the formation of genipin-chitosan-nisin cross-linked network, as described previously. However, higher concentration of genipin (0.2 and 0.4%) could not decrease the SR more because genipin was applied on the surface of the films so it could react and form cross-link network only with the outer surface. Yuan *et al.*, (2007) have reported significant decrease in the SR of the chitosan microspheres due to genipin cross-linking.

The water solubility (WS) of the films is presented in **Figure-3.8(b)**. WS is a very important parameter in the context of food packaging as it makes it possible to predict the stability of the films requiring high water resistance. The higher WS of the uncross-linked nisin films could be due to the depletion of surface adsorbed nisin when kept under water for 24 hr. As the nisin is depleted from the surface, the films lost weight hence the higher WS values. The WS of the surface immobilized nisin films decreased significantly ( $P \leq 0.05$ ) with the incorporation of only 0.05% of genipin, as a result genipin cross-linking improved the stability of the films. However, increase of genipin concentration did not reduce the WS further. Jin *et al.*<sup>18</sup> (2004) have reported improvement in the stability of chitosan/PEO blends films due to genipin cross-linking.

### **3.7.6. Mechanical properties of the films**

Tensile strength is related to the mechanical strength of films whereas the tensile modulus and elongation at break is related to the rigidity and flexibility of the films respectively. The tensile strength, tensile modulus and elongation at break (Eb%) of the uncross-linked (nisin control) and cross-linked with 0.05, 0.1, 0.2 and 0.4% of genipin are presented in **Table-3.1**. The tensile strength and modulus of the films increased significantly ( $P < 0.05$ ) with the incorporation of only 0.05% of genipin. These values are in accordance with Jin *et al.* (2004), where the authors have reported improvement of the mechanical strength of the films due to genipin cross-linking. Other authors such as, Nunes *et al.*, (2013) have reported no significant improvement of the mechanical properties of the chitosan-caffeic acid films due to genipin cross-linking. Qiu *et al.* (2013) reported significant ( $P < 0.05$ ) increase in the compressive elastic modulus of the porcine acellular dermal matrix due to cross-linking with different genipin concentration (0.025 to 0.5%). It is interesting to note that in the current study, both the tensile strength and modulus of the films decreased with high genipin concentration (0.1 to 0.4%). It is interesting to note that both the tensile strength and modulus of the films decreased with high genipin concentration (0.1 to

0.4%). The decrease in the mechanical properties of the films at high genipin concentration could be attributed to the higher heterogeneity on the surface of the films as a result of cross-linking (Rioux *et al.*, 2002). Films cross-linked with high concentration of genipin also exhibited very low bioactivity during the storage experiment. High genipin cross-linking had a positive effect on the flexibility as films cross-linked with 0.2 and 0.4% of genipin significantly ( $P \leq 0.05$ ) improved the flexibility (Eb%) of the films.

### **3.7.7. Antimicrobial activity of the cross-linked films against *L. monocytogenes***

The bacterial growth rate (B) calculation was performed in order to evaluate the effect on genipin cross-linking against *L. monocytogenes* and the results are presented in **Figure-3.9**. It was observed that regardless of the concentration of the nisin, all the antimicrobial films (both the uncross-linked and cross-linked) reduced the B of *L. monocytogenes*, as compared to the control meat samples. The B decreased linearly with the increase in nisin concentration. The B for the control meat samples (B–meat) was 0.28 log CFU/g/day. The growth rate for the films with 18.65  $\mu\text{g}/\text{cm}^2$  of nisin (both the uncross-linked and cross-linked) were 0 log CFU/g/day as they completely inhibited the growth of *L. monocytogenes*. It was interesting to compare the B of the uncross-linked films (B-nisin) with that of cross-linked (B-genipin) films. The B of *L. monocytogenes* was lower for the cross-linked films (with 4.65 and 2.33  $\mu\text{g}/\text{cm}^2$  of nisin) than that of the uncross-linked films at the same nisin concentration. For example, the B of the cross-linked films containing 4.65  $\mu\text{g}/\text{cm}^2$  of nisin (0.15 log CFU/g/day) was 21% lower than that of the uncross-linked films (0.19 log CFU/g/day). The low activity of the un-cross-linked films may have resulted from the enzymatic degradation of nisin due to the interaction with meat components such as, glutathione (Stergiou *et al.*, 2006). The improved antimicrobial activity of

the cross-linked films could be attributed to the better retention of the bioactivity of nisin as a result of cross-linking.

### **3.7.8. Surface morphology of the films**

The surface morphology of the films was analyzed by Scanning electron microscopy (SEM). The surface of the control nanocomposite films (no nisin) revealed a smooth and homogeneous morphology with few white dots (**Figure-3.10a**). The white dots could correspond to the presence of CNC in the films (Khan *et al.*, 2012). An alternation in the surface morphology of films was observed with the increase in nisin concentration from 2.33  $\mu\text{g}/\text{cm}^2$  to 18.65  $\mu\text{g}/\text{cm}^2$ . As the nisin concentration increased the films surface became rougher (**Figure-3.10 b & c**). The increase roughness could be due to the deposition of salt crystals (present in nisin) on the surface of the films. Also, an increase in the quantity of nisin granules adsorbed on the surface of the films was observed. Santiago-Silva *et al.* (2009) have also reported similar changes in the surface morphology of the biopolymeric films due to bacteriocin incorporation. The micrograph of genipin cross-linked films revealed interesting changes in the surface morphology (**Figure-3.10d**). The cross-linked films appeared have fewer granules and seemed to be linked by a continuous surface layer, which could arise due to the formation of heterocyclic cross-linked network between genipin and the surface immobilized nisin. The improvement in the WS (observed previously) of the films could be attributed to this cross-linked layer (Nunes *et al.*, 2013).

## **3.8. Conclusion**

This study has demonstrated the effectiveness of the antimicrobial nanocomposite films to inhibit the growth of pathogenic bacteria in meat products. The antimicrobial activity was attributed to the orientation and adsorption of nisin on the surface of the nanocomposite films. Cross-linking

with low genipin concentration (0.05%) allowed a slow diffusion of nisin from the films and protected its bioactivity during extreme storage condition. Genipin cross-linking improved the water resistance and mechanical strength of the films. The cross-linked films also demonstrated better antimicrobial activity against *L. monocytogenes* compared to the uncross-linked films, by reducing the growth rate of the bacteria in meat samples. This naturally cross-linked nanocomposite films should have high potential to ensure the safety of vacuum packaged RTE deli meat during extended exposure. Further work is necessary to determine if such antimicrobial nanocomposite films could be produced on a larger scale.

### **3.9. Acknowledgements**

This research was supported by the Natural Sciences and Engineering Research Council of Canada (NSERC) and by FPInnovations (Pointe-Claire, Canada) through the RDC program. The authors highly appreciate SEM support from Mrs. Line Mongeon, Technician of the Biomedical Engineering Department and the Facility Electron Microscopy Research (FEMR) at McGill University. The authors would also like to thank Nordion Inc. for irradiation procedures.

### **3.10. References**

- Aider, M. (2010). Chitosan application for active bio-based films production and potential in the food industry: Review. *LWT - Food Science and Technology*, 43(6), 837–842.
- Appendini, P., & Hotchkiss, J. H. (2002). Review of antimicrobial food packaging. *Innovative Food Science and Emerging Technologies*, 3: 113-126.
- Balaguer, M. P., Borne, M., Chalier, P., Gontard, N., Morel, M-H., Peyron, S., Gavara, R., Hernandez-Munoz, P. (2013). Retention and release of cinnamaldehyde from wheat protein matrices. *Biomacromolecules*, 14(5): 1493–1502.

- Baranyi, J., & Roberts, T. A. (1994). A dynamic approach to predicting bacterial growth in food. *International Journal of Food Microbiology*, 23(3-4), 277–294.
- Benech, R., & Kheadr, E. (2002). Antibacterial activities of nisin Z encapsulated in liposomes or produced in situ by mixed culture during cheddar cheese ripening. *Applied and Environmental Microbiology*, 68(11): 5607–5619.
- Bi, L., Yang, L., Bhunia, A. K., & Yao, Y. (2011). Carbohydrate nanoparticle-mediated colloidal assembly for prolonged efficacy of bacteriocin against food pathogen. *Biotechnology and bioengineering*, 108(7): 1529–1536.
- Bigi, a, Cojazzi, G., Panzavolta, S., Roveri, N., & Rubini, K. (2002). Stabilization of gelatin films by crosslinking with genipin. *Biomaterials*, 23(24): 4827–4832.
- Bower, C. K., McGuire, J., & Daeschel, M. A. (1995). Influences on the antimicrobial activity of surface-adsorbed nisin. *Journal of industrial microbiology*, 15(3): 227–233.
- Buonocore, G. G., Del Nobile, M. a, Panizza, a, Corbo, M. R., & Nicolais, L. (2003). A general approach to describe the antimicrobial agent release from highly swellable films intended for food packaging applications. *Journal of controlled release*, 90(1): 97–107.
- Butler, M. F., Clark, A. H., & Adams, S. (2006). Swelling and mechanical properties of biopolymer hydrogels containing chitosan and bovine serum albumin. *Biomacromolecules*, 7(11): 2961–2970.

Butler, M. F., Ng, Y.-F., & Pudney, P. D. A. (2003). Mechanism and kinetics of the crosslinking reaction between biopolymers containing primary amine groups and genipin. *Journal of Polymer Science Part A: Polymer Chemistry*, 41(24): 3941–3953.

Chiono, V., Pulieri, E., Vozzi, G., Ciardelli, G., Ahluwalia, A., & Giusti, P. (2008). Genipin-crosslinked chitosan/gelatin blends for biomedical applications. *Journal of materials science: materials in medicine*, 19(2): 889–898.

Coma, V. (2008). Bioactive packaging technologies for extended shelf life of meat-based products. *Meat Science*, 78: 90–103.

Cooksey, K. (2005). Effectiveness of antimicrobial food packaging materials. *Food additives and contaminants*, 22: 980–987.

Darmadji, P., & Izumimoto, M. (1994). Effect of chitosan in meat preservation. *Meat Science*, 38(2): 243–254.

Davies, E. A, Bevis, H. E., Potter, R., Harris, J., Williams, G. C., & Delves-Broughton, J. (1998). Research note : The effect of pH on the stability of nisin solution during autoclaving. *Letters in Applied Microbiology*, 27(3): 186–188.

Delves-Broughton, J. (1990). Nisin and its application as a food preservative. *Journal of the Society of the Dairy Technology*, 43, 73–76.

Demel, R. A, Peelen, T., Siezen, R. J., De Kruijff, B., & Kuipers, O. P. (1996). Nisin Z, mutant nisin Z and lactacin 481 interactions with anionic lipids correlate with antimicrobial activity. A monolayer study. *European journal of biochemistry*, 235(1-2): 267–274.

Foster, L. J. R., & Butt, J. (2011). Chitosan films are NOT antimicrobial. *Biotechnology letters*, 33(2): 417-421.

Guiga, W., Swesi, Y., Galland, S., Peyrol, E., Degraeve, P., & Sebti, I. (2010). Innovative multilayer antimicrobial films made with Nisaplin® or nisin and cellulosic ethers: Physico-chemical characterization, bioactivity and nisin desorption kinetics. *Innovative Food Science & Emerging Technologies*, 11(2): 352–360.

Harris, R., Lecumberri, E., & Heras, A. (2010). Chitosan-genipin microspheres for the controlled release of drugs: clarithromycin, tramadol and heparin. *Marine drugs*, 8(6): 1750–1762.

Jin, J., Song, M., & Hourston, D. J. (2004). Novel chitosan-based films cross-linked by genipin with improved physical properties. *Biomacromolecules*, 5(1): 162–168.

Jin, T., Liu, L., Zhang, H., & Hicks, K. (2009). Antimicrobial activity of nisin incorporated in pectin and polylactic acid composite films against *Listeria monocytogenes*. *International Journal of Food Science & Technology*, 44(2): 322–329.

Kenawy, E.-R., Worley, S. D., & Broughton, R. (2007). The chemistry and applications of antimicrobial polymers: a state-of-the-art review. *Biomacromolecules*, 8(5): 1359–1384.

Khan, A., Huq, T., Khan, R. a., Riedl, B., & Lacroix, M. (2014). Nanocellulose-based composites and bioactive agents for food packaging. *Critical Reviews in Food Science and Nutrition*, 54(2): 163–174.

Khan, A., Khan, R. A., Salmieri, S., Le Tien, C., Riedl, B., Bouchard, J., Chauve, G., Victor, T., Kamal, M. R., & Lacroix, M. (2012). Mechanical and barrier properties of nanocrystalline

cellulose reinforced chitosan based nanocomposite films. *Carbohydrate Polymers*, 90(4): 1601–1608.

Kim, K. W., Min, B. J., Kim, Y.-T., Kimmel, R. M., Cooksey, K., & Park, S. I. (2011). Antimicrobial activity against foodborne pathogens of chitosan biopolymer films of different molecular weights. *LWT - Food Science and Technology*, 44(2): 565-569.

Le Tien, C., Lacroix, M., Ispas-Szabo, P., & Mateescu, M.-A. (2003). N-acylated chitosan: hydrophobic matrices for controlled drug release. *Journal of Controlled Release*, 93(1): 1–13.

Li, J., Chikindas, M. L., Ludescher, R. D., & Montville, T. J. (2002). Temperature- and Surfactant-Induced Membrane Modifications That Alter *Listeria monocytogenes* Nisin Sensitivity by Different Mechanisms. *Applied and Environmental Microbiology*, 68(12): 5904–5910.

Li, Q., Zhou, J., & Zhang, L. (2009). Structure and properties of the nanocomposite films of chitosan reinforced with cellulose whiskers. *Journal of Polymer Science Part B: Polymer Physics*, 47(11): 1069–1077.

Mangalassary, S., Han, I., Rieck, J., Acton, J., & Dawson, P. (2008). Effect of combining nisin and/or lysozyme with in-package pasteurization for control of *Listeria monocytogenes* in ready to-eat turkey bologna during refrigerated storage. *Food microbiology*, 25(7): 866–870.

Marcos, B., Aymerich, T., Monfort, J. M., & Garriga, M. (2007). Use of antimicrobial biodegradable packaging to control *Listeria monocytogenes* during storage of cooked ham. *International journal of food microbiology*, 120(1-2): 152–158.

Mathew, S., Brahmakumar, M., & Abraham, T. E. (2006). Microstructural imaging and characterization of the mechanical, chemical, thermal and swelling properties of starch-chitosan blend films. *Biopolymers*, 82: 176-187.

Mi, F.-L., Shyu, S.-S., & Peng, C.-K. (2005). Characterization of ring-opening polymerization of genipin and pH-dependent cross-linking reactions between chitosan and genipin. *Journal of Polymer Science Part A: Polymer Chemistry*, 43(10): 1985–2000.

Mi, F.-L., Sung, H.-W., & Shyu, S.-S. (2000). Synthesis and characterization of a novel chitosan-based network prepared using naturally occurring crosslinker. *Journal of Polymer Science Part A: Polymer Chemistry*, 38(15): 2804–2814.

Mi, F., & Sung, H. (2002). Drug release from chitosan-alginate complex beads reinforced by a naturally occurring cross-linking agent. *Carbohydrate Polymers*, 48 : 61–72.

Millette, M., Le Tien, C., Smoragiewicz, W., & Lacroix, M. (2007). Inhibition of *Staphylococcus aureus* on beef by nisin-containing modified alginate films and beads. *Food Control*, 18(7): 878–884.

Moll, G. N., Roberts, G. C. K., Konings, W. N., & Driessen, A. J. M. (1996). Mechanism of lantibiotic-induced pore-formation. *Antonie van Leeuwenhoek*, 69(2): 185–191.

Nguyen, V. T., Gidley, M. J., & Dykes, G. A. (2008). Potential of a nisin-containing bacterial cellulose film to inhibit *Listeria monocytogenes* on processed meats. *Food Microbiology*, 25(3): 471–478.

No, H. K., Meyers, S. P., Prinyawiwatkul, W., & Xu, Z. (2007). Applications of chitosan for improvement of quality and shelf life of foods: a review. *Journal of Food Science*, 72(5): R87-100.

Nunes, C., Maricato, É., Cunha, Â., Nunes, A., da Silva, J. A. L., & Coimbra, M. A. (2013). Chitosan-caffeic acid-genipin films presenting enhanced antioxidant activity and stability in acidic media. *Carbohydrate polymers*, 91(1): 236–243.

Ouattara, B., Simard, R. E., Piette, G., Bégin, A., & Holley, R. A. (2000). Inhibition of surface spoilage bacteria in processed meats by application of antimicrobial films prepared with chitosan. *International Journal of Food Microbiology*, 62(1-2), 139–148.

Pawar, D. D., Malik, S. V, Bhilegaonkar, K. N., & Barbuddhe, S. B. (2000). Effect of nisin and its combination with sodium chloride on the survival of *Listeria monocytogenes* added to raw buffalo meat mince. *Meat science*, 56(3): 215–219.

Prashanth, K.V.H., and Tharanathan, R.N., (2007). Chitin/chitosan: modifications and their unlimited application potential and overview. *Trends in Food Science & Technology*, 18: 117-131.

Qiu, J., Li, J., Wang, G., Zheng, L., Ren, N., Liu, H., Tang, W. Jiang, H. Wang, Y. (2013). In vitro investigation on the biodegradability and biocompatibility of genipin cross-linked porcine acellular dermal matrix with intrinsic fluorescence. *ACS Applied Materials & Interfaces*, 5(2), 344–50.

- Rabea, E. I., Badawy, M. E.-T., Stevens, C. V., Smagghe, G., & Steurbaut, W. (2003). Chitosan as antimicrobial agent: applications and mode of action. *Biomacromolecules*, *4*(6): 1457-1465.
- Revol, J.-F., Bradford, H., Giasson, J., Marchessault, R. H., & Gray, D. G. (1992). Helicoidal self-ordering of cellulose microfibrils in aqueous suspension. *International Journal of Biological Macromolecules*, *14*: 170-172.
- Rhim, J.-W. (2011). Effect of clay contents on mechanical and water vapor barrier properties of agar-based nanocomposite films. *Carbohydrate Polymers*, *86*(2): 691–699.
- Rioux, B., Ispas-Szabo, P., Aït-Kadi, A., Mateescu, M.-A., & Juhász, J. (2002). Structure–properties relationship in cross-linked high amylose starch cast films. *Carbohydrate Polymers*, *50*(4): 371–378.
- Robinson, T. P., Ocio, M. J., Kaloti, a, & Mackey, B. M. (1998). The effect of the growth environment on the lag phase of *Listeria monocytogenes*. *International journal of food microbiology*, *44*(1-2): 83–92.
- Rollema, H. S., Kuipers, O. P., Both, P., de Vos, W. M., & Siezen, R. J. (1995). Improvement of solubility and stability of the antimicrobial peptide nisin by protein engineering. *Applied and environmental microbiology*, *61*(8): 2873–2878.
- Roy, A., Kucukural, A., & Zhang, Y (2010). I-TASSER: a unified platform for automated protein structure and function prediction. *Nature Protocols*, *5*: 725-738.
- Roy, A., Yang, J., & Zhang, Y., (2012). COFACTOR: an accurate comparative algorithm for structure-based protein function annotation. *Nucleic Acids Research*, *40*: W471-W477.

Santiago-Silva, P., Soares, N. F. F., Nóbrega, J. E., Júnior, M. a. W., Barbosa, K. B. F., Volp, A. C. P., Zerdas, E. R. M. A., Würllitzer, N. J. (2009). Antimicrobial efficiency of film incorporated with pediocin (ALTA® 2351) on preservation of sliced ham. *Food Control*, 20(1): 85–89.

Scallan, E., Hoekstra, R. M., Angulo, F. J., Tauxe, R. V., Widdowson, M.-A., Roy, S. L., Jones, J. L., Griffin, P. M. (2011). Foodborne Illness Acquired in the United States—Major Pathogens. *Emerging Infectious Diseases*, 17(1), 7–15.

Sebti, I., Delves-Broughton, J., & Coma, V. (2003). Physicochemical properties and bioactivity of nisin-containing cross-linked hydroxypropylmethylcellulose films. *Journal of agricultural and food chemistry*, 51(22): 6468–6474.

Shai, Y. (1999). Mechanism of the binding, insertion and destabilization of phospholipid bilayer membranes by alpha-helical antimicrobial and cell non-selective membrane-lytic peptides. *Biochimica et biophysica acta*, 1462(1-2) : 55–70.

Song, F., Zhang, L.-M., Yang, C., & Yan, L. (2009). Genipin-crosslinked casein hydrogels for controlled drug delivery. *International journal of pharmaceutics*, 373(1-2): 41–47.

Stergiou, V. A., Thomas, L. V, & Adams, M. R. (2006). Interactions of nisin with glutathione in a model protein system and meat. *Journal of Food Protection*, 69(4), 951–6.

Sung, H.-W., Huang, R.-N., Huang, L. L. H., & Tsai, C.-C. (1999). In vitro evaluation of cytotoxicity of a naturally occurring cross-linking reagent for biological tissue fixation. *Journal of Biomaterials Science, Polymer Edition*, 10(1): 63–78.

Van de Ven, F. J., Van den Hooven, H. W., Konings, R. N., & Hilbers, C. W. (1991). NMR studies of lantibiotics. The structure of nisin in aqueous solution. *European journal of biochemistry*, 202(3): 1181–1188.

Wu, J., Zhong, F., Li, Y., Shoemaker, C. F., & Xia, W. (2013). Preparation and characterization of pullulan–chitosan and pullulan–carboxymethyl chitosan blended films. *Food Hydrocolloids*, 30(1): 82–91.

Yeaman, M. R., & Yount, N. Y. (2003). Mechanisms of antimicrobial peptide action and resistance. *Pharmacological reviews*, 55(1): 27–55.

Yuan, Y., Chesnutt, B. M., Utturkar, G., Haggard, W. O., Yang, Y., Ong, J. L., & Bumgardner, J. D. (2007). The effect of cross-linking of chitosan microspheres with genipin on protein release. *Carbohydrate Polymers*, 68(3): 561–567.

Zhang, Y (2008). I-TASSER server for protein 3D structure prediction. *BMC Bioinformatics*, 9:40.

Zwietering, M. H., Jongenburger, I., Rombouts, F. M., & Van 't Riet, K. (1990). Modeling of the bacterial growth curve. *Applied and Environmental Microbiology*, 56(6), 1875–81.

## Figures

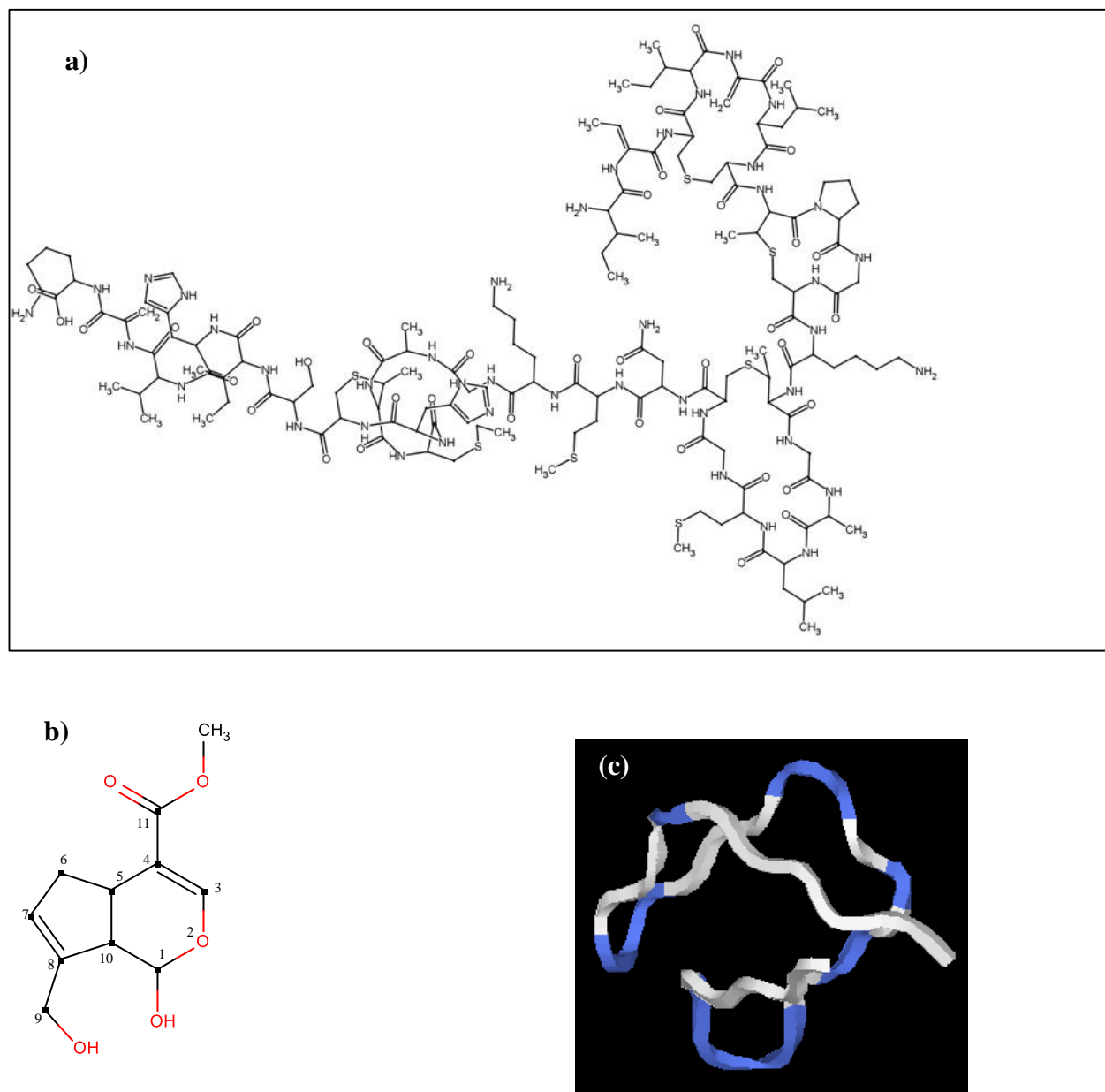


**Figure-3.1:** Chemical structure (a) and (b) genipin (drawn using MarvinSketch 6.2.0, 2014).. The secondary structure of (c) nisin was generated from the nisin peptide sequence using I-TASSER server (Zhang, 2008; Roy et al., 2010 and 2012).

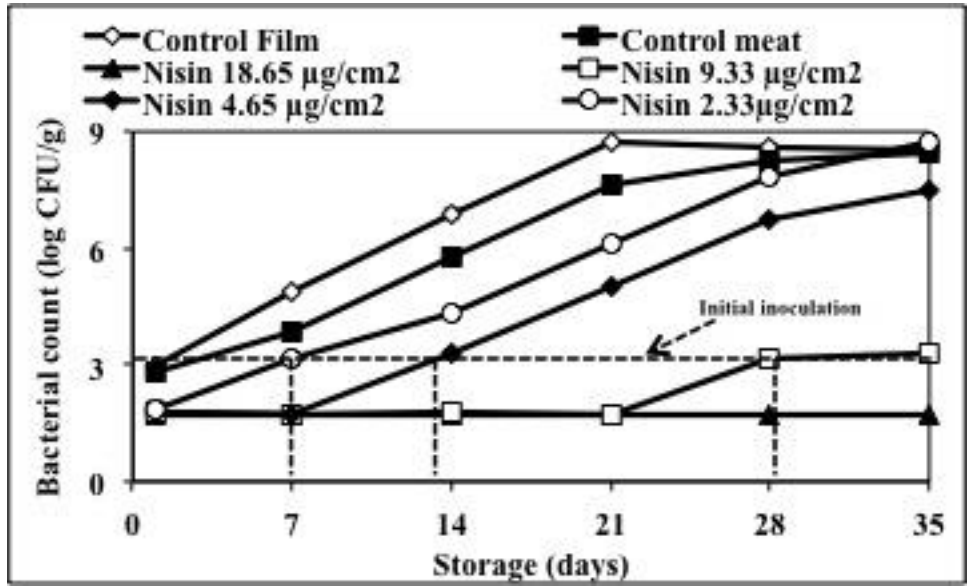


**Figure-3.3:** Antimicrobial activity of nisin films *in situ* against *L. monocytogenes* during storage at 4°C.

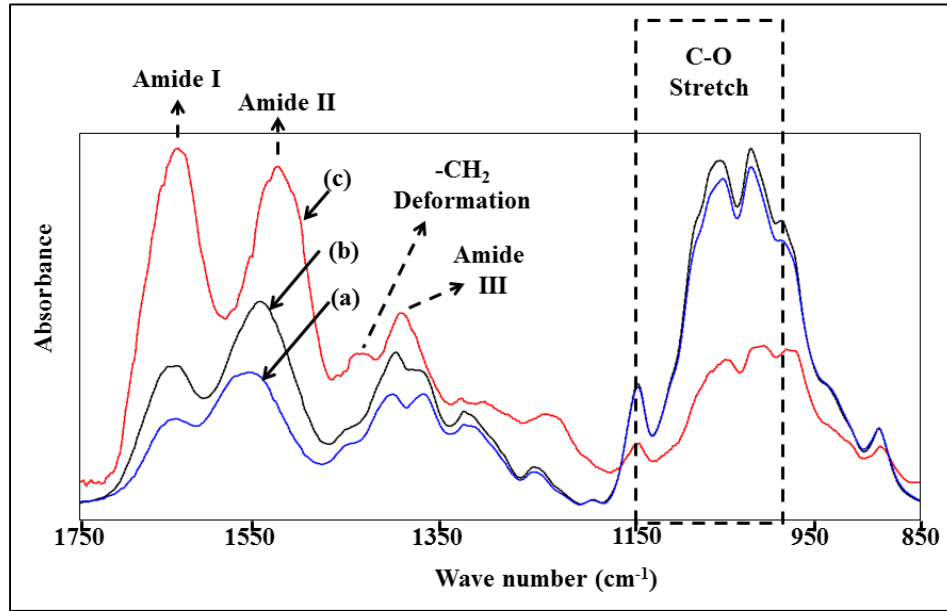


**Figure 3.4:** FT-IR spectra of the (a) control nanocomposite (no nisin) films, nanocomposite films containing (b) 2.33 and (c) 18.65  $\mu\text{g}/\text{cm}^2$  nisin.

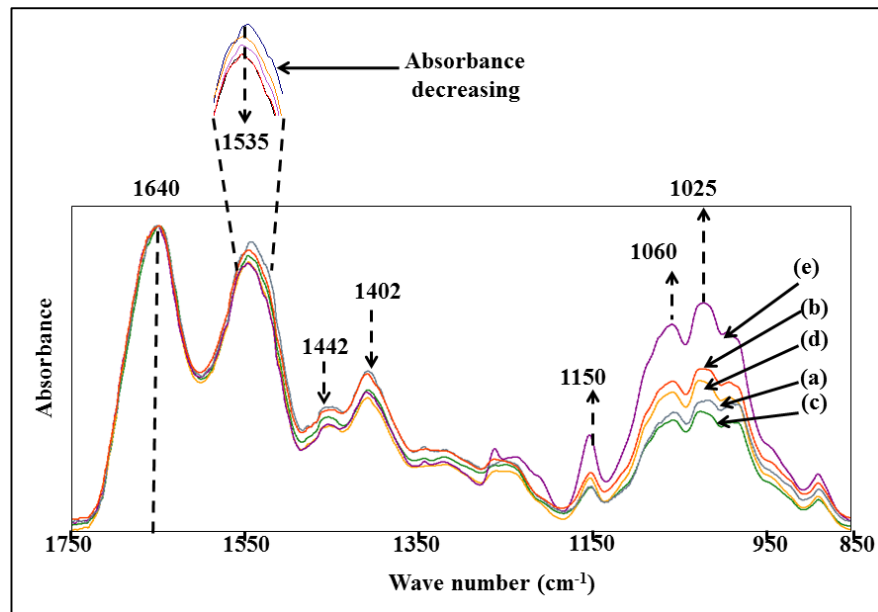


**Figure 3.5:** FT-IR spectra of the (a) uncross-linked, (b) 0.05, (c) 0.1, (d) 0.2 and (e) 0.4% genipin cross-linked films.

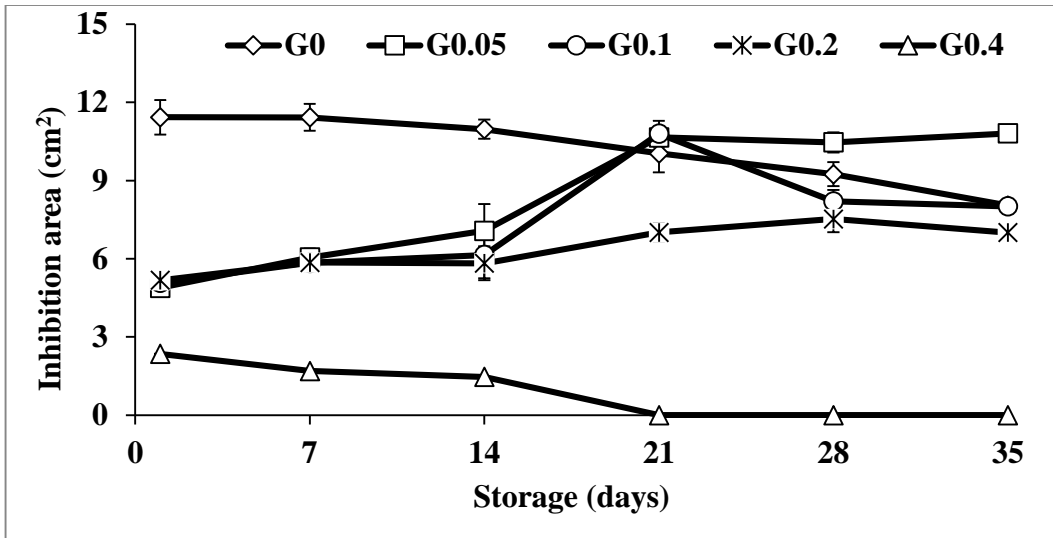


Figure-3.6 (a): The *in vitro* bioactivity of the films during storage at 4°C and 90-100% RH.

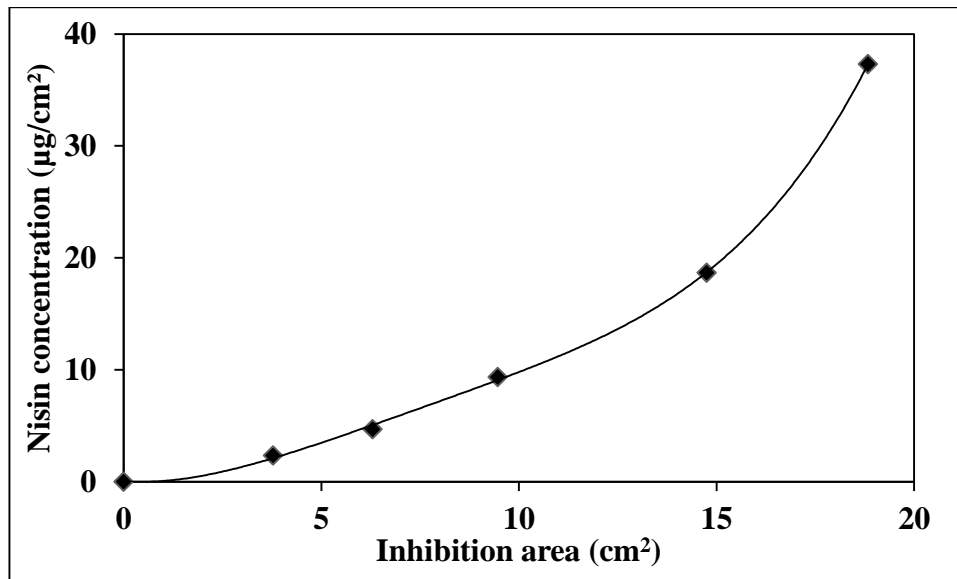
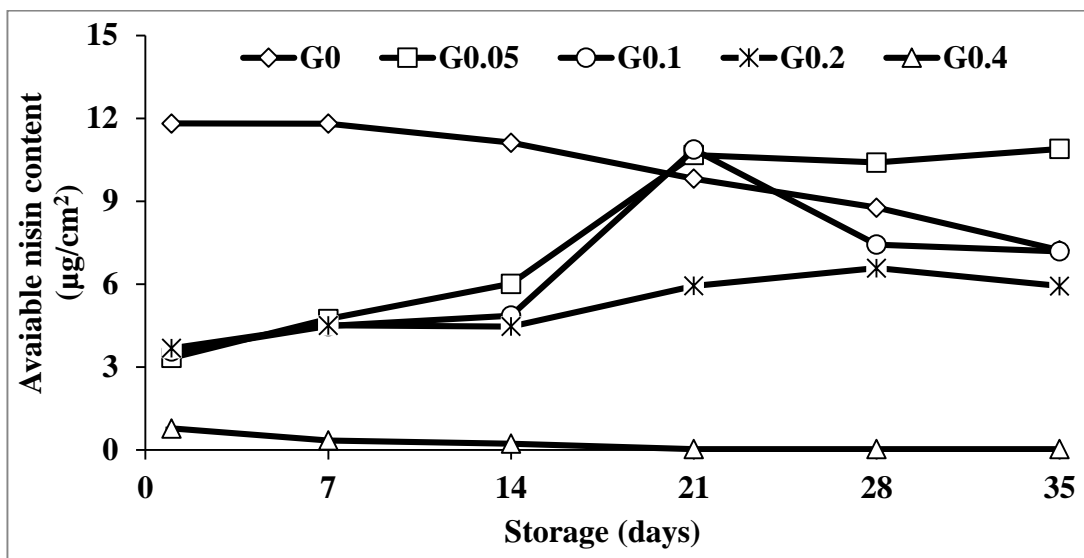
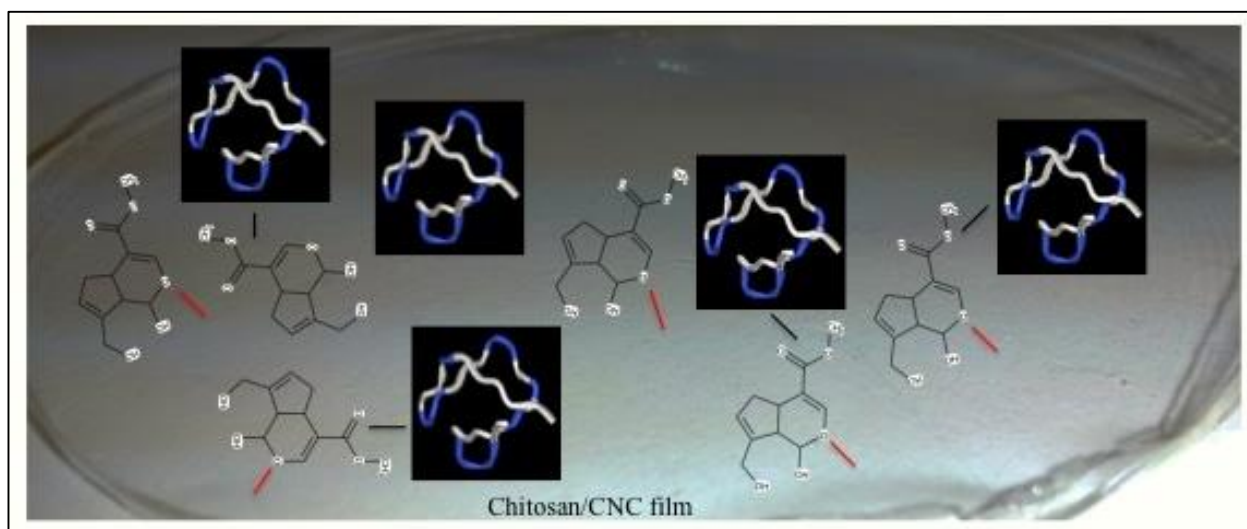


Figure-3.6 (b): A 4<sup>th</sup> order polynomial “standard curve” of inhibition area (cm<sup>2</sup>) versus nisin concentration (µg/cm<sup>2</sup>)



**Figure-3.6 (c):** Available nisin content of the films during storage at 4°C and 90-100% RH.



**Figure-3.7:** Schematic representation of the immobilization of nisin on the surface of the chitosan/CNC films due to genipin cross-linking. Black lines indicate possible linkage between nisin and genipin; red lines indicate possible linkage between genipin and chitosan.

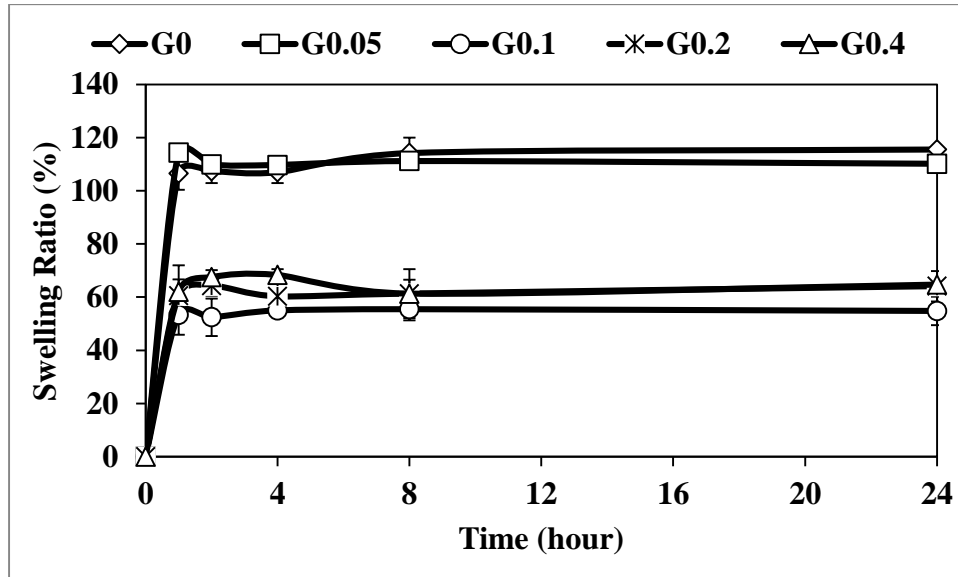


Figure-3.8 (a): The effect of the genipin concentration on the swelling ratio of the films.

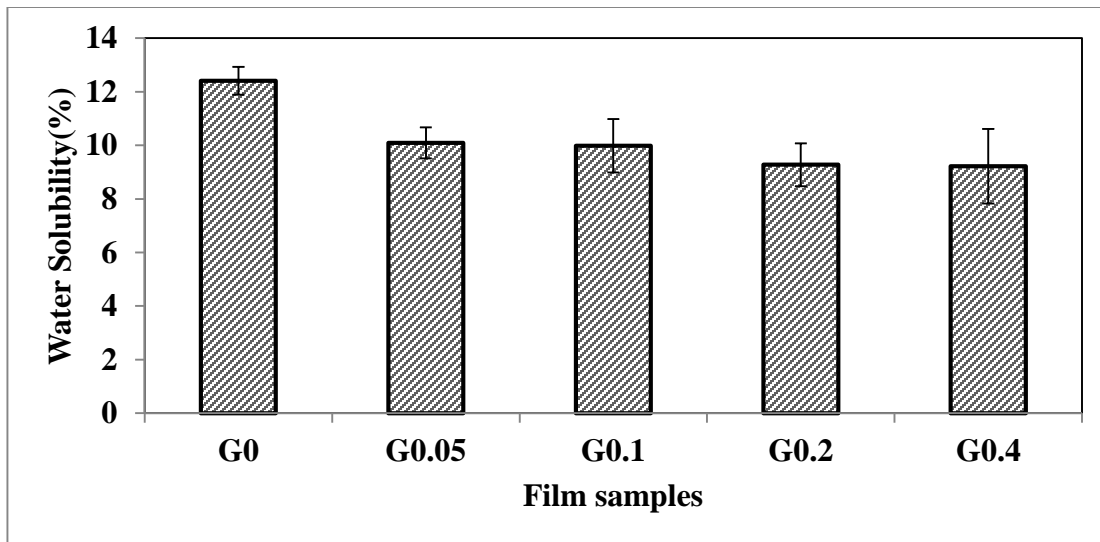
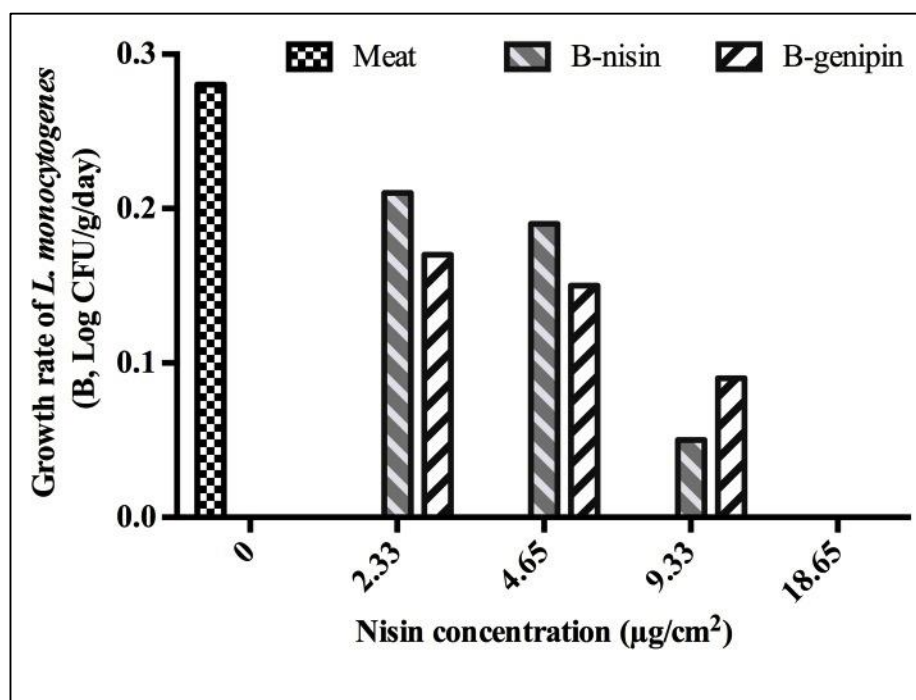


Figure-3.8 (b): Water solubility of the films.

**Table-3.1:** Effect of genipin concentration on the mechanical properties of films\*.

Film samples	Tensile strength (MPa)	Tensile modulus (GPa)	Elongation at break (%)
G0	110.0±5.1 <sup>b</sup>	2.99±0.26 <sup>c</sup>	22.5±2.0 <sup>a</sup>
G0.05	117.5±3.5 <sup>c</sup>	3.61±0.15 <sup>d</sup>	22.4±4.0 <sup>a</sup>
G0.1	108.0±5.3 <sup>b</sup>	2.48±0.29 <sup>b</sup>	21.1±4.0 <sup>a</sup>
G0.2	93.6±5.1 <sup>a</sup>	1.91±0.35 <sup>a</sup>	30.7±3.8 <sup>b</sup>
G0.4	99.1±5.5 <sup>a</sup>	2.15±0.12 <sup>a</sup>	30.6±7.0 <sup>b</sup>

\*Values are means ± standard deviations. Within each column, means with the same lowercase letter are not significantly different ( $P > 0.05$ ).

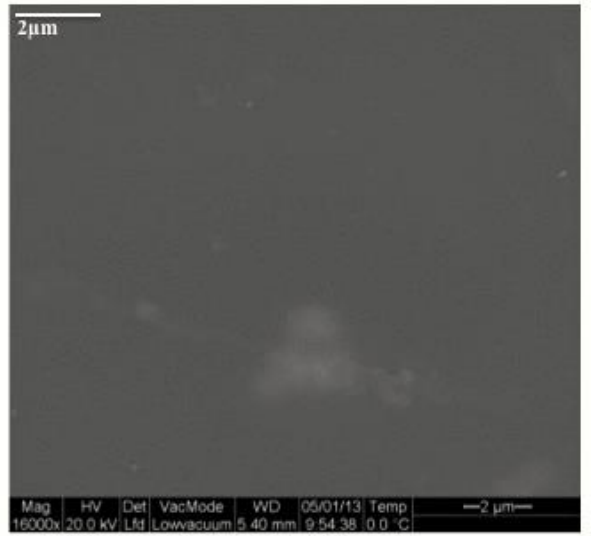
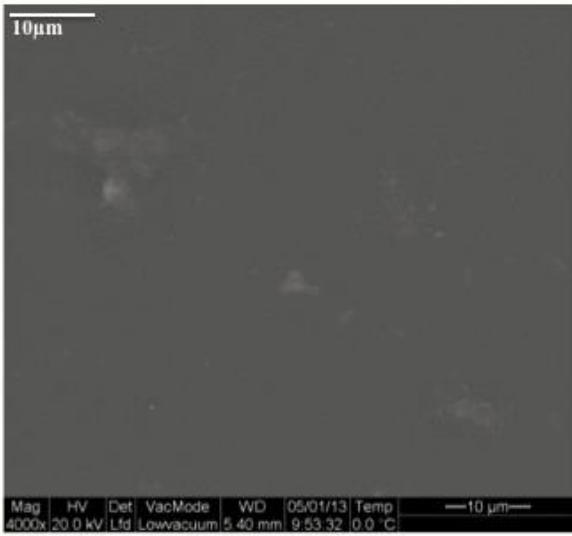


**Figure-3.9:** The effect of the genipin cross-linking on the growth rate of *L. monocytogenes*.

a)



b)



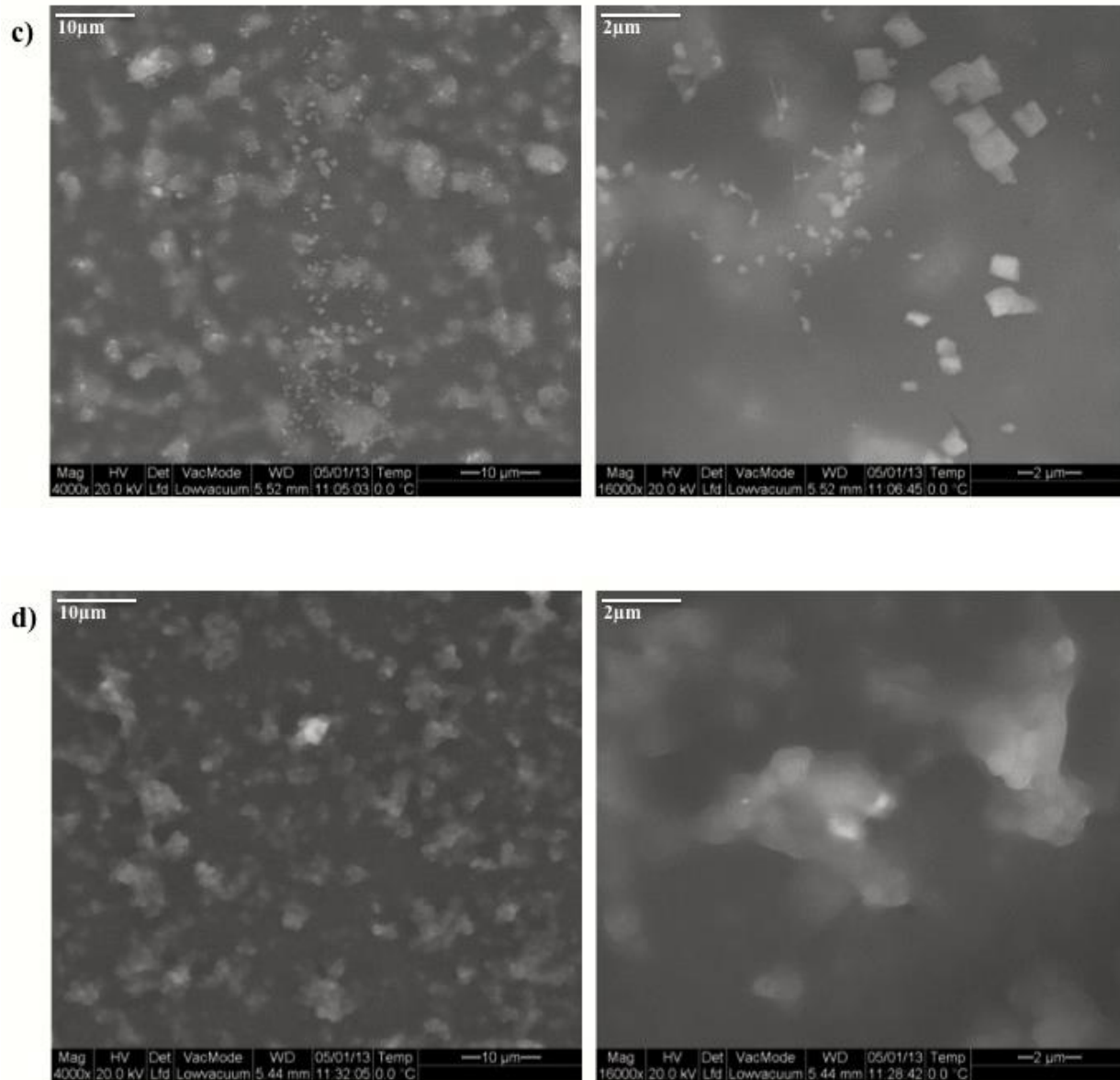


**Figure-3.10:** SEM micrographs of the surface of the a) control nanocomposite (no nisin), b) 2.33 μg/cm<sup>2</sup> nisin c) 18.65 μg/cm<sup>2</sup> nisin and d) 18.65 μg/cm<sup>2</sup> nisin films cross-linked with 0.05% genipin at two different magnification (4000x and 16000x).

### 3.11. General discussion of the Publication-2

In this publication, the antimicrobial CNC/chitosan films demonstrated excellent antimicrobial properties and films containing  $18.65 \mu\text{g}/\text{cm}^2$  of nisin completely inhibited the growth of *L. monocytogenes* during storage. Orientation of nisin on the surface of chitosan films played a major role in the antimicrobial activity of the films. The “Barrel-stave” model explained the mechanism of bactericidal action. Genipin has demonstrated high potential for the protection nisin’s bioactivity during storage. The optimum genipin concentration was found to be 0.05%. Genipin cross-linked films also reduced the swelling and the water solubility and improved mechanical properties of the nanocomposite films. As the growth rate *L. monocytogenes* in RTE meat was not linear, Gompertz function was used to describe and calculate the bacterial growth rate. The genipin cross-linked films reduced the growth rate of *L. monocytogenes* by 21% compared to the un-cross-linked films.

## **CHAPTER 4**

### **Publication 3**

# Optimization of microfluidization for the homogeneous distribution of cellulose nanocrystals (CNCs) in biopolymeric matrix

Avik Khan<sup>1</sup>, Khanh Dang Vu<sup>1</sup>, Gregory Chauve<sup>3</sup>, Jean Bouchard<sup>3</sup>, Bernard Riedl<sup>2</sup> and Monique Lacroix<sup>1\*</sup>

<sup>1</sup>Research Laboratories in Sciences Applied to Food, Canadian Irradiation Centre (CIC), INRS-Institut Armand-Frappier, Université du Québec, 531 Boulevard des Prairies, Laval, Québec, H7V 1B7, Canada

<sup>2</sup>Département des sciences du bois et de la forêt, Faculté de foresterie, géographie et géomatique, Université Laval, Québec-city, Québec, G1V 0A6, Canada

<sup>3</sup>FPIinnovations, 570 Boulevard St. Jean, Pointe-Claire, Québec, H9R 3J9, Canada

## KEYWORDS:

Chitosan, Cellulose nanocrystals, Bionanocomposite, Experimental design, High-pressure-homogenization, Mechanical property, Nanomaterial dispersion, Polyelectrolyte complex.

\* **Corresponding Author:** Prof. Monique Lacroix.

Telephone: +1-450-687-5010; Fax: +1-450-686-5501.

**E-mail:** [monique.lacroix@iaf.inrs.ca](mailto:monique.lacroix@iaf.inrs.ca)

This article is published in *Cellulose* (2014), 21:3457-3468.

#### **4.1. Contribution of the authors**

The experimental works were planned, performed and analyzed by Avik Khan with guidance from Prof. Monique Lacroix. The manuscript was written by Avik Khan. Prof. Monique Lacroix and Prof. Bernard Riedl corrected the main draft. Dr. Khanh Dang Vu helped to design the experimental model and gave valuable advice regarding the use of Response surface methodology. Dr. Gregory Chauve and Dr. Jean Bouchard corrected the main draft and gave valuable suggestions to improve the discussion.

## **4.2. Specific objectives of the Publication-3**

As already mentioned previously that conventional mechanical homogenization could not disperse even 1% CNC suspension into chitosan. In this publication, microfluidization was used to homogeneously distribute a concentrated CNC suspension (2% w/v in water) into chitosan matrix. Use of microfluidization for the dispersion of CNC represent a highly innovative approach and I have not found any similar studies to this day. RSM was used to systematically optimize the CNC concentration, microfluidization pressure and number of microfluidization cycles. RSM allowed optimization of these factors at the same time and eliminated the need for a large number of experimental runs that are otherwise required in a conventional one-factor-at-a-time optimization approach. The mechanical properties of the CNC reinforced chitosan based films were measured and used as an indirect measurement to estimate the homogeneity of CNC dispersion within the chitosan matrix.

### 4.3. Résumé

La microfluidisation, qui est une technique d'homogénéisation à haute pression, a été utilisée pour développer des films nanocomposites à base de chitosane, renforcés de cellulose nanocristalline (CNC) fortement dispersée. Une matrice statistique composite à trois facteurs centraux (CCD) avec cinq niveaux a été conçue et utilisée pour optimiser systématiquement le processus de microfluidisation. Les trois facteurs sont la teneur en CNC, la pression de la microfluidisation et le nombre de cycles de microfluidisation. La méthodologie dite "de surface de réponse" a été utilisée pour obtenir la relation entre les propriétés mécaniques des films nanocomposites et ces facteurs. Des équations polynomiales ont été générées sur la base de l'analyse de régression des facteurs et les propriétés prédites des films nanocomposites sont en bon accord avec les résultats expérimentaux. La microfluidisation permet de réduire efficacement les agrégats CNC-chitosane et d'améliorer les propriétés mécaniques des films nanocomposites. L'analyse microscopique des films nanocomposites microfluidisés a révélé une réduction de 10 à 15 fois de la taille des agrégats par rapport aux films de chitosane/non-microfluidisés CNC et une augmentation de la rugosité de surface (moyenne racine carrée,  $R_q$ ).

#### **4.4. Abstract**

Microfluidization, which is a high-pressure homogenization technique, was used to develop highly dispersed cellulose nanocrystal (CNC) reinforced chitosan based nanocomposite films. A three factor central composite design (CCD) with five levels was designed to systematically optimize the microfluidization process. The three factors were the CNC content, the microfluidization pressure and the number of microfluidization cycles. Response surface methodology was used to obtain relationship between the mechanical properties of the nanocomposite films and the factors. Polynomial equations were generated based on the regression analysis of the factors and the predicted properties of the nanocomposite films were in good agreement with the experimental results. Microfluidization effectively reduced the CNC-chitosan aggregates and improved the mechanical properties of the nanocomposite films. Microscopic analysis of the microfluidized nanocomposite films revealed a 10 to 15 times reduction in the size of the aggregates compared to the non-microfluidized CNC/chitosan films and an increase in the root mean square surface roughness (Rq).

#### **4.5. Introduction**

Cellulose constitutes the main structural component of plant cell walls and is the most abundant of the renewable polymers in nature. Cellulose based nanofiber such as Cellulose nanocrystal (CNC), is a prime example of nanofiber obtained from natural sources. CNCs are natural, non-toxic, highly crystalline, rod shaped nanoparticles that can be extracted through selective isolation from cellulosic sources by a controlled acid hydrolysis process and obtained as an aqueous suspension of nanocrystals (Moon *et al.*, 2011; Habibi *et al.*, 2010). The properties of the CNC suspension can be affected by the selection of acid used for the hydrolysis process. For example, sulfuric acid provides highly stable aqueous suspensions due to the grafting of negatively charged sulfate groups on the surface of the CNC whereas use of hydrochloric acid can lead to CNC with minimal surface charge (Beck-Candanedo *et al.*, 2005). The CNC extracted from bleached softwood pulp with a sulfuric acid hydrolysis exhibit an average length of 110 nm for a width of 5-10 nm (Dong *et al.*, 1998). The stability of CNC suspension is affected by the incorporation of electrolytes in the suspension. The electrolytes reduce the inter particle repulsion of CNC by partially screening the sulfate half-ester groups (Beck-Candanedo *et al.*, 2011). A high-pressure homogenization technique such as microfluidization can be adopted to achieve proper dispersion of the CNC within the polymer matrix. Microfluidization provides an innovative approach to develop processing paths that break down aggregates and maximizes CNC distribution within the polymeric matrix. The applications of a microfluidizer include development of highly stable nanoemulsion or nanodispersions, disruption of cells, micro/nano encapsulation of bioactive compounds in polymer, etc. (Jo and Kwon, 2013; Atalay *et al.*, 2011; Jafari *et al.*, 2007). Microfluidization has also been used effectively for the preparation of cellulose microfibrils from wood (Lee *et al.*, 2009; Zimmermann *et al.*, 2004) and non-wood pulp (Ferrer *et al.*, 2012).

Chitosan is a partially deacetylated derivative of chitin, which is the second most abundant natural polysaccharide in nature after cellulose. Chitosan is a hetero-polysaccharide composed of 2-amino-deoxy- $\beta$ -D-glucopyranose and 2-acetamido-deoxy- $\beta$ -D-glucopyranose (chitin) residues (Kumar *et al.*, 2004). Due to its non-toxic, biodegradable and biocompatible properties, chitosan is used in several fields such as food packaging, biotechnology, medicine, drug delivery, membranes, hydrogels, adhesives, antioxidants, biosensors, artificial bones, and in gene therapy (Prashanth and Tharanatha, 2007). The presence of 2-amino-deoxy- $\beta$ -D-glucopyranose (*N*-glucosamine) allows protonation of chitosan when the pH turns acidic. As a result, the colloidal suspension of chitosan is highly cationic and has the ability to form polyelectrolyte complexes (PECs) with other anionic polysaccharides or molecules (Berger *et al.*, 2004).

Bionanocomposites can be defined as a family of materials consisting of a biopolymeric matrix and reinforced with nano-sized fiber, which is obtained from renewable sources (Habibi *et al.*, 2008). Over the years, CNC based bionanocomposites have attracted significant attention due to their renewable nature as well as potential application in various fields (Khan *et al.*, 2014; Miao & Hamad, 2013; Eichhorn, 2011). Recently, CNC has been used to enhance the mechanical properties of biopolymers such as chitosan (Pereda *et al.*, 2014; Khan *et al.*, 2012). The enhanced mechanical properties of the CNC reinforced chitosan films can be attributed to the formation of PECs due to the favorable interaction between the anionic sulfate groups of CNC and the cationic amine groups of chitosan (De Mesquita *et al.*, 2010). However, if the electrostatic interactions are too strong, precipitation and/or aggregation of the complexes may occur (Berger *et al.*, 2004). As a consequence, the bionanocomposites may not possess desired mechanical properties.

In our previous study, a diluted CNC suspension (0.1% w/v) was used to fabricate chitosan based nanocomposite films and 3 to 5% of CNC (in dry wt.) loading was optimum with regards to the mechanical strength of the films (Khan *et al.*, 2012). However, the mixing of a concentrated CNC suspension (1 to 2%) with a chitosan solution was found to be problematic regardless of the CNC loading, as no significant improvement in the mechanical strength of the films was observed. In order to obtain significant increase in mechanical strength, CNCs should be homogeneously distributed in the chitosan matrix. Microfluidization provides a highly novel and innovative approach for the development of high strength bionanocomposites films by achieving homogeneous distribution of CNC nanofibers. However, to our knowledge there have not been any studies investigating the role of microfluidization on the distribution of CNC nanofibers in biopolymeric matrices.

The main objective of the present study was to achieve proper dispersion of CNC within chitosan matrix by utilizing microfluidization. The mechanical properties of the CNC reinforced chitosan based films were used as an indirect measurement to estimate the homogeneity of CNC dispersion within the chitosan matrix. A central composite design (CCD) and Response surface methodology (RMS) was used to find out the optimized CNC concentration, microfluidization pressure and number of microfluidization cycles. Field emission scanning electron microscopy (FE-SEM) and atomic force microscopy (AFM) was used to investigate the extent of CNC dispersion in the bionanocomposite films.

## **4.6. Materials & Methods**

### **4.6.1. Preparation of the nanocomposite suspensions**

At first, the polymer suspension was prepared by dissolving a 2% w/v of high mol. wt. chitosan (DD: 85-90%, 85/2500 Heppe-medical GmbH, Germany) into a 2% (w/v) of aqueous acetic acid

(Laboratoire Mat, Beauport, Quebec, Canada) solution under magnetic stirring. After that a 0.5% ethylene glycol (Laboratoire Mat, Beauport, Quebec, Canada) was incorporated into the chitosan solution and was magnetically stirred overnight at room temperature. Then, a 2% w/v of aqueous CNC suspension was prepared by dispersing spray dried CNC powder (FPInnovations, Pointe-Claire, QC, Canada) in deionized water under magnetic stirring, followed by ultra-sonication (QSonica Q-500, Misonix, Qsonica, LLC, Newtown, CT, USA) at 1000 J/g of CNC. The prepared CNC suspension was then incorporated into the chitosan/ethylene glycol solution at different concentrations and was pre-homogenized for 3hr with IKA RW-20 (IKA® Works Inc., Wilmington, NC, USA) mechanical homogenizer at 1,500 rpm at room temperature and kept in a beaker prior to microfluidization.

#### **4.6.2. Experimental design**

A central composite design (CCD) is an experimental design, useful in RSM, for building a second order (quadratic) model for the response variable without needing to use a complete three-level factorial experiment. The design consists of 3 distinct sets of experimental runs; 1) a factorial design in the factors studied; 2) a set of center points, experimental runs whose values of each factor are the medians of the values used in the factorial portion. This point is often replicated in order to improve the precision of the experiment; and 3) a set of axial points, experimental runs identical to the center points except for one factor, which will take on values both below and above the median of the two factorial levels, and typically both outside their range. All factors are varied in this way (Adjallé *et al.*, 2011). This experiment was designed using a 3 factor CCD with 3 replicates at the center point to build the response surface model. Multiple center points were chosen as it allows substantial degrees of freedom for estimating pure error of the design. The 3 independent variables were CNC concentration (0-10% w/w of chitosan,  $X_1$ ), microfluidization pressure (5,000-15,000 psi,  $X_2$ ) and number of microfluidization

cycles (0-10,  $X_3$ ). **Table-4.1** represents the principal values of the three independent variables at five levels (-2, -1, 0, 1, 2). Preliminary experiments were carried out to determine the center point values of the independent variables.

#### **4.6.3. Microfluidization of the nanocomposite suspensions**

A schematic representation of the basic operation of a microfluidizer is presented in **Fig. 4.1**. The CNC/chitosan suspensions were introduced in the inlet reservoir of the microfluidizer (Microfluidics Inc., Newton, MA, USA). The on-board electric-hydraulic drive powers a pump capable of operating at a pressure of 5,000 to 30,000 psi (34 to 207 MPa). The pump drives the suspension to the interaction chamber of the machine at constant pressure. The interaction chamber of the microfluidizer is Y-shaped and equipped with micro-channels through which the suspensions are separated and collided with one another from opposite directions at high velocities, thus creating a tremendous shearing action. After that, the microfluidized suspension flows through an external coiling. Ice was placed on the cooling jacket in order to negate overheating of the suspensions due to microfluidization. At this point, microfluidized suspension may be re-circulated through the system for additional cycling or collected from the outlet reservoir. According to the CCD, the CNC/chitosan suspensions were subjected to different microfluidization pressures and number of cycles in a continuous operation mode.

#### **4.6.4. Preparation of the nanocomposite films**

The films were prepared by casting a 15 mL of the CNC/chitosan suspension on Petri dishes which was allowed to dry at room temperature and 30-35% RH. Films were then washed with 1M NaOH (Laboratoire Mat, Beauport, Quebec, Canada) for 2 min, washed several times with deionized water and were allowed to dry. All the films were stored at room temperature in a

desiccator filled with saturated NaBr solution to ensure a stabilized atmosphere of 60% relative humidity.

#### **4.6.5. Measurement of the mechanical properties of the nanocomposite films**

The mechanical properties of the films such as tensile strength (TS), tensile modulus (TM) and elongation at break (Eb%) were measured by using Universal Testing Machine (model H5KT, with a 100N load cell, Tinius-Olsen, Horsham, USA). The samples were cut using ASTM procedure D 638-99 and the film thickness was measured using a Mitutoyo Digimatic Indicator (Type ID-110E; Mitutoyo Manufacturing Co. Ltd., Tokyo, Japan) at five random positions around the film.

#### **4.6.6. Field emission scanning electron microscopy (FE-SEM)**

The field emission scanning electron microscope (FE-SEM) imaging of the film samples (5×5 mm<sup>2</sup>) were performed on an Environmental SEM (ESEM, Quanta 200 FEG, FEI Company Hillsboro, OR, USA) under high vacuum mode with an accelerating voltage of 20.0 kV at 0°C temperature. The microscope was equipped with an energy dispersive X-ray (EDX) spectrometer (Genesis 2000, XMS System 60 with a Sapphire Si/Li detector from EDAX Inc. Mahwah, NJ, USA).

#### **4.6.7. Atomic force microscopy (AFM)**

Nanocomposite films were taped onto magnetic sample holder and the AFM images were captured using a MultiMode Nanoscope IIIa (Digital instrument, Santa Barbara, CA). The topographic height images were obtained in tapping mode in air using silicon cantilevers (Nanoworld, U.S.A). Nanoscope Analysis 1.4 (Bruker, Santa Barbara, CA) software was used to measure the root mean square surface roughness (Rq) of the film samples.

#### 4.6.8. Statistical analysis of the design

RSM was adopted to determine the relationship between the independent variables (CNC concentration, microfluidization pressure and number of cycles) and the dependent variables (TS, TM and Eb%) of the CNC/chitosan films. The mechanical analysis was performed with six different films specimens of the same suspension and the average value was reported. The results of the CCD experiments and values of the dependent variables were analyzed by STATISTICA 12 (STATSOFT Inc., Tulsa, US). The effects of independent variables on the Y response of the dependent variables were analyzed according to a polynomial model of second order of surface response given by the following general equation (**Eq. 4.1**).

$$Y = A_0 + \sum_{i=1}^n A_i X_i + \sum_{j \leq i}^n B_{ij} X_i X_j$$

where  $Y$  is the predicted response;  $A_0$ , intercept;  $X_i$  and  $X_j$  are values of various levels of the independent variables;  $A_i$  is the values of linear coefficients; and  $B_{ij}$  is the values of quadratic coefficients (Adjallé *et al.*, 2011).

### 4.7. Results & Discussions

#### 4.7.1. Regression analysis of the design

An analysis of variance (ANOVA) test was performed on the responses to determine the *lack of fit* and the significant effect of the independent variables on the CNC/chitosan films. The *lack of fit* test is a measure of the failure of the model to represent data in the experimental region in which points were not included in the regression. None of the 3 models demonstrated any significant *lack of fit*. The regression table was used to determine the significance of the linear, quadratic and interaction constant coefficients. The full experimental design with 3 replicates at the center point and the results obtained for the dependent variables are presented in **Table-4.2**.

It was observed that the TS & TM of the nanocomposite films increased with the increase of CNC concentration ( $X_1$ ). Microfluidization pressure ( $X_2$ ) and number of cycles ( $X_3$ ) also affected the values. The response surface regression analyses for the mechanical properties of the films are presented in **Table-4.3**. The  $P$ -values, presented in Table-3, quantify the significance of each factor in the polynomial model. The coefficients with  $P$  value of  $\leq 0.05$  were considered significant. The factors with positive regression coefficient impart a positive effect on the polynomial model and vice-versa. In the current study, the overall regression coefficient ( $R^2$ ) of the response surface model for the TS values was found to be 98.3%. A  $R^2$  value of 98.3% indicates that 98.3% of the variation in the responses could be explained by the combination of the responses. The  $R^2$  value is of prime importance in a predictive modeling system involving optimization of several factors. A high  $R^2$  value implies that the polynomial model is accurate in predicting the responses of the system (Balachandran *et al.*, 2012). The  $R^2$  values for the TM and Eb% of the films were 95.5% and 56.5, respectively.

The linear coefficient of variables CNC ( $X_1$ ), Pressure ( $X_2$ ) and Cycle ( $X_3$ ) all produced statistically significant ( $P \leq 0.01$ ) linear positive and quadratic ( $X_1^2$ ,  $X_2^2$ ,  $X_3^2$ ) negative effects on the TS and TM of the films. It turns out that CNC with higher coefficient values greatly influenced the response surface model of TS and TM, more than the pressure and cycles. There was also statistically significant ( $P < 0.01$ ) negative effect of the interaction coefficient of CNC and Pressure ( $X_1 \times X_2$ ) on the independent variables. Although the interaction coefficient of CNC and Cycles was not statistically significant ( $P > 0.05$ ) but was kept in the polynomial equation in order to negate an underestimation of TS values. Based on the regression analysis, the polynomial equation obtained for the TS and TM is given in **Eq. (4.2)** and **(4.3)**, respectively.

$$TS = 76.86 + 8.95 \times X_1 - 0.42 \times X_1^2 + 6.09 \times 10^{-3} \times X_2 - 2.47 \times 10^{-7} \times X_2^2 + 4.54 \times X_3 - 0.46 \times X_3^2 - 2.48 \times 10^{-4} \times X_1 \times X_2 + 0.12 \times X_1 \times X_3 \quad \text{Eq. (4.2)}$$

$$TM = 978.51 + 540.50 \times X_1 - 23.13 \times X_1^2 + 0.38 \times X_2 - 1.60 \times 10^{-5} \times X_2^2 + 175.38 \times X_3 - 16.22 \times X_3^2 - 0.02 \times X_1 \times X_2 \quad \text{Eq. (4.3)}$$

The Eb% of the films was negatively affected quadratic coefficient of microfluidization cycles ( $X_2^2$ ) whereas the interaction coefficient of pressure and cycle ( $X_2 \times X_3$ ) imparts a positive effect on the values. The linear positive effect of CNC and quadratic positive effect of pressure was not included in the equation as they were not statistically significant ( $P > 0.05$ ). The polynomial equation for Eb% is given in **Eq. (4.4)**.

$$Eb\% = 11.07 - 0.09 \times X_3^2 + 9.05 \times 10^{-5} \times X_2 \times X_3$$

#### 4.7.2. Surface morphology of the nanocomposite films

There was clear visible difference between the microfluidized (**Fig. 4.2b**) and non-microfluidized (**Fig. 4.2a**) suspensions at the same CNC concentration. As a matter of fact, the non-microfluidized nanocomposite suspension exhibited visible aggregation, when kept in a falcon tube for a week. No such aggregation was observed for the microfluidized suspensions. The films prepared from non-microfluidized suspension also appeared to be very opaque (**Fig. 4.3a**). On the contrary, films prepared from the microfluidized CNC/chitosan suspensions appeared to be transparent (**Fig. 4.3b**). The FE-SEM analysis of the CNC/chitosan films was carried out in order to verify the distribution and/or aggregation level of CNC within the chitosan matrix. FE-SEM is a very convenient method of microscopic analysis to verify the presence of aggregates on the nanocomposite films, as it eliminates the need for any conducting coating thus preventing potential damage of the samples due to coating (Kvien *et al.*, 2005). The micrographs

of the non-microfluidized films appeared to have a heterogeneous surface containing cracks and deflection sites (**Fig. 4a**). Large chunks of aggregates were visible throughout the film indicating poor CNC dispersion. As mentioned before, the formation of PECs between CNC and chitosan could be responsible for these aggregations. The micron-sized aggregates were visible even at a low magnification level of 400x and aggregates with sizes as high as 100-150 $\mu$ m could be observed. The microfluidized films exhibited a homogeneous structure (**Fig. 4b**), which indicates proper dispersion of CNC within chitosan. Although few aggregate can still be observed at high magnification level (at 2000x). It is interesting to note that the sizes of the remaining aggregates appeared much smaller than those of non-microfluidized films and were in the range of 5 to 10 $\mu$ m. So, it was possible to reduce the size of the aggregates by 10-15 times by utilizing a microfluidization pressure of 10,000psi and passing the suspension through 5 cycles. Therefore, the improved mechanical properties of films can be attributed to the breakdown of aggregates and homogeneous distribution of CNC in the matrix. The AFM was used to obtain a detailed observation of the nanocomposite films surfaces at high resolution. The AFM images of the non-microfluidized films (**Fig. 5a**) revealed phases of aggregation in agreement with the FE-SEM micrographs. It was not possible to observe the orientation of CNCs within the matrix probably due to the presence of micron-sized aggregates. The CNCs in the microfluidized films appeared to be uniformly distributed thorough out the film (**Fig. 5b**). The root mean square roughness (Rq) of the non-microfluidized films (1.22 to 1.47 nm) was much lower than that of the microfluidized films (2.03 to 2.52 nm). The difference in the Rq value of the films is very interesting because both microfluidized and non-microfluidized films have the same CNC content of 5% w/w. The high Rq value of the micro-fluidized films can be attributed to the better distribution of CNC within the polymer matrix. The Rq of the chitosan films was found to

increase with the incorporation of cellulose based nanofiber (Azeredo *et al.*, 2010). An increase in the Rq of agar based films with increase in nanoclay concentration up to 10% w/w of clay incorporation and then leveled off, which was attributed to the aggregation of clay above the threshold concentration (Rhim, 2011).

#### **4.7.3. Response surface plots**

In order to properly understand the influence of the independent variables on the dependent variables, three-dimensional (3D) response surface plots were drawn. The **Fig. 4.6** presents a 3D response surface plot for the TS of the films as a function of CNC concentration ( $X_1$ ) and microfluidization cycles ( $X_3$ ), while keeping the microfluidization pressure ( $X_2$ ) constant was fixed at 7,000 psi. We can observe that both the CNC ( $X_1$ ) and microfluidization cycles ( $X_3$ ) improved the TS of the films. The TS of the films increased with the increase in CNC concentration up to 9% and no more increase can be observed beyond this value. This could be due to the fact that CNC, having reached this concentration within the matrix, does not participate further in the stress transfer of the nanocomposite films (Huq *et al.*, 2012). The TS of the films demonstrated a parabolic shape with regards to the microfluidization cycles ( $X_3$ ). Both low and high number of cycles resulted in a decrease in TS values, while the optimum condition was located at the middle portion of the graph. By passing the CNC/chitosan suspensions through 5 to 7 microfluidization cycles, it was even possible to improve the TS of the films while keeping the CNC concentration low (2-3%). Based on the analysis of the data presented in **Fig. 4.6**, it turns out that a high CNC concentration and use of 5 to 7 microfluidization cycles is necessary to obtain maximum TS values. The 3D response surface plot presented in **Fig. 4.7** for the TM values of the CNC/chitosan films demonstrated a similar trend as to the TS values. The TM values increased and reached a plateau at 8-9% of CNC. Similar to the TS values, the

highest TM values can be obtained by passing the CNC/chitosan through cycles 5-7 number of microfluidization cycles. The increased TM values correlate to increased TS values of the films. The low TS and TM values of the nanocomposite films at lower number of cycles indicate possible aggregation and uneven distribution of CNC within the chitosan matrix. The strong electrostatic interaction between CNC and chitosan could be responsible for this aggregation (De Mesquita *et al.*, 2010). When polymer suspensions are subjected to microfluidization, high mechanical stress is developed on polymer molecules due to the simultaneous generation of shear, turbulence, impact and cavitation forces (Chen *et al.*, 2013; Tsai *et al.*, 2009; Kasaai *et al.*, 2003). However, at shorter cycles the exposure time of the colliding particles at the interaction chamber was limited. As a result, the critical mechanical stress required to breakdown the aggregation was not achieved and this microscopic phenomenon was reflected on the macroscopic mechanical properties of the films. The increase in the number of microfluidization cycles allowed build up of the mechanical stress sufficient enough to breakdown the CNC-chitosan aggregates and help homogeneous distribution of CNC within the chitosan matrix. Therefore, the reinforcing effect of CNC observed in the current study can be explained by adopting the mean field mechanical model. This model describes mechanical properties of nanofiber-reinforced composites based on homogeneous distribution of CNC in the polymer matrix (Favier *et al.*, 1995). Microfluidization allowed proper dispersion of CNC within the chitosan matrix, which minimized stress concentration and allowed efficient load transfer to the CNC-chitosan network (Kanagaraj *et al.*, 2007). Laneuville *et al.* (2013) reported disruption of large aggregates and reduction in the aggregate concentration of the aqueous xanthan gum suspension due to microfluidization. The increase in the number of cycles increases the exposure time of the nanocomposite suspension towards high shear forces operating in the microfluidizer.

Kasaai *et al.* (2003) reported microfluidization induced degradation of chitosan solution increased with the increase in microfluidization pressure, exposure time and initial molecular weight of chitosan. The authors also reported a linear decrease in degradation with increase in chitosan concentration. Prolonged exposure (higher number of cycles) could have detrimental effect on the nanocomposite suspension as extreme shear forces lead to the chain scission of the polymer matrix (Ferrer *et al.*, 2012; Tsai *et al.*, 2009; Kasaai *et al.*, 2003). The reduction of the TS and TM values of the CNC/chitosan films obtained at higher number of cycles could be attributed to the fragmentation of chitosan chains under extreme shear forces.

The **Fig. 4.8(a)** illustrates 3D response surface plot for the Eb% as a function of CNC concentration ( $X_1$ ) and microfluidization cycles ( $X_3$ ). It is very interesting to note that the Eb% of the films increased with the increase of CNC concentration. While some researchers reported a decrease in the Eb% of the nanocomposite films with the increase in nanofiber concentration (Khan *et al.*, 2012; Azeredo *et al.*, 2010; Aziz Samir *et al.*, 2004), others reported an increase in the Eb% (Dogan and McHugh, 2007; Wu *et al.*, 2007). The improved flexibility of the films was attributed to the better dispersion of the nanofiber within the polymer matrix. In the current study, the interaction coefficient of microfluidization cycles and pressure was found to have a statistically significant ( $P \leq 0.01$ ) positive effect on the Eb% values (**Eq. 4.4**). Therefore, another 3D surface response surface plot for the Eb% was drawn by varying microfluidization pressure ( $X_2$ ) and cycles ( $X_3$ ) while keeping the CNC concentration ( $X_1$ ) constant (**Fig. 4.8b**). From **Fig. 4.8(b)** we can observe that a combination of 6,000-12,000 psi pressure and 3-5 microfluidization cycles provided the maximum Eb%. Therefore the increase of Eb% of the films in the current study can be attributed to the microfluidization operation. The breakdown of CNC-chitosan

aggregates accompanied by homogeneous distribution of CNC in chitosan matrix; may have facilitated to the higher Eb% of the films.

#### **4.7.4. Critical value of the factors**

Based on the analysis of regression, the statistical analysis software (STATISTICA 12) can propose critical values of each factor to obtain a maximum value of the responses (dependent variables). A CNC concentration of 9.2% w/w, a pressure of 7665 psi and a microfluidization cycles of 6 are required to obtain a maximum of 155.5 MPa for TS, whereas, 8.9% w/w CNC, 6662 psi pressure and 5 microfluidization cycles are required to obtain a maximum TM of 5124 MPa. Critical values for Eb% could not be obtained, as the factors did not have any statistically significant ( $P>0.05$ ) linear effect on the response. However, from the response surface plot it is obvious that 14% or more Eb% can be obtained by passing the nanocomposite suspensions at 6,000-12,000 psi pressure and 3-5 microfluidization cycles. Considering the critical values of the responses, we can assume that a 8 to 9% w/w CNC, 6,500 to 8,000 psi pressure and 5 to 6 microfluidization cycles would provide the best mechanical properties of the nanocomposite films.

#### **4.8. Conclusion**

Microfluidization was used to optimize the fabrication of CNC reinforced bionanocomposite films according to a CCD. The mechanical properties of the films were measured and RSM was adopted to analyse the design. The CNC concentration, the microfluidization pressure and the number of microfluidization cycles were found to have statistically significant linear positive effect on both the TS and TM values of the films. Combination of microfluidization pressure and cycles improved the flexibility (Eb%) of the films. The enhanced mechanical properties of the films were attributed to the breakdown of CNC-chitosan aggregates and homogeneous dispersion of CNC within the chitosan matrix. Microscopic analysis of the films confirmed the hypothesis

and revealed a 10-15-fold reduction in the size of the aggregates as a result of microfluidization. Therefore, microfluidization provides an innovative approach to improve CNC distribution in the chitosan matrix to develop bionanocomposites with high mechanical properties.

#### **4.9. Acknowledgements**

This research was supported by the Natural Sciences and Engineering Research Council of Canada (NSERC) and by FPIInnovations (Pointe-Claire, Canada) through the RDC program. The authors highly appreciate SEM support from Mrs. Line Mongeon, Technician of the Biomedical Engineering Department and the Facility Electron Microscopy Research (FEMR) at McGill University.

#### **4.10. References**

Adjallé, K. D., Vu, K. D., Tyagi, R. D., Brar, S. K., Valéro, J. R., & Surampalli, R. Y. (2011). Optimization of spray drying process for *Bacillus thuringiensis* fermented wastewater and wastewater sludge. *Bioprocess and biosystems engineering*, 34(2), 237–46.

ASTM, Standard Test Method for Tensile Strength of Plastics. Annual Book of ASTM Standards, ASTM International, 1999, Method D 638-99.

Atalay, Y. T., Vermeir, S., Witters, D., Vergauwe, N., Verbruggen, B., Verboven, P., ... Lammertyn, J. (2011). Microfluidic analytical systems for food analysis. *Trends in Food Science & Technology*, 22(7), 386–404.

Azeredo, H. M. C., Mattoso, L. H. C., Avena-Bustillos, R. J., Filho, G. C., Munford, M. L., Wood, D., & McHugh, T. H. (2010). Nanocellulose reinforced chitosan composite films as affected by nanofiller loading and plasticizer content. *Journal of Food Science*, 75(1), N1–7.

Azizi Samir, M. A. S., Alloin, F., Sanchez, J. Y., & Dufresne, A. (2004). Cellulose nanocrystals reinforced poly(oxyethylene). *Polymer*, 45, 4149–57.

Balachandran, M., Devanathan, S., Muraleekrishnan, R., & Bhagawan, S. S. (2012). Optimizing properties of nanoclay–nitrile rubber (NBR) composites using Face Centred Central Composite Design. *Materials & Design*, 35, 854–862.

Beck-Candanedo, S., M. Roman, Gray, D. G., (2005). Effect of reaction conditions on the properties and behavior of wood cellulose nanocrystal suspensions. *Biomacromolecules*. 6(2), 1048-1054.

Beck, S., Bouchard, J., & Berry, R. (2011). Controlling the reflection wavelength of iridescent solid films of nanocrystalline cellulose. *Biomacromolecules*, 12(1), 167–72.

Berger, J., Reist, M., Mayer, J., Felt, O., & Gurny, R. (2004). Structure and interactions in chitosan hydrogels formed by complexation or aggregation for biomedical applications. *European Journal of Pharmaceutics and Biopharmaceutics*, 57(1), 35–52.

Chen, J., Liang, R., Liu, W., Li, T., Liu, C., Wu, S., & Wang, Z. (2013). Pectic-oligosaccharides prepared by dynamic high-pressure microfluidization and their in vitro fermentation properties. *Carbohydrate Polymers*, 91(1), 175–82.

- De Mesquita, J. P., Donnici, C. L., & Pereira, F. V. (2010). Biobased nanocomposites from layer-by-layer assembly of cellulose nanowhiskers with chitosan. *Biomacromolecules*, *11*(2), 473–80.
- Dogan, N., & McHugh, T. H. (2007). Effects of microcrystalline cellulose on functional properties of hydroxy propyl methyl cellulose microcomposite films. *Journal of Food Science*, *72*(1), E016–22.
- Dong, X. M., Revol, J. F., & Gray, D. G. (1998). Effect of microcrystallite preparation conditions on the formation of colloid crystals of cellulose. *Cellulose*, *5*, 19-32.
- Eichhorn, S. J. (2011). Cellulose nanowhiskers: promising materials for advanced applications. *Soft Matter*, *7*(2), 303. doi:10.1039/c0sm00142b
- Favier, V., Chanzy, H., & Cavaille., J. Y. (1996). Polymer nanocomposites reinforced by cellulose whiskers. *Macromolecules*, *28*, 6365-6367.
- Ferrer, A., Filpponen, I., Rodríguez, A., Laine, J., & Rojas, O. J. (2012). Valorization of residual Empty Palm Fruit Bunch Fibers (EPFBF) by microfluidization: production of nanofibrillated cellulose and EPFBF nanopaper. *Bioresource Technology*, *125*, 249–55.
- Habibi, Y., Goffin, A.-L., Schiltz, N., Duquesne, E., Dubois, P., & Dufresne, A. (2008). Bionanocomposites based on poly( $\epsilon$ -caprolactone)-grafted cellulose nanocrystals by ring-opening polymerization. *Journal of Materials Chemistry*, *18*(41), 5002.
- Habibi, Y., Lucia, L. A., & Rojas, O. J. (2010). Cellulose nanocrystals: chemistry, self-assembly, and applications. *Chemical reviews*, *110*(6), 3479–500.

Huq T., Salmieri, S., Khan, A., Khan, R.A., Le Tien, C., Riedl, B., Frascinic, C., Bouchard, J., Uribe-Calderon, J., Kamal, M.R. and Lacroix, M., (2012). Nanocrystalline cellulose (NCC) reinforced alginate based biodegradable nanocomposite film. *Carbohydrate Polymers*, 90, 1757–1763.

Jafari, S. M., He, Y., Bhandari, B., (2007). Optimization of nano-emulsions production by microfluidization. *Eur Food Res Technol* 225:733–741.

Jo, Y.-J., & Kwon, Y.-J. (2013). Characterization of  $\beta$ -carotene nanoemulsions prepared by microfluidization technique. *Food Science and Biotechnology*, 23(1), 1–7.

Kanagaraj, S., Varanda, F. R., Zhil'tsova, T. V., Oliveira, M. S. A., & Simões, J. A. O. (2007). Mechanical properties of high density polyethylene/carbon nanotube composites. *Composites Science and Technology*, 67(15-16), 3071-3077.

Kasaai, M. R., Charlet, G., Paquin, P., & Arul, J. (2003). Fragmentation of chitosan by microfluidization process. *Innovative Food Science & Emerging Technologies*, 4(4), 403–413.

Khan, A., Huq, T., Khan, R. A., Riedl, B., & Lacroix, M. (2014). Nanocellulose-Based Composites and Bioactive Agents for Food Packaging. *Critical Reviews in Food Science and Nutrition*, 54(2), 163–174.

Khan, A., Khan, R. A., Salmieri, S., Le Tien, C., Riedl, B., Bouchard, J., Chauve, G., Victor, T., Kamal, M. R., & Lacroix, M. (2012). Mechanical and barrier properties of nanocrystalline cellulose reinforced chitosan based nanocomposite films. *Carbohydrate Polymers*, 90(4), 1601–8.

- Kumar, M. N. V. R., Muzzarelli, R. A. A., Muzzarelli, C., Sashiwa, H., & Domb, a J. (2004). Chitosan chemistry and pharmaceutical perspectives. *Chemical Reviews*, *104*(12), 6017–84.
- Kvien, I., Tanem, B. S., & Oksman, K. (2005). Characterization of cellulose whiskers and their nanocomposites by atomic force and electron microscopy. *Biomacromolecules*, *6*(6), 3160–5.
- Laneuville, S. I., Turgeon, S. L., & Paquin, P. (2013). Changes in the physical properties of xanthan gum induced by a dynamic high-pressure treatment. *Carbohydrate Polymers*, *92*(2), 2327–36.
- Lee, S.-Y., Chun, S.-J., Kang, I.-A., & Park, J.-Y. (2009). Preparation of cellulose nanofibrils by high-pressure homogenizer and cellulose-based composite films. *Journal of Industrial and Engineering Chemistry*, *15*(1), 50–55.
- Moon, R. J., Martini, A., Nairn, J., Simonsen, J., & Youngblood, J. (2011). Cellulose nanomaterials review: structure, properties and nanocomposites. *Chemical Society Reviews*, *40*, 3941-94.
- Pereda, M., Dufresne, A., Aranguren, M. I., & Marcovich, N. E. (2014). Polyelectrolyte films based on chitosan/olive oil and reinforced with cellulose nanocrystals. *Carbohydrate polymers*, *101*, 1018–26.
- Prashanth, K.V.H., and Tharanathan, R.N., (2007). Chitin/chitosan: modifications and their unlimited application potential and overview. *Trends in Food Science & Technology*, *18*, 117-131.
- Rhim, J-W. (2011). Effect of clay contents on mechanical and water vapor barrier properties of agar-based nanocomposite films. *Carbohydrate Polymers*, *86*(2), 691–699.

Tsai, M. L., Tseng, L. Z., & Chen, R. H. (2009). Two-stage microfluidization combined with ultrafiltration treatment for chitosan mass production and molecular weight manipulation. *Carbohydrate Polymers*, 77(4), 767–772.

Wu, Q., Henriksson, M., Liu, X., & Berglund, L. a. (2007). A high strength nanocomposite based on microcrystalline cellulose and polyurethane. *Biomacromolecules*, 8(12), 3687–92.

Zimmermann, T., Pöhler, E., & Geiger, T. (2004). Cellulose Fibrils for Polymer Reinforcement. *Advanced Engineering Materials*, 6(9), 754–761.

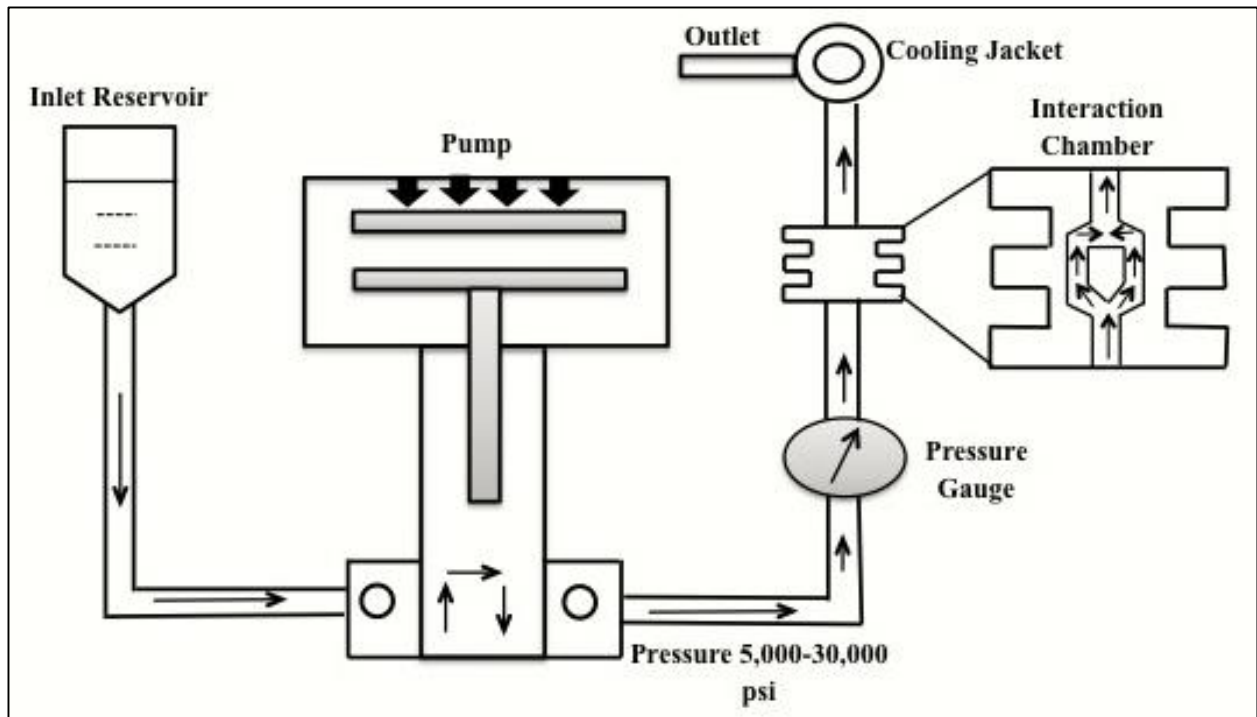


**Figure 4.1:** *Basic principle of a microfluidizer.*

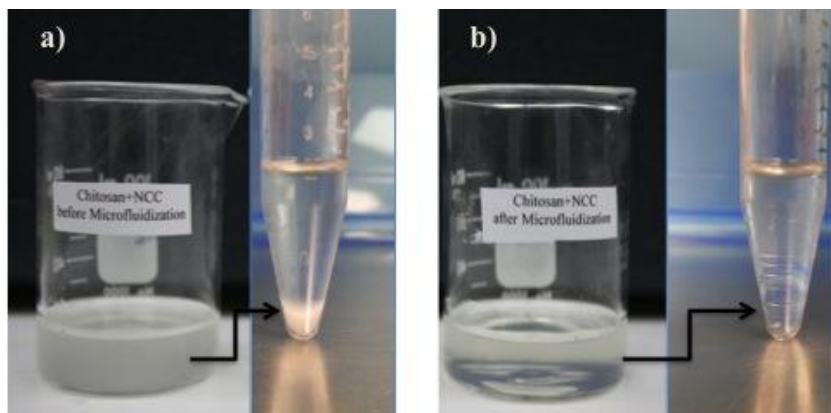


**Figure 4.2:** Digital images of a) non-microfluidized and b) microfluidized CNC/chitosan suspensions.



**Figure 4.3:** Digital images of a) non-microfluidized and b) microfluidized CNC/chitosan films.

**Table-4.1:** Levels of the factor tested in the CCD

Independent Variables	Symbol	Level of factors				
		-2	-1	0	1	2
CNC concentration	X <sub>1</sub> (%)	0	2	5	8	10
Microfluidization Pressure	X <sub>2</sub> (psi)	5,000	7,000	10,000	13,000	15,000
Number Of Cycles	X <sub>3</sub>	0	2	5	8	10

**Table-4.2:** Results of the mechanical properties of the CNC/chitosan films from CCD

Standard Experimental Run (R)	Independent variables			Dependent variables		
	CNC Concentration X <sub>1</sub> (w/w %)	Pressure X <sub>2</sub> (psi)	Number of Cycles X <sub>3</sub>	Tensile Strength TS (MPa)	Tensile Modulus TM (MPa)	Elongation at Break Eb%
1	2	7000	2	128	3978	11
2	2	7000	8	128	3899	12
3	2	13000	2	131	3953	10
4	2	13000	8	134	4256	12
5	8	7000	2	145	4754	14
6	8	7000	8	154	5127	12
7	8	13000	2	144	4399	13
8	8	13000	8	146	4431	14
9	0	10000	5	124	3605	10
10	10	10000	5	153	4895	14
11	5	5000	5	144	4513	12
12	5	15000	5	142	4271	11
13	5	5000	0	130	4210	10
14	5	10000	10	140	4394	9
15	5	10000	5	148	4771	15
16	5	10000	5	150	4896	14
17	5	10000	5	148	4830	13
18	5	10000	5	151	4941	13

**Table-4.3:** Response surface regression analyses for the mechanical properties of the CNC/chitosan films

Terms	Regression analysis					
	Tensile Strength (TS)		Tensile Modulus (TM)		Elongation at breaks (Eb%)	
	Coefficient	P-value	Coefficient	P-value	Coefficient	P-value
Constant	76.86	<0.01	978.51	<0.05	11.07	<0.01
CNC (L) *	8.95	<0.01	540.50	<0.01	0.31	0.26
CNC (Q)*	-0.42	<0.01	-23.13	<0.01	N/A	N/A
Pressure (L)*	$6.09 \times 10^{-3}$	<0.01	0.38	<0.01	N/A	N/A
Pressure (Q)*	$-2.47 \times 10^{-7}$	<0.01	$-1.60 \times 10^{-5}$	<0.01	$-2.13 \times 10^{-8}$	<0.1
Cycles (L)*	4.54	<0.01	175.38	<0.01	N/A	N/A
Cycles (Q)*	-0.46	<0.01	-16.22	<0.01	-0.09	<0.05
CNC×Pressure	$-2.48 \times 10^{-4}$	<0.01	-0.02	<0.01	N/A	N/A
CNC×Cycles	0.12	0.11	N/A	N/A	N/A <sup>#</sup>	N/A
Pressure×Cycles	N/A	N/A	N/A	N/A	$9.05 \times 10^{-5}$	<0.01

\* L represents linear coefficient ( $X_i$ ), Q represents quadratic coefficient ( $X_i^2$ ).

N/A-Not Applicable for the model

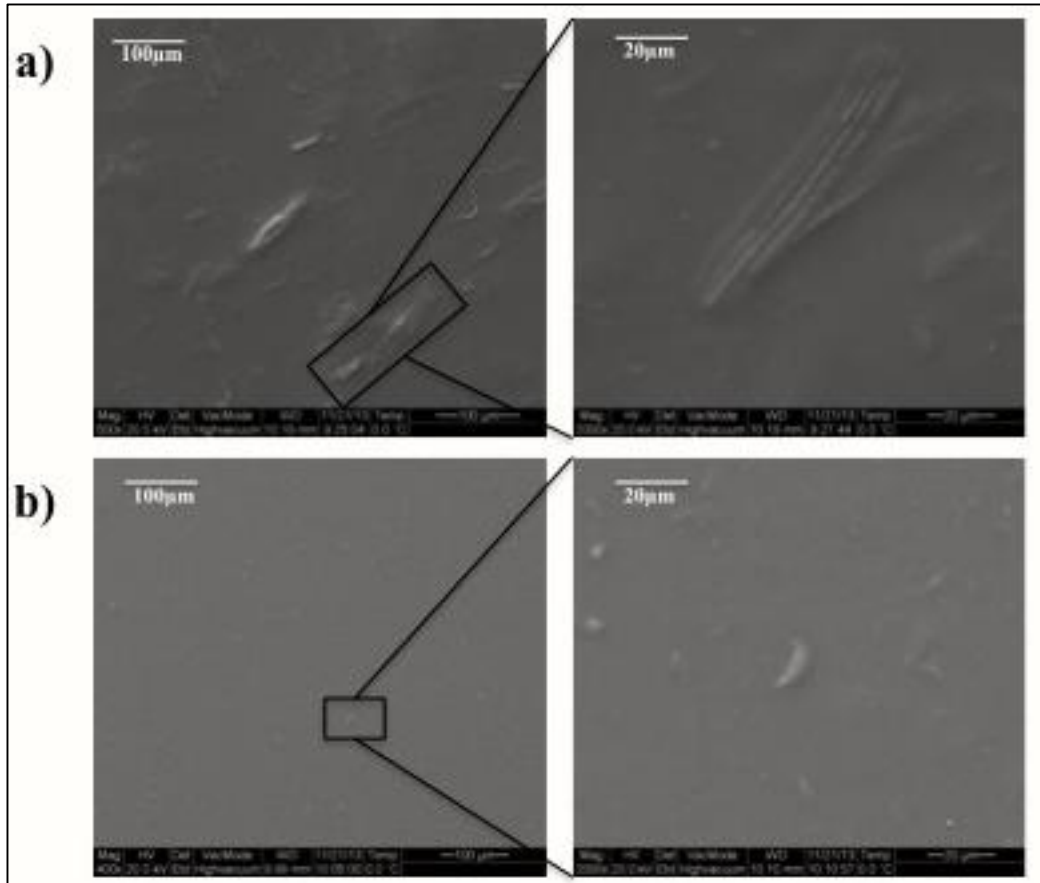


**Figure 4.4:** FE-SEM micrographs of a) non-microfluidized and b) microfluidized CNC/chitosan films at magnification level of 400x and 2000x.

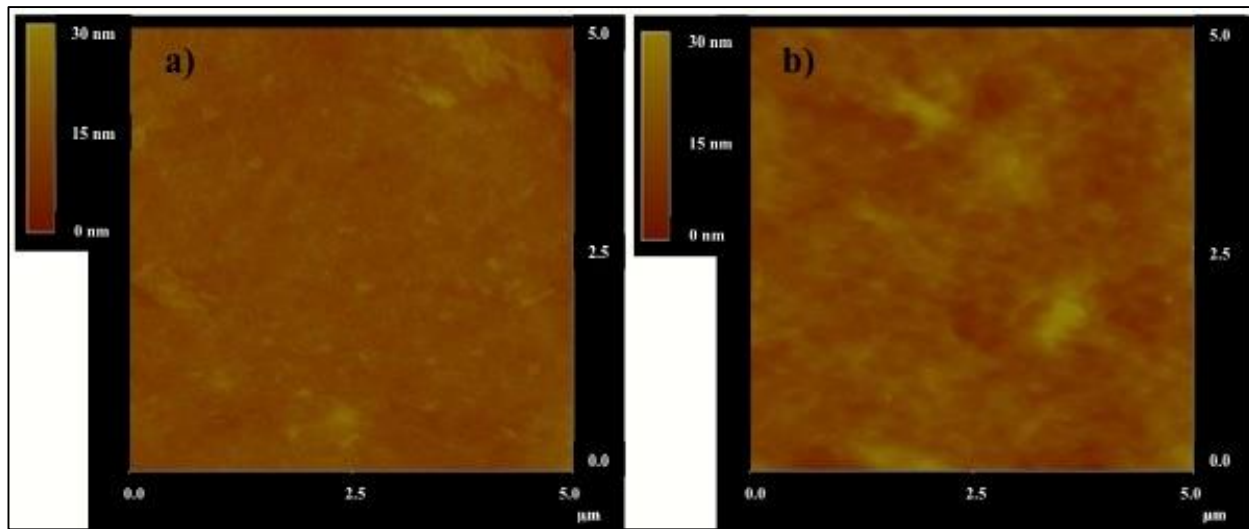


**Figure 4.5:** *The AFM height images of a) non- microfluidized and b) microfluidized nanocomposite films.*

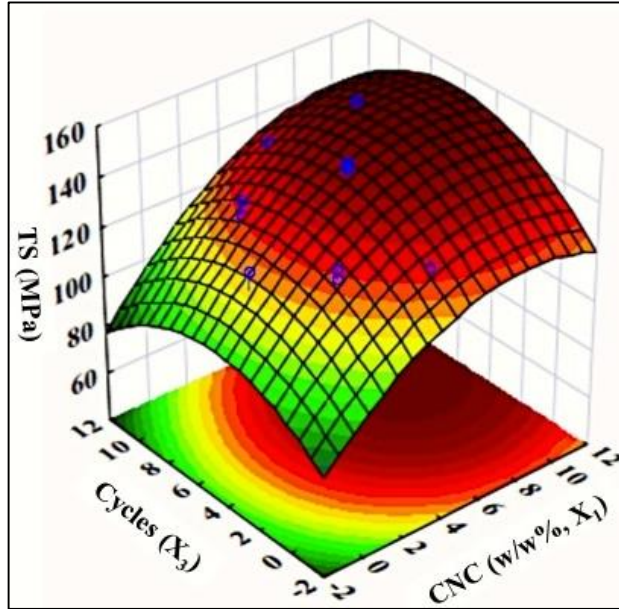


**Figure 4.6:** 3D Response surface plot of TS values obtained by varying CNC concentration ( $X_1$ ) and microfluidization cycles ( $X_3$ ) while keeping microfluidization pressure ( $X_2$ ) constant at 7,000 psi.

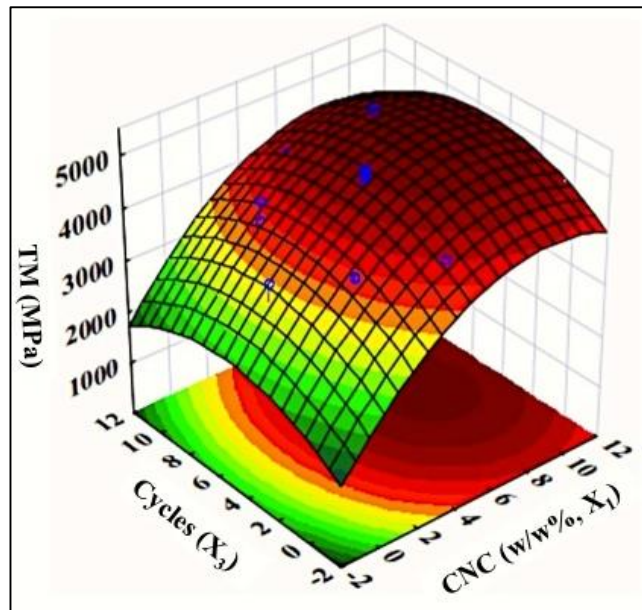


**Figure 4.7:** 3D Response surface plot of TM values obtained by varying CNC concentration ( $X_1$ ) and microfluidization cycles ( $X_3$ ) while keeping microfluidization pressure ( $X_2$ ) constant at 7,000 psi.

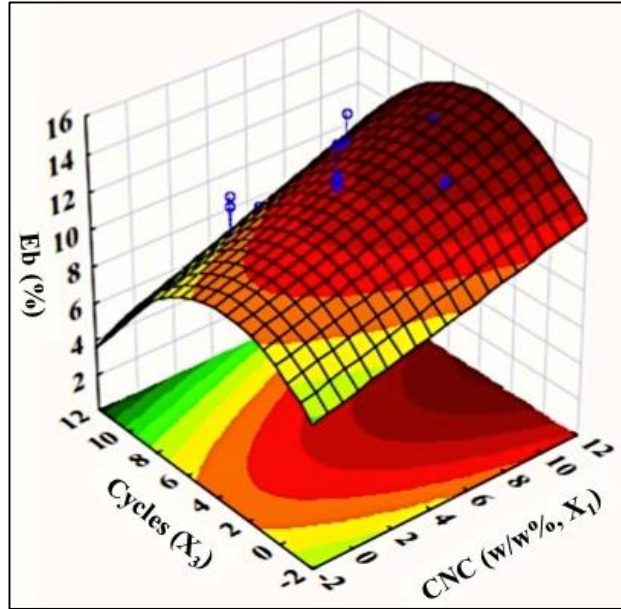


**Figure 4.8(a):** 3D Response surface plot of Eb% obtained by varying CNC concentration ( $X_1$ ) and microfluidization cycles ( $X_3$ ) while keeping microfluidization pressure ( $X_2$ ) constant at 7,000 psi.

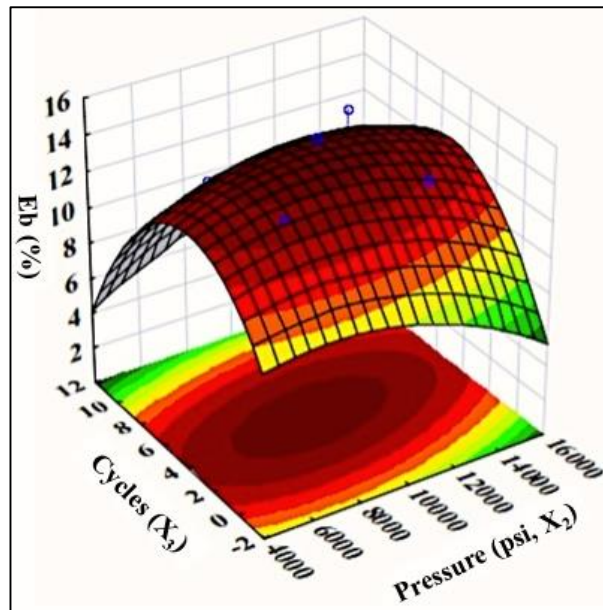


**Figure 4.8(b):** 3D Response surface plot of Eb% obtained by varying microfluidization pressure ( $X_2$ ) and microfluidization cycles ( $X_3$ ) while keeping CNC concentration ( $X_1$ ) constant at 8%.

#### **4.11. General discussion of the Publication-3**

One of the major challenges in the area of nanocomposite is the compatibilization of the nano reinforcements with the polymer matrix to achieve acceptable dispersion of the nanofiller within the polymeric matrix. In this study microfluidization was successfully applied to homogeneously disperse the concentrated CNC suspension into chitosan matrix. Microfluidization offers an innovative approach to disperse cellulosic nanomaterials into biopolymeric matrices. RSM allowed optimization of the CNC concentration, the microfluidization pressure and the number of microfluidization cycles. The experimental data demonstrated a good fit with the polynomial model. CNC concentration was found to be the most important factor affecting the mechanical strength of the films. Microfluidization successfully distributed CNC by reducing chitosan-CNC aggregates and helped to develop high strength CNC/chitosan nanocomposite films. It was possible to reduce the size of the aggregates by 10-15 times by utilizing a microfluidization pressure of 10,000 psi and passing the suspension through 5 cycles. However, prolonged exposure (higher microfluidization pressure and number of cycles) has been found to exhibit a detrimental effect on the mechanical properties of the films, as reported by Ferrer *et al.* (2012) and Tsai *et al.* (2009).

## **CHAPTER 5**

### **Publication 4**

# Optimization of the antimicrobial activity of nisin, Na-EDTA and pH against gram-negative and gram-positive bacteria

Avik Khan<sup>1</sup>, Khanh Dang Vu<sup>1</sup>, Bernard Riedl<sup>2</sup> and Monique Lacroix<sup>1\*</sup>

<sup>1</sup>Research Laboratories in Sciences Applied to Food, Canadian Irradiation Centre (CIC),  
INRS-Institut Armand-Frappier, Université du Québec, 531 Boulevard des Prairies,  
Laval, Québec, H7V 1B7, Canada

<sup>2</sup>Département des sciences du bois et de la forêt, Faculté de foresterie, géographie et géomatique,  
Université Laval, Québec-city, Québec, G1V 0A6, Canada

## KEYWORDS:

Experimental design, EDTA, Response surface methodology, Food safety, *E. coli* 0157:H7,  
*Salmonella* Typhimurium, *Listeria monocytogenes*.

\* **Corresponding Author:** Prof. Monique Lacroix.

Telephone: +1-450-687-5010; Fax: +1-450-686-5501.

**E-mail:** [monique.lacroix@iaf.inrs.ca](mailto:monique.lacroix@iaf.inrs.ca)

This article is under revision at the journal of *LWT-Food Science & Technology*.

## **5.1. Contribution of the authors**

The experimental works were planned, performed, analyzed and the manuscript was written by Avik Khan with constant guidance from Prof. Monique Lacroix. The protocols and results were also discussed with Prof. Monique Lacroix in several meetings. Both Prof. Monique Lacroix and Prof. Bernard Riedl corrected the main draft. Dr. Khanh Dang Vu helped to design the experimental model and corrected the main draft.

## **5.2. Specific objectives of the Publication-4**

In this publication, RSM was used to develop antimicrobial formulation capable of inhibiting selected gram-negative (*E. coli* and *S. typhimurium*) and gram-positive (*L. monocytogenes*) bacteria. So far, to my knowledge there have not been any studies reporting use of RSM to develop antimicrobial formulation by optimizing the Nisin, Na-EDTA concentration and pH. The antimicrobial activity of the formulations was tested by agar diffusion assay.

### 5.3. Résumé

L'activité antimicrobienne de rapports différents de nisine/éthylènediaminetétraacétate disodique (Na-EDTA) a été testé dans une large gamme de pH contre des bactéries Gram-négatives (*E. coli* et *S. typhimurium*) et Gram-positives (*L. monocytogenes*). Un montage expérimental composé de 3 facteurs (nisine, Na-EDTA et pH) a été mis en place pour tester et développer systématiquement une formulation optimisée. La méthodologie dite 'de surface de réponse (RSM)' a été utilisée pour obtenir la relation entre l'activité antimicrobienne des formulations et les autres facteurs. Des équations polynomiales ont été générées sur la base de l'analyse de régression des facteurs et l'activité antimicrobienne des formulations prédite était en bon accord avec les résultats expérimentaux. Une concentration de nisine de 125 à 150 µg/mL et une concentration de Na-EDTA de 20 à 30 mM et un pH de 5-6 ont été déterminées pour inhiber l'ensemble des trois bactéries sélectionnées de façon optimale.

## 5.4. Abstract

The antimicrobial activity of different nisin; disodium ethylenediaminetetraacetate (Na-EDTA) ratio was tested in a broad pH range against selected gram-negative (*E. coli* and *S. typhimurium*) and gram-positive (*L. monocytogenes*) bacteria. An experimental design consisting of 3 factors (nisin, Na-EDTA and pH) was set up to systematically test and develop an optimize formulation. Response surface methodology (RSM) was used to obtain relationship between the antimicrobial activity of the formulations and the factors. Polynomial equations were generated based on the regression analysis of the factors and the predicted antimicrobial activity of the formulations was in good agreement with the experimental results. A nisin concentration of 125-150 µg/mL with a Na-EDTA concentration of 20-30 mM and a pH of 5-6 was found to inhibit all the three selected bacteria.

## 5.5. Introduction

Foodborne diseases are considered as potent public health concern throughout the world and pose serious health risks to consumers. In the United States foodborne diseases are responsible for 9.4 million illnesses, 55,961 hospitalizations and 1,391 deaths each year (Scallan et al., 2011). According to Scallan et al. (2011) norovirus (Norwalk virus), which are the most common cause of stomach and intestine infections, contribute to the majority of the reported illnesses; while nontyphoidal *Salmonella* spp. are the leading causes of hospitalization. Nontyphoidal *Salmonella* spp. and *L. monocytogenes* are responsible for 28% and 19% of the deaths, respectively. In Canada, foodborne pathogens are responsible for approximately 4 million illnesses each year (Thomas et al., 2013). Dairy products such as, unpasteurized cheeses can be susceptible to microbial contamination. In September 2013, *E. coli* outbreak in a British Columbia cheese farm caused several hospitalizations across multiple provinces including tragic death of a woman (CBC News, 2013). Consumption of contaminated meat or meat products has been one of the major causes of foodborne diseases over the years. In 2008, *L. monocytogenes* contamination in a ready-to-eat (RTE) meat product sent shockwaves across Canada. The listeriosis outbreak was responsible for several hospitalizations and claimed the lives of 20 Canadians (Warriner and Namvar, 2009). One of the biggest recalls of beef products in Canadian history was initiated on September 4, 2012; due to the *E. coli* 0157:H7 contamination in an Alberta based Food Company. The contamination made 18 people sick and resulted recall of around 4,000 ton of beef products (Lewis et al., 2013).

The use of natural antimicrobial agents represents a highly effective approach for biopreservation of meat products. Nisin is a bacteriocin produced by the lactic acid bacterium *Lactococcus lactis*, subsp. *lactis* strains and has been found effective to prevent the growth of pathogenic bacteria and extend the shelf life of meat products (Gálvez et al., 2007; Cleveland et al., 2001; Hugas,

1998). Nisin is composed of 34 amino acids and has GRAS (generally considered as safe) status by Food and Drug Administration (FDA) (Delves-Broughton, 1990). The antimicrobial activity of nisin is generally limited to gram-positive bacteria. The outer membrane (OM) of gram-negative bacteria acts as a permeability barrier for the cell and prevents nisin from reaching the cytoplasmic membrane (Stevens *et al.*, 1991). Combination of nisin and chelating agents such as, sodium salts of ethylenediaminetetraacetate (Disodium EDTA) provides an effective approach to improve the antimicrobial activity of nisin against gram-negative bacteria (Vaara, 1992; Gill and Holly, 2003). Disodium EDTA (Na-EDTA) is used as a direct food additive in a wide variety of food products mainly to prevent color and flavor deterioration (Branen and Davidson, 2004). It also has antimicrobial activity and enhances the susceptibility of the gram-negative bacteria towards nisin by binding metal ions in the lipopolysaccharide (LPS) layer of the bacteria (Stevens *et al.*, 1991).

The antimicrobial activity of nisin is strongly influenced by the pH of the nisin solution. The highest activity is exhibited at acidic pH (2 to 3) followed by drastic loss of activity at higher pH (Rollema *et al.*, 1995). On the contrary, the stability of a metal-chelator complex, disodium EDTA, is favored by neutral or alkaline pH (Boziaris and Adams, 1999). So, the pH, along with the concentration of the nisin and Na-EDTA should be optimized in order to obtain an antimicrobial formulation capable of inhibiting both gram-positive and gram-negative bacteria. Traditionally, the optimization of a formulation or process is carried out by a technique called one-variable-at-a-time. The major disadvantage of such an approach is that it is not possible to observe the interactive effects of the variables. This problem can be overcome by utilizing response surface methodology (RSM). RSM can be defined as a set of mathematical and statistical techniques that can provide polynomial equations from the experimental data that are

obtained utilizing experimental design (Bezerra *et al.*, 2008; Baş and Boyac, 2007). RSM allows analysis of multiple factors and eliminates the need for a large number of experimental runs that are otherwise required in a conventional one-factor-at-a-time approach. It is used very effectively to analyze, predict and model systems that require optimization of multiple factors (Balachandran *et al.*, 2012). So far, to our best knowledge there have not been any studies reporting use of RSM to develop antimicrobial formulation by optimizing the Nisin, Na-EDTA concentration and pH.

The objective of the present study was to develop and optimize a new formulation composed by different combinations of nisin, Na-EDTA and pH with antimicrobial activity against selected gram-negative (*E. coli*, *S. typhimurium*) and gram-positive bacteria (*L. monocytogenes*).

## **5.6. Materials & Methods**

### **5.6.1. Bacterial strains**

*E. coli* 0157:H7 (strain EDL933) and *S. typhimurium* (strain SL1344) were obtained from INRS-Institut Armand Frappier (Laval, Quebec, Canada). The *L. monocytogenes* strains HPB 2569 1/2a, 2558 1/2b, 2371 1/2b, 2812 1/2ba and 1043 1/2a were obtained from Health products and Foods Branch of Health Canada (Ottawa, Ontario, Canada). All the microorganisms were kept frozen at -80 °C in Brain heart infusion (BHI, Alpha Biosciences Inc., Baltimore, MD, USA) broth containing glycerol (10% v/v). Before use, the stock cultures were resuscitated through 2 consecutive 24 h growth in BHI at 37 °C to obtain the working cultures containing approximately 10<sup>9</sup> CFU/mL. The five *L. monocytogenes* strains were mixed together (2mL each) to obtain a cocktail mixture.

### **5.6.2. Preparation of antimicrobial formulations**

A stock solution of nisin (Niprosin™, purity 2.5%, 77.5% salt and 20% vegetable protein, Profood, IL, USA) was prepared by dissolving 1g of the Niprosin™ powder in 100 ml of deionized water under magnetic stirring. The pH of the suspension was adjusted to 3.0 with dilute lactic acid (3% w/v in water; Laboratoire Mat, Beauport, Quebec, Canada). The solution was magnetically stirred and kept overnight at 4 °C. Then it was centrifuged for 15 min at 2500 rpm to remove the insoluble fractions and the supernatant was collected and stored at 4°C. The antimicrobial formulations were prepared by dissolving Na-EDTA (Laboratoire Mat, Beauport, Quebec, Canada) in the nisin solution. The final volume of all the formulations was fixed at 25 mL and the pH of the formulations was adjusted either with dilute lactic acid or with 1M NaOH (Laboratoire Mat, Beauport, Quebec, Canada). All formulations were filtered through a 0.45µm filter.

### **5.6.3. Agar diffusion assay**

The antimicrobial activity of the formulations was tested by agar diffusion assay. Test mediums containing 3.7% (w/v) BHI and 0.75% (w/v) agar (Alpha Biosciences Inc., Baltimore, MD, USA) were prepared, autoclaved and were allowed to cool at 50 °C in a water bath. Test mediums used for *L. monocytogenes* were prepared by incorporating 1.0% (w/v) Tween 20, a surfactant, into the solution prior to autoclave. After cooling, the mediums were inoculated with 1.0% (v/v) BHI broth containing the bacterial cultures ( $10^8$  CFU/mL) to obtain a final bacterial population of approximately  $10^6$  CFU/mL. A 25 mL of the inoculated medium was added to each Petri dish (95mm×15mm) and was allowed to solidify. Thereafter, holes measuring 7.0 mm in diameter were dug and 100 µL of the antimicrobial formulations were added to each hole. The plates were incubated for 24 h at 37 °C temperature and diameter (mm) of the inhibition zones were measured to determine the antimicrobial activity of the formulations.

#### 5.6.4. Central composite design (CCD)

For the current study, a central composite design (CCD) was chosen as the experimental design.

A CCD consists of a full or fractional factorial design; an additional star design in which the star points are at a distance ( $\alpha$ ) from its center; and a center point, which is often replicated in order to improve the precision of the experiment (Adjallé *et al.*, 2011; Bezerra *et al.*, 2008). It requires an experimental run according to **Eq. (1)**.

$$N = K^2 + 2K + C_n$$

Where  $N$  is the experimental runs,  $K$  is the number of factors (can also be termed as independent variable) and  $C_n$  is the number of replicates in the center points. The values of  $\alpha$  depend on the number of factors and can be calculated by  $\alpha = (2^k)^{1/4}$ . Where  $K$  is the number of factors. All the factors have five levels ( $-\alpha, -1, 0, +1, +\alpha$ ).

As discussed before, pH, nisin and Na-EDTA concentrations are the 3 factors that affect the antimicrobial activity against the selective bacteria. So, a 3 factor CCD with 3 replicates at the center point was designed to build the response surface model. For a 3 factor CCD the value of  $\alpha$  is 1.68. **Table-5.1** presents the principal values and codes of the 3 factors at five levels. Preliminary experiments were carried with each factor alone and with few combinations in order to determine the optimal values of the factors.

#### 5.6.5. Statistical analysis of the design

The relationship between the factors and antimicrobial activity (response) of the formulations was determined by utilizing RSM. Each experimental run was performed in triplicate and the average values for the zone of inhibition (D) was reported. The results of the CCD experiments and values of the responses were analyzed by STATISTICA 12 (STATSOFT Inc., Tulsa, US). The effects of factors on the responses (Y) can be presented according to the second-order polynomial equation (**Eq. 5.2**).

$$Y = A_0 + \sum_{i=1}^n A_i X_i + \sum_{j \leq i}^n B_{ij} X_i X_j$$

Where  $Y$  represents predicted response;  $A_0$ , constant term;  $X_i$  and  $X_j$ , values of various levels of the factors;  $A_i$ , values of linear coefficients; and  $B_{ij}$ , values of quadratic coefficients (Adjallé *et al.*, 2011).

## 5.7. Results

### 5.7.1. Regression analysis of the design

The full experimental design along with inhibition zone values obtained against *E. coli*, *S. typhimurium* and *L. monocytogenes* are presented in **Table-5.2**. An analysis of variance (ANOVA) test was performed on the responses and regression table was used to determine the significance of the linear, quadratic and interaction coefficients. The coefficients with a statistical significance level of less than 0.05 ( $P \leq 0.05$ ) were considered significant. The regression analyses for the responses are presented in **Table-5.3**. The regression coefficient ( $R^2$ ) of the response surface model for *E. coli*, *S. typhimurium* and *L. monocytogenes* were 95.1%, 98.5% and 90.1%, respectively. The importance of  $R^2$  is very high in a predictive modeling system, as it indicates how well polynomial model fits the experimental observations. In the current study, the  $R^2$  for the 3 polynomial models was higher than 90%, which represents a good fit of the experimental data with the polynomial model. The *lack of fit test* provides another way to evaluate the model. It is a measurement of the failure of the model to represent data in the experimental region in which points were not included in the regression and it is important to not have any significant *lack of fit*. None of the 3 models demonstrated any significant *lack of fit*. From **Table-5.3**, it can be observed that the linear coefficient of responses nisin ( $X_1$ ), Na-EDTA ( $X_2$ ) and pH ( $X_3$ ) produced statistically significant linear positive and quadratic ( $X_1^2$ ,  $X_2^2$ ,  $X_3^2$ ) negative effects on the antimicrobial activity of the formulations against *E. coli*. Based on the

regression analyses, the polynomial equation obtained for the inhibition of *E. coli* ( $D_E$ ) is presented in **Eq. (5.3)**.

$$D_E = -6.52 + 0.04 \times X_1 - 1.60E - 04 \times X_1^2 + 0.4 \times X_2 - 4.26E - 03 \times X_2^2 + 3.66 \times X_3 - 0.33 \times X_3^2$$

Against *S. typhimurium*, nisin ( $X_1$ ), Na-EDTA ( $X_2$ ) and pH ( $X_3$ ) showed linear positive effects, balanced by quadratic negative effects of nisin ( $X_1^2$ ) and pH ( $X_3^2$ ). Linear positive effect of nisin ( $X_1$ ), Na-EDTA ( $X_2$ ), pH ( $X_3$ ) accompanied by quadratic negative effects of pH ( $X_3^2$ ) was found on the inhibition zone of the formulations against *L. monocytogenes*. Based on the regression analyses, the polynomial equation obtained for the inhibition of *S. typhimurium* ( $D_S$ ) and *L. monocytogenes* ( $D_L$ ) are presented **Eq. (5.4)** and **(5.5)**, respectively.

$$D_S = -3.2018 + 0.04 \times X_1 - 1.70E - 04 \times X_1^2 + 0.18 \times X_2 + 2.95 \times X_3 - 0.26 \times X_3^2 \quad \text{Eq. (5.4)}$$

$$D_L = 7.27 + 0.01 \times X_1 + 0.15 \times X_2 + 1.56 \times X_3 - 0.16 \times X_3^2 \quad \text{Eq. (5.5)}$$

### 5.7.2. Response surface plots

The three-dimensional (3D) response surface plots offer visualization of the predicted polynomial equation. Usually, this graphical representation allows two-dimensional representation of a three-dimensional plot (Bezerra *et al.*, 2008). As we have 3 factors in the current study, one of the factors needs to be set to a constant value in order to visualize the plots.

**Fig. 5.1a** presents a 3D response surface plot for  $D_E$  as a function of pH ( $X_3$ ) and Na-EDTA ( $X_2$ ), while keeping the nisin concentration ( $X_1$ ) constant at 125 ( $\mu\text{g/mL}$ ). The dots in the 3D response surface plot represent actual experimental points. The response surface plot was mostly affected

by the change in pH. The inhibition zone ( $D_E$ ) varied in a parabolic shape with regards to the pH of the formulations. Both low and high pH resulted in a decrease in the antimicrobial activity, while the optimum condition was located at the middle portion of the graph. The optimum pH values seem to be in the region of 5 to 6. The  $D_E$  also increased with the increase in Na-EDTA concentration and seems to reach plateau after 30 mM. The effect of nisin ( $X_1$ ) and pH ( $X_3$ ) on the  $D_E$  (Na-EDTA fixed at 20 mM) is presented in **Fig. 5.1b**. The  $D_E$  increased with the increase in nisin concentration up to 150  $\mu\text{g/mL}$  and decreased thereafter. The optimum nisin concentration seems to be 125 to 150  $\mu\text{g/mL}$ . The graph fits very well with **Eq. 5.3**, where statistically significant linear positive and quadratic negative effect of nisin on  $D_E$  has been reported. The graph also reinforced the influence of pH on the inhibition zone, as similar to Na-EDTA; nisin demonstrated a pH dependent antimicrobial activity. The maximum antimicrobial activity can be found at pH 5.5 to 6. The 3D response surface plot for the inhibition against *S. typhimurium* ( $D_S$ ) is presented in **Fig. 5.2a**. *S. typhimurium* being a gram-negative bacterium, the plots demonstrated a trend similar to that obtained for *E. coli*. The  $D_S$  increased with the increase in Na-EDTA concentration and the maximum point seems to move outside the experimental region. The activity of nisin  $D_S$  was found to be similar to that discussed for *E. coli* and the optimum concentration varied over a range of 100 to 200  $\mu\text{g/mL}$ . However, pH proved to be the factor that is most influential with regards to the antimicrobial activity of the formulations. The inhibition zone ( $D_S$ ) appears to have maximum value at a pH of 4.5 to 6.5, regardless of the Na-EDTA or nisin concentration. Against *L. monocytogenes*, Na-EDTA (**Fig. 5.3a**) demonstrated a linear positive effect on the inhibition zone ( $D_L$ ). The pH also influenced the antilisterial activity of the formulations and the optimum pH was in the range of 4 to 5. The  $D_L$  increased with the increase in nisin concentration, when the Na-EDTA concentration was fixed at 125  $\mu\text{g/mL}$  (**Fig.**

**5.3b).** It is interesting to note that the antilisterial activity seems to be stable at a wide pH range and the maximum  $D_L$  could be obtained at pH 4 to 6. The inhibition zones were generally much higher than that obtained against *E. coli* and *S. typhimurium*.

## **5.8. Discussions**

The hydrophobic residues (N-terminal position) of nisin are considered to be responsible for its antimicrobial activity. These hydrophobic residues of nisin disrupt the cytoplasmic membrane of susceptible bacteria through the formation of pores in the membrane (Shai, 1999). However, nisin is rendered inactive against gram-negative bacteria such as, *E. coli* and *S. typhimurium*. The OM of these bacteria is composed of asymmetric lipid-protein bilayer. Virtually all the LPS are placed to the outer leaflet and non-polar phospholipids on the inner membrane. The divalent cations present in the OM play an important role in the stabilization of the core anionic charges of the LPS molecules and constitute a hydrophilic surface (Beveridge, 1999; Ellison *et al.*, 1988). As a result, the hydrophilic LPS provide penetration barrier towards hydrophobic molecules. In the current study, both nisin and Na-EDTA has been found to have positive influence on the bactericidal activity against *E. coli* and *S. typhimurium*. It can be hypothesized that Na-EDTA removes the divalent cations from their binding sites and reduces the interaction between LPS molecules. The loss of LPS may lead to the appearance of phospholipids in the outer leaflet of the OM and form channels thorough, which hydrophobic molecules could diffuse (Gill and Holley, 2003; Vaara, 1992; Stevens *et al.*, 1991). Thereafter, the bacterial membrane is susceptible to the attack and pore formation by the molecules like nisin. Incorporation of Na-EDTA also improved the antimicrobial activity of nisin against *L. monocytogenes* (**Eq. 5.5**). The reason could be that combination of nisin with EDTA allowed simultaneous attack on different targets in bacterial cell membrane. A simultaneous attack, as a result of combination of different antimicrobials, is more difficult for bacteria to overcome (Gill and Holley, 2003). Branen and

Davidson, (2004) also reported that the combination of EDTA-nisin produced a synergistic effect against *E. coli* and *L. monocytogenes* but not against *S. typhimurium*. Contrary to the current experiment, the authors reported that an increase of EDTA levels did not further enhance the inhibition by nisin. It is interesting to note that, the inhibition zones obtained for *S. typhimurium* were generally lower than that of *E. coli*, regardless of the nisin, Na-EDTA concentration or pH. Other researchers also reported lower sensitivity of *Salmonella* spp., compared to that of *E. coli*, to the action of nisin-EDTA combination (Boziaris and Adams, 1999; Stevens *et al.*, 1991).

In the current study the linear coefficient of pH (**Table-5.3**) was found to be higher than that of nisin and Na-EDTA, in the all the three polynomial models. As a result, pH could be considered to be the most influential factor affecting the antimicrobial activity of the formulations against both gram-positive and gram-negative bacteria. This is due to the contrasting pH condition required for bactericidal activity of nisin and EDTA. The ionization of a metal-chelator complex such as Na-EDTA depends upon the pH of the formulation. The ionized carboxylate groups of EDTA are an excellent donor group. However, lowering of pH decreases the proportion of EDTA in its ionized form; hence, the stability of Na-EDTA complex decreases (Boziaris and Adams, 1999). As a result, at acidic pH, Na-EDTA cannot bind and replace the metal ions from the OM of the gram-negative bacteria. This explains the low inhibition zone of the formulations against both the gram-negative bacteria at acidic pH (2-4). The decrease of inhibition zone at alkaline pH (8-10) can be associated with the low antimicrobial activity of nisin at this pH range (Rollema *et al.*, 1995). Although Na-EDTA is able of chelate metals ions better at alkaline pH, loss of nisin activity meant no combined effect of the antimicrobials could be observed. So, a nisin concentration of 125-150 µg/mL, Na-EDTA concentration of 20-30 mM and pH of 5-6 favor the maximum inhibition of *E. coli* and *S. typhimurium*. It is interesting to observe that

against *L. monocytogenes*, the formulations demonstrated good antilisterial activity over a broad pH range (3.5-7.5). The efficacy of nisin over a broad pH range makes it a very favorable prospect for food application requiring neutral pH condition.

## **5.9. Conclusion**

RSM was adopted to develop and optimize the antimicrobial activity of nisin, Na-EDTA and pH according to an experimental design. The antimicrobial activity of the formulations against *E. coli*, *S. typhimurium* and *L. monocytogenes* was measured by agar diffusion assay. Na-EDTA enhanced the antimicrobial activity of nisin against all the selected bacteria. Nisin concentration, Na-EDTA concentration and pH were found to have statistically significant linear positive effect on the antimicrobial activity of the formulations. The study presented an optimized formulation capable of inhibiting both gram-positive and gram-negative bacteria. *In situ* studies will be carried out in the future to test the efficacy of this formulation in meat system against *E. coli*, *S. typhimurium* and *L. monocytogenes*.

## **5.10. Acknowledgements**

This research was supported by the Natural Sciences and Engineering Research Council of Canada (NSERC) and FPInnovation (Pointe-Claire, Canada) through the RDC program.

## **5.11. References**

Adjallé, K. D., Vu, K. D., Tyagi, R. D., Brar, S. K., Valéro, J. R., & Surampalli, R. Y. (2011). Optimization of spray drying process for *Bacillus thuringiensis* fermented wastewater and wastewater sludge. *Bioprocess and biosystems engineering*, 34(2), 237–46.

Balachandran, M., Devanathan, S., Muraleekrishnan, R., & Bhagawan, S. S. (2012). Optimizing properties of nanoclay–nitrile rubber (NBR) composites using Face Centred Central Composite Design. *Materials & Design*, 35, 854–862.

Baş, D., & Boyacı, İ. H. (2007). Modeling and optimization I: Usability of response surface methodology. *Journal of Food Engineering*, 78(3), 836–845.

Beveridge, T. J. (1999). Structures of gram-negative cell walls and their derived membrane vesicles. *Journal of Bacteriology*, 181(16), 4725–4733.

Bezerra, M. A., Santelli, R. E., Oliveira, E. P., Villar, L. S., & Escaleira, L. A. (2008). Response surface methodology (RSM) as a tool for optimization in analytical chemistry. *Talanta*, 76(5), 965–977.

Boziaris, I. S., & Adams, M. R. (1999). Effect of chelators and nisin produced in situ on inhibition and inactivation of gram negatives. *International Journal of Food Microbiology*, 53(2-3), 105–113.

Branen, J. K., & Davidson, P. M. (2004). Enhancement of nisin, lysozyme, and monolaurin antimicrobial activities by ethylenediaminetetraacetic acid and lactoferrin. *International Journal of Food Microbiology*, 90(1), 63–74.

CBC News (2013). Quebec E. coli illness linked to B.C. cheese recall. Retrieved from <http://www.cbc.ca/news/canada/british-columbia/quebec-e-coli-illness-linked-to-b-c-cheese-recall-1.1863369>

Delves-Broughton, J. (1990). Nisin and its application as a food preservative. *Journal of the Society of the Dairy Technology*, 43, 73–76.

Ellison, R. T., Giehl, T. J., & LaForce, F. M. (1988). Damage of the outer membrane of enteric gram-negative bacteria by lactoferrin and transferrin. *Infection and Immunity*, 56(11), 2774–2781.

Gálvez, A., Abriouel, H., López, R. L., & Ben Omar, N. (2007). Bacteriocin-based strategies for food biopreservation. *International Journal of Food Microbiology*, 120(1-2), 51–70.

Gill, A. O., & Holley, R. A. (2003). Interactive inhibition of meat spoilage and pathogenic bacteria by lysozyme, nisin and EDTA in the presence of nitrite and sodium chloride at 24 °C. *International Journal of Food Microbiology*, 80(3), 251–259.

Hosseini, S. M., Hosseini, H., Mohammadifar, M. A., German, J. B., Mortazavian, A. M., Mohammadi, A., Khosravi-Daranic, K., Shojaee-Aliabadia, S., & Khaksar, R. (2014). Preparation and characterization of alginate and alginate-resistant starch microparticles containing nisin. *Carbohydrate Polymers*, 103, 573–80.

Khare, A. K., Biswas, A. K., & Sahoo, J. (2014). Comparison study of chitosan, EDTA, eugenol and peppermint oil for antioxidant and antimicrobial potentials in chicken noodles and their effect on colour and oxidative stability at ambient temperature storage. *LWT - Food Science and Technology*, 55(1), 286–293.

Lewis, R., Corriveau, A., & Osborne, W. (2013). *Independent Review of XL Foods Inc. Beef Recall 2012*. Retrieved from [http://www.salubritedesaliments.gc.ca/english/xl\\_reprt-rappрте.pdf](http://www.salubritedesaliments.gc.ca/english/xl_reprt-rappрте.pdf)

Rohani, S. M. R., Moradi, M., Mehdizadeh, T., Saei-Dehkordi, S. S., & Griffiths, M. W. (2011). The effect of nisin and garlic (*Allium sativum* L.) essential oil separately and in combination on the growth of *Listeria monocytogenes*. *LWT - Food Science and Technology*, *44*(10), 2260–2265.

Rollema, H. S., Kuipers, O. P., Both, P., de Vos, W. M., & Siezen, R. J. (1995). Improvement of solubility and stability of the antimicrobial peptide nisin by protein engineering. *Applied and environmental microbiology*, *61*(8), 2873–2878.

Scallan, E., Hoekstra, R. M., Angulo, F. J., Tauxe, R. V., Widdowson, M.-A., Roy, S. L., Jones, J. L., & Griffin, P. M. (2011). Foodborne Illness Acquired in the United States—Major Pathogens. *Emerging Infectious Diseases*, *17*(1), 7–15.

Shai, Y. (1999). Mechanism of the binding, insertion and destabilization of phospholipid bilayer membranes by alpha-helical antimicrobial and cell non-selective membrane-lytic peptides. *Biochimica et biophysica acta*, *1462*(1-2), 55–70.

Stevens, K. A., Sheldon, B. W., Klapes, N. A., & Klaenhammer, T. R. (1991). Nisin treatment for inactivation of *Salmonella* species and other gram-negative bacteria. *Applied and Environmental Microbiology*, *57*(12), 3613–3615.

Thomas, M. K., Murray, R., Flockhart, L., Pintar, K., Pollari, F., Fazil, A., Nesbitt, A., & Marshall, B. (2013). Estimates of the burden of foodborne illness in Canada for 30 specified pathogens and unspecified agents, circa 2006. *Foodborne Pathogens and Disease*, *10*(7), 639–648.

Vaara, M. (1992). Agents that increase the permeability of the outer membrane. *Microbiological Reviews*, 56(3), 395–411.

Viedma, M. P., Ercolini, D., Ferrocino, I., Abriouel, H., Ben Omar, N., López, R. L., & Gálvez, A. (2010). Effect of polythene film activated with enterocin EJ97 in combination with EDTA against *Bacillus coagulans*. *LWT - Food Science and Technology*, 43(3), 514–518.

Wan Norhana, M.N., Poole, S.E., Deeth, H.C., & Dykes, G.A. (2012). Effects of nisin, EDTA and salts of organic acids on *Listeria monocytogenes*, *Salmonella* and native microflora on fresh vacuum packaged shrimps stored at 4 °C. *Food Microbiology*, 31, 43–50.

Warriner, K., & Namvar, A. (2009). What is the hysteria with *Listeria*? *Trends in Food Science & Technology*, 20(6-7), 245–254.

**Table-5.1:** Levels of the factor tested in the CCD

Factors	Symbol (Unit)	Level of factors				
		$-\alpha$	-1	0	+1	$+\alpha$
Nisin concentration	$X_1$ ( $\mu\text{g/mL}$ )	19.8	62.5	125.5	18.75	230
Na-EDTA concentration	$X_2$ (mM)	3.18	10	20	30	36.18
pH	$X_3$	2.14	3.5	5.5	7.5	8.86

**Table-5.2:** Results of the inhibition zones of the formulations from CCD.

Run	Nisin X <sub>1</sub> (µg/mL)	Na-EDTA X <sub>2</sub> (mM)	pH X <sub>3</sub>	Inhibition Zone (D, mm)		
				D <sub>E</sub> (mm)	D <sub>S</sub> (mm)	D <sub>L</sub> (mm)
1	62.50	10.00	3.50	7.8	7.8	13.4
2	62.50	10.00	7.50	7.4	7.8	12.2
3	62.50	30.00	3.50	13.6	11.4	16.8
4	62.50	30.00	7.50	12.7	11.8	15.0
5	187.50	10.00	3.50	8.3	7.5	15.4
6	187.50	10.00	7.50	7.9	7.5	14.5
7	187.50	30.00	3.50	11.3	10.7	18.5
8	187.50	30.00	7.50	12.9	11.0	16.7
9	19.90	20.00	5.50	10.0	9.0	14.6
10	230.10	20.00	5.50	10.9	9.1	16.7
11	125.00	3.18	5.50	7.4	7.5	12.4
12	125.00	36.82	5.50	14.7	13.8	18.0
13	125.00	20.00	2.14	8.4	7.7	13.6
14	125.00	20.00	8.86	8.6	8.2	14.2
15 (C)	125.00	20.00	5.50	12.5	11.2	15.8
16 (C)	125.00	20.00	5.50	12.8	11.0	16.2
17 (C)	125.00	20.00	5.50	12.1	11.3	15.9
18 (C)	125.00	20.00	5.50	12.6	11.2	16.3

**Table-5.3:** Response surface regression analyses for the inhibition zones of the formulations.

Terms	Regression analysis					
	<i>E. Coli</i> (D)		Salmonella (D)		<i>L. monocytogenes</i> (D)	
	Coefficient	<i>P</i> -value	Coefficient	<i>P</i> -value	Coefficient	<i>P</i> -value
Constant	-6.52	≤0.01	-3.20	≤0.01	7.27	≤0.01
Nisin (L)*	0.04	≤0.01	0.04	≤0.01	0.01	≤0.01
Nisin (Q)*	-1.60×10 <sup>-4</sup>	≤0.01	-1.70×10 <sup>-4</sup>	≤0.01	N/A	N/A
Na-EDTA (L)*	0.40	≤0.01	0.18	≤0.01	0.15	≤0.01
Na-EDTA (Q)*	-4.26×10 <sup>-3</sup>	≤0.05	N/A	N/A	N/A	N/A
pH (L)*	3.66	≤0.01	2.95	≤0.01	1.56	≤0.01
pH (Q)*	-0.33	≤0.01	-0.26	≤0.01	-0.16	≤0.01

\* L represents linear coefficient ( $X_i$ ), Q represents quadratic coefficient ( $X_i^2$ ).  
 N/A-Not Applicable for the model

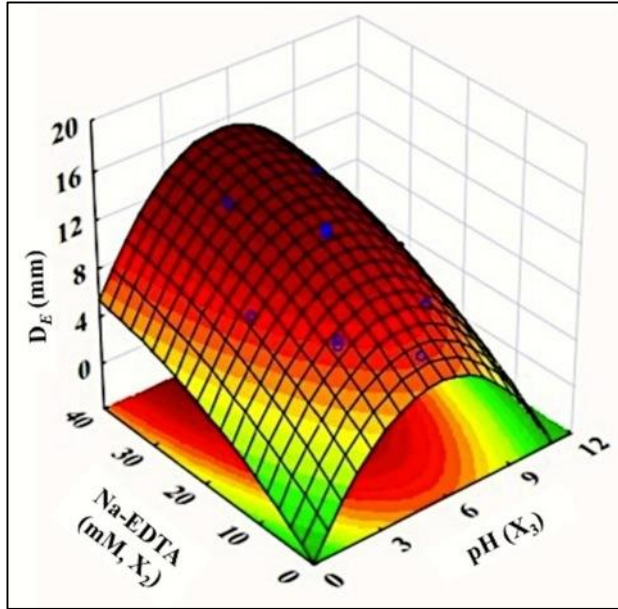


**Figure 5.1(a):** 3D response surface plot for  $D_E$  as a function of pH ( $X_3$ ) and Na-EDTA ( $X_2$ ), while keeping the nisin ( $X_1$ ) constant at 125 ( $\mu\text{g/mL}$ ).

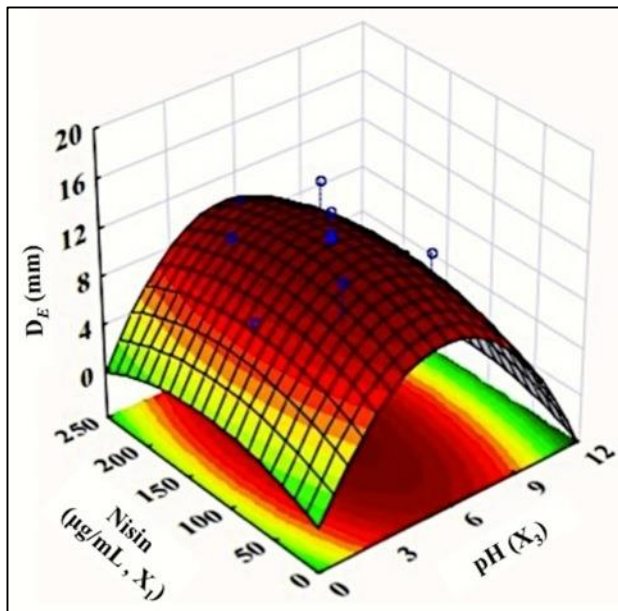


**Figure 5.1(b):** 3D response surface plot for  $D_E$  as a function of pH ( $X_3$ ) and nisin ( $X_1$ ), while keeping the Na-EDTA ( $X_2$ ) constant at 20 mM.

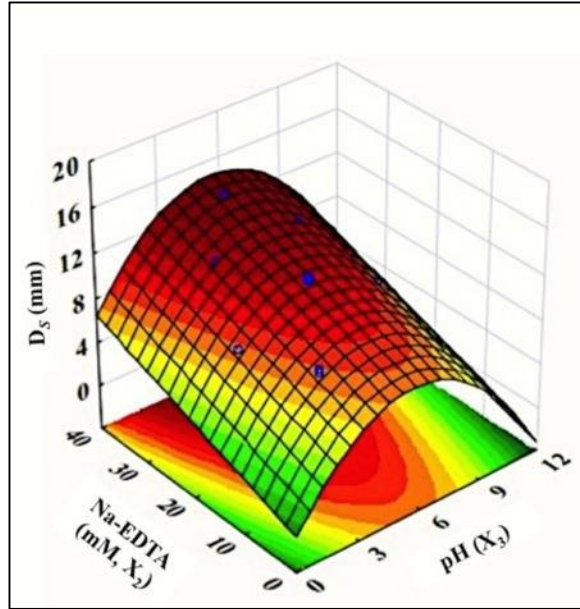


**Figure 5.2(a):** 3D response surface plot for  $D_S$  as a function of pH ( $X_3$ ) and Na-EDTA ( $X_2$ ), while keeping the nisin ( $X_1$ ) constant at 125 ( $\mu\text{g/mL}$ ).

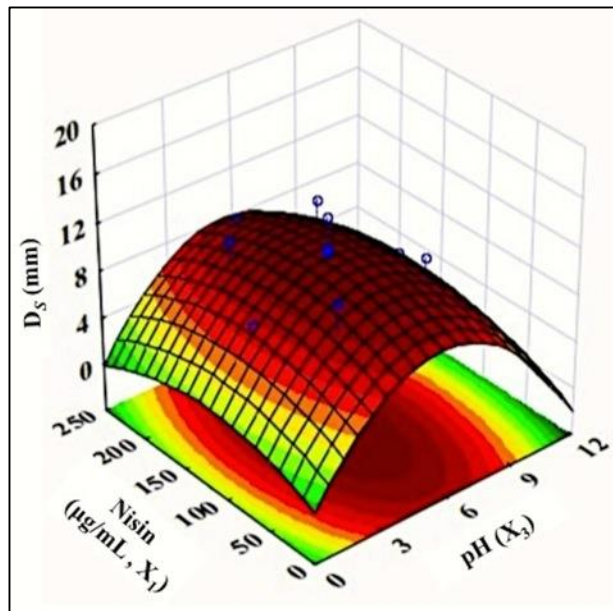


**Figure 5.2(b):** 3D response surface plot for  $D_S$  as a function of pH ( $X_3$ ) and nisin ( $X_1$ ), while keeping the Na-EDTA ( $X_2$ ) constant at 20 mM.

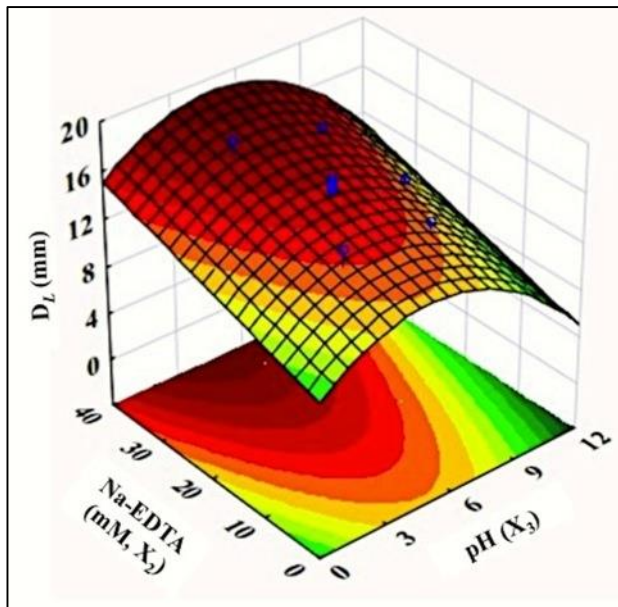


**Figure 5.3(a):** 3D response surface plot for  $D_L$  as a function of pH ( $X_3$ ) and Na-EDTA ( $X_2$ ), while keeping the nisin ( $X_1$ ) constant at 125 ( $\mu\text{g/mL}$ ).

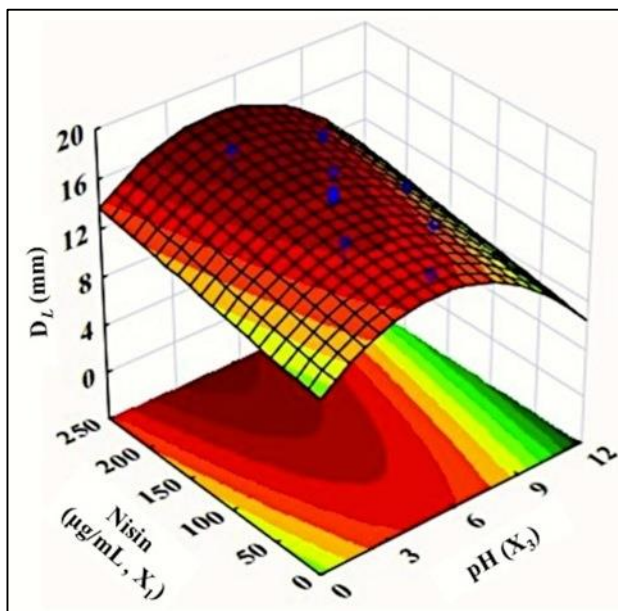


**Figure 5.3(b):** 3D response surface plot for  $D_L$  as a function of pH ( $X_3$ ) and nisin ( $X_1$ ), while keeping the Na-EDTA ( $X_2$ ) constant at 20 mM.

### **5.12. General discussion of the Publication-4**

Among the 3 factors studied (nisin, Na-EDTA and pH) in this publication, pH was found to be the most influential factor affecting the antimicrobial activity of the formulations against both gram-positive and gram-negative bacteria. Combinations nisin and Na-EDTA demonstrated effective bactericidal activity against *E. coli* and *S. typhimurium*. A nisin concentration of 125-150 µg/mL, Na-EDTA concentration of 20-30 mM and pH of 5-6 favor the maximum inhibition of *E. coli* and *S. typhimurium*. Incorporation of Na-EDTA also improved the antimicrobial activity of nisin against *L. monocytogenes*. One of the significant outcomes of this research was the antilisterial activity of nisin over a broad pH range (3.5-7.5). Generally, the antilisterial activity of nisin is limited to acidic pH range (2-4), which limits the potential use of nisin for food applications sensitive to the change of pH (Steven *et al.*, 1991). A nisin concentration of 125-150 µg/mL, Na-EDTA concentration of 20-30 mM and pH of 5-6 was found optimum to inhibit all three selected pathogenic bacteria.

## **CHAPTER 6**

### **Publication 5**

# Genipin cross-linked antimicrobial nanocomposite films to prevent the surface growth of bacteria in fresh meats

Avik Khan<sup>1</sup>, Jean Bouchard<sup>3</sup>, Bernard Riedl<sup>2</sup> and Monique Lacroix<sup>1\*</sup>

<sup>1</sup>Research Laboratories in Sciences Applied to Food, Canadian Irradiation Centre (CIC),  
INRS-Institut Armand-Frappier, Université du Québec, 531 Boulevard des Prairies,  
Laval, Québec, H7V 1B7, Canada

<sup>2</sup>Département des sciences du bois et de la forêt, Faculté de foresterie, géographie et géomatique,  
Université Laval, Québec-city, Québec, G1V 0A6, Canada

<sup>3</sup>FPIinnovations, 570 Boulevard St. Jean, Pointe-Claire, Québec, H9R 3J9, Canada

**KEYWORDS:** Cellulose Nanocrystal, Genipin, Nisin, EDTA, Food Safety, *E. coli* 0157:H7,  
Total Viable Count, *Listeria monocytogenes*.

\* **Corresponding Author:** Prof. Monique Lacroix.

Telephone: +1-450-687-5010; Fax: +1-450-686-5501.

**E-mail:** [monique.lacroix@iaf.inrs.ca](mailto:monique.lacroix@iaf.inrs.ca)

This article has been submitted to the *International Journal of Food Microbiology*.

## **6.1. Contribution of the authors**

The experimental works were planned, performed and analyzed by Avik Khan with guidance from Prof. Monique Lacroix. Prof. Monique Lacroix and Prof. Bernard Riedl corrected the main draft. Dr. Jean Bouchard also corrected the main draft.

## 6.2. Specific objectives of the Publication-5

The optimized nisin-EDTA formulation (from Publications-4) was immobilized on the surface of the microfluidized CNC/chitosan (from Publications-3) by using the optimized genipin concentration (0.05% w/v) from Publications-2. The antimicrobial activity of the films were tested *in vitro* and *in situ* against *L. monocytogenes* and *E. coli* during storage at 4 °C. Boneless pork loin meat was chosen as a meat model for the *in situ* analysis. The films were gamma irradiated to examine the possible synergy between genipin cross-linking and gamma-irradiation. Psychrotrophs, mesophiles and *lactobacillus* spp. (LAB) are the three groups of bacteria that are relevant to fresh meat or meat products and are divided according to the temperature range within which they can grow. The growth of these bacteria dictates the microbiological quality and shelf life of fresh meat products. So, the films were also tested for their ability to restrict the growth of these bacteria in fresh meat.

### 6.3. Résumé

La nisine et l'éthylènediaminetétraacétate disodique ont été immobilisés à la surface de films nanocomposites de cellulose nanocristalline (CNC)/chitosane en utilisant la gènipine comme agent de réticulation. L'effet de l'irradiation aux rayons gamma à faible dose sur l'activité antimicrobienne des films a été testée *in vitro* contre *E. coli* et *L. monocytogenes*. Les films réticulés à la gènipine ayant subi une irradiation à 1,5 kGy ont démontré la plus forte activité antimicrobienne contre les bactéries à la fin des 35 jours de stockage. Les films ont limité le développement des psychrotrophes, mésophiles et lactobacillus spp. (LAB) sur des échantillons de viandes de longe de porc frais et augmenté la durée de vie microbiologique des échantillons de viande de plus de 5 semaines. Ces films ont également réduit le nombre de *E. coli* et *L. monocytogenes* dans des échantillons de viande de 4,4 et 5,7 log UFC/g, respectivement, après 35 jours de stockage.

## 6.4. Abstract

Nisin and disodium ethylenediaminetetraacetate were immobilized on the surface of cellulose nanocrystal (CNC)/chitosan nanocomposite films by using genipin as a cross-linking agent. The effect of low dose gamma irradiation on the antimicrobial activity of the films was tested *in vitro* against *E. coli* and *L. monocytogenes*. The genipin cross-linked films prepared by irradiating at 1.5 kGy demonstrated the highest antimicrobial activity against both the bacteria at the end of 35 days of storage. The films restricted the growth of psychrotrophs, mesophiles and *lactobacillus* spp. (LAB) in fresh pork loin meats and increased the microbiological shelf life of meat sample by more than 5 weeks. The films also reduced the count of *E. coli* and *L. monocytogenes* in meat samples by 4.4 and 5.7 log CFU/g, respectively, after 35 days of storage.

## 6.5. Introduction

In the context of a constantly growing population and globalization of markets, prevention of food contamination by microorganisms or pathogens, is becoming increasingly important. Foodborne diseases are responsible for 9.4 million illnesses, 55,961 hospitalization and 1,391 deaths each year in the United States (Scallan *et al.*, 2011). Microbial contamination, which is considered to be the main reason for food spoilage, can drastically reduce the shelf life of foods and increase the risk of foodborne illnesses. Consumption of contaminated fresh meats or ready-to-eat (RTE) products poses serious health risk and can result in hospitalization or even deaths. Microbial contamination of meat products usually occurs at the surface due to post processing handling, processing or cutting. Antimicrobial packaging is gaining interest from researchers and industries due to its potential to prevent the surface growth of pathogenic bacteria in meat products (Quintavalla and Vicini, 2002). Direct incorporation of antimicrobials onto meat surface may provide limited efficacy due to the migration of the active substances into the bulk food matrix. Also, drastic loss of antimicrobial activity may occur due to the interaction and/or inactivation of the active substances by food components (Coma *et al.*, 2008). Antimicrobial packaging provides an innovative alternative to some of the traditional meat preservation methods and can reduce the addition of larger quantities of antimicrobials that are usually incorporated directly into the bulk of the food (Cooksey, 2005; Quintavalla and Vicini, 2002). Bionanocomposites can be defined as a novel class of materials consisting of a biopolymeric matrix, which is reinforced with a nanofiber. The nanofiber should be non-toxic, natural and obtainable from renewable sources. Cellulose nanofiber reinforced bionanocomposite films have attracted significant attention during recent years, due to their renewable nature and high potential in the field of food packaging (Khan *et al.*, 2014a; Moon *et al.*, 2011). Cellulose based nanofiber such as Cellulose nanocrystal (CNC) can be extracted through selective cellulosic

sources by a controlled acid hydrolysis process (Habibi *et al.*, 2010). CNC is made up of highly crystalline, rod shaped, nanoparticles and exhibits an average length of 100-110 nm and width of 5-10 nm (Dong *et al.*, 1998). CNC has been found very effective to improve the mechanical properties of biopolymeric films such as, chitosan, alginate, carrageenan, starch etc. (Pereda *et al.*, 2014; Khan *et al.*, 2012; Huq *et al.*, 2012; Chang *et al.*, 2010; Sanchez-Garcia *et al.*, 2010). Chitosan is a natural hetero-polysaccharide composed of 2-amino deoxy- $\beta$ -D-glucopyranose and 2-acetamido-deoxy- $\beta$ -D-glucopyranose (chitin) residues. It is a partially deacetylated derivative of chitin, which is the second most abundant natural polysaccharide in nature after cellulose. Chitosan, due to its non-toxic, biodegradable and biocompatible properties, has found application in several fields including food packaging (Prashanth and Tharanatha, 2007).

Lactic acid bacteria (LAB) produce a wide range of antimicrobial agents including bacteriocins such as, nisin. Nisin is produced by the lactic acid bacterium *Lactococcus lactis*, subsp. *lactis* strains. It is composed of 34 amino acids and belongs to the class of small peptides (<4 kDa) called lantibiotics (Hyde *et al.*, 2006; O'Sullivan *et al.*, 2002). Nisin is used as food additive in at least 48 countries and is the only bacteriocin that has GRAS (generally considered as safe) status by Food and Drug Administration (FDA) (Delves-Broughton, 1990). Nisin can inhibit a broad range of gram-positive bacteria including pathogens such as, *L. monocytogenes*. However, lack of inhibition against gram-negative bacteria remains a bottleneck for the use of nisin in food products, which requires inhibition of both gram-positive and gram-negative bacteria. Combination of nisin with other antimicrobials such as EDTA has proved to be effective to improve the antimicrobial activity of nisin against gram-negative bacteria (Vaara, 1992).

The activity of nisin may be lost in fresh and RTE meat products due to an interaction with glutathione (GSH). GSH is a strong reducing agent and is found in plants, animals,

microorganisms as well as meats such as, beef, chicken and pork (Stergiou *et al.*, 2006; Rose *et al.*, 1999). Nisin can be cross-linked onto the surface of the packaging in order to protect its activity in meat products. Genipin represents a highly potential cross-linking agent for food packaging applications due to its biocompatibility and low toxicity compared to other similar cross-linking agent such as glutaraldehyde (Sung *et al.*, 1999). It is derived from the fruit *Genipa americana* and has the ability to cross-link with amino acids or proteins (Mi *et al.*, 2002).

The objective of the present study was to investigate the antimicrobial efficacy of genipin cross-linked bionanocomposite films containing nisin and EDTA. The antimicrobial efficacy of the films were tested *in vitro* and *in situ* against *E. coli* and *L. monocytogenes* on fresh pork loin meat samples during storage at 4°C. The microbiological quality of the meat samples was also tested during storage.

## **6.6. Materials and methods**

### **6.6.1. Bacterial strains**

*E. coli* 0157:H7 (strain EDL933) was obtained from INRS-Institut Armand Frappier (Laval, Quebec, Canada). The *L. monocytogenes* strains HPB 2569 1/2a, 2558 1/2b, 2371 1/2b, 2812 1/2ba and 1043 1/2a were obtained from Health products and Foods Branch of Health Canada (Ottawa, Ontario, Canada). All the microorganisms were kept frozen at -80°C in Brain heart infusion (BHI, Alpha Biosciences Inc., Baltimore, MD, USA) broth containing glycerol (10% v/v). Before use, the stock cultures were resuscitated through 2 consecutive 24 h growth in BHI at 37°C to obtain the working cultures containing approximately 10<sup>9</sup> CFU/mL. The five *L. monocytogenes* were mixed together (2mL each) to obtain a mixture.

### **6.6.2. Preparation of nisin-EDTA antimicrobial formulation**

The antimicrobial formulation was prepared according to Khan *et al.* (2014d). A 125 µg/mL of nisin solution was prepared by dissolving the Niprosin™ powder (2.5% nisin, 77.5% salt and

20% vegetable protein, Profood, IL, USA) in deionized water. The pH of the solution was adjusted to 3.0 with dilute lactic acid (Laboratoire Mat, Beauport, Quebec, Canada), followed by centrifugation for 15 min at 2500×g. A 30 mM of disodium ethylenediaminetetraacetate (EDTA, Laboratoire Mat, Beauport, Quebec, Canada) was mixed with the nisin supernatant and the pH of the formulation was adjusted to 5.5 with 1M NaOH (Laboratoire Mat, Beauport, Quebec, Canada). The nisin-EDTA formulation was then filtered through a 0.45µm filter and stored at 4°C.

### **6.6.3. Preparation of the nanocomposite films**

In our previous study, microfluidization was found very useful for the fabrication of high strength CNC/chitosan nanocomposite films. Microfluidization allowed proper dispersion of CNC within the chitosan matrix (data not shown). In the current study, the nanocomposite films were prepared from the optimized CNC content, microfluidization pressure and number of cycles; obtained from Khan *et al.* (2014c). At first, 2% w/v of high mol. wt. chitosan (DD: 85-90%, 85/2500 Heppe-medical GmbH, Germany) and 0.5% ethylene glycol (Laboratoire Mat, Beauport, Quebec, Canada) was dissolved into a 2% w/v of aqueous acetic acid (Laboratoire Mat, Beauport, Quebec, Canada) solution. A 2% w/v of aqueous CNC (FPInnovations, Pointe-Claire, QC, Canada) suspension was prepared and incorporated (8% w/w of chitosan) into the chitosan/ethylene glycol solution. The CNC/chitosan nanocomposite suspension was then pre-homogenized for 3h with a homogenizer (IKA RW-20; IKA® Works Inc., Wilmington, USA), microfluidized at 7,000 psi and 6 microfluidization cycles. The nanocomposite films were made by casting the microfluidized suspension on Petri dishes which was allowed to dry at room temperature and 30-35% RH. Films were then treated with 1M NaOH (Laboratoire Mat, Beauport, Quebec, Canada) for 2 min, washed several times with deionized water and were allowed to dry.

#### **6.6.4. Preparation of the antimicrobial nanocomposite films**

The antimicrobial films were prepared by casting 15 mL of the nisin-EDTA antimicrobial solution on the surface of the nanocomposite films. The genipin cross-linked films were prepared by mixing 0.05% w/v of genipin (Challenge Bio-products, Yun-Lin Hsien, Taiwan) with the nisin-EDTA formulation at pH 5.5 and the reaction was carried out for 24 h at room temperature (khan *et al.*, 2014b). The films were allowed to dry for 2 days. After drying the films were peeled off the Petri dishes and stored at 4°C in a desiccator filled with deionized water. All the films were  $\gamma$ -irradiated at doses 0.5 and 1.5 kGy at the Canadian Irradiation Centre (CIC, Laval, Quebec, Canada) at room temperature. The uncross-linked films were coded as N-0kGy, N-0.5kGy and N-1.5kGy. The genipin cross-linked films were coded as G-0kGy, G-0.5kGy and G-1.5kGy. All the films were stored at 4°C in a desiccator filled with deionized water to obtain 90-100% RH.

#### **6.6.5. *In vitro* analysis**

The films were tested *in vitro* against *E. coli* and *L. monocytogenes* according to a modified disk diffusion assay. At first, test media (3.7% w/v BHI and 0.75% w/v agar) were prepared, autoclaved and were cooled to 50°C in a water bath. Test mediums used for *L. monocytogenes* were prepared by incorporating 1.0% w/v Tween 20, a surfactant, into the solution prior to autoclave. After cooling, a 1.0% v/v of the bacterial cultures ( $10^8$  CFU/mL) was mixed with test media to obtain a final bacterial population of approximately  $10^6$  CFU/mL. A 25 mL of the inoculated medium was added to each Petri dish (95mm×15mm) and was allowed to solidify. The films were cut into square shapes (1.44 cm), and were put on the surface of the inoculated plates. The plates were incubated for 24 h at 37°C temperature and diameter (mm) of the inhibition zones were measured. The inhibition zones of the films (at 4°C and 90-100% RH) were measured during 1, 4, 7, 14, 21 and 35 days of storage.

#### **6.6.6. *In situ* analysis**

The meat samples were purchased from a local grocery store (IGA, Laval, Quebec, Canada). A 10 g of meat samples (as purchased) were cut, sandwiched between two films, vacuum packaged and stored at 4°C. The meat samples were analyzed for the total viable count (TVC) of psychrotrophs, mesophiles and LAB. Two pathogenic bacteria, *E. coli* and *L. monocytogenes*, were chosen as model bacteria to investigate the antimicrobial activity of the films in case of a meat contamination by pathogenic bacteria. Different meat samples were inoculated with *E. coli* and *L. monocytogenes* (approximately 10<sup>3</sup> CFU/g of meat), prior to vacuum packaging.

#### **6.6.7. Microbiological and chemical analysis**

Meat samples were analyzed during storage for microbial growth at 1, 4, 7, 14, 21 and 35 days. On each day of analysis, 3 meat samples were placed in a sterile filter sample bag (Whirl-Pak; Nasco, Fort Atkinson, WI, USA), diluted 5 folds with peptone water (0.1%; BD, Sparks, MD, USA) and homogenized in a Lab-blender 400 stomacher (Seward Medical, London, UK) for 2 min at 360 rpm. From this homogenate, appropriate dilutions were mixed (according to pour plate method) with brain heart infusion agar (Alpha Biosciences Inc., Baltimore, MD, USA) for the enumeration of mesophilic and psychrotropic bacteria. The solidified agar plates were incubated at 37 °C for 2 days for the mesophilic and at 4 °C for 7 days for the psychrotropic bacteria. For the enumeration of LAB present in the meat, De-Mann, Rogosa and Sharpe (MRS) agar plates were used and were incubated at 37 °C for 48 h. Following the bacterial enumeration, the homogenates were used to analyze the pH of the meat samples during storage. The pH values were measured using a digital pH meter (Accumet Basic AB15, Fisher Scientific, ON, Canada). MacConkey Sorbital (Alpha Biosciences) agar was used for the selective enumeration of *E. coli*. PALCAM (Alpha Biosciences) agar supplemented with antibiotics acriflavine (5 mg/mL), polymyxin B (10 mg/mL) and ceftazidime (8 mg/mL); was used for the selective enumeration of

*L. monocytogenes*. The plates were incubated at 37 °C for 48 h. Following incubation, the colonies forming unit (CFU) were counted using a magnifier. Detection limit for all microbial analysis was 5 CFU/g of meat. All bacterial counts were transformed to logarithmic (log<sub>10</sub>) values.

#### **6.6.8. Statistical analysis**

The mechanical analysis was performed with six different films specimens and the average value was reported. All the other experiments and analysis were performed in triplicate. An analysis of variance (ANOVA) and multiple comparison tests of Turkey's-b were used to compare all the results. Differences between means were considered significant when the confidence interval is smaller than 5% ( $P \leq 0.05$ ). The analysis was performed with the PASW Statistics 18 software (SPSS Inc., Chicago, IL, USA).

### **6.7. Results and Discussions**

#### **6.7.1. Antimicrobial activity of the films *in vitro***

The *in vitro* antimicrobial activity of the films against *E. coli* is presented in **Fig. 6.1**. At day 1, the inhibition zones of the film formulations N-0kGy, N-0.5kGy, N-1.5kGy, G-0kGy, G-0.5kGy and G-1.5kGy were 28.2, 24.7, 23.6, 26.2, 25.7 and 23.4 mm, respectively. The antimicrobial activity of the uncross-linked film (N-0kGy) was significantly higher ( $P \leq 0.05$ ) than all the other film formulations. The inhibition zone of the unirradiated genipin cross-linked films (G-0kGy) was also significantly higher ( $P \leq 0.05$ ) than those of the irradiated films (G-0.5kGy and G-1.5kGy). However, the combination of gamma irradiation and genipin cross-linking positively influenced the antimicrobial activity of the films during storage. The activity of the unirradiated (both cross-linked and uncross-linked) films decreased significantly ( $P \leq 0.05$ ) during storage. At day 14, the inhibition zones obtained for N-0kGy and G-0kGy was 21.2 and 21.8 mm; whereas the zones for N-0.5kGy, N-1.5kGy, G-0.5kGy and G-1.5kGy were 22.6, 22.3, 24.7, 23.9 mm,

respectively. The activity of the G-0.5kGy was stable thorough out the storage experiment as there were no significant ( $P>0.05$ ) change in the inhibition zones from day 1 to 35. It is interesting to note that the activity of the cross-linked films irradiated at 1.5 kGy (G-1.5kGy) improved during storage. At day 35, the inhibition zone (27.1 mm) obtained for G-1.5kGy was significantly higher ( $P\leq 0.05$ ) than all the other film formulations. **Fig. 6.2** represents the zone of inhibitions obtained against *L. monocytogenes*. At day 1, the inhibition zones of the film formulations N-0kGy, N-0.5kGy, N-1.5kGy, G-0kGy, G-0.5kGy and G-1.5kGy were 21.1, 22.2, 29.3, 27.7, 22.6 and 23.8 mm, respectively. The antimicrobial activity of the irradiated uncross-linked film (N-1.5kGy) was significantly higher ( $P\leq 0.05$ ) than that of all the other film formulations. However, the activity decreases significantly ( $P\leq 0.05$ ) during storage and at day 35 the inhibition zone was 22.1 mm. While the inhibition zone for N-0kGy increased from 21.1 to 30.5 during day 1 to 7; it began to decrease thereafter and was found to 21.4 mm at day 35. The activity of the un-irradiated cross-linked films (G-0kGy) decreased from 27.7 (at day 1) to 21.8 (at day 35) mm during storage. The cross-linked films irradiated at 1.5 kGy demonstrated the highest antimicrobial activity during storage. The inhibition zones (27.7 mm) obtained for G-1.5kGy films were significantly higher ( $P\leq 0.05$ ) than the other film formulations.

Initial low activity of the cross-linked films could be attributed to the immobilization of the antimicrobial formulation on to the surface of the nanocomposite films could be due to the cross-linking reaction of nisin with genipin. It was reported that the antimicrobial activity of the cross-linked nisin-hydroxypropylmethylcellulose (HPMC) films was lower compared to that of the uncross-linked nisin-HPMC films (Sebti *et al.*, 2003). At pH 5 to 6, genipin can undergo cross-linking reaction with the primary amine groups present in nisin via two different sites on its structure. One of the reaction mechanisms is the formation of secondary amide linkage due to the

nucleophilic substitution of the ester group of genipin by primary amine group present in nisin, while the other reaction mechanism is the formation of a heterocyclic cross-linked compound due to the ring opening reaction of the genipin molecule at C-3 position (Butler *et al.*, 2003; Mi *et al.*, 2000). The reduction in the antimicrobial activity of the uncross-linked films coincided with the increase in the activity of the cross-linked films. These phenomena can be attributed to the high RH (90 to 100%) storage condition. High RH could have facilitated desorption or depletion of nisin from the surface of the uncross-linked films; hence low antimicrobial activity during storage (Balaguer *et al.*, 2013). On the other hand, the cross-linked network may have initially (1 to 7 days) restricted desorption or depletion of nisin-EDTA from the surface of the films. But prolonged storage (14 to 35 days) caused chain-relaxation of the cross-linked network; as a result more nisin-EDTA was available on the surface of the films. In the current study, films prepared by the combination of low dose gamma irradiation (1.5 kGy) and genipin cross-linking exhibited the highest antimicrobial activity during storage. Gamma irradiation may have limited the loss of antimicrobial agents through diffusion and stabilized the films. Le Tien *et al.* (2000) reported preparation of cross-linked whey protein concentrate (WPC) films using gamma irradiation. Gamma irradiation modified the conformation of proteins, which became more stable and ordered. The results from the *in vitro* analysis showed that the genipin cross-linked films prepared by 1.5kGy (G-1.5kGy) exhibited maximum antimicrobial activity against both *E. coli* and *L. monocytogenes*. As a result, the G-1.5kGy films were selected to test the antimicrobial efficacy of the film *in situ*.

#### **6.7.2. Total count for psychrotrophic and mesophilic bacteria**

The bacteria count for psychrotrophs and mesophiles are presented **Fig. 6.3** and **Fig. 6.4**, respectively. The initial bacterial counts (at day 1) for psychrotrophs and mesophiles in the meat samples were 5.2 and 4.4 log CFU/g, respectively. From the bacterial counts, it is evident that

both mesophilic and psychrotrophic bacteria constitute the initial microflora of fresh meats. While bacteria such as, *Acinetobacter baumannii*, *Buttiauxella* spp., *Serratia* spp. etc. are regarded as mesophilic populations; *Carnobacterium maltaromaticum* and *Carnobacterium divergens* are the species found in both mesophilic and psychrotrophic populations. Under refrigerated or chilled condition, the bacteria developing in meat are predominately psychrotrophic. This explains initial higher count of psychrotrophs (5.2 log CFU/g) in meat samples as compared to mesophiles (4.4 log CFU/g). Both gram positive, such as LAB, and gram negative, such as *Pseudomonas* spp. and *Enterobacteriaceae* belong to the psychrotrophic group of bacteria (Ercolini *et al.*, 2009). The psychrotrophs (**Fig. 6.3**) and mesophiles (**Fig. 6.4**) grew rapidly before entering stationary phase after 14 days of storage. The maximum count obtained for psychrotrophs were 8.4 log CFU/g at day 14; whereas that obtained for mesophiles were 8.4 at day 21. At day 35, the counts for psychrotrophs and mesophiles were 7.4, and 7.3 log CFU/g.

It is interesting to note that the bacterial counts for psychrotrophs and mesophiles crossed 6 log CFU/g, which is considered to be the limit for microbiological shelf life of fresh meats, within 4 to 5 days of storage. The microbiological shelf life of meat or meat products, which can be defined as the maximum acceptable bacterial level in meat, is directly related to its spoilage. A total viable count (TVC) of 6 log CFU/g is considered to be the maximum acceptable limit of bacteria in meat (Gram *et al.*, 2002; Jiang *et al.*, 2010). If the bacterial count crosses this limit the meat is spoiled; slime and discoloration may also appear at 8 log CFU/g (Borch *et al.*, 1996; Mano *et al.*, 1995).

Low dose (1.5 kGy) gamma irradiation reduced the count of psychrotrophic and mesophilic bacteria and increased the shelf life of meat up to 14 days. At day 14, the psychrotrophic and

mesophilic bacteria count for the irradiated meat samples were 6.0 and 6.4 log CFU/g, which were significantly lower ( $P \leq 0.05$ ) than those of the unirradiated meat samples. Therefore, irradiation of the meat samples at 1.5 kGy reduced the count of psychrotrophs and mesophiles by 2.4 and 1.5 log CFU/g, respectively. Dogbevi et al. (2000) also reported that irradiation of fresh pork loin meat at 1 kGy reduced the count of psychrotrophic and mesophilic bacteria by 2.5 and 0.5 log CFU/g, respectively. Similar to the current study, the authors also reported mesophiles were more resistant to gamma radiation than psychrotrophs. Dussault et al. (2012) reported more than 2 log CFU/g reduction in the initial count of psychrotrophs and mesophiles due to the irradiation of pork sausage meat at 1.5 kGy. The antimicrobial films (G-1.5kGy) were found to be very effective in controlling the growth of bacteria in meat samples. The bacterial count did not cross the shelf life limit during the storage period. At day 35, the counts for psychrotrophs and mesophiles were 3.6 and 2.8 log CFU/g. Therefore, the films reduced the count of psychrotrophs and mesophiles by 3.4 and 4.6 log CFU/g, respectively, after 35 days of storage. Ercolini et al. (2010) reported significant reduction of food spoilage microbial population and enhanced microbiological quality of beef samples due to the use of antimicrobial packaging containing nisin, HCl and EDTA.

### **6.7.3. Total count for LAB**

The bacterial count for LAB in meat samples is presented in **Fig. 6.5**. The initial count (at day 1) for LAB was 4.2 log CFU/g. The LAB also grew over storage but entered death phase after day 14. The bacterial count crossed 6 log CFU/g within 4 days of storage and the maximum count obtained was 7.9 log CFU/g at 14. The presence of LAB in meat is associated with the development of acidic off-odor and spoilage of meat due to the production of organic acids from glucose by fermentation (Dussault *et al.*, 2012). The presence of LAB is particularly important for vacuum packaged meats. When meat in vacuum-packaged, the composition of the gaseous

phase changes during storage: a carbon dioxide rich environment develops due to the decrease in oxygen concentration. As a result, bacterial flora is gradually shifted towards LAB, which is carbon dioxide tolerant (Jiang *et al.*, 2010). *Lactobacillus sakei* is among the most common psychrotrophic lactobacilli detected in refrigerated vacuum packaged fresh meat samples (Doulgeraki *et al.*, 2012). Other psychrotrophic LAB such as, *Lactobacillus curvatus*, *fuchuensis*, *algidus* can also be found during storage under vacuum at refrigerated condition (Doulgeraki *et al.* 2010; Nieminen *et al.*, 2011). Gamma irradiation (1.5 kGy) reduced the count of LAB and prevented the spoilage of the meat samples. At day 14, the LAB count for the irradiated meat samples was 5.6 log CFU/g, which was significantly lower ( $P \leq 0.05$ ) than that of the unirradiated meat samples. Therefore, irradiation of the meat samples at 1.5 kGy reduced the count of LAB by 2.2 log CFU/g, respectively. The antimicrobial films successfully inhibited the growth of LAB in meat products and at day 35 the LAB count was 1.7 log CFU/g. Therefore, the films reduced the count of LAB by 5.6 log CFU/g.

#### **6.7.4. pH of the meat samples**

The results for the pH analysis of the meat samples during storage are shown in **Fig. 6.6**. The initial pH of the meat samples was approximately 5.6. There was no significant ( $P > 0.05$ ) difference in the pH of the irradiated and non-irradiated meat samples. The pH of meat samples reduced slightly from 5.6 to 5.3 during storage time. The pH reduction of the meat samples can be associated with the growth of LAB in meat. The growth of LAB may result in the production of organic acids and subsequent reduction in the pH (Dussault *et al.*, 2012). It is interesting to note that the pH of the meat samples with antimicrobial films was approximately 6.6, which was significantly higher ( $P \leq 0.05$ ) than that of control meat samples. The high pH of the meat with G-1.5kGy films may be attributed to the suppression of LAB in meat. The antimicrobial packaging (G-1.5kGy) also kept the pH of the meat stable during storage time.

#### **6.7.5. Antimicrobial activity against pathogenic bacteria**

The *in situ* antimicrobial activity of the films against *E. coli* and *L. monocytogenes* is presented in **Fig. 6.7a** and **6.7b**, respectively. The initial count (at day 1) for *L. monocytogenes* and *E. coli* in meat samples was 3.0 and 4.1 log CFU/g, respectively. Both the bacteria grew during storage and at day 35 the count for *L. monocytogenes* and *E. coli* was 5.1 and 6.4 log CFU/g, respectively. The films completely inhibited the growth of *L. monocytogenes* in meat samples and the bacterial count was below the detection limit (0.7 log CFU/g) during the storage experiment. As a result, a 4.4 log CFU/g reduction in the count of *L. monocytogenes* was obtained due to the use antimicrobial films. A gradual decrease in the count of *E. coli* was also observed in the meat samples wrapped with films. The films reduced the count of *E. coli* by 5.7 log CFU/g after 35 days of storage.

In the current study, the antimicrobial films successfully inhibited the growth of *E. coli* and *L. monocytogenes*. The films also restricted the growth psychrotrophs, mesophiles and LAB. The antimicrobial activity of the films can be attributed to the cross-linked nisin-EDTA formulation. Nisin disrupt the cytoplasmic membrane of susceptible gram-positive bacteria through the formation of pores in the membrane (Shai, 1999). However, presence of divalent cations in the outer membrane (OM) of gram-negative bacteria promotes a hydrophilic surface and excludes nisin from reaching the cytoplasmic membrane. EDTA replaces the divalent cations from the OM and allows diffusion of nisin to the cytoplasmic membrane of gram-negative bacteria (Gill and Holley, 2003; Vaara, 1992). A zein film containing lysosome and EDTA has been found to be effective against both gram-positive (*Bacillus subtilis* and *Lactobacillus plantarum*) and gram-negative (*E. coli*) bacteria (Mecitoğlu *et al.*, 2006).

## 6.8. Conclusion

This study has demonstrated the effectiveness of a naturally cross-linked antimicrobial nanocomposite films to restrict and inhibit the growth of non-pathogenic and pathogenic bacteria in fresh pork meats. Combination of low dose gamma irradiation and genipin cross-linking was found to be very useful to protect the antimicrobial activity of nisin-EDTA formulation in the films during storage at high RH. The gamma irradiated cross-linked films increased the microbiological shelf life of pork meats by more than 5 weeks by restricting the growth of psychrotrophs, mesophiles and LAB below 6 log CFU/g. The films also inhibited the growth of *E. coli* and *L. monocytogenes* in meat samples. This study offers an innovative and highly potential approach for the use of gamma irradiation in food packaging application. However, more studies are required in order to elicit the mechanism of action involved in effect of gamma irradiation on genipin cross-linking and its role in the protection of the activity of antimicrobial agents.

## 6.9. Acknowledgements

This research was supported by the Natural Sciences and Engineering Research Council of Canada (NSERC), FPInnovations (Pointe-Claire, Canada) and by International Atomic Energy Agency (IAEA). The authors would also like to thank and Nordion Inc. for irradiation procedures.

## 6.10. References

Balaguer, M. P., Borne, M., Chalier, P., Gontard, N., Morel, M.-H., Peyron, S., Gavara, R., Hernandez-Munoz, P. (2013). Retention and release of cinnamaldehyde from wheat protein matrices. *Biomacromolecules*, *14*(5), 1493–1502.

- Borch, E., Kant-Muermans, M-L., & Blixt, Y. (1996). Bacterial spoilage of meat and cured meat products. *International Journal of Food Microbiology*, 33(1), 103–120.
- Butler, M. F., Clark, A. H., & Adams, S. (2006). Swelling and mechanical properties of biopolymer hydrogels containing chitosan and bovine serum albumin. *Biomacromolecules*, 7(11), 2961–2970.
- Chang, P. R., Jian, R., Zheng, P., Yu, J., & Ma, X. (2010). Preparation and properties of glycerol plasticized-starch (GPS)/cellulose nanoparticle (CN) composites. *Carbohydrate Polymers*, 79(2), 301–305.
- Cleveland, J., Montville, T. J., Nes, I. F., & Chikindas, M. L. (2001). Bacteriocins: safe, natural antimicrobials for food preservation. *International Journal of Food Microbiology*, 71(1), 1–20.
- Coma, V. (2008). Bioactive packaging technologies for extended shelf life of meat-based products. *Meat Science*, 78, 90–103.
- Cooksey, K. (2005). Effectiveness of antimicrobial food packaging materials. *Food additives and contaminants*, 22, 980–987.
- Delves-Broughton, J. (1990). Nisin and its application as a food preservative. *Journal of the Society of the Dairy Technology*, 43, 73–76.
- Dogbevi, M., Vachon, C., & Lacroix, M. (2000). The effect of gamma irradiation on physicochemical and microbiological quality of fresh pork loins. *Radiation Physics and Chemistry*, 57, 261–263.
- Dong, X. M., Revol, J. F., & Gray, D. G. (1998). Effect of microcrystallite preparation conditions on the formation of colloid crystals of cellulose. *Cellulose*, 5, 19-32.

- Doulgeraki, A. I., Ercolini, D., Villani, F., & Nychas, G-J. E. (2012). Spoilage microbiota associated to the storage of raw meat in different conditions. *International Journal of Food Microbiology*, *157*(2), 130–141.
- Doulgeraki, A. I., Paramithiotis, S., Kagkli, D. M., & Nychas, G-J. E. (2010). Lactic acid bacteria population dynamics during minced beef storage under aerobic or modified atmosphere packaging conditions. *Food Microbiology*, *27*(8), 1028–1034.
- Dussault, D., Benoit, C., & Lacroix, M. (2012). Combined effect of  $\gamma$ -irradiation and bacterial-fermented dextrose on microbiological quality of refrigerated pork sausages. *Radiation Physics and Chemistry*, *81*(8), 1098–1102.
- Ercolini, D., Ferrocino, I., La Storia, A., Mauriello, G., Gigli, S., Masi, P., & Villani, F. (2010). Development of spoilage microbiota in beef stored in nisin activated packaging. *Food Microbiology*, *27*(1), 137–143.
- Ercolini, D., Russo, F., Nasi, A., Ferranti, P., & Villani, F. (2009). Mesophilic and psychrotrophic bacteria from meat and their spoilage potential in vitro and in beef. *Applied and Environmental Microbiology*, *75*(7), 1990–2001.
- Gill, A. O., & Holley, R. A. (2003). Interactive inhibition of meat spoilage and pathogenic bacteria by lysozyme, nisin and EDTA in the presence of nitrite and sodium chloride at 24 degrees C. *International Journal of Food Microbiology*, *80*(3), 251–259.
- Gram, L., Ravn, L., Rasch, M., Bruhn, J. B., Christensen, A. B., & Givskov, M. (2002). Food spoilage-interactions between food spoilage bacteria. *International Journal of Food Microbiology*, *78*(1-2), 79–97.
- Habibi, Y., Lucia, L. A., & Rojas, O. J. (2010). Cellulose nanocrystals: chemistry, self-assembly, and applications. *Chemical reviews*, *110*(6), 3479–3500.

Huq T., Salmieri, S., Khan, A., Khan, R.A., Le Tien, C., Riedl, B., Frascinic, C., Bouchard, J., Uribe-Calderon, J., Kamal, M.R. and Lacroix, M., (2012). Nanocrystalline cellulose (NCC) reinforced alginate based biodegradable nanocomposite film. *Carbohydrate Polymers*, 90, 1757–1763.

Hyde, A. J., Parisot, J., McNichol, A., & Bonev, B. B. (2006). Nisin-induced changes in Bacillus morphology suggest a paradigm of antibiotic action. *Proceedings of the National Academy of Sciences of the United States of America*, 103(52), 19896–19901.

Jiang, Y., Gao, F., Xu, X. L., Su, Y., Ye, K. P., & Zhou, G. H. (2010). Changes in the bacterial communities of vacuum-packaged pork during chilled storage analyzed by PCR-DGGE. *Meat Science*, 86(4), 889–895.

Khan, A., Huq, T., Khan, R. a., Riedl, B., & Lacroix, M. (2014a). Nanocellulose-Based Composites and Bioactive Agents for Food Packaging. *Critical Reviews in Food Science and Nutrition*, 54(2), 163–174.

Khan, A., Salmieri, S., Frascini, C., Jean, B., Riedl, B., & Lacroix, M. (2014b). Genipin cross-linked nanocomposite films for the immobilization of antimicrobial agent. Published in *ACS-Applied Materials & Interfaces*.

Khan, A., Khanh, V. D., Chauve, G., Jean, B., Riedl, B., & Lacroix, M. (2014c). Optimization of microfluidization for the homogeneous distribution of cellulose nanocrystals (CNCs) in biopolymeric matrix. *Cellulose* 21:3457-3468.

Khan, A., Khanh, V. D., Riedl, B., & Lacroix, M. (2014d). Enhancement and optimization of the antimicrobial activity of nisin against gram-negative and gram-positive bacteria. Under revision at *LWT-Food Science & Technology*.

- Khan, A., Khan, R. A., Salmieri, S., Le Tien, C., Riedl, B., Bouchard, J., Chauve, G., Victor, T., Kamal, M. R., & Lacroix, M. (2012). Mechanical and barrier properties of nanocrystalline cellulose reinforced chitosan based nanocomposite films. *Carbohydrate Polymers*, *90*(4), 1601–1608.
- Le Tien, C., Letendre, M., Ispas-Szabo, P., Mateescu, M. a, Delmas-Patterson, G., Yu, H. L., & Lacroix, M. (2000). Development of biodegradable films from whey proteins by cross-linking and entrapment in cellulose. *Journal of Agricultural and Food Chemistry*, *48*(11), 5566–5575.
- Mano, S. B., De Fernando, G. D. G., Lopez-Galvez, D., Selgas, M. D., Garcia, M. L., Camero, M. I., & Ordoñez, J. A. (1995). Growth/survival of natural flora and listeria monocytogenes on refrigerated uncooked pork and turkey packaged under modified atmospheres. *Journal of Food Safety*, *15*(4), 305–319.
- Mecitoğlu, Ç., Yemenicioğlu, A., Arslanoğlu, A., Elmacı, Z. S., Korel, F., & Çetin, A. E. (2006). Incorporation of partially purified hen egg white lysozyme into zein films for antimicrobial food packaging. *Food Research International*, *39*(1), 12–21.
- Mi, F-L., Sung, H-W., & Shyu, S-S. (2000). Synthesis and characterization of a novel chitosan-based network prepared using naturally occurring crosslinker. *Journal of Polymer Science Part A: Polymer Chemistry*, *38*(15): 2804–2814.
- Mi, F., & Sung, H. (2002). Drug release from chitosan-alginate complex beads reinforced by a naturally occurring cross-linking agent. *Carbohydrate Polymers*, *48*, 61–72.
- Moon, R. J., Martini, A., Nairn, J., Simonsen, J., & Youngblood, J. (2011). Cellulose nanomaterials review: structure, properties and nanocomposites. *Chemical Society Reviews*, *40*, 3941-3994.

- Nieminen, T. T., Vihavainen, E., Paloranta, A., Lehto, J., Paulin, L., Auvinen, P., Solismaa, M., Björkroth, K. J. (2011). Characterization of psychrotrophic bacterial communities in modified atmosphere-packed meat with terminal restriction fragment length polymorphism. *International Journal of Food Microbiology*, *144*(3), 360–366.
- O’Sullivan, L., Ross, R. P., & Hill, C. (2002). Potential of bacteriocin-producing lactic acid bacteria for improvements in food safety and quality. *Biochimie*, *84*(5-6), 593–604.
- Pereda, M., Dufresne, A., Aranguren, M. I., & Marcovich, N. E. (2014). Polyelectrolyte films based on chitosan/olive oil and reinforced with cellulose nanocrystals. *Carbohydrate polymers*, *101*, 1018–1026.
- Prashanth, K.V.H., and Tharanathan, R.N., (2007). Chitin/chitosan: modifications and their unlimited application potential and overview. *Trends in Food Science & Technology*, *18*, 117-131.
- Quintavalla, S., & Vicini, L. (2002). Antimicrobial food packaging in meat industry. *Meat Science*, *62*(3), 373–380.
- Rhim, J-W., & Ng, P. K. W. (2007). Natural biopolymer-based nanocomposite films for packaging applications. *Critical Reviews in Food Science and Nutrition*, *47*(4), 411–433.
- Rose, N. L., Sporns, P., Stiles, M. E., & McMullen, L. M. (1999). Inactivation of Nisin by Glutathione in Fresh Meat. *Journal of Food Science*, *64*(5), 759–762.
- Sanchez-Garcia, M. D., Hilliou, L. and Lagaron, J. M. (2010). Morphology and water barrier properties of nanobiocomposites of k/l-hybrid carrageenan and cellulose nanowhiskers. *Journal of Agricultural and Food Chemistry*, *58*, 12847–12857.

Scallan, E., Hoekstra, R. M., Angulo, F. J., Tauxe, R. V., Widdowson, M.-A., Roy, S. L., Jones, J. L., Griffin, P. M. (2011). Foodborne Illness Acquired in the United States—Major Pathogens. *Emerging Infectious Diseases*, 17(1), 7–15.

Shai, Y. (1999). Mechanism of the binding, insertion and destabilization of phospholipid bilayer membranes by alpha-helical antimicrobial and cell non-selective membrane-lytic peptides. *Biochimica et biophysica acta*, 1462(1-2), 55–70.

Stergiou, V. A, Thomas, L. V, & Adams, M. R. (2006). Interactions of nisin with glutathione in a model protein system and meat. *Journal of Food Protection*, 69(4), 951–956.

Sung, H.-W., Huang, R.-N., Huang, L. L. H., & Tsai, C.-C. (1999). In vitro evaluation of cytotoxicity of a naturally occurring cross-linking reagent for biological tissue fixation. *Journal of Biomaterials Science, Polymer Edition*, 10(1), 63–78.

Vaara, M. (1992). Agents that increase the permeability of the outer membrane. *Microbiological Reviews*, 56(3), 395–411.

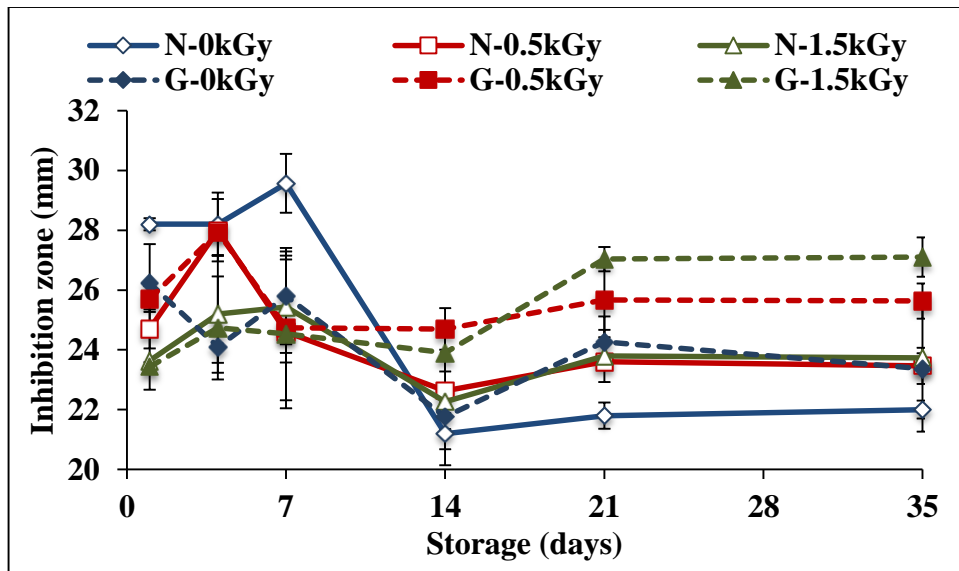


Figure 6.1: Antimicrobial activity of the films in vitro against *E. coli* during storage at 4 °C.

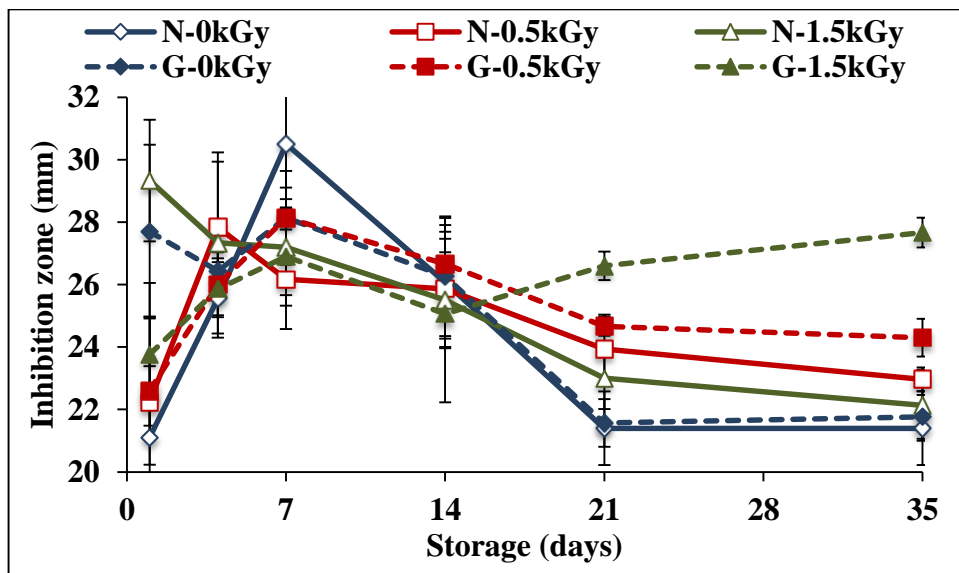
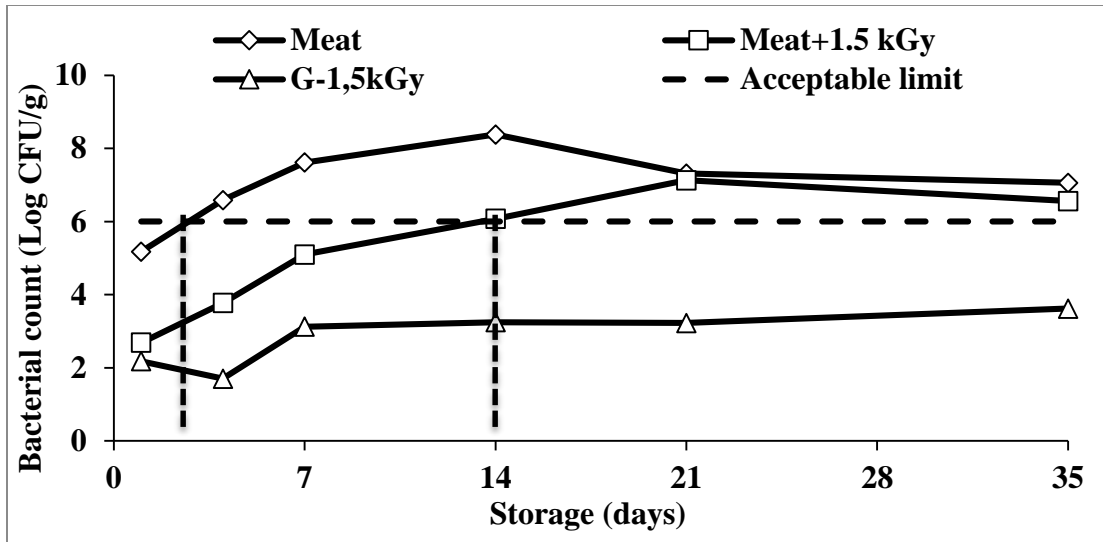
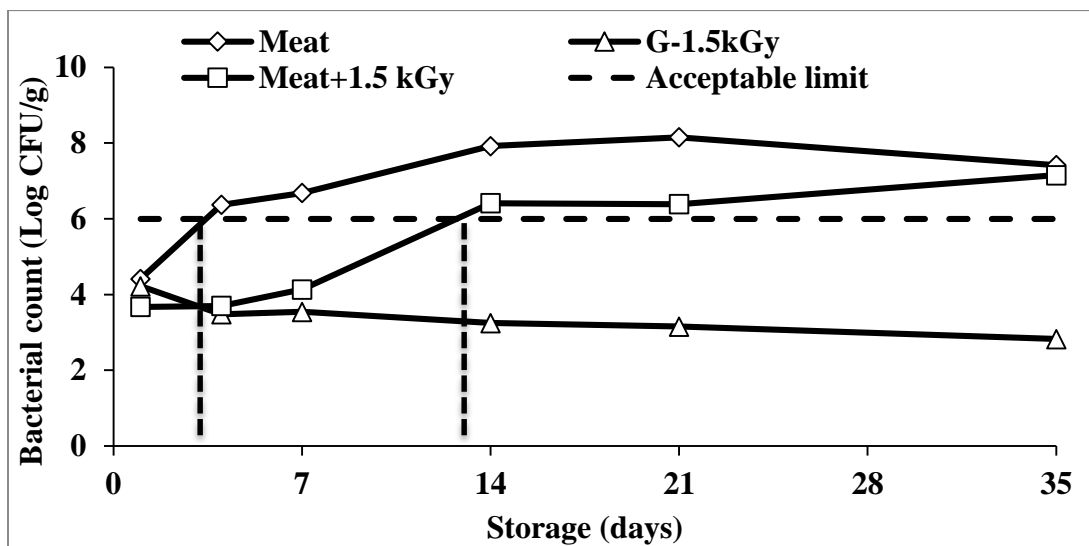


Figure 6.2: Antimicrobial activity of the films in vitro against *L. monocytogenes* during storage at 4 °C.



**Figure 6.3:** Total count of psychrotrophic bacteria in fresh pork during storage at 4 °C.



**Figure 6.4:** Total count of mesophilic bacteria in fresh pork during storage at 4 °C.

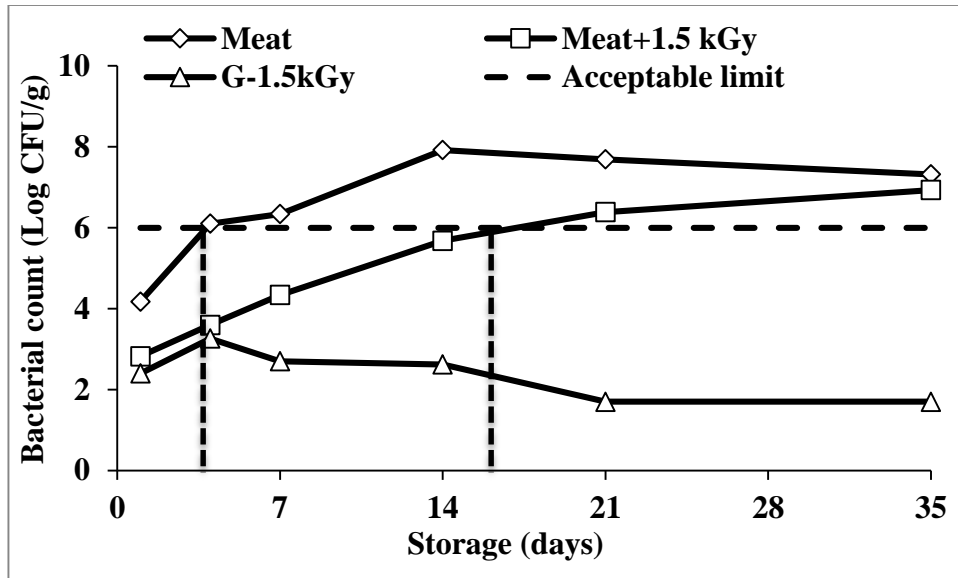


Figure 6.5: Total count of LAB in fresh pork during storage at 4 °C.

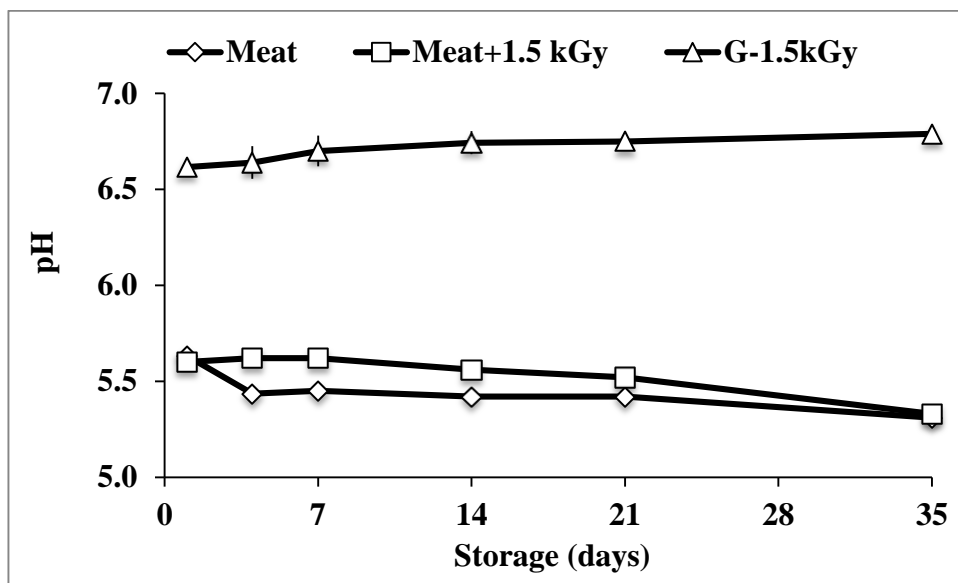
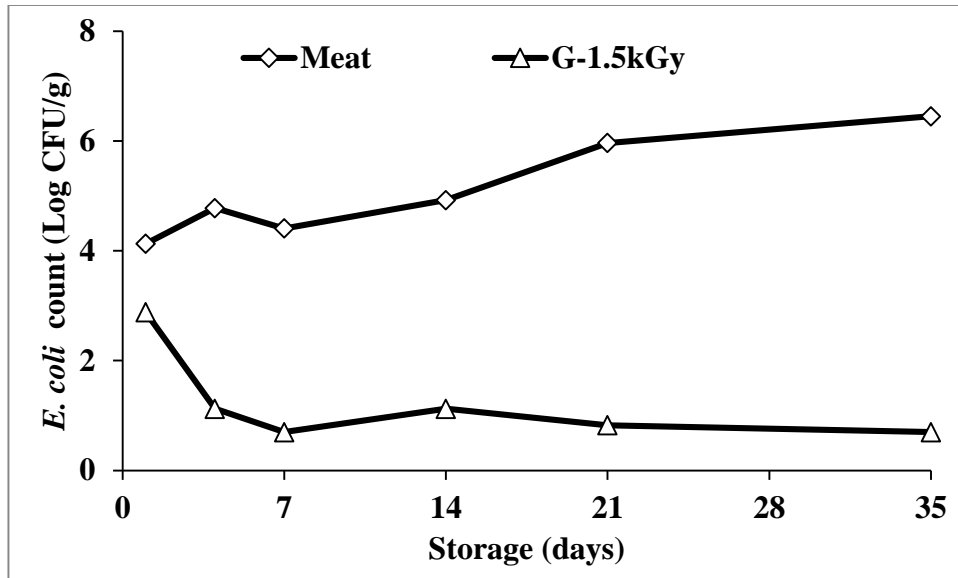
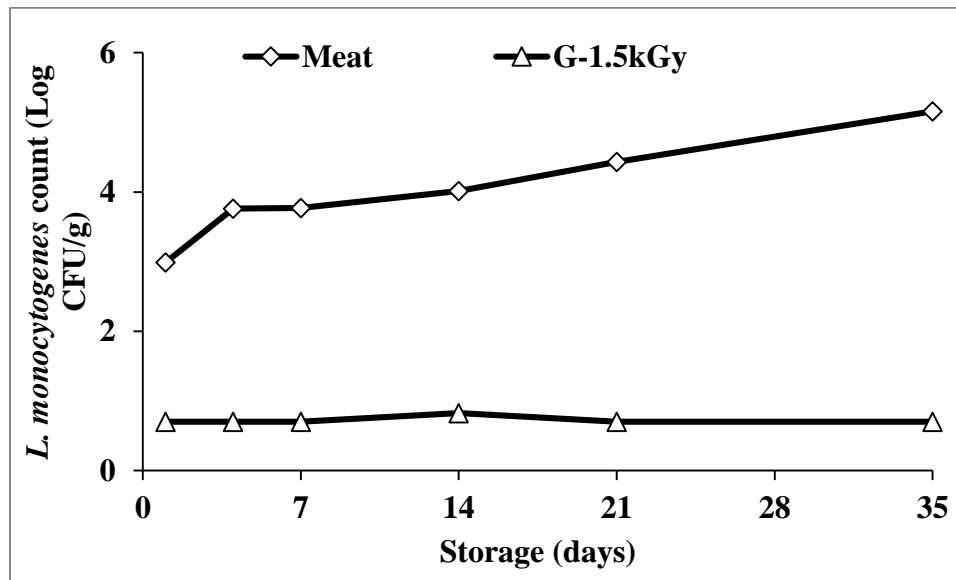


Figure 6.6: pH of the fresh pork during storage at 4 °C.



**Figure 6.7(a):** Antimicrobial activity of the films in situ against *E. coli* during storage at 4 °C.



**Figure 6.7(b):** Antimicrobial activity of the films in situ against *L. monocytogenes* during storage at 4 °C.

## 6.11. General discussion of the Publication-5

In this publication, gamma irradiation worked synergistically with genipin cross-linked films to protect the activity of the antimicrobials *in vitro* during storage. Genipin cross-linked films prepared by gamma irradiation (at 1.5kGy) exhibited maximum antimicrobial activity against both *E. coli* and *L. monocytogenes*. The films inhibited the growth of *L. monocytogenes* and *E. coli* in meat. The films also increased the microbiological shelf life of pork meats by more than 35 days by restricting the growth of psychrotrophs, mesophiles and LAB below 6 log CFU/g. It is interesting to note that, the pH of the meat samples were also stable during storage.

## **CHAPTER 7**

### **General Discussion, Conclusions and Future Perspectives**

From the literature review, it was evident that CNC has high potential to act as reinforcing fillers in polymer matrices and enhance the mechanical properties of the matrices (Dieter-Klemm *et al.*, 2009; Azeredo *et al.*, 2010; Cao *et al.*, 2008). However, when I began my research project, the first problem I found is the lack of reinforcing effect of CNC with chitosan matrix. It was little bewildering for me, considering all the literature review suggested that CNC should reinforce well with biopolymers. After months of hard work I found the solution to the problem. I used to make a 1% w/v CNC suspension in deionized water and then used this suspension to fabricate the CNC/chitosan films. But, there was visible aggregation in the films (regardless of the CNC content) and it was not possible to remove them (the aggregates) by homogenization. I realized that the aggregates are due to the interaction of CNC and chitosan. Due to the presence of negatively charged sulfate half-ester groups, the stability of CNC suspension is affected by the incorporation of electrolytes in the suspension. The colloidal suspension of chitosan, being highly cationic (in acidic pH), may electrostatically interact with CNC. As a result, instead of using a 1% CNC suspension, I diluted it to 0.1% and it worked. The CNC/chitosan films made in this way (Publication-1) exhibited better mechanical and barrier properties compared to that of chitosan. The optimum CNC concentration was found to be 5% w/w in chitosan. This also highlights the importance of CNC using a dilute CNC suspension for chitosan or other highly cationic polymers. As previously mentioned (in the publication) the optimum CNC concentration reported by Li *et al.* (2009) was very high (15-20% w/w of CNC). The CNC length and width reported in this manuscript was 400 nm in length and 24 nm in width, which is almost 4 times longer than the CNC used in the current study. Also, the authors may have used a concentrated CNC suspension. These could be the reasons why such a high nanocrystal loading (15-20% w/w) was required to reinforce chitosan.

In the second publication, the CNC/chitosan films were treated with NaOH. The treatment was carried out in order to make the film insoluble in water. When the un-treated CNC/chitosan films were used to wrap the ham samples, within 1 week of storage the films dissolved on the surface of the ham samples. It was evident that the films are not sufficiently water resistance to be used for this sort of packaging application. As a result, I came up with this simple yet highly efficient treatment involving NaOH. After films are formed, I treated the films with NaOH for a short time (2 min), followed by washing with water. The treatment worked and the films were insoluble. However, we could not peel off the films from the Petri dish and carry out the treatment. If we did so, the films lost their shape and shrank a lot during drying (after washing with water). So, the treatment must be carried out when the films are dried but firmly stuck on the petri dish. In this way there were no loss in the shape or size of the films and films were stable. The CNC/chitosan films (treated in this way) were highly water resistant. The films exhibited only 4% water solubility after immersion in water for 24h. The most amazing fact about this treatment is that there was no statistically significant ( $P>0.05$ ) difference between the mechanical properties of the untreated and treated films. The reinforcing effect of CNC was retained after the treatment. Nisin was selected as an antimicrobial agent in order to make the films antimicrobial. However, incorporation of nisin inside the CNC/chitosan films did not show promising antimicrobial properties. As a result, nisin was immobilized on the surface of the CNC/chitosan films.

Nisin is a very effective at inhibiting the growth of pathogenic bacteria in food; however, the activity of nisin may quickly deplete during storage after initial application (Benech and Kheadr, 2002). It is a challenge for the food industry to find a way to protect the efficacy of nisin. Although numerous studies have been carried out about genipin cross-linked films (Chiono *et*

*al.*, 2008; Bigi *et al.*, 2002; Butler *et al.*, 2006) or nisin (Jin *et al.*, 2009; Millette *et al.*, 2007), their combinational application is not yet reported. So, genipin cross-linking presents a novel approach to protect the activity of nisin in meat products.

A broad range of pathogenic gram-positive and gram-negative bacteria can contaminate fresh meat and meat products. While *L. monocytogenes* (gram-positive) has a fatality rate of 20-30%; *E. coli* and *S. typhimurium* (gram-negative) can also cause severe health complications and result in fatality (Thomas *et al.*, 2013). However, the antimicrobial activity of nisin is generally limited to gram-positive bacteria (Rohani *et al.*, 2011). The outer membrane (OM) of gram-negative bacteria such as, *E. coli* and *S. typhimurium* acts as a permeability barrier for the cell and prevents nisin from reaching the cytoplasmic membrane. Combination of nisin and chelating agents such as, sodium salts of ethylenediaminetetraacetate (Disodium EDTA) provides an effective approach to improve the antimicrobial activity of nisin against broad spectrum of bacteria (Khare *et al.*, 2014). As a result, RSM was used to develop antimicrobial formulation capable of inhibiting selected gram-negative (*E. coli* and *S. typhimurium*) and gram-positive (*L. monocytogenes*) bacteria (Publication-4).

The important findings and conclusions from the thesis have been summarized below:

- The CNC/chitosan films prepared with 0.1% CNC suspension exhibited superior mechanical and barrier properties compared to that of chitosan (Publication-1). The optimum CNC concentration was found to be 5% w/w in chitosan. So, CNC acted as a good reinforcing agent in chitosan.
- The antimicrobial films prepared by immobilizing nisin on the surface of the optimized CNC/chitosan films were very effective to inhibit the growth of *L. monocytogenes* on

RTE ham samples (Publication-2). Films prepared with  $18.65\mu\text{g}/\text{cm}^2$  completely inhibited the growth of *L. monocytogenes* during storage. Even films containing low concentration ( $2.33\mu\text{g}/\text{cm}^2$ ) of nisin reduced the count of *L. monocytogenes* by 1.2 log CFU/g.

- Genipin cross-linking presented a novel approach to protect the antimicrobial activity of nisin during storage (Publication-2). The nisin content of the films cross-linked with 0.05% genipin films were significantly higher ( $P<0.05$ ) than the uncross-linked films. The cross-linked films reduced the swelling and the water solubility and improved mechanical properties of the nanocomposite films. The cross-linked films also demonstrated high efficacy during *in situ* study and reduced the growth rate of *L. monocytogenes* by 21% compared to the un-cross-linked films.
- Microfluidization was successfully applied to homogeneously distribute a concentrated CNC suspension into chitosan matrix (Publication-3). CNC concentration was found to be the most important factor affecting the mechanical strength of the films. Microfluidization reduced the chitosan-CNC aggregates and helped to develop high strength CNC/chitosan nanocomposite films. It was possible to reduce the size of the aggregates by 10-15 times by utilizing a microfluidization. An 8 to 9% w/w CNC, 6,500 to 8,000 psi pressure and 5 to 6 microfluidization cycles was found to be the optimum parameters to provide the best mechanical properties of the nanocomposite films.
- Combination of nisin with Na-EDTA enhanced the antimicrobial activity of nisin against *E. coli*, *S. typhimurium* and *L. monocytogenes* (Publication-4). Nisin concentration, Na-EDTA concentration and pH were found to have statistically significant linear positive effect on the antimicrobial activity of the formulations.

- Gamma irradiation worked synergistically with genipin cross-linked films to protect the activity of the antimicrobials *in vitro* during storage (Publiaction-5). The films increased the microbiological shelf life of pork meats by more than 35 days by restricting the growth of psychrotrophs, mesophiles and LAB below 6 log CFU/g.

For future perspective, it would be interesting to check the effect of CNC directly in combination with the antimicrobials rather than inside the biopolymeric films. CNC can be used for the nano-encapsulation of spice extracts such as, essential oils (EOs). Microfluidization can be used in great effect to reduce the emulsion droplet size (EDP) and to stabilize the active compound. It would be interesting to attach nisin with CNC. Nisin, being positively charged (in acidic pH), should have electrostatic interaction with CNC. The modification of CNC for the attachment of antioxidant molecules has high potential not only in the field of food packaging but also in cosmetic and pharmaceutical industry. The modified CNC can be used to protect the oxidation of food products, develop anti-aging/anti-oxidant skin care products, and extend the shelf life of oxygen sensitive drugs. It will also be interesting to investigate the mechanism of action involving genipin cross-linking with gamma-irradiation by adopting variety of techniques such as, XRD and X-ray photoelectron spectroscopy (XPS), etc.

## References

Azeredo, H. M. C., Mattoso, L. H. C., Wood, D., Williams, T. G., Bustillos, R. J. A., & McHugh, T. H. (2010). Nanocomposite edible films from mango puree reinforced with cellulose nanofibers. *Journal of Food Science*, 74(5), 31-35.

- Bigi, a, Cojazzi, G., Panzavolta, S., Roveri, N., & Rubini, K. (2002). Stabilization of gelatin films by crosslinking with genipin. *Biomaterials*, 23(24): 4827–4832.
- Butler, M. F., Clark, A. H., & Adams, S. (2006). Swelling and mechanical properties of biopolymer hydrogels containing chitosan and bovine serum albumin. *Biomacromolecules*, 7(11): 2961–2970.
- Cao, X., Dong, H., & Li, C. M. (2007). New nanocomposite materials reinforced with flax cellulose nanocrystals in waterborne polyurethane. *Biomacromolecules*, 8, 899-904.
- Chiono, V., Pulieri, E., Vozzi, G., Ciardelli, G., Ahluwalia, A., & Giusti, P. (2008). Genipin-crosslinked chitosan/gelatin blends for biomedical applications. *Journal of materials science: materials in medicine*, 19(2): 889–898.
- Dieter-Klemm, D., Schumann, D., Kramer, F., Hessler, N., Koth, D., & Sultanova, B. (2009). Nanocellulose materials: different cellulose, different functionality. *Macromolecular Symposia*, 280, 60–71.
- Khare, A. K., Biswas, A. K., & Sahoo, J. (2014). Comparison study of chitosan, EDTA, eugenol and peppermint oil for antioxidant and antimicrobial potentials in chicken noodles and their effect on colour and oxidative stability at ambient temperature storage. *LWT - Food Science and Technology*, 55(1), 286–293.

**ANNEXE A**  
**(Unfinished publication)**

## **Modification of cellulose nanocrystal (CNC) for the attachment of antioxidant molecules**

Active packaging can be defined as an innovative type of packaging that prevents or slows deterioration of packaged food quality. Oxygen scavengers, carbon dioxide scavengers/emitters, moisture absorbers and ethanol generators are some examples of active packaging. Active packaging also involves the release of antioxidants and/or antimicrobial substances onto the food surface (Appendini and Hotchkiss 2002). Gallic acid is a natural phenolic antioxidant extractable from plants, especially green tea (Lu *et al.*, 2006). It is widely used in foods, drugs, and cosmetics to prevent rancidity induced by lipid peroxidation and spoilage. CNC is a highly crystalline nanometer sized rod like particles that is obtained as a stable aqueous colloidal suspension. This CNC was extracted from softwood bleached kraft pulp with an acid hydrolysis process inspired from the literature (Beck-Candanedo *et al.*, 2005). The CNC was found to exhibit an average length of 110 nm long for a 5-10nm width (Revol *et al.*, 1992).

Gallic acid can be grafted on the surface of CNC following a reduction-oxidation (Redox) reaction with H<sub>2</sub>O<sub>2</sub> and ascorbic acid according to a modified process as described by Curcio *et al.* 2011. The modified CNC with containing antioxidant moiety has the potential to provide value added nanomaterial for the next generation of packaging.

### **Synthesis of CNC-antioxidant conjugates**

The conjugation of the antioxidant moiety on the CNC chains was performed by free radical-induced grafting reaction. A biocompatible and water-soluble system, an ascorbic acid/hydrogen peroxide pair, was chosen as redox initiator system. The interaction mechanism between the two components of the redox pair involves the oxidation of ascorbic acid by H<sub>2</sub>O<sub>2</sub> at room temperature with the formation of ascorbate and hydroxyl radicals, which initiate the reaction. A 5ml of 1M H<sub>2</sub>O<sub>2</sub> was mixed with 0.25g ascorbic acid and was added to 25ml of 1% CNC

suspension. After mixing for 1hr different quantity of gallic acid (25, 50 and 100 mg; coded as CNC25, CNC50, and CNC100, respectively) was introduced and the reaction was carried out for 1 day at room temperature. The gallic acid grafted CNC particles was then introduced into dialysis tubes (MWCO 1000 Da), dipped into distilled water for 1 day with two changes of water, in order to purify and remove any unreacted molecules.

### **Antiradical Test**

The antiradical properties of the control (unmodified CNC) and modified CNC was measured following the procedure of Salmieri and Lacroix, (2006), using *N,N*-diethyl-*p*-phenylenediamine (DPPD) reagent. A fixed volume of the modified CNC suspension (200  $\mu$ l) was placed in an electrolytic cell (platinum electrodes) containing 3 ml of 0.15 M NaCl and was subjected to electrolysis for 1 min (10 mA direct current, 400 V). After electrolysis, an aliquot of 200  $\mu$ l of the electrolyte was added to 2 ml of DPPD solution. The generated reactive oxygen species (ROS) such as superoxide anions ( $\cdot\text{O}_2^-$ ), singlet oxygen ( $^1\text{O}_2$ ), hydroxyl radicals ( $\cdot\text{OH}$ ), and their byproducts react instantly with DPPD. A red coloration that was measured at 515 nm using a DMS spectrophotometer (Varian Canada Inc., Mississauga, ON, Canada) was produced. The antiradical activity of the suspension is equivalent to their capacity to inhibit the accumulation of oxidative species and so the red coloration. The colorimetric reaction was calibrated using the non-electrolyzed NaCl solution (no oxidative species, ascribed to 100% scavenging) and the electrolyzed NaCl solution (0% scavenging, in the absence of any antioxidants). The scavenging percentage was calculated using the equation,

$$\text{Scavenging (\%)} = [1 - (A_{\text{sample}} - A_{(-)}) / (A_{(+)} - A_{(-)})] \times 100$$

Where,  $A_{\text{sample}}$  is the absorbance sample,  $A_{(+)}$  and  $A_{(-)}$  is the absorbance of electrolyzed and non-electrolyzed NaCl solution in the absence of sample. The degree of discoloration

indicates the scavenging potential of the product. The reaction was standardized with Trolox<sup>®</sup> (Sigma-Aldrich Ltd), from a calibration curve made of Trolox<sup>®</sup> (6-hydroxy-2,5,7,8-tetramethylchroman-2-carboxylic acid) and Vitamin C.

### **Determination of grafting efficiency**

The gallic acid content in the modified CNC was determined by a standard curve plotting known solutions of gallic (mg/ml) acid against the scavenging (%). The grafting efficiency was calculated by comparing the scavenging (%) of the modified CNC with that of the 2<sup>nd</sup> order polynomial equation obtained from the standard curve.

$$\text{Grafting Efficiency (GE)} = 1 - [(1 - G_t) / G_o] \times 100$$

Where,

$G_t$  = Quantity (mg) of gallic acid grafted on to CNC, which was determined by comparing the scavenging (%) of the modified CNC with that of the 2<sup>nd</sup> order polynomial equation obtained from the standard curve.

$G_o$  = Initial quantity (mg) of gallic acid incorporated in the reaction.

### **Preparation of chitosan based nanocomposite films**

At first a 2% (w/v) of aqueous acetic acid solution is incorporated into a diluted (0.1%) unmodified (control) and optimized modified CNC suspension (CNC50) under magnetic stirring. The suspension is then subjected to ultra-sonication. After that a 0.5% ethylene glycol (Laboratoire Mat, Beauport, Quebec, Canada) and 2% high mol. wt. chitosan (DD: 85-90%, 85/2500 Heppe-medical, GmbH) is incorporated in the suspension. The suspension is then

magnetically stirred overnight followed by homogenization with IKA RW-20 mechanical homogenizer. After homogenization, a paraffin film is wrapped on top of the beaker and kept for few hours to remove all the bubbles. The films are prepared by casting on Petri dishes and allowed to dry at room temperature and 30-35% RH. After that films are treated with NaOH and washed several times with deionized water to render the films insoluble.

## **Results**

Reaction with 50mg CNC has inhibited more than 91% of the free radicals and demonstrated the highest grafting efficiency (almost 60%). The nanocomposite films were made from the optimized modified CNC suspension (CNC50). The films were irradiated to check the effect of low dose irradiation on the antiradical property of the films. The CNC/chitosan films inhibited more than 51% of the free radicals. The irradiated films did not demonstrate any significant ( $P \geq 0.05$ ) loss of antiradical property.

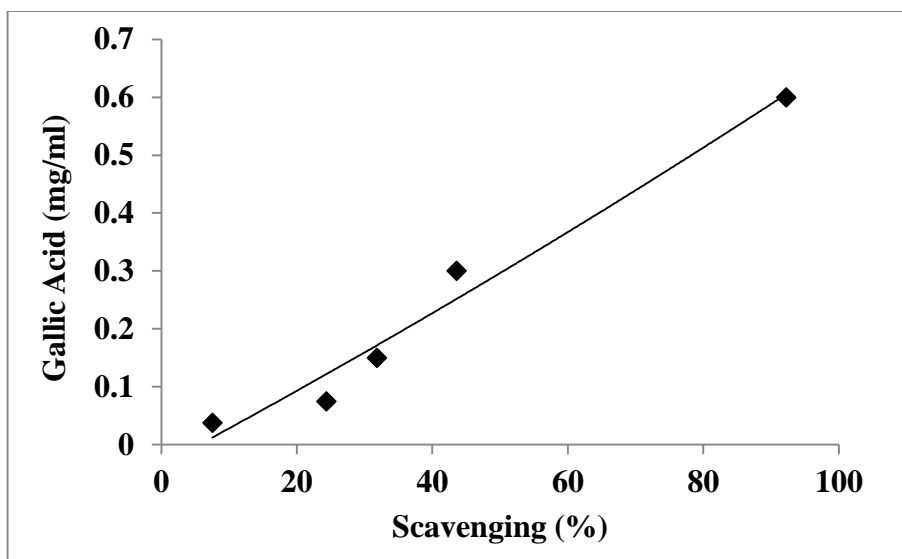


**Figure-A1:** Standard curve with gallic acid

**Table-A1:** The antiradical properties of the gallic acid grafted CNC

Sample	Antiradical properties			GE (%)
	Scavenging (%)	Vit. C eq (mg/ml) of CNC	Trolox <sup>®</sup> eq mM/ml of CNC	
CNC control	3.90±2.88 <sup>a</sup>	0.70±0.12 <sup>a</sup>	0.16±0.52 <sup>a</sup>	0 <sup>a</sup>
CNC25	40.19±2.12 <sup>b</sup>	7.26±0.09 <sup>b</sup>	1.64±0.38 <sup>b</sup>	22.95±1.45 <sup>c</sup>
<b>CNC50</b>	<b>91.23±0.54<sup>d</sup></b>	<b>16.47±0.1<sup>d</sup></b>	<b>3.73±0.02<sup>d</sup></b>	<b>59.8±0.41<sup>d</sup></b>
CNC100	43.26±10.53 <sup>c</sup>	7.81±0.29 <sup>c</sup>	1.77±1.27 <sup>c</sup>	8.36±1.61 <sup>b</sup>

**Table-A2:** The antiradical properties of the nanocomposite films

Nanocomposite Film Samples	Antiradical properties		
	Scavenging (%)	Vit. C eq (mg/ml) of CNC	Trolox <sup>®</sup> eq mM/ml of CNC
Unmodified CNC	5.26±3.24 <sup>a</sup>	0.95±0.56 <sup>a</sup>	0.22±0.13 <sup>a</sup>
Modified CNC	51.69±2.25 <sup>b</sup>	9.3±0.40 <sup>b</sup>	2.11±0.10 <sup>b</sup>
Modified CNC +0.5 kGy	47.07±3.36 <sup>b</sup>	8.5±0.61 <sup>b</sup>	1.92±0.14 <sup>b</sup>
Modified CNC +1.5 kGy	47.6±5.47 <sup>b</sup>	8.6±0.99 <sup>b</sup>	1.95±0.22 <sup>b</sup>

### References:

Appendini P, Hotchkiss JH. 2002. Review of antimicrobial food packaging. *Innov Food Sci Emerg Technol* 3(2):113–26.

Beck-Candanedo, S., M. Roman, Gray, D. G. Effect of reaction conditions on the properties and behavior of wood cellulose nanocrystal suspensions. *Biomacromolecules* **2005**, 6(2), 1048-1054

Curcio, M., Puoci, F., Iemma, F., Parisi, O. I., Cirillo, G., Spizzirri, U. G., & Picci, N. (2009). Covalent insertion of antioxidant molecules on chitosan by a free radical grafting procedure. *Journal of agricultural and food chemistry*, 57(13), 5933–8.

Lu, Z.; Nie, G.; Belton, P. S.; Tang, H.; Zhao, B. Structure-activity relationship analysis of antioxidant ability and neuroprotective effect of gallic acid derivatives. *Neurochem. Int.* 2006, 48, 263–274.

Revol, J.-F.; Bradford, H.; Giasson, J.; Marchessault, R. H.; Gray, D. G. (1992). *Int. J. Biol. Macromol.* **1992**, 14, 170-172.

Salmieri, S., & Lacroix, M. (2006). Physicochemical properties of alginate/polycaprolactone-based films containing essential oils. *Journal of agricultural and food chemistry*, 54(26), 10205–14.

## **ANNEXE B**

**(Supplementary information)**

## Chemical structures and images

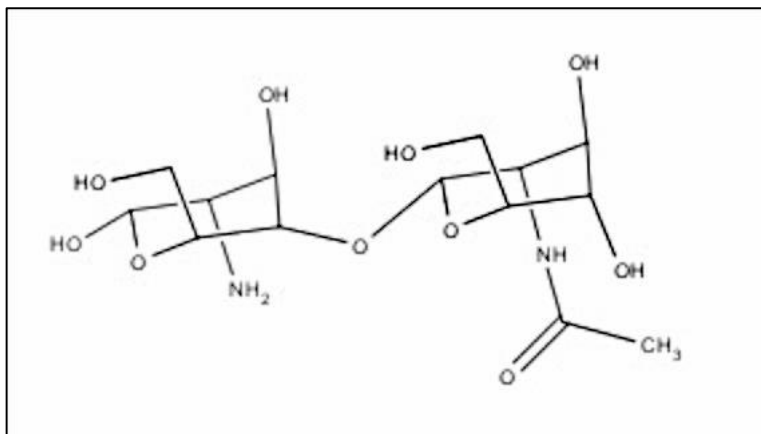


**Figure-B1:** Chemical structure of chitosan

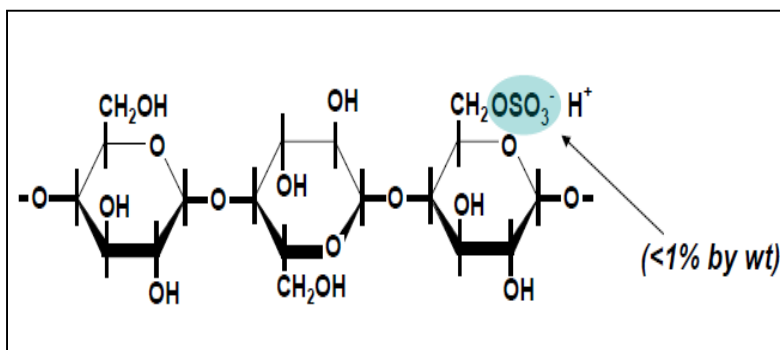


**Figure-B2:** Chemical structure of CNC (Revol et al., 1998)

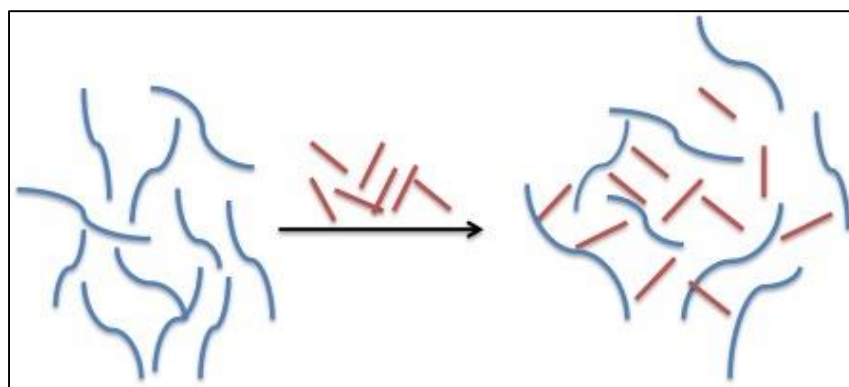


**Figure-B3:** Schematic representation of the polyelectrolytic complex formation between chitosan

(blue lines) and CNC (red lines) (adopted from Wang and Roman, 2010)

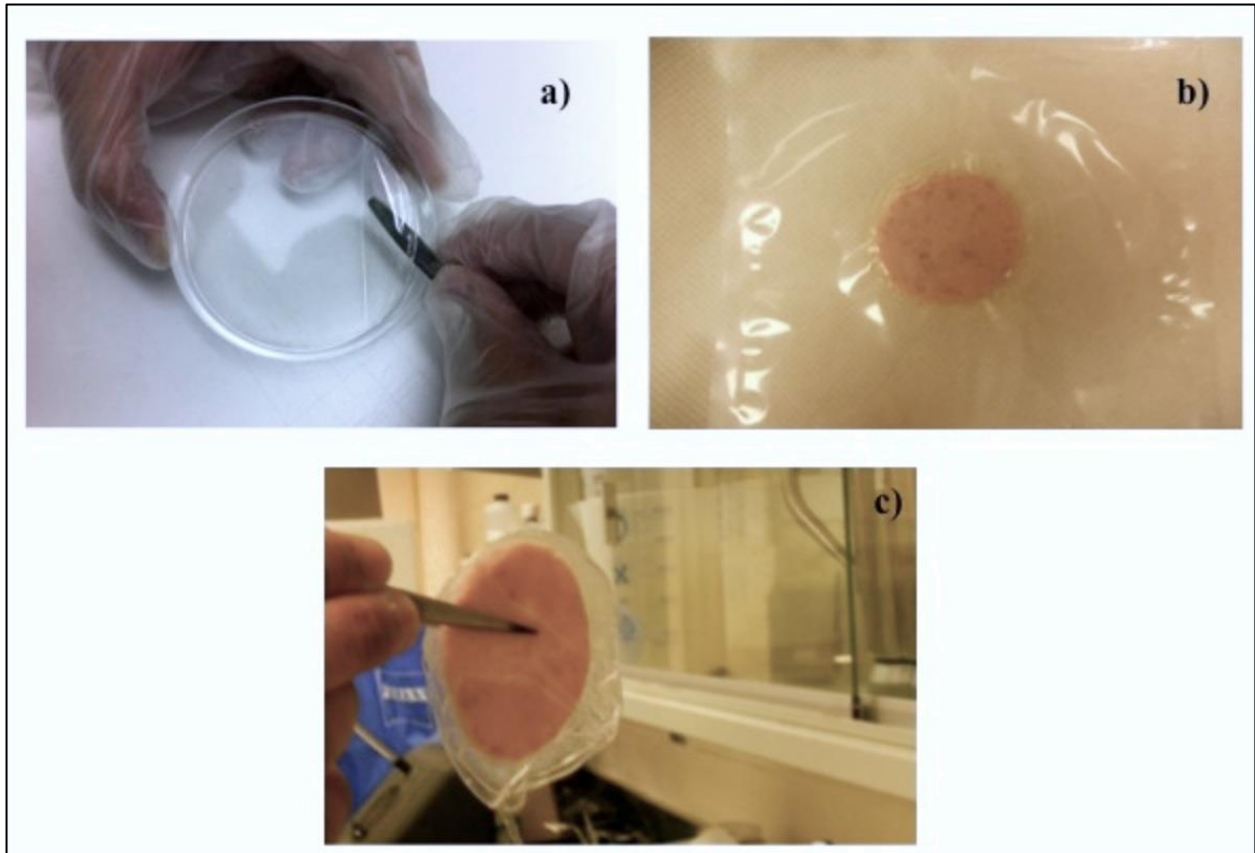


**Figure-B4:** *Digital images of a) CNC/chitosan film, b) RTE ham samples sandwiched between two films and c) Microbial analysis of the RTE ham samples during storage.*

## **Effect of $\gamma$ -irradiation on the activity of nisin solution and nisin treated films**

Generally all the films are sterilized by gamma irradiation prior to any microbial analysis. Antimicrobial activity of films containing natural antimicrobial agents such as, nisin maybe affected  $\gamma$ -irradiation. So it was essential to investigate the effect  $\gamma$ -irradiation on the activity of nisin treated films and compared to that of the nisin solution.

### ***Gamma irradiation***

The nisin stock solution and the nisin treated biofilm formulation (18.65  $\mu\text{g}/\text{cm}^2$ ) were irradiated at doses 0 to 60 kGy in the Canadian Irradiation Center (CIC) at room temperature (20 °C). A UC-15A irradiator equipped with a  $^{60}\text{Cobalt}$  source was used to deliver radiation at a mean rate of 16.2 kGy  $\text{h}^{-1}$ .

### ***Inhibition test***

The effect of  $\gamma$ -irradiation on the activity of nisin was determined using the disk diffusion assay against *L. sakei*. A 20  $\mu\text{L}$  of each solution was put on top of sterile cellulose disks (the disk diameter was 7 mm) and the experiment was performed as described in Chapter 2.

### ***Results***

The inhibition area for the control (0 kGy) nisin solution and nisin treated films was found to be 17.26 and 14.75  $\text{cm}^2$ , respectively. A drastic decrease in the activity of nisin solution was observed at doses 2.5 kGy. The inhibition area decreased from 17.26 to only 4.23  $\text{cm}^2$ , which is more than 80% decrease in the activity of nisin from the control. The activity decreased slowly after from 5 to 15 kGy. At doses 30 kGy the activity of nisin was completely lost (no inhibition area). The nisin treated films exhibited much better resistance and retention activity against  $\gamma$ -irradiation than the nisin solution. There was no significant decrease ( $P \geq 0.05$ ) in the inhibition zone at doses from 0 to 7.5 kGy. The activity decreased significantly ( $P \leq 0.05$ ) from 7.5 to 12.5

kGy. The films retained activity even at doses 60 kGy (inhibition area 6.43 cm<sup>2</sup>). So, the retention of nisin activity is much better in films than in solutions.

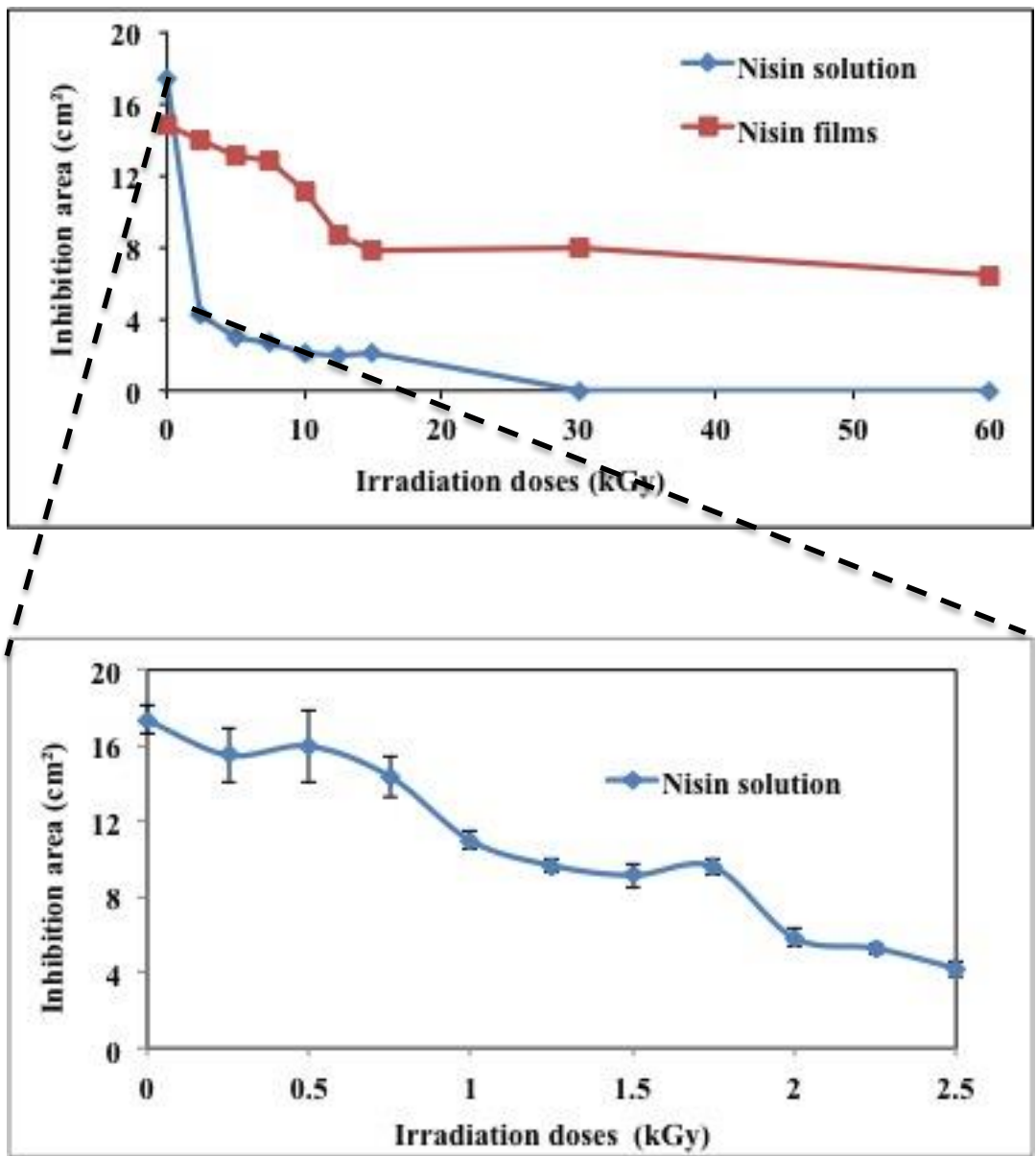


**Figure-B4:** Effect of  $\gamma$ -irradiation on the activity of nisin solution and nisin treated films (0 to 60 kGy)

## **ANNEXE C**

**(Biography)**

## Publications

1. **Khan, A.**, Salmieri, S., Frascini, C., Jean, B., Riedl, B., & Lacroix, M. (2014b). Genipin cross-linked nanocomposite films for the immobilization of antimicrobial agent. Published in *Applied Materials & Interfaces*.
2. **Khan, A.**, Khanh, V. D., Chauve, G., Jean, B., Riedl, B., & Lacroix, M. (2014c). Optimization of microfluidization for the homogeneous distribution of cellulose nanocrystals (CNCs) in biopolymeric matrix. *Cellulose* 21:3457-3468.
3. Khan, A., Khanh, V. D., Chauve, G., Jean, B., Riedl, B., & Lacroix, M. (2014c). Optimization of microfluidization for the homogeneous distribution of cellulose nanocrystals (CNCs) in biopolymeric matrix. *Cellulose* 21:3457-3468.
4. **Khan, A.**, Khanh, V. D., Riedl, B., & Lacroix, M. (2014d). Enhancement and optimization of the antimicrobial activity of nisin against gram-negative and gram-positive bacteria. Under revision in *LWT-Food Science & Technology*.
5. **Khan, A.**, Jean, B., Riedl, B., & Lacroix, M. (2014e). Genipin cross-linked antimicrobial nanocomposite films to prevent the surface growth of bacteria in fresh meats. Submitted to *International Journal of Food Microbiology*.
6. **Khan, A.**, Huq, T., Khan, R. A., Riedl, B., & Lacroix, M. (2014a). Nanocellulose-Based Composites and Bioactive Agents for Food Packaging. *Critical Reviews in Food Science and Nutrition*, 54(2), 163–174.
7. Huq, T., **Khan, A.**, Khan, R. A., Riedl, B., & Lacroix, M. (2013). Encapsulation of probiotic bacteria in biopolymeric system. *Critical Reviews in Food Science and Nutrition*, 53(9), 909–16.
8. **Khan, A.**, Khan, R. A., Salmieri, S., Le Tien, C., Riedl, B., Bouchard, J., Chauve, G., Victor, T., Kamal, M. R., & Lacroix, M. (2012). Mechanical and barrier properties of nanocrystalline

cellulose reinforced chitosan based nanocomposite films. *Carbohydrate Polymers*, 90(4), 1601–1608.

9. Huq T., Salmieri, S., **Khan, A.**, Khan, R.A., Le Tien, C., Riedl, B., Frascinic, C., Bouchard, J., Uribe-Calderon, J., Kamal, M.R. and Lacroix, M., (2012). Nanocrystalline cellulose (CNC) reinforced alginate based biodegradable nanocomposite film. *Carbohydrate Polymers*, 90, 1757–1763.
10. **Khan, A.**, Huq, T., Khan, R. A., Dussault, D., Salmieri, S., & Lacroix, M. (2012). Effect of gamma radiation on the mechanical and barrier properties of HEMA grafted chitosan-based films. *Radiation Physics and Chemistry*, 81(8), 941–944.
11. Huq, T., **Khan, A.**, Dussault, D., Salmieri, S., Khan, R. A., & Lacroix, M. (2012). Effect of gamma radiation on the physico-chemical properties of alginate-based films and beads. *Radiation Physics and Chemistry*, 81(8), 945–948.

### **Poster Presentations**

1. **Avik Khan**, Khanh Dang Vu, Gregory Chauve, Stephane Salmieri, Bernard Riedl, Jean Bouchard & Monique Lacroix. Development of biobased nanocomposite films using microfluidization. International Conference on Bio-based Materials and Composites (ICBMC'14). Montreal, Canada, May 13-16.
2. **Avik Khan**, Dominic Dussault, Stephane Salmieri, Bernard Riedl, Jean Bouchard & Monique Lacroix. *Combined effect of  $\gamma$ -irradiation and antimicrobial films on the shelf life of refrigerated pork sausage meat*. 58th International Congress of Meat Science and Technology-2012. Montreal, Canada, August 12-17.

3. **Avik Khan**, Dominic Dussault, Bernard Riedl and Monique Lacroix. *Antimicrobial nanocomposite films for food packaging*. TAPPI International Conference on Nanotechnology for Renewable Materials-2012. 4 to 7<sup>th</sup> June, Montreal, Canada.
4. **Avik Khan**, Ruhul A. Khan, Dominic Dussault, Bernard Riedl and Monique Lacroix. *Use of microfluidization for the preparation of nanocrystalline cellulose reinforced biobased nanocomposites*. NanoQuebec Conference-2012. 20 to 21<sup>th</sup> March, Montreal, Canada.
5. **Avik Khan**, Tanzina Huq, Ruhul A. Khan, Dominic Dussault, Bernard Riedl and Monique Lacroix. *Effect of Gamma Radiation on the Mechanical, Barrier and Thermal Properties of Chitosan*. International Meeting on Radiation Processing (IMRP 2011), 13<sup>th</sup> to 16<sup>th</sup> June, 2011, Montréal, Canada.
6. Tanzina Huq, **Avik Khan**, Ruhul A. Khan, Dominic Dussault, Bernard Riedl and Monique Lacroix. *Effect of Gamma Radiation on the Physico-chemical Properties of Alginate Based Films and Beads*. Accepted to the International Meeting on Radiation Processing (IMRP 2011), 13<sup>th</sup> to 16<sup>th</sup> June, 2011, Montréal, Canada.

### **Conference Proceedings**

1. **Avik Khan**, Dominic Dussault, Stephane Salmieri, Bernard Riedl, Jean Bouchard & Monique Lacroix. (2012). *Combined effect of  $\gamma$ -irradiation and antimicrobial films on the shelf life of refrigerated pork sausage meat*. Proceedings of the 58th International Congress of Meat Science and Technology, Montreal, Canada, August 12-17. SAFMICROP-34, 1-4.

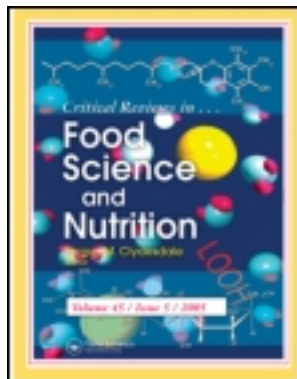
**ANNEXE D**  
**(Other contributions)**

This article was downloaded by: [INRS - Service de documentation et d'information spécialisées (SDIS)], [Avik Khan]

On: 05 November 2013, At: 05:50

Publisher: Taylor & Francis

Informa Ltd Registered in England and Wales Registered Number: 1072954 Registered office: Mortimer House, 37-41 Mortimer Street, London W1T 3JH, UK



## Critical Reviews in Food Science and Nutrition

Publication details, including instructions for authors and subscription information:

<http://www.tandfonline.com/loi/bfsn20>

### Nanocellulose-Based Composites and Bioactive Agents for Food Packaging

Avik Khan<sup>a</sup>, Tanzina Huq<sup>a</sup>, Ruhul A. Khan<sup>a</sup>, Bernard Riedl<sup>b</sup> & Monique Lacroix<sup>a</sup>

<sup>a</sup> Research Laboratories in Sciences Applied to Food, Canadian Irradiation Center (CIC), INRS-Institute Armand-Frappier, University of Quebec, 531 Boulevard des Prairies, Laval, Quebec, H7V 1B7, Canada

<sup>b</sup> Centre de recherche sur le bois, Faculté de foresterie, de géomatique et de géographie, Université Laval, Quebec, G1V 0A6, Canada

Accepted author version posted online: 04 Sep 2012. Published online: 04 Nov 2013.

To cite this article: Avik Khan, Tanzina Huq, Ruhul A. Khan, Bernard Riedl & Monique Lacroix (2014) Nanocellulose-Based Composites and Bioactive Agents for Food Packaging, *Critical Reviews in Food Science and Nutrition*, 54:2, 163-174, DOI: [10.1080/10408398.2011.578765](https://doi.org/10.1080/10408398.2011.578765)

To link to this article: <http://dx.doi.org/10.1080/10408398.2011.578765>

PLEASE SCROLL DOWN FOR ARTICLE

Taylor & Francis makes every effort to ensure the accuracy of all the information (the "Content") contained in the publications on our platform. However, Taylor & Francis, our agents, and our licensors make no representations or warranties whatsoever as to the accuracy, completeness, or suitability for any purpose of the Content. Any opinions and views expressed in this publication are the opinions and views of the authors, and are not the views of or endorsed by Taylor & Francis. The accuracy of the Content should not be relied upon and should be independently verified with primary sources of information. Taylor and Francis shall not be liable for any losses, actions, claims, proceedings, demands, costs, expenses, damages, and other liabilities whatsoever or howsoever caused arising directly or indirectly in connection with, in relation to or arising out of the use of the Content.

This article may be used for research, teaching, and private study purposes. Any substantial or systematic reproduction, redistribution, reselling, loan, sub-licensing, systematic supply, or distribution in any form to anyone is expressly forbidden. Terms & Conditions of access and use can be found at <http://www.tandfonline.com/page/terms-and-conditions>

# Nanocellulose-Based Composites and Bioactive Agents for Food Packaging

AVIK KHAN,<sup>1</sup> TANZINA HUQ,<sup>1</sup> RUHUL A. KHAN,<sup>1</sup> BERNARD RIEDL,<sup>2</sup>  
and MONIQUE LACROIX<sup>1</sup>

<sup>1</sup>Research Laboratories in Sciences Applied to Food, Canadian Irradiation Center (CIC), INRS-Institute Armand-Frappier, University of Quebec, 531 Boulevard des Prairies, Laval, Quebec H7V 1B7, Canada

<sup>2</sup>Centre de recherche sur le bois, Faculté de foresterie, de géomatique et de géographie, Université Laval, Quebec, G1V 0A6, Canada

*Global environmental concern, regarding the use of petroleum-based packaging materials, is encouraging researchers and industries in the search for packaging materials from natural biopolymers. Bioactive packaging is gaining more and more interest not only due to its environment friendly nature but also due to its potential to improve food quality and safety during packaging. Some of the shortcomings of biopolymers, such as weak mechanical and barrier properties can be significantly enhanced by the use of nanomaterials such as nanocellulose (NC). The use of NC can extend the food shelf life and can also improve the food quality as they can serve as carriers of some active substances, such as antioxidants and antimicrobials. The NC fiber-based composites have great potential in the preparation of cheap, lightweight, and very strong nanocomposites for food packaging. This review highlights the potential use and application of NC fiber-based nanocomposites and also the incorporation of bioactive agents in food packaging.*

**Keywords** Packaging materials, nanocellulose, biodegradable films, nanocomposites, bioactive polymers, biopolymers, essential oils

## INTRODUCTION

The purpose of food packaging is to preserve the quality and safety of the food it contains, from the time of manufacture to the time it is used by the consumer. An equally important function of packaging is to protect the product from physical, chemical, or biological damages. The outer covering should also inform the consumer about the product. The packaging also has a secondary function, i.e., reduction of loss, damage, and waste for distributor and customer, and facilitates its storage, handling, and other commercial operations. About 50% of agricultural products are destroyed because of the absence of packaging. The causes of this loss are bad weather and physical, chemical, and microbiological deteriorations. Progress in the packaging of foodstuffs will prove crucial over the next few years mainly because of new consumer patterns, demands creation, and world population growth which is estimated to be 15 billion by 2025. The most well-known packaging materials that meet

these criteria are polyethylene- or copolymer-based materials, which have been in use by the food industry for over 50 years. These materials are not only safe, inexpensive, versatile, but also flexible. However, one of the limitations with plastic food packaging materials is that it is meant to be discarded, with very little being recycled (Cha and Chinnan, 2004; Villanueva et al., 2006). Currently, almost all the plastics, which are widely used in the various sectors, are produced from petrochemical products. With rising petroleum costs, there is concern with finding cost-effective ways to manufacture packaging materials. In addition to the above environmental issues, food packaging has been impacted by notable changes in food distribution, including globalization of the food supply, consumer trends for more fresh and convenient foods as well as a desire for safer and better quality foods. Given these and previously mentioned issues, consumers are demanding that food packaging materials be more natural, disposable, potentially biodegradable as well as recyclable (Chandra and Rustgi, 1998; Fischer et al., 1999).

Bio-based packaging is defined as packaging containing raw materials originating from agricultural sources, i.e., produced from renewable, biological raw materials such as starch, cellulose, and bio-derived monomers. To date, biodegradable packaging has commanded great attention, and numerous projects

Address correspondence to Monique Lacroix, Research Laboratories in Sciences Applied to Food, Canadian Irradiation Center (CIC), INRS-Institute Armand-Frappier, University of Quebec, 531 Boulevard des Prairies, Laval, Quebec H7V 1B7, Canada. E-mail: monique.lacroix@iaf.inrs.ca

are under way in this field. One important reason for this attention is the marketing of environmentally friendly packaging materials. Furthermore, use of biodegradable packaging materials has the greatest potential in countries where landfill is the main waste management tool. Bio-based packaging materials include both edible films and edible coatings along with primary and secondary packaging materials (Siro and Plackett, 2010; Khan et al., 2010b). Unfortunately, so far the use of biodegradable films for food packaging has been strongly limited because of the poor barrier properties and weak mechanical properties shown by natural polymers. For this reason natural polymers were frequently blended with other synthetic polymers or, less frequently, chemically modified with the aim of extending their applications in more special or severe circumstances (Weber et al., 2002; Khan et al., 2010a).

Cellulose is one of the most abundant biopolymers on earth, occurring in wood, cotton, hemp, and other plant-based materials and serving as the dominant reinforcing phase in plant structures. Plant fibers are mainly composed of cellulose, hemicellulose, and lignin. Cellulose, which awards the mechanical properties of the complete natural fiber, is ordered in microfibrils enclosed by the other two main components: hemicellulose and lignin (Bledzki & Gassan 1999). Cellulose microfibrils can be found as intertwined microfibrils in the cell wall (2–20 nm diameter and 100–40,000 nm length depending on its source). In these microfibrils, there exist nanofibers (also composed by cellulose) with diameters of 5–50 nm and lengths of several millimetres conformed by nanocrystalline domains and amorphous regions (Darder et al., 2007). Cellulose is a linear carbohydrate polymer chain consisting of D-glucopyranose units joined together by  $\beta$ -1,4-glycosidic linkages. In the unit cell of cellulose, two chains are joined by hydrogen bonding to each other in a parallel conformation, which is called cellulose. These units are packed side-by-side to form microfibrils of cellulose, which also contain disordered or amorphous regions. The arrangement of the cellulose microfibrils in the primary wall is random. Secondary cell walls of plants contain cellulose (40–80%), hemicellulose (10–40%), and lignin (5–25%), where cellulose microfibrils are embedded in lignin. Hemicellulose is a highly branched polymer compared to the linearity of cellulose. Its structure contains a variety of sugar units, whereas cellulose contains only 1,4- $\beta$ -D-glucopyranose units and its degree of polymerization is 10–100 times lower than that of cellulose. Finally, lignin is a complex hydrocarbon polymer with both aliphatic and aromatic constituents (Soykeabkaew et al., 2008).

The cellulose molecules are always biosynthesized in the form of nanosized fibrils, which are in turn assembled into fibers, films, walls, etc. The cellulose nanofibers are called nanocellulose (NC). The molecular arrangements of these fibrillar bundles are so small that the average diameter of the bundle is about 10 nm. These cellulose nanofibers are with diameters of 5–50 nm and lengths of thousands of nanometers. NC is a cellulose derivative composed of a nanosized fiber network which determines the product properties and its functionality. NC fibers are very interesting nanomaterials for production of

cheap, lightweight, and very strong nanocomposites. Generally, NC is produced by the bio-formation of cellulose via bacteria and also by the disintegration of plant celluloses using shear forces in refiner techniques. Wood-derived NC can also be prepared by electrospinning from pulp solutions (Dufresne, 1997) or by controlled acid hydrolysis of wood pulp (Beck-Candanedo et al., 2005). Cellulose nanofibers are recognized as being more effective than their microsized counterparts to reinforce polymers due to interactions between the nanosized elements that form a percolated network connected by hydrogen bonds, provided there is a good dispersion of the nanofibers in the matrix. It is predicted that NC reinforcements in the polymer matrix may provide value-added materials with superior performance and extensive applications for the next generation of biodegradable materials. NC is expected to show high stiffness since the Young's modulus (YM) of the cellulose crystal is as high as 134 GPa. The tensile strength of the crystal structure was assessed to be approximately 0.8 up to 10 GPa (Cao et al., 2008; Dieter-Klemm et al., 2009; Azeredo et al., 2010).

Polymer composites are mixtures of polymers with inorganic or organic additives having certain geometries (fibres, flakes, spheres, particulates). The use of nanoscale fillers is leading to the development of polymer nanocomposites and represents a radical alternative to the conventional polymer composites ((Dieter-Klemm et al., 2006). Polymer nanocomposites have generated enormous interest since Toyota<sup>®</sup> researchers in the late 1980s showed that as little as 5% addition of nanosized clays to nylons greatly increased their modulus and heat distortion temperature (Kojima et al., 1993). The use of nanocomposites serve a number of important functions, such as extending the food shelf life, enhancing food quality because they can serve not only as barriers to moisture, water vapor, gases, and solutes, but also serve as carriers of some active substances, such as antioxidants and antimicrobials (Rhim and Hong, 2006). These nanocomposites are significant due to their nanoscale dispersion with size less than 1,000 nm (Sanguansri and Augustin, 2006). Addition of relatively low levels of nanoparticles (less than 5%) have been shown to substantially improve the properties of the finished plastic, increasing the deformability and strength, and reducing the electrical conductivity and gas permeability (Sorrentino and Gorrasi, 2007).

The review discusses potential use, application, and advantages of nanocomposites, especially nanocellulose in the field of food packaging. This review highlights the potential of biopolymers (alginate, chitosan, etc.) for food packaging and also the incorporation of bioactive agents or antimicrobials (organic acids, bacteriocins, essential oils, etc.) into packaging to improve the quality and safety of food products during storage.

## NANOCOMPOSITES

Nanocomposites are mixture of polymers with nanosized inorganic or organic fillers with particular size, geometry, and surface chemistry properties. The polymers used are normally

hydrocolloids, such as proteins, starches, pectins, and other polysaccharides. Various inorganic nanoparticles have been recognized as possible additives to enhance the polymer performance (John and Thomas, 2008). Nanofillers include solid layered clays, synthetic polymer nanofibers, cellulose nanofibers, and carbon nanotubes. Up to now, only the layered inorganic solids like layered silicate have attracted the attention of the packaging industry. This is due to their ready availability and low cost, and also their significant enhancement of finished product properties and relative simple processing (Sorrentino and Gorrasi, 2007).

### ***Advantages of Nanocomposites***

When polymers are combined with nanofillers, the resulting nanocomposites exhibit significant improvements in mechanical properties, dimensional stability, and solvent or gas resistance with respect to the pristine polymer. Owing to the nanosize particles obtained by dispersion, these nanocomposites can exhibit many advantages such as biodegradability, enhanced organoleptic characteristics of food, such as appearance, odor, and flavor; reduced packaging volume, weight, and waste; extended shelf life and improved quality of usually nonpackaged items; individual packaging of small particulate foods, such as nuts and raisins; function as carriers for antimicrobial and antioxidant agents; controlled release of active ingredients; annually renewable resources (Hitzky et al., 2005; Rhim, 2007).

Nanocomposites also offer extra benefits like low density, transparency, good flow, better surface properties, and recyclability. The enhancement of many properties resides in the fundamental length scales dominating the morphology and properties of these materials. The nanofiller particles have at least one dimension in the nanometer (from 1 to 100 nm) range. It means that a uniform dispersion of these particles can lead to ultra-large interfacial area between the constituents. The very large organic or inorganic interface alters the molecular mobility and the relaxation behavior, improves the mechanical properties of nanocomposites both in solid and melt states, and the thermal stability and melt viscosity of renewable polymers also increase after nanocomposite preparation (Han and Floros, 1997; Penner and Lagaly, 2001; Sorrentino and Gorrasi, 2007). Manias et al. (2001), reported that small additions—typically less than 6 wt% of nanoscale inorganic fillers could promote concurrently several of the polypropylene material properties, including improved tensile characteristics, higher heat deflection temperature, retained optical clarity, high barrier properties, better scratch resistance, and increased flame retardancy. Strawhecker and Manias (2000) suggested that for a 5% montmorillonite (MMT) exfoliated composite, the softening temperature of nanocomposites increased by 25°C, the water permeability reduced by 60%, and the nanocomposites could retain their optical clarity. For these reasons, these are far lighter in weight than conventional biodegradable composites and make them competitive with other materials for specific applications,

especially food packaging (Petersen et al., 1999). Another advantage of nanocomposite is that it can be biodegraded efficiently. Degradation of a polymer may result from the action of microbes, macro-organisms, photo degradation or chemical degradation (Avella et al., 2005).

### ***Application of Nanocomposites in Food Packaging***

The use of proper packaging materials and methods to minimize food losses and provide safe and wholesome food products have always been the focus of food packaging. In addition, consumer trends for better quality, fresh-like, and convenient food products have intensified during the last decades. Therefore, a variety of active packaging technologies have been developed to provide better quality, wholesome, and safe foods, and also to limit package-related environmental pollution and disposal problems. The application of nanocomposites may open a new possibility to solve these problems. Nanocomposite packaging materials have great potential for enhanced food quality, safety, and stability as an innovative packaging and processing technology. The unique advantage of the natural biopolymer packaging may lead to new product development in food industry, such as individual packaging of particulate foods, carriers for functionally active substances, and nutritional supplements (Ozdemir and Floros, 2004).

### ***NANOCELLULOSE (NC)***

Nanocelluloses (NCs) are described as celluloses composed of nanosized fibers and nanofiber structuring which determines the product's properties. The similar term *nanosized cellulose* is used in case of isolated crystallites and whiskers formed by acid-catalyzed degradation of celluloses. This field and the application of that nanosized cellulose, e.g., in composites, have been intensively investigated. Typical examples have been reported (Ljungberg et al., 2005; Masa et al., 2005).

### ***Types of Nanocellulose***

As described above, one type of NC is formed directly as the result of biosynthesis of special bacteria, and these types of NCs are called bacterial NC. A very pure product with subsequently reported important properties is formed that necessitates challenging biosynthesis/biotechnological handling and the development of large-scale production. Another kind of NC can be prepared from the nearly inexhaustible source of feedstock wood using controlled mechanical disintegration steps to produce the favored product properties (Masa et al., 2005).

### ***Nanocellulose from Bacteria***

In 1886, A. J. Brown discovered bacterial cellulose (BC) as a biosynthetic product of *Gluconacetobacter xylinus* strains

(Klemm et al., 1998). He identified a gelatinous mass, formed on the solution during the vinegar fermentation as cellulose. It is mentioned that in the middle of the 20th century, a special culture medium was developed for *Gluconacetobacter xylinus* to optimize cellulose formation on the laboratory scale. As a result of systematic and comprehensive research over the last decade, broad knowledge of the formation and structure of BC has been acquired. This work is an important part of the integration of biotechnological methods into polysaccharide chemistry and the development of cellulose products with new properties and application potential (Tischer et al., 2011).

### **Nanocellulose from Wood**

In contrast to BC, cellulose from wood is composed of fibers that are about 100 times thicker. Because of the complex and expensive cultivation of BC (sophisticated medium and long cultivation time), it is also a challenge to produce nanofibrillated celluloses from wood. The substructures of wood are only accessible by chemical treatment (Klemm et al., 1998) and mechanical disintegration procedures. In the last 25 years, there have been efforts to reduce wood fibers in size. As a first step, in the early 1980s, Turbak et al. (1983) developed micro fibrillated cellulose (MFC). Today, there are different ways to produce materials with controlled fiber diameters. At first, a water suspension of pulp has to go through a mechanical treatment that consists of a spring-loaded valve assembly (refiner), where the slurry is pumped at high pressure. The formed MFC is moderately degraded and extremely expanded in surface area. In recent years, cellulose with a nanoscale web-like structure has been made. The fiber diameters are in the range 10–100 nm (Nakagaito & Yano, 2004, 2005). The degree of fibrillation depends on the number of passes through the refiner. Another technique to prepare wood MFC/NC is described by Takahashi et al. (2005). The aim was the creation of strong composites in tension using hot-pressed fibers without synthetic polymers but with the original wood components hemicelluloses and lignin as binders. The starting material was bamboo because of its high cellulose content. Bamboo-fiber bundles and monofilaments were ground under high-speed conditions using stone disks. A combination of thermal and alkali pretreatments, given the appropriate ratio of cellulose, hemicelluloses and lignin in the monofilaments led to strong adhesion between the fibers under the hot-press conditions. Suzuki and Hattori (2004) treated a pulp with a solid concentration of 1–6% with a disk refiner more than 10 times. The fibers obtained had a length of less than 0.2 mm. There have also been some investigations into the properties of NC from wood, which has an amazing water-storage capacity, similar to BC. A dispersion of these cellulose fibers in water with a solid content of only 2% leads to a mechanically stable transparent gel. The wood NC fibers are suitable for solidification of emulsion paints and filter aids, useful for both primary rough filtration and precision filtration. Furthermore, NC from wood is used in paper-making as a coating

and dye carrier in paper tinting. Moreover, it can be utilized in the food industry as a thickening agent, a gas-barrier, and in moisture resistant paper laminate for packaging. In cosmetics, wood NC is suitable as an additive in skin-cleansing cloths, and as part of disposal diapers, sanitary napkins, and incontinence pads. Possible medical applications are directed to excipients such as binders, fillers, and/or disintegrants in the development of solid dosage forms (Fukuda et al., 2001; Kumar, 2002; Kyomori et al. 2005).

Besides application in its pure form, it is possible to use NC from wood in polymer composites. In embedding tests, the tensile strength of such composites was five times higher than that of the original polymers. This result, as well as its natural origin, makes this NC attractive for combination with different biopolymers. Possible applications for such reinforced biopolymers could arise in areas such as medicine, food industry, and gardening (Nakagaito and Yano, 2004, 2005). In these sectors, properties such as biodegradability, high mechanical strength, and where required optical transparency are important. It should also be mentioned that the application of wood NC prepared by the described techniques, where the cell wall is further disintegrated by mechanical treatment, leads to lower-strength cellulose fiber-reinforced composites than in the corresponding BC materials (Gindl and Keckes, 2004).

### **Application of Nanocellulose**

In recent years due to the exceptional properties of these innovative NC polymers, many widespread utilization have been observed. Membranes and composites from cellulose and cellulose esters are important domains in the development and application of these polymeric materials. The most important segment by volume in the chemical processing of cellulose contains regenerated cellulose fibers, films, and membranes. In the case of the cellulose esters, mainly cellulose nitrate and cellulose acetate as well as novel high-performance materials are created, which are widely used as laminates, composites, optical/photographic films, and membranes, or as other separation media. The direct formation of stable and manageable BC fleeces as the result of bacterial biosynthesis in the common static culture is significant. This and their exciting properties have led to the increasing use of BC as a membrane material and composite component. Contaminations incorporated from the culture medium and bacterial cells can be removed from the BC by smooth purification methods depending on the application area. One recent example of the formation and application of foils/membranes of unmodified bacterial NC is described by George and coworkers (George et al., 2005). The processed membrane seems to be of great relevance as a packaging material in the food industry, where continuous moisture removal and minimal-oxygen-transmission properties play a vital role. The purity, controllable water capacity, good mechanical stability, and gas-barrier properties of bacterial NC are important parameters for this application.

### *Nanocellulose Based Composites*

There have been several researches on the use of NC as a reinforcing agent in polymer matrices. Nanocomposites based on nanocellulosic materials have been prepared with petroleum-derived nonbiodegradable polymers such as polyethylene (PE) or polypropylene (PP) and also with biodegradable polymers such as polylactic acid (PLA), polyvinyl alcohol (PVOH), starch, polycaprolactone (PCL), methylcellulose, and chitosan.

Bruce et al. (2005) prepared composites based on Swede root MFC and different resins including four types of acrylic and two types of epoxy resins. All the composites were significantly stiffer and stronger than the unmodified resins. The main merit of the study was that it demonstrated the potential for fabricating nanocomposites with good mechanical properties from vegetable pulp in combination with a range of resins. Apart from good mechanical properties, high composite transparency can be important for some applications (e.g., in the optoelectronics industry). Iwamoto et al. (2005, 2008) reported that because of the size of nanofibers reinforced acrylic resin retains the transparency of the matrix resin even at fiber contents as high as 70 wt%. The BC with nanofiber widths of 10 nm also has potential as a reinforcing material for transparent composites. As for example, Nogi et al. (2005, 2006a, 2006b) obtained transparent composites by reinforcing various acrylic resins with BC at loadings up to 70 wt% by reducing the average fiber size (diameter 15 nm). Abe et al. (2007) fabricated an NC (from wood) containing acrylic resin nanocomposite with transmittance higher than that of BC nanocomposite in the visible wavelength range and at the same thickness and filler content. This finding indicated that nanofibers obtained from wood were more uniform and thinner than BC nanofibers.

Another remarkable and potentially useful feature of NC is their low thermal expansion coefficient (CTE), which can be as low as 0.1 ppm K<sup>-1</sup> and comparable with that of quartz glass (Nishino et al., 2004). This low CTE combined with high strength and modulus could make NC a potential reinforcing material for fabricating flexible displays, solar cells, electronic paper, panel sensors and actuators, etc. As an example, Nogi and Yano (2008) prepared a foldable and ductile transparent nanocomposite film by combining low-YM transparent acrylic resin with 5 wt% of low CTE and high-YM of BC. The same researchers reported that transparent NC sheets prepared from NC and coated with acrylic resin have low CTEs of 8.5–14.9 ppm K<sup>-1</sup> and a modulus of 7.2–13 GPa (Nogi and Yano, 2009). Polyurethane (PU), which is a polar polymer, has the potential to interact with the polar groups of cellulose molecules leading to enhanced mechanical and interfacial properties of the composites. PU-MFC composite materials were prepared recently using a film stacking method in which the PU films and nonwoven cellulose fibril mats were stacked and compression moulded (Seydibeyoglu and Oksman, 2008). The thermal stability and mechanical properties of the pure PU were improved by MFC reinforcement. Nanocomposites with 16.5 wt% fibril

content had tensile strength and YM values nearly 5 and 30 times higher, respectively, than that of the corresponding values for the matrix polymer.

Polyvinyl alcohol (PVOH) is a water-soluble alcohol, which is biocompatible, biodegradable, and also has excellent chemical resistance. Therefore, PVOH has a wide range of practical applications. In particular, PVOH is an ideal candidate for biomedical applications including tissue reconstruction and replacement, cell entrapment and drug delivery, soft contact lens materials, and wound covering bandages for burn victims (Ding et al., 2004). Sun-Young Lee et al. (2009) reported the fabrication of PVOH-NC composites by the reinforcement of NC into a PVOH matrix at different filler loading levels and subsequent film casting. The NC was prepared by acid hydrolysis of MCC at different hydrobromic acid (HBr) concentration. Chemical characterization of NC was performed for the analysis of crystallinity (Xc), degree of polymerization (DP), and molecular weight (Mw). The acid hydrolysis decreased steadily the DP and Mw of MCC. The crystallinity of MCC with 1.5 M and 2.5 M HBr showed a significant increase due to the degradation of amorphous domains in cellulose. The mechanical and thermal properties of the NC reinforced PVOH films were also measured for tensile strength and thermo-gravimetric analysis (TGA). The tensile strength (TS) of pure PVOH film was 49 MPa. The TS of NC-reinforced PVOH films after 1.5 M HBr hydrolysis showed the highest value (73 MPa) at the loading of 1 wt%. This value was 49% higher than pure PVOH film. However, the NC loading of 3 and 5 wt% to PVOH matrix gradually decreased the values of TS. The TS of PVOH films with 3 and 5 wt% NC were 3.0 and 55.3% lower, respectively, compared to those with 1 wt% NC. The TGA of NC-reinforced PVOH films revealed three main weight loss regions. The first region at a temperature of 80–140°C is due to the evaporation of physically weak and chemically strong bound water, and the weight loss of the film in those ranges is about 10 wt%. The second transition region at around 230–370°C is due to the structural degradation of PVOH composite films and the total weight loss in those ranges was about 70%. The third stage weight loss occurred above 370°C, due to the cleavage backbone of PVOH composite films or the decomposition of carbonaceous matter. Wan et al. (2006) tested BC as a potential reinforcing material in PVOH for medical device applications. These authors developed a PVOH-BC nanocomposite with mechanical properties tuneable over a broad range, thus making it appropriate for replacing different tissues. A number of applications using MFC for reinforcing PVOH have been reported. For example, Zimmermann et al. (2004) dispersed MFC into PVOH and generated fibril-reinforced PVOH nanocomposites (fibril content 20 wt%) with up to three times higher YM and up to five times higher TS when compared to the reference polymer. A blend containing 10% NC obtained from various sources, such as flax bast fibers, hemp fibers, kraft pulp or rutabaga and 90% PVOH was used for making nanofiber-reinforced composite material by a solution casting procedure (Bhatnagar and Sain, 2005). Both TS and YM were improved compared to neat PVOH film, with a pronounced four- to five-fold increase in YM observed. Poly(caprolactone)

(PCL), a biodegradable polymer, is suitable as a polymer matrix in biocomposites. Lönnberg et al. (2008) prepared MFC-grafted PCL composites via ring-opening polymerization (ROP). This changes the surface characteristics of MFC, for grafting made it possible to obtain a stable dispersion of MFC in a nonpolar solvent. It also improved the compatibility of MFCs with PCL. The thermal behavior of MFC grafted with different amount of PCL has been investigated using thermal gravimetric analysis (TGA) and differential scanning calorimetry (DSC). The crystallization and melting behavior of free PCL and MFC-PCL composites were studied with DSC, and a significant difference was observed regarding melting points, crystallization temperature (T<sub>g</sub>), degree of crystallinity, as well as the time required for crystallization.

Khan et al. (2010c) prepared methylcellulose (MC)-based films casted from its 1% aqueous solution containing 0.5% vegetable oil, 0.25% glycerol, and 0.025% Tween80<sup>®</sup>. Puncture strength (PS), puncture deformation (PD), viscoelasticity coefficient, and water vapor permeability (WVP) were found to be 147 N/mm, 3.46 mm, 41%, and 6.34 g.mm/m<sup>2</sup>.day.kPa, respectively. Aqueous NC solution (0.1–1%) was incorporated into the MC-based formulation, and it was found that both PS and WVP values were improved by 117 and 26%, respectively. Films containing 0.25% NC were found to be the optimum. Khan et al. (2010c) also reported the effect of gamma radiation on the NC containing MC-based composites. The films were irradiated from 0.5 to 50 kGy doses, and it was revealed that mechanical properties of the films were slightly increased at low doses because of NC fibers reorientation, whereas barrier properties were further improved to 29% at 50 kGy.

Dufresne and Vignon (1998, 2000) prepared potato starch-based nanocomposites, while preserving the biodegradability of the material through addition of MFC. The cellulose filler and glycerol plasticizer content were varied between 0–50 wt% and 0–30 wt%, respectively. MFC significantly reinforced the starch matrix, regardless of the plasticizer content, and the increase in YM as a function of filler content was almost linear. The YM was found to be about 7 GPa at 50 wt% MFC content compared to about 2 GPa for unreinforced samples (0% MFC). However, it was noted that when the samples were conditioned at high relative humidity (75% RH), the reinforcing effect of the cellulose filler was strongly diminished. Since starch is more hydrophilic than cellulose, in moist conditions it absorbs most of the water and is then plasticized. The cellulosic network is surrounded by a soft phase and the interactions between the filler and the matrix are strongly reduced. Besides improving mechanical properties of starch, addition of MFC to the matrix resulted in a decrease of both water uptake at equilibrium and the water diffusion coefficient. Nanocomposites from wheat straw nanofibers and thermoplastic starch from modified potato starch were prepared by the solution casting method (Alemdar and Sain, 2008). Thermal and mechanical performance of the composites was compared with the pure thermoplastic starch (TPS) using TGA, dynamic mechanical analysis (DMA), and

tensile testing. The TS and YM were significantly enhanced in the nanocomposite films, which could be explained by the uniform dispersion of nanofibers in the polymer matrix. The YM of the TPS increased from 111 to 271 MPa with maximum (10 wt%) nanofiber filling. In addition, the glass transition (T<sub>g</sub>) of the nanocomposites was shifted to higher temperatures with respect to the pure TPS. Azeredo et al. (2010) developed NC-reinforced chitosan films with different NC and glycerol (plasticizer) content. They evaluated the effect of different concentration of NC and glycerol on the TS, YM, T<sub>g</sub>, elongation at break (Eb), and WVP of the chitosan-based composite films. They have an optimum condition of 18% glycerol and 15% NC, based on the maximization of TS, YM, T<sub>g</sub>, and decreasing WVP values while maintaining a acceptable Eb of 10%. Pereda et al. (2010) developed sodium caseinate films with NC by dispersing the fibrils into film forming solutions, casting, and drying. Composite films have been reported to be less transparent and had a more hydrophilic surface than neat sodium caseinate films. However, the global moisture uptake was almost not affected by the NC concentration. Addition of NC to the neat sodium caseinate films produced an initial increase in the WVP and then decreased as filler content increased. The TS and TM of the composite films have been reported to increase significantly with a more than two times increase in TS and TM than the native films at 3% NC content.

### CLASSIFICATION OF BIOPOLYMERS

A vast number of biopolymers or biodegradable polymers are chemically synthesized or biosynthesized during the growth cycles of all organisms. Some micro-organisms and enzymes capable of degrading them have been identified (Averous & Boquillon, 2004). Figure 1, proposes a classification with four different categories, depending on the synthesis:

- (a) Polymers from biomass such as the agro-polymers from agro-resources, e.g., starch, cellulose.
- (b) Polymers obtained by microbial production, e.g., poly(hydroxyalkanoates).
- (c) Polymers chemically synthesized using monomers obtained from agro-resources, e.g., poly(lactic acid).
- (d) Polymers whose monomers and polymers are both obtained by chemical synthesis from fossil resources, e.g., poly(caprolactone), polyester amide, etc.

Except the fourth family, which is of fossil origin, most polymers of family (a)–(c) are obtained from renewable resources (biomass). The first family is agro-polymers (e.g., polysaccharides) obtained from biomass by fractionation. The second and third families are polyesters, obtained respectively by fermentation from biomass or from genetically modified plants (e.g., polyhydroxyalkanoate) and by synthesis from monomers obtained from biomass (e.g. polylactic acid). The fourth family

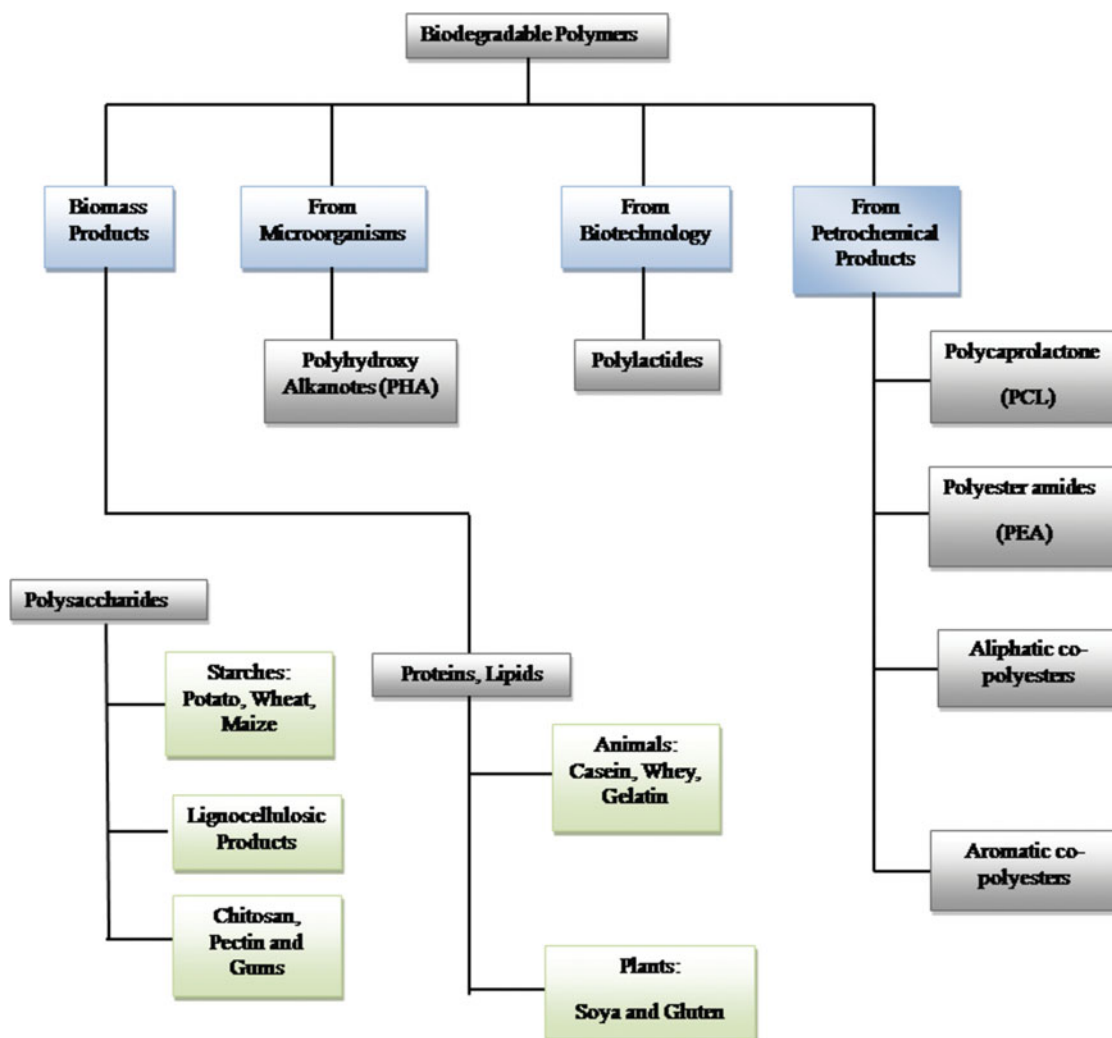


Figure 1 Classification of biodegradable polymer (adopted from John & Thomas, 2008). (Color figure available online.)

is polyesters, totally synthesized by the petrochemical process (e.g., polycaprolactone; polyester amide; aliphatic or aromatic copolyesters). A large number of these biopolymers are commercially available. They show a large range of properties and they can compete with nonbiodegradable polymers in different industrial fields (John and Thomas, 2008).

### BIOACTIVE PACKAGING

Bioactive packaging is gaining interest from researchers and industries due to its potential to provide quality and safety benefits. The reason for incorporating bioactive agents into the packaging is to prevent surface growth of micro-organisms in foods where a large portion of spoilage and contamination occurs (Appendini and Hotchkiss, 2002; Coma, 2008). This approach can reduce the addition of larger quantities of antimicrobials that are usually incorporated into the bulk of the food. A controlled

release from packaging film to the food surface has numerous advantages over dipping and spraying. In the latter processes, in fact, antimicrobial activity may be rapidly lost due to inactivation of the antimicrobials by food components or dilution below active concentration due to migration into the bulk food matrix (Janjarasskul and Krochta, 2010). Numerous researchers have demonstrated that bioactive polymers such as, alginate, chitosan, gelatine, etc., and antimicrobial compounds such as organic acids (acetic, propionic, benzoic, sorbic, lactic, lauric), potassium sorbate, bacteriocins (nisin, lacticin), grape seed extracts, spice extracts (thymol, p-cymene, cinnamaldehyde), thio-sulfonates (allicin), enzymes (peroxidase, lysozyme), proteins (conalbumin), isothiocyanates (allylisothiocyanate), antibiotics (imazalil), fungicides (benomyl), chelating agents (ethylenediaminetetraacetic acid-EDTA), metals (silver), or parabens (heptylparaben) could be added to edible films to reduce bacteria in solution, on culture media, or on a variety of muscle foods (Cutter, 2002 and 2006). A short discussion on some of the bioactive polymers and bioactive agents is given here:

## Bioactive Polymers

Bioactive polymers such as, alginate, chitosan, gelatin, etc., can be used for the packaging of food products. Alginates are linear copolymers of  $\beta$ -(1-4)-linked D-mannuronic acid and  $\alpha$ -(1-4)-linked L-guluronic acid units, which exist widely in many species of brown seaweeds. Since it was discovered by Stanford in 1881, alginate has been used in a wide range of industries, such as food, textile printing, paper and pharmaceuticals, and for many other novel end-uses (Khan et al., 2010b). Study found that alginate coatings retarded oxidative off-flavors, improved flavor, and juiciness in re-heated pork patties (Earle & McKee, 1976). Other researchers have extended the shelf life of shrimp, fish, and sausage with alginate coatings (Cutter and Samner, 2002). Sodium alginate coatings extended the shelf life of salted and dried mackerel (Jo et al., 2001). Chitosan is a linear polysaccharide consisting of 1, 4-linked 2- amino-deoxy- $\beta$ -D-glucan, is a deacetylated derivative of chitin, which is the second most abundant polysaccharide, found in nature after cellulose. Chitosan has been found to be nontoxic, biodegradable, biofunctional, biocompatible, and was reported by several researchers to have strong antimicrobial and antifungal activities. Chitosan has been compared with other biomolecule-based active films used as packaging materials and the reported results showed that chitosan has more advantages because of its antibacterial activity and bivalent minerals chelating ability (Chen et al., 2002). Chitosan films have been successfully used as a packaging material for the quality preservation of a variety of foods (Ouattara et al., 2000). Antimicrobial films have been prepared by including various organic acids and essential oils in a chitosan matrix, and the ability of these bio-based films to inhibit the growth of indigenous (*Lactic acid bacteria* and *Enterobacteriaceae*) or inoculated bacteria (*Lactobacillus sakei* and *Serratia liquefaciens*) onto the surfaces of vacuum-packed cured meat products have been investigated. Release of organic acids (acetic and propionic) was found to be initially fast, when the gradient of ion concentration between the inside of the polymer matrix and the outside environment was high, then decreased as the release of acids progressed. At the same time, it was shown that the antimicrobial activity of the bio-based films under study did not affect growth and activity of lactic acid bacteria, whereas the growth of *Enterobacteriaceae* and *S. liquefaciens* was delayed or completely inhibited after storage during 21 days at 4°C (Quintavalla and Vicini, 2002). Recently, a chitosan–starch film has been prepared using microwave treatment which may find potential application in the food packaging technology (Dutta et al., 2009; Aider, 2010). Chitosan films have been made via treatments with various acids and incorporated into packaging films for processed meats and seafood, as well as combined with nisin and coated onto the surfaces of paper for inhibiting microorganisms (Vartiainen et al., 2004). Durango et al. (2006) also developed and evaluated an edible film made from 3% or 5% chitosan and starch against *S. enteritidis* in suspensions. When applied directly to cell suspensions, 1% chitosan reduced the pathogen  $>4\log_{10}$  CFU/mL (or

99.99%). Subsequent experiments demonstrated that chitosan-treated films made with 3% or 5% chitosan reduced populations of *S. enteritidis*  $> 1\log_{10}$  CFU/mL (or 90%). The authors demonstrated that chitosan-treated films made with 5% chitosan were the most efficient treatment for inhibiting *S. enteritidis* in solution and that the application of these films to foodstuffs was in progress. In another study, Cooksey (2005) incorporated nisin into chitosan to inhibit *L. monocytogenes*. In solution and in agar diffusion assays, the antimicrobial film inhibited the pathogen, but no further studies were conducted in meat systems (Cha and Chinnan, 2004).

## Organic Acids

Organic acids, such as acetic, benzoic, lactic, citric, nalidixic, maleic, tartaric, propionic, fumaric, sorbic, etc., are one of the most common ingredients used for bioactive packaging. Yamanaka et al. (2000), described the influence of bioactive organic agents such as nalidixic acid as additives to the bacterial cellulose (BC) culture medium. In that case, not only the crystallization of the fibers and the material properties were influenced but the *Gluconacetobacter* cells were also changed. Using antibiotics in a concentration of 0.1 mM, a 2–5 times elongation of the cell length was observed due to inhibition of cell division. The fibers became 1–2 times wider compared to common BC. Ghosh et al. (1977), developed fungistatic wrappers with sorbic acid and applied them to bread. This wrapper necessitated heating the wrapped bread at 95–100°C for a period of 30 to 60 minutes. The incorporation of an antioxidant in the treated wrapper and also the use of an odor adsorbent inside the bread packs minimized off-flavor development. Sliced bread, based on sensory evaluation, was found acceptable up to 1 month, and as a sandwich up to 3 months. The fungistatic wrappers were made by coating grease-proof paper with an aqueous dispersion of sorbic acid in 2% carboxymethyl cellulose solution. Using this sorbic acid-treated paper and then enclosing the food in a polyethylene bag could preserve foods that are generally amenable to spoilage by mold for minimum of 10 days. Han and Flores (1997) studied the incorporation of 1.0% w/w potassium sorbate in low density polyethylene films. A 0.1-mm-thick film was used for physical measurements. It was found that potassium sorbate lowered the growth rate and maximum growth of yeast, and lengthened the lag period before mold growth became apparent. Weng et al. (1999) developed the technique of combining polyethylene-co-methacrylic acid (PEMA) with benzoic and sorbic acid to form antimicrobial food packaging material. Devlieghere et al. (2000) studied the antimicrobial activity of ethylene vinyl alcohol (EVA)/linear low density polyethylene (LLDPE) containing potassium sorbate. Because of the limited migration of K-sorbate from LLDPE film, the inhibition effect of this film against *Candida* spp., *Pichia* spp., *Trichosporon* spp., and *Penicillium* spp. appeared very weak. Moreover, no significant differences could be observed for yeast and mold growth on the cheese cubes

compared to a reference film during storage of cheese packaged in a *K*-sorbate film. Benzoic anhydride-incorporated antimicrobial polyethylene films and minimal microwave heating were used to control the microbial growth of Tilapia fish fillets.

### Bacteriocins

The bacteriocin such as nisin, which is produced by the lactic acid bacterium, *Lactococcus lactis*, is one of the most effective agents when it comes to antimicrobial packaging. It is the most effective against lactic acid bacteria and other gram-positive organisms, notably the *Clostridia* species (Jin and Zhang, 2008). Imran et al. (2010) developed hydroxypropyl methylcellulose films with nisin and evaluated the antimicrobial activity of the films against *Listeria*, *Staphylococcus*, *Enterococcus*, and *Bacillus* strains. It has been reported that film bioactivity demonstrated efficacy against *Listeria* > *Enterococcus* > *Staphylococcus* > *Bacillus* spp. Scannell et al. (2000) developed bioactive food packaging materials using immobilized nisin and lactacin 3147. The antimicrobial packaging reduced the lactic acid bacteria counts in sliced cheese and ham at refrigeration temperatures, thus, extending the shelf life. Nisin adsorbed bioactive inserts reduced levels of *Listeria innocua* by below 2 log units in cheese and ham and *Staphylococcus aureus* in cheese (~1.5 log units) and ham (~2.8 log units). Ming et al. (1997) applied nisin and pediocin to cellulose casings to reduce *L. monocytogenes* in meats and poultry. Pediocin-coated bags completely inhibited the growth of inoculated *L. monocytogenes* through 12 weeks storage at 4°C. Pediocin is another bacteriocin, which was found to be effective against *L. monocytogenes*. Wilhoit (1996 and 1997) has received a patent for the method of employing pediocin-coated cellulose casings on meat for inhibiting the growth of *L. monocytogenes*. Cutter and Siragusa (1997) reported that immobilization of the bacteriocin nisin in calcium alginate gels not only resulted in greater reductions of bacterial populations on lean and adipose beef surfaces, but also resulted in greater and sustained bacteriocin activity when the tissues were ground and stored under refrigerated conditions for up to 7 days, as compared to nisin-only controls.

### Essential Oils and Plant Extracts

The antimicrobial activity of essential oils and plant extracts has been recognized for many years. Ouattara et al. (2001) evaluated the combined effect of low-dose gamma irradiation and protein-based coatings with thyme oil and trans-cinnamaldehyde to extend the shelf life of pre-cooked shrimp. The product's shelf life was significantly extended without altering the appearance and taste of shrimp for thymol treatment concentrations of up to 0.9%. Oussalah et al. (2007) developed alginate-based edible films with 1% (w/v) essential oils of Spanish oregano (O; *Corydothymus capitatus*), Chinese cinnamon (C; *Cinnamomum cassia*), or winter savory (S; *Satureja mon-*

*tana*) to control pathogen growth on bologna and ham slices. The bologna and ham slices were inoculated with *Salmonella* Typhimurium or *Listeria monocytogenes* at 10<sup>3</sup> CFU/cm<sup>2</sup>. On bologna, C-based films were the most effective against the growth of *Salmonella* Typhimurium and *L. monocytogenes*. *L. monocytogenes* was the more sensitive bacterium to O-, C-, and S-based films. *L. monocytogenes* concentrations was found to be below the detection level (<10 CFU/mL) after five days of storage on bologna coated with O-, C-, or S-based films. On ham, a 1.85 log CFU/cm<sup>2</sup> reduction of *Salmonella* Typhimurium ( $P \leq 0.05$ ) have been reported after five days of storage with C-based films. *L. monocytogenes* was highly resistant in ham, even in the presence of O-, C-, or S-based films. However, C-based films were the most effective against the growth of *L. monocytogenes*. Oussalah et al. (2004), also developed milk protein-based edible films containing 1.0% (w/v) oregano, 1.0% (w/v) pimento, or 1.0% oregano-pimento (1:1) essential oils mix were applied on beef muscle slices. The application of bioactive films on meat surfaces containing 10<sup>3</sup> CFU/cm<sup>2</sup> of *Escherichia coli* O157:H7 or *Pseudomonas* spp. showed that film containing oregano was the most effective against both the bacteria, whereas film containing pimento oils was reported to have least effect against these two bacteria. A 0.95 log reduction of *Pseudomonas* spp. level, as compared to samples without film, was observed at the end of storage in the presence of films containing oregano extracts. A 1.12 log reduction of *E. coli* O157:H7 level was reported in samples coated with oregano-based films. Hammer et al. (1999) investigated 52 plant oils and extracts for activity against *Acinetobacter baumannii*, *Aeromonas veronii* biogroup *sobria*, *Candida albicans*, *Enterococcus faecalis*, *Escherichia coli*, *Klebsiella pneumoniae*, *Pseudomonas aeruginosa*, *Serratia marcescens* and *Staphylococcus aureus*, using an agar dilution method. Lemongrass, oregano, and bay inhibited all organisms at concentrations of  $\leq 2.0\%$  (v/v). Six oils did not inhibit any organisms at the highest concentration, which was 2.0% (v/v) oil for apricot kernel, evening primrose, macadamia, pumpkin, sage and sweet almond. Variable activity was recorded for the remaining oils. Twenty of the plant oils and extracts were investigated, using a broth microdilution method, for activity against *C. albicans*, *S. aureus* and *E. coli*. The lowest minimum inhibitory concentrations were 0.03% (v/v) thyme oil against *C. albicans* and *E. coli*, and 0.008% (v/v) vetiver oil against *S. aureus*. Smith-Plamer et al. (1998) investigated antimicrobial properties of 21 plant essential oils and two essences were investigated against five important food-borne pathogens, *Campylobacter jejuni*, *Salmonella enteritidis*, *Escherichia coli*, *Staphylococcus aureus* and *Listeria monocytogenes*. The oils of bay, cinnamon, clove, and thyme were the most inhibitory, each having a bacteriostatic concentration of 0.075% or less against all five pathogens. In general, gram-positive bacteria were more sensitive to inhibition by plant essential oils than the gram-negative bacteria. *Campylobacter jejuni* was the most resistant of the bacteria investigated to plant essential oils, with only the oils of bay and thyme having a bacteriocidal concentration of less than 1%. At 35°C, *L. monocytogenes* was extremely

sensitive to the oil of nutmeg. A concentration of less than 0.01% was bacteriostatic and 0.05% was bacteriocidal, but when the temperature was reduced to 4°C, the bacteriostatic concentration was increased to 0.5% and the bacteriocidal concentration to greater than 1%.

## CONCLUSION

Among the many different materials that mankind is currently dependent on, nonbiodegradable polymers are arguably still one of the most important considering their widespread usage in food packaging industries. Currently, almost all the nonbiodegradable polymers that are widely used in various sectors are produced from petrochemical products. Due to concerns for the global environment and the increasing difficulty in managing solid wastes, biodegradable polymeric materials, bio-nanocomposites, and bioactive packaging may be among the most suitable alternatives for many applications. Addition of bioactive polymers (alginate, chitosan, etc.) or bioactive agents such as organic acids, essential oils, and plant extracts, bacteriocins can significantly enhance the quality and safety of food products during storage and can also prevent the growth of microorganisms in food. Similarly, NC-based composites, due to their excellent mechanical and barrier properties and their role as the carrier of bioactive substances, have great potential in food packaging industries. The field of food packaging represents a promising and exciting field for the use of nanotechnology. Use of nanotechnology in food packaging can not only increase the mechanical and barrier properties of the films but can also increase the safety and shelf life of the packaged food products by allowing a controlled or sustained release of antimicrobials or bioactive agents. However, there has been little study on the combination of NC with bioactive agents to have composite films that will fulfill both mechanical and antimicrobial properties required for food packaging. So, composites films with both NC and bioactive agents, represent a promising field of research and should have an enormous impact on food packaging over the coming years.

## ACKNOWLEDGMENTS

We thank the Natural Sciences and Engineering Research Council of Canada (NSERC) and FP Innovation (Pointe-Claire, Canada) for their research support and funding.

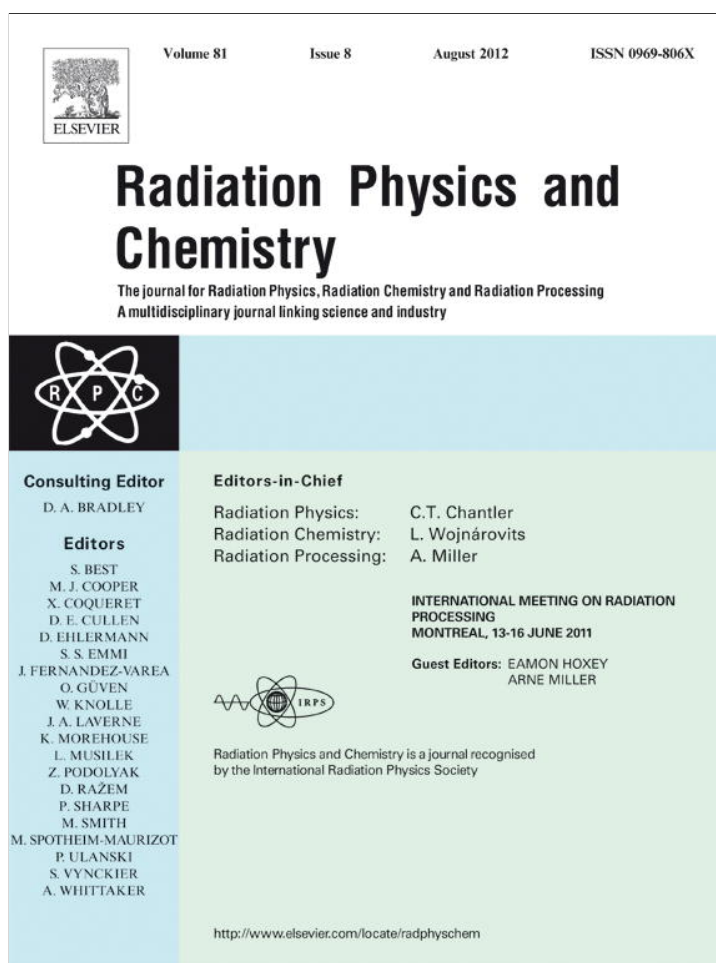
## REFERENCES

Abe, K., Iwamoto, S. and Yano, H. (2007). Obtaining cellulose nanofibers with a uniform width of 15 nm from wood. *Biomacromolecules* **8**:3276–3278.  
 Aider, M. (2010). Chitosan application for active bio-based films production and potential in the food industry: Review. *LWT - Food Sci. Technol.* **43**:837–842.

Alemdar, A. and Sain, M. (2008). Biocomposites from wheat straw nanofibers: Morphology, thermal and mechanical properties. *Compos. Sci. Technol.* **68**:557–565.  
 Appendini, P. and Hotchkiss, J. H. (2002). Review of antimicrobial food packaging. *Innovative Food Sci. Emerging Technol.* **3**:113–126.  
 Avella, M., Vlieger, J. J. D., Errico, M. E., Fischer, S., Vacca, P. and Volpe, M. G. (2005). Biodegradable starch/clay nanocomposite films for food packaging applications. *Food Chem.* **93**:467–474.  
 Averous, L. and Boquillon, N. (2004). Biocomposites based on plasticized starch: Thermal and mechanical behaviors. *Carbohydr. Polym.* **56**:111–122.  
 Azeredo, H. M., Mattoso, L. H., Avena-Bustillos, R. J. A., Filho, G. C., Munford, M. L., Wood, D. and Mchugh, T. H. (2010). Nanocellulose reinforced chitosan composite films as affected by nanofiller loading and plasticizer content. *J. Food Sci.* **75**(1):N1–N7.  
 Beck-Candanedo, S., Roman, M. and Gray, D. G. (2005). Effect of reaction conditions on the properties and behavior of wood cellulose nanocrystal suspensions. *Biomacromolecules* **6**(2):1048–1054.  
 Bhatnagar, A. and Sain, M. (2005). Processing of cellulose nano fiber reinforced composites. *J. Reinf. Plast. Comp.* **24**:1259–1268.  
 Bledzki, A. K. and Gassan, J. (1999). Composites reinforced with cellulose based fibres. *Prog. Polym. Sci.* **24**:221–274.  
 Bruce, D. M., Hobson, R. N., Farrent, J. W. and Hepworth, D. G. (2005). High-performance composites from low-cost plant primary cell walls. *Compos. Part A - Appl. Sci. Manufact.* **36**:1486–1493.  
 Cao, X., Chen, Y., Chang, P. R., Muir, A. D. and Falk, G. (2008). Starch-based nanocomposites reinforced with flax cellulose nanocrystals. *Polym. Lett.* **2**(7):502–510.  
 Cha, D. and Chinnan, M. (2004). Biopolymer-based antimicrobial packaging: A review. *Crit. Rev. Food Sci.* **44**(4):223–237.  
 Chandra, R. and Rustgi, R. (1998). Biodegradable polymers. *Prog. Polym. Sci.* **23**:1273–1335.  
 Chen, X. G., Zheng, L., Wang, Z., Lee, C. Y. and Park, H. J. (2002). Molecular affinity and permeability of different molecular weight chitosan membranes. *J. Agric. Food Chem.* **50**(21):5915–5918.  
 Coma, V. (2008). Bioactive packaging technologies for extended shelf life of meat-based products. *Meat Sci.* **78**:90–103.  
 Cooksey, K. (2005). Effectiveness of antimicrobial food packaging materials. *Food Addit. Contam.* **22**:980–987.  
 Cutter, C. N. and Siragusa, G. R. (1997). Growth of *Brochothrix thermosphacta* in ground beef following treatments with nisin in calcium alginate gels. *Food Microbiol.* **14**:425–430.  
 Cutter, C. N. and Sumner, S. S. (2002). Application of edible coatings on muscle foods. In: Protein-Based Films and Coatings, pp. 467–484. Gennadios, A., Ed., CRC Press, Boca Raton, FL.  
 Cutter, C. N. (2002). Microbial control by packaging: A review. *Crit. Rev. Food Sci.* **42**:151–161.  
 Cutter, C. N. (2006). Opportunities for bio-based packaging technologies to improve the quality and safety of fresh and further processed muscle foods. *Meat Sci.* **74**:131–142.  
 Darder, M., Aranda, P. and Ruiz-Hitzky, E. (2007). Bionanocomposites: A new concept of ecological, bioinspired, and functional hybrid materials. *Adv Mater.* **19**:1309–1319.  
 Devlieghere, F., Vermeiren, L., Bockstal, A. and Debevere, J. (2000). Study on antimicrobial activity of a food packaging material containing potassium sorbate. *Acta Alimentaria* **29**:137–146.  
 Dieter-Klemm, D., Schumann, D., Kramer, F., Hessler, N., Hornung, M., Schmauder, H. P. and Marsch, S. (2006). Nanocelluloses as innovative polymers in research and application. *Adv. Polym. Sci.* **205**:49–96.  
 Dieter-Klemm, D., Schumann, D., Kramer, F., Hessler, N., Koth, D. and Sultanova, B. (2009). Nanocellulose materials: Different cellulose, different functionality. *Macromol. Symp.* **280**:60–71.  
 Ding, B., Kimura, E., Sato, T., Fujita, S. and Shiratori, S. (2004). Fabrication of blend biodegradable nanofibrous nonwoven mats via multi-jet electrospinning. *Polym.* **45**:1895–1902.  
 Dufresne, A. (1997). Mechanical behavior of films prepared from sugar beet cellulose microfibrils. *J. Appl. Polym. Sci.* **64**(6):1185–1194.

- Dufresne, A., Dupuyre, D. and Vignon, M. R. (2000). Cellulose microfibrils from potato tuber cells: Processing and characterization of starch-cellulose microfibril composites. *J Appl. Polym. Sci.* **76**:2080–2092.
- Dufresne, A. and Vignon, M. R. (1998). Improvement of starch film performances using cellulose microfibrils. *Macromolecules* **31**:2693–2696.
- Durango, A. M., Soares, N. F. F., Benevides, S., Teixeira, J., Carvalho, M., Wobeto, C. and Andrade, N. J. (2006). Development and evaluation of an edible antimicrobial films based on yam starch and chitosan. *Packag. Technol. Sci.* **19**:55–59.
- Dutta, P. K., Tripathi, S., Mehrotra, G. K. and Dutta, J. (2009). Perspectives for chitosan based antimicrobial films in food applications. *Food Chem.* **114**(4):1173–1182.
- Earle, R. D. and McKee, D. H. (1976). US Patent 3991218, November 9.
- Fischer, H. R., Gielgens, L. H. and Koster, T. P. M. (1999). Nanocomposites from polymers and layered minerals. *Acta Polymerica* **50**:122–126.
- Fukuda, S., Takahashi, M., Yuyama, M. and Oka, N. (2001). JP Patent 2001293033.
- George, J., Ramana, K. V., Sabapathy, S. N. and Bawa, A. S. (2005). Physicochemical properties of chemically treated bacterial (*Acetobacter xylinum*) cellulose membrane. *World J. Microb. Biot.* **21**:1323–1327.
- Ghosh, K. G., Srivatsava, A. N., Nirmala, N. and Sharma, T. R. (1977). Development and application of fungistatic wrappers in food preservation. Part II. Wrappers made by coating process. *J. Food Sci. Technol.* **14**:261–264.
- Giannelis, E. P. (1996). Polymer layered silicate nanocomposites. *Adv. Mat.* **8**(1):29–35.
- Gindl, W. and Keckes, J. (2004). Tensile properties of cellulose acetate butyrate composites reinforced with bacterial cellulose. *Comp. Sci. Technol.* **64**(15):2407–2413.
- Hammer, K. A., Carson, C. F. and Riley, T. V. (1999). Antimicrobial activity of essential oils and other plant extracts. *J. Appl. Microb.* **86**:985–990.
- Han, J. H. and Floros, J. D. (1997). Casting antimicrobial packaging films and measuring their physical properties and antimicrobial activity. *J. Plast. Film Sheeting* **13**:287–298.
- Hitzky E. R., Darder, M. and Pilar, A. (2005). Functional biopolymer nanocomposites based on layered solids. *J. Mater. Chem.* **15**:3650–3662.
- Imran, M., El-Fahmy, S., Revol-Junelles, A. M. and Desobry, S. (2010). Cellulose derivative based active coatings: Effects of nisin and plasticizer on physico-chemical and antimicrobial properties of hydroxypropyl methylcellulose films. *Carbohydr. Polym.* **81**(2):219–225.
- Iwamoto, S., Abe, K. and Yano, H. (2008). The effect of hemicelluloses on wood pulp nanofibrillation and nanofiber network characteristics. *Biomacromolecules* **9**:1022–1026.
- Iwamoto, S., Nakagaito, A. N., Yano, H. and Nogi, M., (2005). Optically transparent nanocomposites reinforced with plant fiber-based nanofibers. *Appl. Phys. A-Mater. Sci. Process.* **81**:1109–1112.
- Janjarasskul, T. and Krochta, J. M. (2010). Edible packaging materials. *Annual Rev. Food Sci. Technol.* **1**:415–448.
- Jin, T. and Zhang, H. (2008). Biodegradable polylactic acid polymer with nisin for use in antimicrobial food packaging. *J. Food Sci.* **73**(3):M127–M134.
- Jo, C., Lee, J. W., Lee, K. H. and Byun, M. W. (2001). Quality properties of pork sausage prepared with water-soluble chitosan oligomer. *Meat Sci.* **59**(4):369–375.
- John, M. J. and Thomas, S. (2008). Biofibres and biocomposites. *Carbohydr. Polym.* **71**:343–364.
- Khan, A., Huq, T., Saha, M., Khan, R. A. and Khan, M. A. (2010a). Surface modification of calcium alginate fibers with silane and methyl methacrylate monomers. *J. Reinf. Plast. Comp.* **29**(20):3125–3132.
- Khan, A., Huq, T., Saha, M., Khan, R. A., Khan, M. A. and Gofur, M. A. (2010b). Effect silane treatment on the mechanical and interfacial properties of calcium alginate fiber reinforced polypropylene composite. *J. Comp. Mater.* **24**:2875–2886.
- Khan, R. A., Salmieri, S., Dussault, D., Calderon, J. U., Kamal, M. R., Safrany, A. and Lacroix, M. (2010c). Production and properties of nanocellulose reinforced methylcellulose-based biodegradable films. *J. Agric. Food Chem.* **58**(13):7878–7885.
- Klemm, D., Philipp, B., Heinze, T., Heinze, U. and Wagenknecht, W. (1998). Comprehensive Cellulose Chemistry: Functionalization of Cellulose, Vol. 2, Ch. 4, Systematics of Cellulose Derivatization, p. 29. Wiley-VCH Verlag, Weinheim, Germany.
- Kojima, Y., Usuki, A., Kawasumi, M., Okada, A., Fukushima, Y., Kurauchi, T. and Kamigaito, O. (1993). Mechanical properties of Nylon 6-clay hybrid. *J. Mater. Res.* **8**(5):1185–1189.
- Kumar, V. (2002). WO Patent 2002022172.
- Kyomori, K., Tadokoro, I. and Matsumura, T. (2005). JP Patent 2005126867.
- Lee, S. Y., Mohan, D. J., Kang, I. A., Doh, G. H., Lee, S. and Han, S. O. (2009). Nanocellulose reinforced PVA composite films: Effects of acid treatment and filler loading. *Fibers. Polym.* **10**(1):77–82.
- Ljungberg, N., Bonini, C., Bortolussi, F., Boisson, C., Heux, L. and Cavaille, J. Y. (2005). New nanocomposite materials reinforced with cellulose whiskers in atactic polypropylene: Effect of surface and dispersion characteristics. *Biomacromolecules* **6**:2732–2739.
- Lönnberg, H., Fogelström, L., Said, M. A., Samir, A., Berglund, L., Malmström, E. and Anders Hult, A. (2008). Surface grafting of microfibrillated cellulose with poly( $\epsilon$ -caprolactone)—Synthesis and characterization. *European Polym. J.* **44**:2991–2997.
- Manias, E., Touny, A., Wu, L., Strawhecker, K., Lu, B. and Chung, T. C. (2001). Polypropylene/montmorillonite nanocomposites. Review of the synthetic routes and materials properties. *Chem. Mater.* **13**:3516–3523.
- Masa, S., Alloin, F. and Dufresne, A. (2005). Review of recent research into cellulosic whisker, their properties and their application in nanocomposite filed. *Biomacromolecules* **6**:612–626.
- Ming, X., Weber, G. H., Ayres, J. W. and Sandine, W. E. (1997). Bacteriocins applied to food packaging materials to inhibit *Listeria monocytogenes* on meats. *J. Food Sci.* **62**(2):413–415.
- Nakagaito, A. N. and Yano, H. (2004). The effect of morphological changes from pulp fiber towards nano-scale fibrillated cellulose on the mechanical properties of high-strength plant fiber based composites. *Appl. Phys. A.* **78**:547–552.
- Nakagaito, A. N. and Yano, H. (2005). Novel high-strength biocomposites based on microfibrillated cellulose having nanoorder-unit web-like network structure. *Appl. Phys. A.* **80**:155–159.
- Nishino, T., Matsuda, I. and Hirao, K. (2004). All-cellulose composite. *Macromolecules* **37**:7683–7687.
- Nogi, M., Abe, K., Handa, K., Nakatsubo, F., Ifuku, S. and Yano, H. (2006a). Property enhancement of optically transparent bionanofiber composites by acetylation. *Appl. Phys. Lett.* **89**(23):1–3.
- Nogi, M., Handa, K., Nakagaito, A. N. and Yano, H. (2005). Optically transparent bionanofiber composites with low sensitivity to refractive index of the polymer matrix. *Appl. Phys. Lett.* **87**(24):1–3.
- Nogi, M., Ifuku, S., Abe, K., Handa, K., Nakagaito, A. N. and Yano, H. (2006b). Fiber-content dependency of the optical transparency and thermal expansion of bacterial nano fiber reinforced composites. *Appl. Phys. Lett.* **88**(13):1–3.
- Nogi, M. and Yano, H. (2008). Transparent nanocomposites based on cellulose produced by bacteria offer potential innovation in the electronics device industry. *Adv. Mater.* **20**:1849–1852.
- Nogi, M. and Yano, H. (2009). Optically transparent nanofiber sheets by deposition of transparent materials: A concept for roll-to-roll processing. *Appl. Phys. Lett.* **94**(23):1–3.
- Quattara, B., Sabato, S. F. and Lacroix, M. (2001). Combined effect of antimicrobial coating and gamma irradiation on shelf life extension of pre-cooked shrimp (*Penaeus spp.*). *Int. J. Food Microbiol.* **68**:1–9.
- Quattara, B., Simard, R. E., Piette, G., Begin, A. and Holley, R. A. (2000). Diffusion of acetic and propionic acids from chitosan-based antimicrobial packaging films. *J. Food Sci.* **65**(5):768–773.
- Oussalah, M., Caillet, S., Salmieri, S., Saucier, L. and Lacroix, M. (2007). Antimicrobial effects of alginate-based films containing essential oils on *Listeria monocytogenes* and *Salmonella typhimurium* present in bologna and ham. *J. Food Protec.* **70**(4):901–908.
- Oussalah, M., Caillet, S., Salmieri, S., Saucier, L. and Lacroix, M. (2004). Antimicrobial and antioxidant effects of milk protein-based film containing essential oils for the preservation of whole beef muscle. *J. Agric. Food Chem.* **52**(18):5598–5605.

- Ozdemir, M. and Floros, J. D. (2004). Active food packaging technologies. *Crit. Rev. Food Sci.* **44**:185–193.
- Penner, D. and Lagaly, G. (2001). Influence of anions on the rheological properties of clay mineral dispersions. *Appl. Clay Sci.* **19**(1–6):131–142.
- Pereda, M., Amica, G., Rácz, L., Norma, E. and Marcovich, N. E. (2010). Structure and properties of nanocomposite films based on sodium caseinate and nanocellulose fibers. *J. Food Eng.* **103**(1):76–83.
- Petersen, K., Nielsen, P. V., Bertelsen, G., Lawther, M., Olsen, M. B., Nilsson, N. H. and Mortensen, G. (1999). Potential of bio-based materials for food packaging. *Trends Food Sci. Tech.* **10**:52–68.
- Quintavalla, S. and Vicini, L. (2002). Antimicrobial food packaging in meat industry. *Meat Sci.* **62**(3):373–380.
- Ray, S. S. and Okamoto, M. (2003). Polymer/layered silicate nanocomposites: A review from reinforced with bacterial cellulose. *Comp. Sci. Technol.* **64**:2407–2413.
- Rhim, J. W. (2007). Natural biopolymer-based nanocomposite films for packaging applications. *Crit. Rev. Food Sci. Nutr.* **47**(4):411–433.
- Rhim, J. W. and Hong, S. I. (2006). Preparation and characterization of chitosan nanocomposite films with antimicrobial activity. *J. Agric. Food Chem.* **54**(16):5814–5822.
- Sanguansri, P. and Augustin, M. A. (2006). Nanoscale materials development—A food industry perspective. *Trends Food Sci. Tech.* **17**(10):547–556.
- Scannell, A. G. M., Hill, C., Ross, R. P., Marx, S., Hartmeier, W. and Arendt, K. E. (2000). Development of bioactive food packaging materials using immobilized bacteriocins Lacticin 3147 and Nisaplin. *Int. J. Food Microbiol.* **60**:241–249.
- Seydibeyoglu, M. O. and Oksman, K. (2008). Novel nanocomposites based on polyurethane and microfibrillated cellulose. *Compos. Sci. Technol.* **68**:908–914.
- Siro, I. and Plackett, D. (2010). Microfibrillated cellulose and new nanocomposite materials: A review. *Cellulose* **17**:459–494.
- Smith-Palmer, A., Stewart, J. and Fyfe, L. (1998). Antimicrobial properties of plant essential oils and essences against five important food-borne pathogens. *Letters Appl. Microbiol.* **26**:118–122.
- Sorrentino, A. and Gorrasi, G. (2007). Potential perspectives of bio-nanocomposites for food packaging applications. *Trends Food Sci. Tech.* **18**(2):84–95.
- Soykeabkaew, N., Arimoto, N., Nishino, T. and Peijs, T. (2008). All-cellulose composites by surface selective dissolution of aligned ligno-cellulosic fibres. *Compos. Sci. Technol.* **68**:2201–2207.
- Strawhecker, K. E. and Manias, E. (2000). Structure and properties of poly(vinyl alcohol)/Na<sup>+</sup> montmorillonite nanocomposites. *Chem. Mater.* **12**:2943–2949.
- Suzuki, M. and Hattori, Y. (2004). WO Patent 2004009902.
- Takahashi, N., Okubo, K. and Fujii, T. (2005). Development of green composite using microfibrillated cellulose extracted from bamboo. *Bamboo J.* **22**:81–92.
- Tischer, P. C. S. F., Sierakowski, M. R., Westfahl, H. Jr. and Cesar Augusto Tischer, C. A. (2011). Nanostructural reorganization of bacterial cellulose by ultrasonic treatment. *Biomacromolecules* **11**:1217–1224.
- Turbak, A. F., Snyder, F. W. and Sandberg, K. R. (1983). *J. Appl. Polym. Sci. Appl. Polym. Symp.* **37**:815–827.
- Vartiainen, J., Motion, R., Kulonen, K., Ratto, M., Skytta, E. and Advenainen, R. (2004). Chitosan-coated paper: Effects of nisin and different acids on the antimicrobial activity. *J. Appl. Polym. Sci.* **94**:986–993.
- Villanueva, M. P., Cabedo, L., Feijoo, J. L., Lagaron, J. M. and Gimenez, E., (2006). Optimization of biodegradable nanocomposites based on a PLA/PCL blends for food packaging applications. *Macromolecular Sympos.* **233**:191–197.
- Wan, W. K., Hutter, J. L., Millon, L. E. and Guhados, G., (2006). Bacterial cellulose and its nanocomposites for biomedical applications. In: Cellulose nanocomposites. Processing Characterization, and Properties, pp. 221–241, Oksman, K. and Sain, M. Eds., American Chemical Society, Washington, DC.
- Weber, C. J., Haugaard, V., Festersen, R. and Bertelsen, G. (2002). Production and applications of biobased packaging materials for the food industry. *Food Addit. Contam.* **19**:172–177.
- Weng, Y. M., Chen, M. J. and Chen, W. (1999). Antimicrobial food packaging materials from poly(ethylene-co-methacrylic acid). *Food Sci. Technol.* **32**(4):191–195.
- Wilhoit, D. L. (1996). Film and method for surface treatment of foodstuffs with antimicrobial compositions. US Patent 557379.
- Wilhoit, D. L. (1997). Antimicrobial compositions, film and method for surface treatment of foodstuffs. EU Patent No. EP0 750 853 A2.
- Yamanaka, S., Ishihara, M. and Sugiyama, J. (2000). Structural modification of bacterial cellulose. *Cellulose* **7**:213–225.
- Zimmermann, T., Pohler, E. and Geiger, T. (2004). Cellulose fibrils for polymer reinforcement. *Adv. Eng. Mater.* **6**:754–761.



This article appeared in a journal published by Elsevier. The attached copy is furnished to the author for internal non-commercial research and education use, including for instruction at the authors institution and sharing with colleagues.

Other uses, including reproduction and distribution, or selling or licensing copies, or posting to personal, institutional or third party websites are prohibited.

In most cases authors are permitted to post their version of the article (e.g. in Word or Tex form) to their personal website or institutional repository. Authors requiring further information regarding Elsevier's archiving and manuscript policies are encouraged to visit:

<http://www.elsevier.com/copyright>



## Effect of gamma radiation on the mechanical and barrier properties of HEMA grafted chitosan-based films

Avik Khan, Tanzina Huq, Ruhul A. Khan, Dominic Dussault, Stephane Salmieri, Monique Lacroix\*

Research Laboratories in Sciences Applied to Food, Canadian Irradiation Center (CIC), INRS-Institut Armand-Frappier, Institute of Nutraceuticals and Functional Foods, University of Quebec, 531 Boulevard des Prairies, Laval, Quebec, Canada H7V 1B7

### ARTICLE INFO

#### Article history:

Received 10 June 2011

Accepted 24 November 2011

Available online 13 December 2011

#### Keywords:

Gamma irradiation

chitosan

HEMA

Monomer grafting

Biopolymer

### ABSTRACT

Chitosan films were prepared by dissolving 1% (w/v) chitosan powder in 2% (w/v) aqueous acetic acid solution. Chitosan films were prepared by solution casting. The values of puncture strength (PS), viscoelasticity coefficient and water vapor permeability (WVP) of the films were found to be 565 N/mm, 35%, and 3.30 g mm/m<sup>2</sup> day kPa, respectively. Chitosan solution was exposed to gamma irradiation (0.1–5 kGy) and it was revealed that PS values were reduced significantly ( $p \leq 0.05$ ) after 1 kGy dose and it was not possible to form films after 5 kGy. Monomer, 2-hydroxyethyl methacrylate (HEMA) solution (0.1–1%, w/v) was incorporated into the chitosan solution and the formulation was exposed to gamma irradiation (0.3 kGy). A 0.1% (w/v) HEMA concentration at 0.3 kGy dose was found optimal-based on PS values for chitosan grafting. Then radiation dose (0.1–5 kGy) was optimized for HEMA grafting. The highest PS values (672 N/mm) were found at 0.7 kGy. The WVP of the grafted films improved significantly ( $p \leq 0.05$ ) with the rise of radiation dose.

© 2011 Elsevier Ltd. All rights reserved.

### 1. Introduction

Bio-based packaging is defined as packaging containing raw materials originating from agricultural sources, such as chitosan, alginate, starch, cellulose, and bio-derived monomers. Bio-based packaging materials include both edible films and edible coatings along with primary and secondary packaging materials (Siro and Plackett, 2010; Salmieri and Lacroix, 2006). Chitosan is prepared from chitin, which is the second most abundant polysaccharide, found in nature after cellulose. Chitosan is a linear polysaccharide and is composed of glucosamine and *N*-acetyl glucosamine residues with a  $\beta$ -1, 4-linkage. Chitosan is non-toxic, biodegradable, bio-functional, biocompatible, and have strong antimicrobial and antifungal activities (Dutta et al., 2009; Aider, 2010). Chitosan-based films were compared with other biopolymer-based active films used as packaging materials and was reported that chitosan has advantages over other bio-polymers (Kim et al., 2011).

Chitosan films have been successfully used as a packaging material for the preservation of a variety of foods quality (Chen et al., 2009). However, natural polymers such as chitosan are usually hydrophilic in nature. So, modification of chitosan is required to improve its properties. Modifications on the chitosan

structure can be carried out in order to adequate it to various applications, such as, drug carrier by *N*-acylation (Le Tien et al., 2003); for biomedical applications by graft copolymerization (Prashanth and Tharanathan, 2007), etc. The general effect of radiation on chitosan has been evaluated by Chmielewski (2010). Among the various methods of modification used to improve chitosan properties, graft copolymerization is widely used (Sun et al., 2003). The modification of polymeric materials by graft copolymerization is reported elsewhere (Khan et al., 2010; Sashiwa and Aiba, 2004) because it can provide materials with desired properties through the appropriate choice of the side chain to be grafted (Casimiro et al., 2005). Chitosan bears, two types of reactive groups, that can be modified by grafting: the C-2 free amino groups on deacetylated units and the hydroxyl groups in the C-3 and C-6 either in acetylated or deacetylated units (Berger et al., 2004). The monomer, 2-hydroxyethyl methacrylate (HEMA) is a synthetic and water soluble vinyl monomer. Singh and Ray (1994) were the first to prepare HEMA grafted chitosan films. It is reported (Sultana et al., 2010) that HEMA can cross-link with gelatin by gamma radiation and the grafted films possessed high mechanical strength. The advantage of using gamma radiation is that it does not require the addition of chemical initiators or lethal agents to promote the polymerization reaction and, at the same time, promotes the inactivation of pathogenic micro-organisms (Casimiro and Gil, 2010). The main objective of this study was to find out the suitability of gamma radiation for the preparation of HEMA grafted chitosan films for food packaging applications.

\* Corresponding author. Tel.: +1 450 687 5010; fax: +1 450 686 5501.  
E-mail address: monique.lacroix@iaf.inrs.ca (M. Lacroix).

## 2. Materials and methods

### 2.1. Materials

Chitosan (molecular wt. 700 kDa; degree of deacetylation 88–89%) was obtained from Kitomer Marinard (Quebec, Canada). Monomer, 2-hydroxyethyl methacrylate (HEMA) was purchased from Sigma-Aldrich Canada Ltd.

### 2.2. Film preparation

1% (w/v) chitosan was dissolved in 2% aqueous acetic acid solution. The chitosan solution was then  $\gamma$ -irradiated from 0.1 to 5 kGy. Then the irradiated solution was casted onto Petri dishes and was allowed to dry at room temperature (RH was 40–50%). The HEMA grafted chitosan films were prepared by slowly incorporating HEMA (0.1–1%, w/v) into the chitosan solution under constant stirring. The solution was stirred for 1 h and then subjected to gamma irradiation at different doses under air. After irradiation treatment, the solution was again stirred for 1 h and the films were prepared by casting.

### 2.3. Irradiation

Irradiation of both chitosan and chitosan/HEMA solution was conducted with  $\gamma$ -rays generated from a  $^{60}\text{Co}$  source at room temperature, at a dose rate of 17.878 kGy/h in an Underwater Calibrator-15A Research Irradiator (Nordion Inc., Kanata, ON, Canada). The solutions were irradiated from 0.1 kGy to 25 kGy.

### 2.4. Film thickness

Film thickness was measured using a Mitutoyo Digimatic Indicator (Type ID-110E; Mitutoyo Manufacturing Co. Ltd., Tokyo, Japan) with a resolution of 0.001 mm, at five random positions around the film, by slowly reducing the micrometer gap until the first indication of contact.

### 2.5. Puncture strength (PS)

PS was measured by the Stevens-LFRA texture analyzer (model TA-1000; Texture Technologies Corp., Scarsdale, NY). Films were fixed between two perforated Plexiglas plates (3.2 cm diameter), and the holder was held tightly with two screws. A cylindrical probe (2 mm diameter; scale, 0–900 g; sensitivity, 2 V) was moved perpendicularly to the film surface at a constant speed (1 mm/s) until it passed through the film. Strength values at the puncture point are used to calculate the hardness of the film. The PS values were divided by the thickness of the films to avoid any variation related to this parameter. PS is calculated using the equation  $\text{PS (N/mm)} = (9.81 F)/x$ , where  $F$  is the recorded force value,  $x$  is the film thickness, and 9.81 is the gravitational acceleration.

### 2.6. Viscoelasticity coefficient ( $Y$ )

Viscoelastic properties were evaluated using relaxation curves. The same puncture test procedure described above was used, but the probe is stopped to 3 mm after film contact and maintained for 1 min. The relaxation coefficient  $Y$  is calculated using the equation:

$$Y(\%) = [(F_i - F_f)/F_i] \times 100$$

where,  $F_i$  is the initial recorded value (g) and  $F_f$  the second value measured after 1 min of relaxation. A low relaxation coefficient ( $Y \rightarrow 0\%$ ) indicates high film elasticity, whereas a high coefficient

( $Y \rightarrow 100\%$ ) indicates high film plasticity related to a more rigid and easily distorted material.

### 2.7. Water vapor permeability (WVP)

WVP tests were conducted gravimetrically using an ASTM 15.09: E96 procedure (ASTM, 1983). Films were mechanically sealed onto Vapometer cells (No. 68-1, Twining-Albert Instrument Co., West Berlin, NJ) containing 30 g of anhydrous calcium chloride (0% RH). The cells were initially weighed and placed in a Shellab 9010L controlled humidity chamber (Sheldon Manufacturing Inc., Cornelius, OR) maintained at 25 °C and 64% RH for 24 h. The amount of water vapor transferred through the film and absorbed by the desiccant is determined from the weight gain of the cell. The assemblies were weighed initially and after 24 h for all samples and up to a maximum of 10% gain. WVP is calculated according to the combined Fick and Henry laws for gas diffusion through coatings and films.

### 2.8. Statistical analysis

To validate the results obtained during different experimental procedure each analysis was carried out in triplicate. An analysis of variance (ANOVA) and multiple comparison tests of Duncan's were used to compare all the results. Differences between means were considered significant when the confidence interval is smaller than 5% ( $p \leq 0.05$ ). The results were analyzed by the PASW Statistics 18 software (IBM Corporation, Somers, NY, USA).

## 3. Results and discussion

### 3.1. Effect of gamma irradiation and HEMA treatment on puncture strength

The puncture strength (PS) of control chitosan films was found to be 565 N/mm. Fig. 1 depicts the effect of gamma radiation on the PS of chitosan and HEMA grafted chitosan films. It was found that PS of irradiated chitosan films increased at low radiation doses ( $\leq 0.3$  kGy). The PS values of the irradiated (0.3 kGy) chitosan films reached to 597 N/mm, which is 5.7% higher than control samples. The increase of PS of the films at low radiation doses may be due to the formation of dimmer (formation of chitosan oligomers) with acetic acid (Park et al., 2002). At doses  $> 0.3$  kGy, a decrease in PS was observed. At 5 kGy, the PS of the films decreased by 47% as compared to the control, which may be due to the radiation degradation of chitosan. It was not possible to prepare chitosan films from solutions

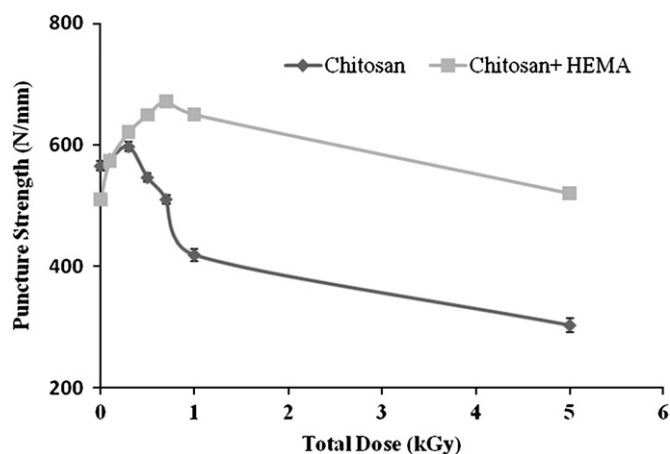


Fig. 1. Effect of gamma radiation on the puncture strength of films.

irradiated at doses higher than 5 kGy. HEMA solution (0.1–1% w/v) was incorporated into the chitosan solution then exposed to gamma radiation. It was found that films containing 0.1% (w/v) HEMA exhibited the highest PS (621 N/mm) at doses 0.3 kGy. So, the optimized HEMA concentration (0.1%, w/v) was exposed to gamma radiation at doses from 0.1 to 5 kGy. The PS of the films increased with the increase of radiation dose up to 0.7 kGy. At 0.7 kGy, HEMA grafted chitosan films exhibited a PS of 672 N/mm, which is 20% higher than that of the control chitosan films. The increase in PS may be attributed to the reaction of acrylic groups of HEMA with amino group of chitosan. However, the PS of the films sharply decreased at doses >0.7 kGy. The decrease of the mechanical strength could be due to the formation of poly(HEMA) by homo polymerization and also due to the degradation of chitosan. The glycosidic linkage of the natural polymer may generally break under gamma irradiation. At higher doses, the polymer may undergo scission and may be broken into smaller fragments. As a result, the mechanical strength of the polymer decreases (Vanichvattanadecha et al., 2010; Huang et al., 2007).

### 3.2. Effect of gamma irradiation on the viscoelasticity ( $Y$ ) coefficient

Fig. 2 shows the effect of gamma irradiation on the viscoelasticity coefficient ( $Y$ ) of the chitosan and HEMA grafted chitosan films. It was found that  $Y$  coefficient values of the chitosan films decreased significantly ( $p \leq 0.05$ ) at doses 0.3–5 kGy. However, the  $Y$  coefficient values of the HEMA grafted chitosan films increased significantly ( $p \leq 0.05$ ) with the increase of radiation dose up to 0.5 kGy. The  $Y$  coefficient values of the HEMA treated but non-irradiated (0 kGy) chitosan films were found to be 43%. When treated at 0.5 kGy,  $Y$  coefficient value was found to be 63% ( $p \leq 0.05$ ). At 0.5 kGy, the  $Y$  coefficient reached to a plateau. So, it was evident that HEMA grafted chitosan films showed better elastic property than the control chitosan films.

### 3.3. Effect of gamma radiation on the WVP

Fig. 3 represented the effects gamma radiation on the WVP of control and HEMA treated chitosan films. The WVP of the chitosan films was found to be 3.30 g mm/m<sup>2</sup> day kPa. At 0.1 kGy, the WVP of the chitosan films decreased sharply and showed a value of 3.07 g mm/m<sup>2</sup> day kPa, which is almost 7% lower than that of the chitosan films. However, at radiation doses (> 0.1 kGy), the WVP of the films increased and at 5 kGy the WVP value was 3.41 g mm/m<sup>2</sup> day kPa. So, a very low radiation dose (0.1 kGy) contributed the chitosan films more water vapor resistant. The WVP of the HEMA treated chitosan films decreased with the increase of radiation doses.

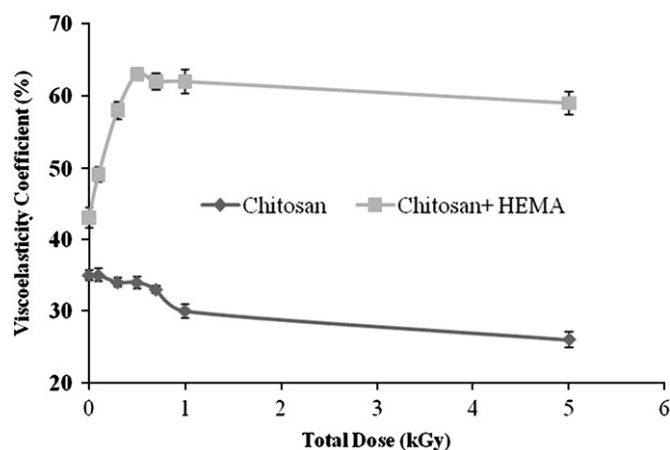


Fig. 2. Effect of gamma radiation on the viscoelasticity coefficient (%) of films.

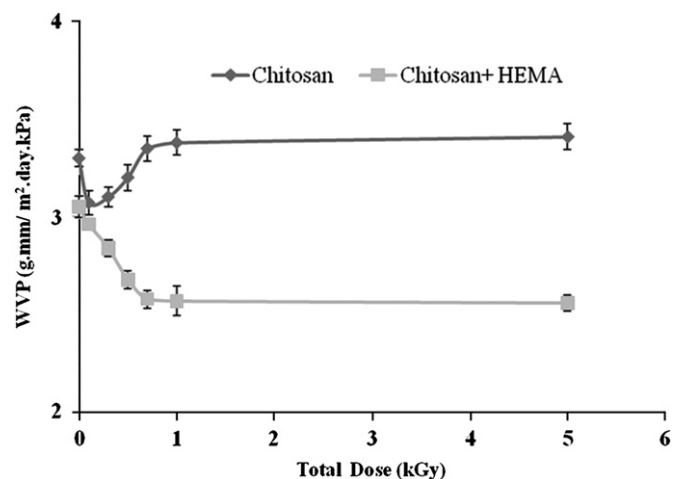


Fig. 3. Effect of gamma radiation on the WVP of films.

At 0.7 kGy the WVP of the HEMA treated chitosan films was found to be 2.58 g mm/m<sup>2</sup> day kPa. Therefore, a 22% reduction of WVP was obtained by treating chitosan with HEMA followed by the exposure of 0.7 kGy dose.

## 4. Conclusion

From this study it was found that low radiation doses (0.1–0.3 kGy) on chitosan solution improved the mechanical strength of the films. The HEMA grafted chitosan films possessed better mechanical and barrier properties compared to the control chitosan samples. So, gamma radiation can be considered as a safe and good source for the preparation of monomer grafted films.

## Acknowledgment

Authors are grateful to the Natural Sciences and Engineering Research Council of Canada (NSERC) and BSA Food Ingredients s.e.c./l.p. (Montreal, Qc, Canada). The authors would also like to thank Nordion Inc. for irradiation procedures.

## References

- Aider, M., 2010. Chitosan application for active bio-based films production and potential in the food industry: review. *LWT—Food Sci. Technol.* 43, 837–842.
- ASTM, 1983. Standard test method for water vapor transmission of materials. American Society for Testing and Materials, Philadelphia, PA Method 15.09:E96.
- Berger, J., Reist, M., Mayer, J.M., Felt, O., Gurny, R., 2004. Structure and interactions in chitosan hydrogels formed by complexation or aggregation for biomedical applications. *Eur. J. Pharm. Biopharm.* 57, 35–52.
- Casimiro, M.H., Gil, M.H., 2010. Suitability of gamma irradiated chitosan based membranes as matrix in drug release system. *Int. J. Pharm.* 395, 142–146.
- Casimiro, M.H., Botelho, M.L., Leal, J.P., Gil, M.H., 2005. Study on chemical, UV and gamma radiation-induced grafting of 2-hydroxyethyl methacrylate onto chitosan. *Radiat. Phys. Chem.* 72, 731–735.
- Chen, F., Shi, Z., Neoh, K.G., Kang, E.T., 2009. Antioxidant and antibacterial activities of eugenol and carvacrol-grafted chitosan nanoparticles. *Biotechnol. Bioeng.* 104, 30–39.
- Chmielewski, A.G., 2010. Chitosan and radiation chemistry. *Radiat. Phys. Chem.* 79 (3), 272–275.
- Dutta, P.K., Tripathi, S., Mehrotra, G.K., Dutta, J., 2009. Perspectives for chitosan based antimicrobial films in food applications. *Food Chem.* 114 (4), 1173–1182.
- Huang, L., Zhai, M., Peng, J., Li, J., Wei, G., 2007. Radiation-induced degradation of carboxymethylated chitosan in aqueous solution. *Carbohydr. Polym.* 67, 305–312.
- Khan, A., Huq, T., Saha, M., Khan, R.A., Khan, M.A., 2010. Surface modification of calcium alginate fibers with silane and methyl methacrylate monomers. *J. Reinf. Plast. Compos.* 29 (20), 3125–3132.

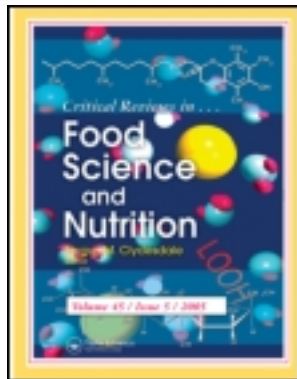
- Kim, K.W., Min, B.J., Kim, Y.T., Kimmel, R.M., Cooksey, K., Park, S.I., 2011. Antimicrobial activity against foodborne pathogens of chitosan biopolymer films of different molecular weights. *LWT—Food Sci. Technol.* 44, 565–569.
- Le Tien, C., Lacroix, M., Ispas-Szaboa, P., Mateescu, M.A., 2003. N-acylated chitosan: hydrophobic matrices for controlled drug release. *J. Control Release* 93, 1–13.
- Park, S.Y., Marsh, K.S., Rhim, J.W., 2002. Characteristics of different molecular weight chitosan films affected by the type of organic solvents. *J. Food Sci.* 67 (1), 194–197.
- Prashanth, K.V.H., Tharanathan, R.N., 2007. Chitin/chitosan: modifications and their unlimited application potential and overview. *Trends Food Sci. Technol.* 18, 117–131.
- Salmieri, S., Lacroix, M., 2006. Physicochemical properties of alginate/polycaprolactone based films with essential oils. *J. Agric. Food Chem.* 54, 10205–10214.
- Sashiwa, H., Aiba, S.I., 2004. Chemically modified chitin and chitosan as biomaterials. *Prog. Polym. Sci.* 29, 887–908.
- Singh, D.K., Ray, A.R., 1994. Graft copolymerization of 2-hydroxyethylmethacrylate onto chitosan films and their blood compatibility. *J. Appl. Polym. Sci.* 53 (8), 1115–1121.
- Siro, I., Plackett, D., 2010. Microfibrillated cellulose and new nanocomposite materials: a review. *Cellulose* 17, 459–494.
- Sultana, S., Khan, R.A., Shahruzzaman, M., Khan, M.A., Mustafa, A.I., Gafur, M.A., 2010. Effect of gamma radiation on the physico and thermo-mechanical properties of gelatin-based films using 2-hydroxyethyl methacrylate (HEMA). *Polym. Plast. Technol.* 49 (7), 662–671.
- Sun, T., Xu, P., Qing Liu, Q., Xue, J., Xie, W., 2003. Graft copolymerization of methacrylic acid onto carboxymethyl chitosan. *Eur. Polym. J.* 39, 189–192.
- Vanichvattanadecha, C., Supaphol, P., Nagasawa, N., Tamada, M., Tokura, S., Furuike, T., Tamura, H., Rujiravanit, R., 2010. Effect of gamma radiation on dilute aqueous solutions and thin films of N-succinyl chitosan. *Polym. Degrad. Stabil.* 95, 234–244.

This article was downloaded by: [Avik Khan]

On: 15 June 2013, At: 07:23

Publisher: Taylor & Francis

Informa Ltd Registered in England and Wales Registered Number: 1072954 Registered office: Mortimer House, 37-41 Mortimer Street, London W1T 3JH, UK



## Critical Reviews in Food Science and Nutrition

Publication details, including instructions for authors and subscription information:

<http://www.tandfonline.com/loi/bfsn20>

### Encapsulation of Probiotic Bacteria in Biopolymeric System

Tanzina Huq<sup>a</sup>, Avik Khan<sup>a</sup>, Ruhul A. Khan<sup>a</sup>, Bernard Riedl<sup>b</sup> & Monique Lacroix<sup>a</sup>

<sup>a</sup> Research Laboratories in Sciences Applied to Food, Canadian Irradiation Center (CIC), INRS-Institute Armand-Frappier, University of Quebec, 531 Boulevard des Prairies, Laval, Quebec, H7V 1B7, Canada

<sup>b</sup> Centre de recherche sur le bois, Faculté de foresterie, de géomatique et de géographie Université Laval, Québec, G1V0A6, Canada

Accepted author version posted online: 24 Feb 2012. Published online: 14 Jun 2013.

To cite this article: Tanzina Huq, Avik Khan, Ruhul A. Khan, Bernard Riedl & Monique Lacroix (2013): Encapsulation of Probiotic Bacteria in Biopolymeric System, Critical Reviews in Food Science and Nutrition, 53:9, 909-916

To link to this article: <http://dx.doi.org/10.1080/10408398.2011.573152>

PLEASE SCROLL DOWN FOR ARTICLE

Full terms and conditions of use: <http://www.tandfonline.com/page/terms-and-conditions>

This article may be used for research, teaching, and private study purposes. Any substantial or systematic reproduction, redistribution, reselling, loan, sub-licensing, systematic supply, or distribution in any form to anyone is expressly forbidden.

The publisher does not give any warranty express or implied or make any representation that the contents will be complete or accurate or up to date. The accuracy of any instructions, formulae, and drug doses should be independently verified with primary sources. The publisher shall not be liable for any loss, actions, claims, proceedings, demand, or costs or damages whatsoever or howsoever caused arising directly or indirectly in connection with or arising out of the use of this material.

# Encapsulation of Probiotic Bacteria in Biopolymeric System

TANZINA HUQ,<sup>1</sup> AVIK KHAN,<sup>1</sup> RUHUL A. KHAN,<sup>1</sup> BERNARD RIEDL,<sup>2</sup>  
and MONIQUE LACROIX<sup>1</sup>

<sup>1</sup>Research Laboratories in Sciences Applied to Food, Canadian Irradiation Center (CIC), INRS-Institute Armand-Frappier, University of Quebec, 531 Boulevard des Prairies, Laval, Quebec, H7V 1B7, Canada

<sup>2</sup>Centre de recherche sur le bois, Faculté de foresterie, de géomatique et de géographie Université Laval, Québec, G1V0A6, Canada

*Encapsulation of probiotic bacteria is generally used to enhance the viability during processing, and also for the target delivery in gastrointestinal tract. Probiotics are used with the fermented dairy products, pharmaceutical products, and health supplements. They play a great role in maintaining human health. The survival of these bacteria in the human gastrointestinal system is questionable. In order to protect the viability of the probiotic bacteria, several types of biopolymers such as alginate, chitosan, gelatin, whey protein isolate, cellulose derivatives are used for encapsulation and several methods of encapsulation such as spray drying, extrusion, emulsion have been reported. This review focuses on the method of encapsulation and the use of different biopolymeric system for encapsulation of probiotics.*

**Keywords** Probiotics, biopolymers, prebiotics, encapsulation, SGF, SIF

## INTRODUCTION

Probiotics are live microorganisms that transit the gastrointestinal tract and, in doing so, benefit the health of the consumer. They are recognized as very potential bacteria and are also thought that they remove the harmful bacteria from the intestine. Therapeutic benefits have led to an increase in the incorporation of probiotic bacteria such as lactobacilli and bifidobacteria in dairy products, especially yogurts. The efficiency of added probiotic bacteria depends on dose level, and their viability must be maintained throughout storage, products' shelf-life, and they must survive in adverse environment. Hence, viability of probiotic bacteria is of paramount importance in the marketability of probiotic-based food products (Adhikari et al., 2000; Ariful et al., 2010).

Encapsulation of bacterial cells is currently gaining attention to increase viability of probiotic bacteria in acidic products such as yogurt. Encapsulation is a process by which one material or mixture of materials is coated with, or entrapped within, another material or system. The material that is coated or entrapped is

referred to by various names such as core material, payload, actives, fill or internal phase. The material that forms the coating is referred to as the wall material, carrier, membrane, shell or coating. Coating protects the active content from environmental stresses such as acidity, oxygen, and gastric conditions and can be used, for example, to help the content pass through the stomach (Hassan et al., 1996; Dave and Shah, 1997; Godward and Kailasapathy, 2003). Encapsulation segregates the cells from adverse environment, thus potentially reducing cell injury. Encapsulation has been used as a technology that can provide protection against the sensitive probiotic cultures, improving their stability and viability in food products and performing the target delivery in gastrointestinal tract. There is a need for encapsulation of probiotic bacteria to survive human gastric juice in the stomach, where the pH can be as low as 2. The viability of *Bifidobacterium pseudolongum* and *B. longum* in simulated gastric fluid (SGF) environment was improved by encapsulation technology. Encapsulated bacteria showed a higher protection from freezing and freeze drying. A higher stability also showed for Lactic acid bacteria (LAB) during storage of dairy products by using encapsulation (Rao et al., 1989; Lee and Heo, 2000; Shah and Ravula, 2000).

For example, it was reported that encapsulation using calcium-induced alginate–starch polymers, in potassium induced *k*-carrageenan polymers and in whey protein polymers

Address correspondence to Monique Lacroix, Research Laboratories in Sciences Applied to Food, Canadian Irradiation Center (CIC), INRS-Institute Armand-Frappier, University of Quebec, 531 Boulevard des Prairies, Laval, Quebec, H7V 1B7, Canada. E-mail: monique.lacroix@iaf.inrs.ca

have increased the survival and viability of probiotic bacteria in yogurt during storage. The encapsulant materials such as alginate, chitosan, starch, carrageenan, and whey protein are commonly used as food stabilizers in the manufacture of stirred yogurts to prevent syneresis. Alginate is a natural polysaccharide extracted from brown sea weeds and it enhances viscosity and binds water, hence reduces syneresis in stirred yogurts. Divalent cations, such as calcium, bind preferentially to the alginate polymer and, hence, increase viscosity or form gels depending on the concentration. Hi-maize resistant starch has improved thickening and gelling properties and bind water and thicken when added to yogurt hence prevent syneresis and improve textural properties (Siitonen et al., 1990; Sultana et al., 2000).

The aim of this review is to discuss the suitable method of encapsulation for probiotics and also about the encapsulation of probiotic bacteria in biopolymeric system in order to improve the viability and quality of food products during storage and in gastrointestinal tracts.

## PROBIOTIC BACTERIAS

People use LAB for more than 4000 years for foods' fermentation. Today, probiotics are also used in a variety of fermented dairy products and their manufacture involves fermentation: microbial process by which lactose is converted into lactic acid. Food and Agriculture Organization (FAO) of the United Nations and the World Health Organization (WHO) define probiotics as "Live microorganisms (bacteria or yeasts), which when ingested or locally applied in sufficient numbers confer one or more specified demonstrated health benefits for the host" (FAO/WHO, 2001). LABs are the most important probiotic microorganisms typically associated with the human gastrointestinal tract. These bacteria are gram-positive, rod-shaped, non-spore-forming, catalase-negative organisms that are devoid of cytochromes and are of non-aerobic habit but are aero-tolerant, fastidious, acid-tolerant, and strictly fermentative; lactic acid is the major end-product of sugar fermentation. A few of the known LABs that are used as probiotic are *Lactobacillus acidophilus*, *Lactobacillus amylovorus*, *Lactobacillus casei*, *Lactobacillus crispatus*, *Lactobacillus delbrueckii*, *Lactobacillus gasseri*, *Lactobacillus johnsonii*, *Lactobacillus paracasei*, *Lactobacillus plantarum*, *Lactobacillus reuteri*, *Lactobacillus rhamnosus*, etc. (Anal and Singh, 2007). Lactobacilli, as a part of the commensal microbial flora of humans and mammals and main representatives of the probiotic bacteria, might be useful candidates in prevention and treatment of infections caused by multiresistant bacteria due to their ability to modulate the immune responses of the host and to protect the host from pathogens by competitive exclusion (Brachkova et al., 2010; Mohammadi et al., 2011). Other common probiotic microorganisms are the bifidobacteria. Bifidobacteria are also gram-positive and rod-shaped but are strictly anaerobic. These bacteria can grow at pH in the range 4.5–8.5. Bifidobacteria actively ferment carbohydrates, producing mainly acetic acid and lactic acid in a molar ratio

of 3:2 (v/v), but not carbon dioxide, butyric acid or propionic acid. The most recognized species of bifidobacteria that are used as probiotic organisms are *Bifidobacterium adolescentis*, *Bifidobacterium animalis*, *Bifidobacterium bifidum*, *Bifidobacterium breve*, *Bifidobacterium infantis*, *Bifidobacterium lactis* and *Bifidobacterium longum*. Other than these bacteria, *Bacillus cereus* var. *toyoi*, *Escherichia coli* strain nissle, *Propionibacterium freudenreichii*, and some types of yeasts, e.g., *Saccharomyces cerevisiae* and *Saccharomyces boulardii* have also been identified as having probiotic effects (Holzapfel et al., 2001).

## IMPORTANCE OF PROBIOTICS

### Intestinal Tract Health

A number of studies have found probiotic consumption to be useful in the treatment of many types of diarrhoea, including antibiotic-associated diarrhoea in adults, travellers' diarrhoea, and diarrhoeal diseases in young children caused by rotaviruses. The most commonly studied probiotic species in these studies have been *Lactobacillus GG*, *L. casei*, *B. bifidum*, and *S. thermophilus*. Because diarrhoea is a major cause of infant death worldwide and can be incapacitating in adults, the widespread use of probiotics could be an important, non-invasive means to prevent and treat these diseases, particularly in developing countries. Probiotic bacteria have also been shown to preserve intestinal integrity and mediate the effects of inflammatory bowel diseases, irritable bowel syndrome, colitis, and alcoholic liver disease. In addition, LAB may improve intestinal mobility and relieve constipation (Isolauri et al., 1991; Nanji et al., 1994; Pitino et al., 2010).

### Nutrient Synthesis and Bioavailability

Fermentation of food with LAB has been shown to increase folic acid content of yogurt, bifidus milk, and kefir, and to increase niacin and riboflavin levels in yogurt, vitamin B<sub>12</sub> in cottage cheese, and vitamin B<sub>6</sub> in Cheddar cheese. In addition to nutrient synthesis, probiotics may improve the digestibility of some dietary nutrients such as protein and fat. Short-chain fatty acids such as lactic acid, propionic acid, and butyric acid produced by lactic acid bacteria may help maintain an appropriate pH and protect against pathological changes in the colonic mucosa (Kruis et al., 1997; Chen and Subirade, 2009).

### Probiotic Antimicrobial Activity

The importance of probiotics in human nutrition has been gaining recognition in recent years. This study proposed an improved in vitro model for the study of probiotic antimicrobial activity against enteropathogens, by attempting to re-create, in a common culture medium, environmental growth conditions comparable to those present in the small intestine. A preliminary

experiment was carried out in order to find a culture medium able to support both probiotics and pathogens. This was done with the aim of obtaining correct assessment of the interaction under shared growth conditions. Brain Heart Infusion (BHI) medium was selected as the common culture medium and was therefore used in antimicrobial activity assays. The interactions between *Salmonella* 1344 and *Lactobacillus rhamnosus* and *Lactobacillus reuteri* were then assessed at different pH and oxygen availability conditions mimicking the small intestinal environment. *L. rhamnosus* GG ATCC 53103 had the strongest antimicrobial effect, in particular under anaerobic conditions and at lower pH levels. Its antagonistic activity involved both lactic acid and secreted non-lactic acid molecules (Marianelli et al., 2010).

### **Probiotics for Cancer Prevention**

Studies of the effect of probiotic consumption on cancer appear promising. Colorectal cancer (CRC) is the biggest cause of death from cancer in the Western world. Approximately 70% of CRC is associated with environmental factors, probably mainly the diet. The fermented milk containing probiotic cultures can play a protective role against CRC. Interventional studies have shown a shift of intermediate markers of CRC risk in human subjects from a high to low risk pattern after ingestion of fermented milk or probiotics. Animal studies consistently show a reduction in chemically induced colorectal tumor incidence and aberrant crypt formation accompanying probiotic administration. In vitro studies also provide evidence of protection, and permit a better understanding of active compounds involved, and of the mechanisms underlying their anticarcinogenic effects. Probiotics may beneficially modulate several major intestinal functions: detoxification, colonic fermentation, transit, and immune status, which may accompany the development of colon cancer (Saikali et al., 2004). LAB or a soluble compound produced by the bacteria may interact directly with tumour cells in culture and inhibit their growth. LAB significantly reduced the growth and viability of the human colon cancer cell line HT-29 in culture, and dipeptidyl peptidase IV and brush border enzymes were significantly increased, suggesting that these cells may have entered a differentiation process (Baricault et al., 1995; Hirayama and Rafter, 2000).

## **ENCAPSULATION TECHNOLOGY**

Encapsulation can be used for many applications in food industry, including stabilizing the core material, controlling the oxidative reaction, providing sustained or controlled release (both temporal and time-controlled release), masking flavors, colors or odors, extending the shelf-life and protecting components against nutritional loss. A microcapsule consists of a semi-permeable, spherical, thin, and strong membrane surrounding a solid or liquid core, with a diameter varying from a few microns to 1 mm. For enhancing the viability of bacteria, encapsula-

tion facilitates handling of cells and allows a controlled dosage. Food-grade polymers such as alginate, chitosan, carboxymethyl cellulose (CMC), carrageenan, gelatin, and pectin are mainly applied, using various encapsulation technologies (Anal and Singh, 2007).

### **Extrusion Method**

Extrusion method is a simple and cheap method with gentle operations which makes cell injuries minimal and causes relatively high viability of probiotic cells. Biocompatibility and flexibility are some of the other specifications of this method. A hydrocolloid solution is first prepared, probiotics are added, and the solution is dripped through a syringe needle or nozzle. The droplets are allowed to fall into a hardening solution. In this technique, alginate, *k*-carrageenan, *k*-carrageenan plus locust bean gum, xanthan plus gellan, alginate plus corn starch and whey proteins have been used as wall materials for encapsulation of lactobacilli and bifidobacteria. The size of the microcapsules is affected by the nozzle size. The diameter of the obtained alginate beads is also increased as the concentration of sodium alginate increases, but the alginate concentration does not significantly influence the numbers of free cells. A mixture of gellan and xanthan has better technological properties than alginate, *k*-carrageenan, or locust bean gums, but the shape and size of the gellan and xanthan gum capsules have been found to be varying (Rokka and Rantamaki, 2010).

### **Emulsion Method**

Emulsion technique has been successfully applied for the microencapsulation of LAB. In contrary with the extrusion technique, it can be easily scaled up and the diameter of produced beads is considerably smaller (25  $\mu\text{m}$ –2 mm). However, this method requires more cost for performance compared with the extrusion method due to need of using vegetable oil for emulsion formation. In this technique, a small volume of cell/polymer slurry (as a dispersed phase) is added to the large volume of vegetable oil (as a continuous phase) such as soy-, sun flower-, corn-, millet or light paraffin oil. Resulting solution becomes well homogeneous by proper stirring/agitating, till water-in-oil emulsion forms. Emulsifiers can be used for better emulsion formation. Tween 80 at the concentration of 0.2% has been recommended as the best choice. Once W/O emulsion forms, the water soluble polymer becomes insoluble after addition of calcium chloride, by means of cross linking and thus makes gel particles in the oil phase. Smaller particles of the water phase in W/O emulsion will lead to the formation of beads with smaller diameters. Agitation rate of the mixture and type of emulsifier used are also determinable factors from the beads diameter point of view. Using emulsifiers causes formation of beads with smaller diameters, because these components decrease interfacial tension of the water and oil phases. It has been claimed that by applying emulsifiers of tween 80 and lauryl sulphate together,

beads with a range of 25–35  $\mu\text{m}$  in diameter can be produced. In the emulsion technique relevant to alginate, a fat soluble acid such as acetic acid is usually added to the encapsulation mixture. Thereby, pH of alginate solution is reduced to approximately 6.5, at which gelation process of alginate with calcium ions starts. After gel formation, the encapsulated mixture is poured into water to separate the oil phase by decantation. It has been reported that concentration and viscosity of the encapsulation mix before gelation and its agitation rate are the main parameters that control the diameter of the final formed microbeads. It should be reminded that the beads diameter, apart from having a crucial effect on the viability of probiotic cells, their metabolic rate and sensory properties of the final product, also affects distribution and dispersion quality of the microbeads within the product (Krasaekoopt et al., 2003; Picot and Lacroix, 2003).

### **Drying Method**

Drying of the encapsulated mixture in order to produce cell powders/granules can be achieved by different methods. The most important of these methods are freeze drying, spray drying, and fluidized bed drying. Typical survival rates in the spray-drying and freeze drying processes are in the range of 70–85%. Although a survival rate may be acceptable, the prolonged storage stability of the product is often low. The presence of deoxidant and desiccant has been found to improve cell survival. In general, the drying process causes some injuries to the microbeads, release of some cells and reducing viability of the cells. In the freeze drying technique, heat injuries to the cells are minimal compared with other techniques. Also, cryo protectants must be used to inhibit cold injuries to the cells. Spray drying has been recommended for this reason because it is a relatively cheap method and large volumes of solutions can be processed by this technique. However, viability loss of the cells is high due to presence of both dehydration and heating factors, simultaneously. It seems that achieving the best method can be possible by modified techniques of spray drying. This procedure was economic with high ability of maintaining probiotic cells viability. The method consists of coating milk fat droplets containing powder particles of freeze dried cells with polymers of whey proteins, in a condition where emulsifier is used. The size of the starter culture powder particles had a determinable impact on their homogeneous distribution within the oil phase (hydrophobic phase). This size should be bigger than bacterial cells (2–4  $\mu\text{m}$ ) and smaller than selected fat droplets (10–50  $\mu\text{m}$ ) for achieving appropriate encapsulation. Mentioned size regulations were carried out by the micronization process. It was reported that optimum diameter of fat droplets for the mentioned process was 10–50  $\mu\text{m}$ . Micronization can be done by the size reduction system such as the impact mill, jet mill, mill with agate motor, and ball mill systems. Jet mills form the best systems on both the laboratory and industrial scales. This mill has been used to produce various types of wheat flour, protein powders, and pharmaceutical powders (Dimantov et al., 2003; Picot and Lacroix, 2003).

It was evaluated that the effect of process factors including grind air pressure and feeding rate on the diameter of powder particles and cells viability along with the effect of reducing powder particles size (micronization) on the heat resistance of bacterial cells during the spray-drying process was studied. Micronization was found necessary to reach the homogeneous emulsion system; however, excessive reduction of particles size led to mechanical damage of the cells and considerably decreased their heat resistance during the spray-drying process, especially when high temperatures were used. Therefore, micronization should be carried out with special care and in a particular limit (particularly at high temperatures of spray drying) to avoid mentioned damages. In the research, it was found that dispersing of *Bifidobacterium* spp. fresh cells (unfrozen dried cells) in a suspension of heat-treated whey protein base containing milk fat droplets followed by spray drying of the mixture is a suitable method on the industrial scale with respect to cells viability and economics (Picot and Lacroix, 2004).

## **ENCAPSULATION OF PROBIOTIC BACTERIA IN DIFFERENT BIO-POLYMERIC SYSTEM**

### **Encapsulation of Probiotics in Alginate Systems**

The conventional encapsulation method, with sodium alginate in calcium chloride ( $\text{CaCl}_2$ ), has been used to encapsulate *L. acidophilus* to protect this organism from the harsh acidic conditions in gastric fluid. Studies have shown that calcium-alginate immobilized cell cultures are better protected, shown by an increase in the survival of bacteria under different conditions, than the non-encapsulated state. The results from these studies indicate that the viability of encapsulated bacteria in SGF increases with an increase in capsule size (Anal and Singh, 2007). However, it was reported that very large calcium alginate beads (>1 mm) cause a coarseness of texture in live microbial feed supplements and that small beads of size less than 100  $\mu\text{m}$  do not significantly protect the bacteria in SGF, compared with free cells. These studies indicate that these bacteria should be encapsulated within a particular size range. They tested nine different strains of *Bifidobacterium* spp. for their tolerance to simulated gastrointestinal conditions, and observed some variations among the strains for resistance to gastric fluid (pH 2–3) and bile salts (5 and 10 g/L). Among these strains, only a strain *B. lactis* Bb-12 was found to be resistant to low pH and bile salts. They also encapsulated some of the strains in alginate microspheres to evaluate their resistance properties in gastric fluid and to bile salts. They obtained alginate microspheres (20–70  $\mu\text{m}$ ) by emulsifying the mixture of cells and sodium alginate in vegetable oil and subsequently cross-linking with  $\text{CaCl}_2$ . Cryo-scanning electron microscopy revealed that these microparticles were densely loaded with probiotic bacteria and were porous. The loaded alginate microparticles remained stable during storage at 4°C in 0.05 M  $\text{CaCl}_2$  and in milk (2% fat), sour cream, and yogurt for up to 16 days, and in SGF (pH 2.0)

for 1 h at 37°C. However, the microparticles exposed to low pH did not improve the survival of acid sensitive bifidobacteria. They also showed that *B. bifidum* survived in higher numbers in frozen milk in beads made from alginate than in beads made from *k*-carrageenan (Hansen et al., 2002; Kebary, 1996).

### **Encapsulation of Probiotics in Proteins and Polysaccharide Mixtures**

Gelatin is useful as a thermally reversible gelling agent for encapsulation. Due to its amphoteric nature, it is also an excellent candidate for incorporating with anionic gelforming polysaccharides, such as gellan gum. These hydrocolloids are miscible at pH >6, because they both carry net negative charges and repel one another. However, the net charge of gelatin becomes positive when the pH is adjusted below its isoelectric point and causes a strong interaction with the negatively charged gellan gum. High concentrations of gelatine (24% w/v) were also used to encapsulate *Lactobacillus lactis* by cross-linking with toluene-2, 4-diisocyanate for biomass production (Mortazavian et al., 2007). It was reported that encapsulated *Bifidobacterium* cells in a mixed gel composed of alginate, pectin, and whey proteins. They investigated the protective effects of gel beads without extra membrane and gel beads coated with extra membranes, formed by the conjugation of whey protein and pectin, in simulated gastric pH and bile salt solutions on the survival of free and encapsulated *B. bifidum*. After 1 h of incubation in acidic solution (pH 2.5), the free cell counts decreased by 4.75 log, compared with a decrease of 7.1 log for entrapped cells. The free cells did not survive after 2 h of incubation at pH 2.5, whereas the immobilized cells decreased by about only 2 log. After incubation (1 or 3 h) in 2 and 4% bile salt solutions, the mortality for *B. bifidum* cells in membrane-free gel beads (4–7 log) was greater than that for free cells (2–3 log). However, the counts of cells immobilized in membrane coated gel beads decreased by <2 log. The double membrane coating enhanced the resistance of the cells to acidic conditions and higher bile salt concentrations (Hyndman et al., 1993; Guerin et al., 2003).

### **Chitosan-Coated Alginate Encapsulate System**

Chitin is a homopolymer comprised only of 2-acetamido-2-deoxy- $\beta$ -D-glucopyranose residues, whereas chitosan is a heteropolymer mainly composed of 2-amino-2-deoxy- $\beta$ -D-glucopyranose repeating units but still retaining a small amount of 2-acetamido-2-deoxy- $\beta$ -D-glucopyranose residues. Chitin is the second most abundant organic material on earth after cellulose. Chitosan gel beads and microspheres can be obtained by cross-linking with polyphosphates and sodium alginate (Anal et al., 2003; Anal and Stevens, 2005). Chitosan coating provides stability to alginate microparticles for effective encapsulation of therapeutic live cells. The positively charged amino groups of chitosan and negatively charged carboxylic acid groups of alginate form a membrane on the microparticle surface, which

reduces the leakage of entrapped materials from the particles. Various research works were carried out to investigate the potentiality of a chitosan-coated alginate microparticulate system for increasing the survival and stability of entrapped live probiotic bacterial cells. The survival and stability of probiotic bacteria loaded into chitosan-coated alginate microparticles are largely dependent on the molecular weight of chitosan. *Lactobacillus bulgaricus* KFRI 673-loaded alginate microparticles were coated with chitosans of three different molecular weights to investigate the survival and stability of *Lactobacillus bulgaricus* KFRI 673 in SGF (pH 2.0) and simulated intestinal fluid (SIF) (pH 7.4). Before encapsulation, the authors examined the survival of free *L. bulgaricus* KFRI 673 in SGF of pH 2.0 and in SIF of pH 7.4. In SGF, none of the cells survived after 60 min (Huguet et al, 1996). On the other hand, survival of the *Lactobacillus* strain was fully maintained in SIF over the time period until 120 min, suggesting that *L. bulgaricus* KFRI 673 is pH sensitive and cannot survive in acidic pH conditions. Therefore, encapsulation of the *Lactobacillus* is essential for its survival when given orally. After encapsulation, the survival of *L. bulgaricus* KFRI 673 was investigated for all microparticle batches after sequential incubation in SGF and SIF. The incubation time in SGF was optimized at 0, 30, 90, and 180 min. After then, 180-min incubation was carried out in SIF as for sequential incubation. The microparticles prepared with high molecular weight chitosan provided a higher survival rate (46%) compared with the microparticles made with low molecular weight chitosan (36%). Chitosan-uncoated alginate microparticles showed lower survival (25%) of *L. bulgaricus* KFRI 673. The prepared microparticles stability was also investigated at 4°C and 22°C during a four-week period. Both the free and the encapsulated cells showed similar stabilities at 4°C, whereas high molecular weight chitosan-coated alginate microparticles appreciably improved the *Lactobacillus* stabilities at 22°C compared with free cells and the other respective batches. This was due to the thicker membrane of the microparticles made with high molecular weight chitosan, which protected the encapsulated *Lactobacillus* better than the microparticles made with low and medium molecular weight chitosans and non-encapsulated cells (Lee et al., 2004).

### **Encapsulation of Probiotics in Cellulose Derivatives**

It has been reported that gastric juice resistant tablet formulations of LAB were developed, using hydroxypropylmethylcellulose acetate succinate (HPMCAS) as well as alginates, apple pectin, and Metolose<sup>®</sup> as matrix forming components. To optimize the formulation—using survival rate in acid medium and disintegration time in intestinal fluid as test parameters—tablets were modified with respect to LAB content, amount of applied excipients per tablet, and compaction forces. A decrease of viable cells of not more than one log unit after 2 h of incubation in acid medium was desired, as well as a disintegration time of 1 h in phosphate buffer pH 6.8. It was found that the amount of

HPMCAS in the tablet correlates with gastric juice resistance. As HPMCAS also leads to a decrease of disintegration time in intestinal fluid, slight amounts of this excipient were preferred. The best protective qualities against artificial gastric juice were observed when tablets were prepared from compaction mixtures of LAB, HPMCAS, and sodium alginate (Stadler and Viernstein, 2003). In another report they showed the potential use of compression coating as an alternative method for the encapsulation of probiotic bacteria *Lactobacillus acidophilus* to improve their storage stability. Microbial cell containing powders were first compressed into a pellet, which was then encapsulated with a coating material of a combination of sodium alginate and hydroxypropyl cellulose by further compression. The effect of compression pressure on cell viability was studied. Results showed that compression of the microbial cell containing powders at pressures up to 90 MPa caused little loss of viability of the bacteria. Beyond 90 MPa, the cell viability decreased almost linearly with the compression pressure. Further compression to form a coating did not cause significant reduction in the cell viability. The stability of the encapsulated bacteria using the compression pressures up to 60 MPa was approximately 10 times higher than free cell containing powders and cell pellets after 30 days storage at 25°C (Chan and Zhang, 2002). In another report, they used sodium alginate and hydroxypropyl cellulose as a coating material for encapsulation of Probiotics in acidic medium. Sodium alginate, which can form gels after being hydrated, has been exploited as the prime coating material. Probiotic cell containing powders were first compressed into a pellet, which was then encapsulated with the coating material by further compression. Results indicated significant improvement in survival of encapsulated cells when exposed to acidic media of pH 1.2 and 2. The encapsulated cells showed 10<sup>4</sup>–10<sup>5</sup>-fold increment in cell survival when compared to free cells under the test conditions. The formation of a hydrogel barrier by the compacted sodium alginate layer has shown to retard the permeation of the acidic fluid into the cells. This contributed to the enhanced cell survival. In addition, it could be deduced from in vitro tests that the release of encapsulated cells in the human digestive tract could occur near the end of the ileum and beginning of the colon. The mechanism of cell release is primarily due to the erosion of the alginate gel layer (Chan and Zhang, 2005).

It was reported that cellulose acetate phthalate (CAP) contains ionizable phthalate groups. For this reason, this cellulose derivative polymer is insoluble in acid media at pH 5 and lower but is soluble at pH higher than 6. In addition, CAP is physiologically inert when administered in vivo, and is, therefore, widely used as an enteric coating material for the release of core substances for intestinal targeted delivery systems. It was also reported that the encapsulation of *B. pseudolongum* in CAP used an emulsion technique. Encapsulated bacteria survived in larger numbers (10<sup>9</sup> CFU/mL) in an acidic environment than non-encapsulated organisms, which did not retain any viability when exposed to a simulated gastric environment for 1 h. Encapsulated *B. lactis* and *L. acidophilus* in CAP polymer used a spray-drying method. This study evaluated the resistance of

encapsulated microorganisms in acid and high bile salt concentrations. Spray-dried microcapsules of CAP containing *B. lactis* and *L. acidophilus* were effective in protecting both these microorganisms when inoculated into media with pH values similar to those in the human stomach. Encapsulated *L. acidophilus* suffered a reduction of only 1 log at pH 1 after 2 h of incubation, and the population of *B. lactis* was reduced by only 1 log immediately after inoculation into a pH 1 medium and between 1 and 2 h after inoculation into a pH 2 medium. After inoculation of the CAP microcapsules loaded with bacteria into bile solution (pH 7), complete dissolution of the powder indicated that both the wall material and the process used in the preparation of the microcapsules were adequate in protecting the bacteria, to pass undamaged through the acidic conditions of the stomach, followed by their rapid liberation in the pH of the intestine (Anal and Singh, 2007).

#### **Encapsulation of Probiotics in Whey Protein Gel particles**

Encapsulation of probiotics in whey protein gel particles could offer protection during processing and storage as well as extending the food applications of the bacteria to biscuits, vegetable, and frozen cranberry juice. Whey protein isolate (WPI) has the potential for the encapsulation of *L. rhamnosus* strain. Beads were prepared by extruding the denatured WPI-concentrated bacteria solution and 96% of the probiotic cells were in the whey protein particles. The protein-based technique can provide an alternative for encapsulation with alginate-type gels or spray-coating with fats, the two most widely-used probiotic encapsulation methods. The protein matrix would have different cell release properties than the other encapsulation methods (polymer or fat based). Thus, applications can extend to other foods for protection during processing as well as stability during storage but also in nutraceuticals for protection and cell release in the gastrointestinal tract (Champagne et al., 2006).

#### **Encapsulation of Live Probiotics in Modified Alginate System**

Modified alginates were also investigated for encapsulation of live probiotic bacteria to improve their survival in acidic condition. In this regard, succinylated alginate and N-palmitoylaminoethyl alginate were prepared. *Lactobacillus rhamnosus* was microencapsulated into unmodified and modified alginate beads to investigate their acid resistance and viability in acidic condition. To investigate the acid resistance of free cells and encapsulated cells, all the formulations loaded with *Lactobacillus rhamnosus* were incubated in SGF (pH 1.5) for 30 min. For free cells, the initial count was dropped from 1.0 × 10<sup>8</sup> CFU/ml to an uncountable level after 30 min. Moderate protection was achieved by the unmodified alginate beads loaded with *L. rhamnosus*. Succinylated alginate and succinylated chitosan beads loaded with the probiotic bacteria showed better protection in SGF, with a slight decrease of viability, although

no significant ( $P > 0.05$ ) differences were achieved in protection of encapsulated cells between these two formulations. The best protection in SGF was obtained for N-palmitoylaminoethyl alginate with a slight decrease in bacterial cell viability from  $2.5 \times 10^7$  to  $2.2 \times 10^7$  CFU/ml. The minor loss of encapsulated cells from N-palmitoylaminoethyl alginate beads could have occurred from near or on the bead surface. N-Palmitoylaminoethyl alginate beads showed a promising formulation to protect the live bacteria from acidic environment and to improve their survival and stability (Le-Tien et al., 2004).

### **Effect of Prebiotic for Probiotic Encapsulate System**

Adding the prebiotic inulin to yoghurt boosted the growth of probiotic bacteria and when used in a novel double encapsulation, extended the survival rates of the friendly bacteria. The various prebiotic fibers protect the stability and viability of probiotic *Lactobacillus rhamnosus* strains during freeze-drying, storage in freeze-dried form and after formulation into apple juice and chocolate-coated breakfast cereals. The studied prebiotics were: sorbitol, mannitol, lactulose, xylitol, inulin, fructooligosaccharide (FOS), and raffinose (Ann et al., 2007).

Incorporation of Hi-Maize starch (a prebiotic) improved encapsulation of viable bacteria as compared to when the bacteria were encapsulated without starch. Inclusion of glycerol (a cryoprotectant) with alginate mix increased the survival of bacteria when frozen at  $-20^\circ\text{C}$ . The acidification kinetics of encapsulated bacteria showed that the rate of acid produced was lower than that of free cultures. The encapsulated bacteria, however, did not demonstrate a significant increase in survival when subjected to in vitro high acid and bile salt conditions. A preliminary study was carried out in order to monitor the effects of encapsulation on the survival of *Lactobacillus acidophilus* and *Bifidobacterium* spp. in yogurt over a period of eight weeks. It showed that the survival of encapsulated cultures of *L. acidophilus* and *Bifidobacterium* spp. showed a decline in viable count of about 0.5 log over a period of eight weeks while there was a decline of about 1 log in cultures which were incorporated as free cells in yogurt (Sultana et al., 2000; Vidhyalakshmi et al., 2009). It was reported that prebiotics (FOS or isomaltooligosaccharides) were used as growth promoter (peptide) and sodium alginate as coating materials to encapsulate different probiotics such as *L. acidophilus*, *L. casei*, *B. bifidum*, and *B. longum*. A mixture containing sodium alginate (1% w/v) mixed with peptide (1% w/w) and FOS (3% w/w) as coating materials produced the highest survival in terms of probiotic count (Chen et al., 2005).

### **CONCLUSION AND FUTURE CHALLENGES**

In the food processing industry, encapsulation of probiotics is playing a vital role to protect the viability and enhance the survival of probiotic bacteria against the adverse environmen-

tal conditions. Encapsulated probiotic bacteria can be used in many fermented dairy products, such as yogurt, cheese, cultured cream, and frozen dairy desserts, and for biomass production. In the health food industry, capsules, tablets, suspensions, creams, and powders will be increasingly using encapsulation technology for direct consumption and for external application of probiotics. Encapsulation of probiotic bacteria in foods on an industrial scale faces technological, microbiological, and financial challenges and also questions linked to consumer behaviour. The main challenge in applying encapsulation of probiotics to new foods to meet consumer interests has to do with finding the appropriate encapsulation technique, safe and effective encapsulating materials and potent bacterial strains. Encapsulation is expected to extend the shelf life of probiotics at room temperature in various food matrices, increase their heat resistance, improve their compression and shear stress resistance, and enhance their acid tolerance. Biopolymers are the best effective materials for encapsulation of probiotics. But when only one biopolymer is used for encapsulation, it does not exhibit appropriate effect on encapsulation. Mixture of biopolymers could have the best potential for the encapsulation of probiotics. The future challenge would be the uses of biopolymeric blends for encapsulation of probiotics which will be efficiently protect the probiotics through the gastrointestinal tract where they can interact with specific receptors.

### **ACKNOWLEDGMENTS**

The authors would like to thank the Natural Sciences and Engineering Research Council of Canada (NSERC) and FP Innovation (Pointe-Claire, Canada) for their research support and funding.

### **REFERENCES**

- Adhikari, K., Mustapha, A., Grun, I. U. and Fernando, L. (2000). Viability of microencapsulated bifidobacteria in set yogurt during refrigerated storage. *J. Dairy Sci.* **83**:1946–1951.
- Anal, A. K. and Singh, H. (2007). Recent advances in microencapsulation of probiotics for industrial applications and targeted delivery. *Trends Food Sci. Tech.* **18**:240–251.
- Anal, A. K. and Stevens, W. F. (2005). Chitosan-alginate multilayer beads for controlled release of ampicillin. *Int. J. Pharm.* **290**:45–54.
- Anal, A. K., Bhopatkar, D., Tokura, S., Tamura, H. and Stevens, W. F. (2003). Chitosan-alginate multilayer beads for gastric passage and controlled intestinal release of protein. *Drug. Dev. Ind. Pharm.* **29**:713–724.
- Ann, E. Y., Kim, Y., Oh, S., Imm, J. Y., Park, D. J., Han, K. S., and Kim, S. H., (2007). Microencapsulation of *Lactobacillus acidophilus* ATCC 43121 with prebiotic substrates using a hybridisation system. *Int. J. Food Sci. Technol.* **42**:411–419.
- Ariful, M. I., Yun, C. H., Choi, Y. J. and Cho, C. S., (2010). Microencapsulation of live probiotic bacteria. *J. Microbiol. Biotechnol.* **20**(10):1367–1377.
- Baricault, L., Denariaz, G., Hourri, J. J., Bouley, C., Sapin, C. and Trugnan, G. (1995). Use of HT-29, a cultured human colon cancer cell line, to study the effect of fermented milks on colon cancer cell growth and differentiation. *Carcinogenesis.* **16**:245–252.

- Brachkova, I. M., Duarte, A. M. and Pinto, F. J., (2010). Preservation of viability and antibacterial activity of *Lactobacillus* spp. in calcium alginate beads. *Eur. J. Pharm. Sci.* **41**:589–596.
- Champagne, C. P., Reid, A. A., Gardner, N., Fustier, P. and Vuilleumard, J. C. (2006). Survival in food systems of *Lactobacillus rhamnosus* R011 micro-entrapped in whey protein gel particles. *J. Food Sci.* **72**(1):M31–M37.
- Chan, E. S. and Zhang, Z. (2002). Encapsulation of probiotic bacteria *Lactobacillus acidophilus* by direct compression. *Trans IChEME.* **80**:Part C.
- Chan, E. S. and Zhang, Z. (2005). Bioencapsulation by compression coating of probiotic bacteria for their protection in an acidic medium. *Process Biochem.* **40**:3346–3351.
- Chen, K. N., Chen, M. J., Liu, J. R., Lin, C. W. and Chiu, H. Y. (2005). Optimization of incorporated prebiotics as coating materials for probiotic microencapsulation. *J. Food Sci.* **70**:260–266.
- Chen, L. and Subirade, M. (2009). Elaboration and characterization of Soy/Zein protein microspheres for controlled nutraceutical delivery. *Biomacromolecules.* **10**:3327–3334.
- Dave, R. I. and Shah, N. P. (1997). Viability of yogurt and probiotic bacteria in yogurts made from commercial starter cultures. *Int. Dairy J.* **7**:31–41.
- Dimantov, A., Greenberg, M., Kesselman, E. and Shimoni (2003). Study of high amylase corn starch as food grade enteric coating in a microcapsule model systems. *Innov. Food Sci. Eng. Technol.* **5**:93–100.
- FAO/WHO Experts' Report. (1–4 October 2001). Health and nutritional properties of probiotics in food including powder milk with live lactic acid bacteria. Cordoba, Argentina.
- Godward, G. and Kailasapathy, K. (2003). Viability and survival of free, encapsulated and co-encapsulated probiotic bacteria in yoghurt. *Milk Sci. Int. (Milchwissenschaft).* **58**:396–399.
- Guerin, D., Vuilleumard, J. C. and Subirade, M. (2003). Protection of bifidobacteria encapsulated in polysaccharide-protein gel beads against gastric juice and bile. *J. Food Protect.* **66**:2076–2084.
- Hansen, L. T., Allan-Wojtas, P. M., Jin, Y. L. and Paulson, A. T. (2002). Survival of Ca-alginate microencapsulated *Bifidobacterium* spp. in milk and simulated gastrointestinal conditions. *Food Microbiol.* **19**:35–45.
- Hassan, A. N., Frank, J. F., Schmidt, K. A. and Shalabi, S. I. (1996). Textural properties of yoghurt made with encapsulated non-ropy lactic cultures. *J. Dairy Res.* **79**:2098–2103.
- Hirayama, K. and Rafter, J. (2000). The role of probiotic bacteria in cancer prevention. *Microbes Infect.* **2**:681–686.
- Holzapfel, W. H., Haberer, P., Geisen, R., Bjorkroth, J. and Schillinger, U. (2001). Taxonomy and important features of probiotic microorganisms in food and nutrition. *Am. J. Clin. Nutr.* **73**:365–373.
- Huguet, M. L., Neufeld, R. J. and Dellacherie, E. (1996). Calcium-alginate beads coated with polycationic polymers: Comparison of chitosan and DEAE-dextran. *Process Biochem.* **31**:347–353.
- Hyndman, C. L., Groboillot, A. F., Poncelet, D., Champagne, C. P. and Neufeld, R. J. (1993). Microencapsulation of *Lactococcus lactis* within cross-linked gelatin membranes. *J. Chem. Technol. Biotechnol.* **56**:259–263.
- Isolauri, E., Juntunen, M., Rautanen, T., Sillanauke, P. and Koivula, T. (1991). A human *Lactobacillus* strain (*Lactobacillus casei* sp. Strain GG) promotes recovery from acute diarrhea in children. *Pediatrics.* **88**:90–97.
- Keব্য, K. M. K., (1996). Viability of *Bifidobacterium bifidum* and its effect on quality of frozen Zabady. *Food Res. Int.* **29**:431–437.
- Krasaekoopt, W., Bhandari, B. and Deeth, H. (2003). Evaluation of encapsulation techniques of probiotics for yoghurt. *Int. Dairy J.* **13**:3–13.
- Kruis, W., Schutz, E., Fric, P., Fixa, B., Judmaier, G. and Stolte, M. (1997). Double-blind comparison of an oral *Escherichia coli* preparation and mesalazine in maintaining remission of ulcerative colitis. *Aliment Pharmacol. Ther.* **11**:853–858.
- Le-Tien, C., Millette, M., Mateescu, M. A. and Lacroix, M., (2004). Modified alginate and chitosan for lactic acid bacteria immobilization. *Biotechnol. Appl. Biochem.* **39**: 347–354.
- Lee, J. S., Cha, D. S. and Park, H. J. (2004). Survival of freeze-dried *Lactobacillus bulgaricus* KFRI 673 in chitosan-coated calcium alginate microparticles. *J. Agr. Food Chem.* **52**:7300–7305.
- Lee, K.Y. and Heo, T.R., (2000). Survival of *Bifidobacterium longum* immobilized in calcium-alginate beads in simulated gastric juices and bile salt solution. *Appl. Env. Microbiol.* **66**:869–873.
- Majamaa, H. and Isolauri, E. (1997). Probiotics: A novel approach in the management of food allergy. *J. Allergy Clin. Immun.* **99**:179–185.
- Marianelli, C., Cifani, N. and Pasquali, P. (2010). Evaluation of antimicrobial activity of probiotic bacteria against *Salmonella enterica* subsp. *enterica* serovar typhimurium 1344 in a common medium under different environmental conditions. *Res. Microbiol.* **161**:673–680.
- Mohammadi, R., Mortazavian, M. A., Khosrokhavar, R. and Cruz, D. G. A. (2011). Probiotic ice cream: Viability of probiotic bacteria and sensory properties. *Ann. Microbiol.* [http://link.springer.com/article/10.1007%2F978-94-007-0100-0\\_10](http://link.springer.com/article/10.1007%2F978-94-007-0100-0_10)
- Mortazavian, A., Razavi, H. S., Ehsani, R. M. and Sohrabvandi, S. (2007). Principles and methods of microencapsulation of probiotic microorganisms. *Iranian J. Biotechnol.* **5**(1):1–18.
- Nanji, A. A., Khettry, U. and Sadrzadeh, S. M. H. (1994). *Lactobacillus* feeding reduces endotoxemia and severity of experimental alcoholic liver (disease). *Proc. Soc. Exp. Biol. Med.* **205**:243–247.
- Picot, A. and Lacroix, C. (2003). Effects of micronization on viability and thermotolerance of probiotic freeze-dried cultures. *Int. Dairy J.* **13**:455–462.
- Picot, A. and Lacroix, C. (2004). Encapsulation of bifidobacteria in whey protein-based microcapsules and survival in simulated gastrointestinal conditions and in yoghurt. *Int. Dairy J.* **14**:505–515.
- Pitino, I., Randazzo, C. L., Mandalari, G., Curto, A. L., Faulks, M. R., Marc, L.Y., Bisignano, C., Caggia, C. and Wickham, J. S. M. (2010). Survival of *Lactobacillus rhamnosus* strains in the upper gastrointestinal tract. *Food Microbiol.* **27**:1121–1127.
- Rao, A. V., Shiwnarain, N. and Maharaj, I., (1989). Survival of microencapsulated *Bifidobacterium pseudolongum* in simulated gastric fluid and intestinal juice. *Can. Inst. Food Sci. Tech.* **22**:345–349.
- Rokka, S. and Rantamaki, P. (2010). Protecting probiotic bacteria by microencapsulation: Challenges for industrial applications. *Eur. Food Res. Technol.* **231**:1–12.
- Saikali, J., Picard, C., Freitas, M. and Holt, R. P. (2004). Fermented milks, probiotic cultures, and colon cancer. *Nutr. Cancer* **49**(1):14–24.
- Shah, N. P. and Ravula, R. R. (2000). Microencapsulation of probiotic bacteria and their survival in frozen fermented dairy dessert. *Austral. J. Dairy. Technol.* **55**:139–144.
- Siitonen, S., Vapaatalo, H., Salminen, S., Gordin, A., Saxelin, M., Wikberg, R. and Kirkkola, A. L. (1990). Effect of *Lactobacillus* GG yogurt in prevention of antibiotic associated diarrhoea. *Ann. Med.* **22**:57–59.
- Stadler, M. and Viernstein, H. (2003). Optimization of a formulation containing viable lactic acid bacteria. *Int. J. Pharm.* **256**:117–122.
- Sultana, K., Godward, G., Reynolds, N., Arumugaswamy, R., Peiris, P. and Kailasapathy, K. (2000). Encapsulation of probiotic bacteria with alginate–starch and evaluation of survival in simulated gastrointestinal conditions and in yogurt. *Int. J. Food Microbiol.* **62**:47–55.
- Vidhyalakshmi, R., Bhakayaraj, R. and Subhasree, R. S. (2009). Encapsulation “The future of probiotics”—A review. *Adv. Biol. Res.* **3**(3–4):96–103.



ELSEVIER

Contents lists available at [SciVerse ScienceDirect](http://www.sciencedirect.com)

## Radiation Physics and Chemistry

journal homepage: [www.elsevier.com/locate/radphyschem](http://www.elsevier.com/locate/radphyschem)

## Effect of gamma radiation on the physico-chemical properties of alginate-based films and beads

Tanzina Huq, Avik Khan, Dominic Dussault, Stephane Salmieri, Ruhul A. Khan, Monique Lacroix\*

Research Laboratories in Sciences Applied to Food, Canadian Irradiation Center (CIC), INRS-Institute Armand-Frappier, University of Quebec, 531 Boulevard des Prairies, Laval, Quebec, Canada H7V1B7

## ARTICLE INFO

## Article history:

Received 10 June 2011

Accepted 24 November 2011

Available online 6 December 2011

## Keywords:

Gamma irradiation

Alginate

Physico-chemical properties

Ionotropic gelation

## ABSTRACT

Alginate solution (3%, w/v) was prepared using deionized water from its powder. Then the solution was exposed to gamma radiation (0.1–25 kGy). The alginate films were prepared by solution casting. It was found that gamma radiation has strong effect on alginate solution. At low doses, mechanical strength of the alginate films improved but after 5 kGy dose, the strength started to decrease. The mechanism of alginate radiolysis in aqueous solution is discussed. Film formation was not possible from alginate solution at doses > 5 kGy. The mechanical properties such as puncture strength (PS), puncture deformation (PD), viscoelasticity (Y) coefficient of the un-irradiated films were investigated. The values of PS, PD and Y coefficient of the films were 333 N/mm, 3.20 mm and 27%, respectively. Alginate beads were prepared from 3% alginate solution (w/v) by ionotropic gelation method in 5% CaCl<sub>2</sub> solution. The rate of gel swelling improved in irradiated alginate-based beads at low doses (up to 0.5 kGy).

© 2011 Elsevier Ltd. All rights reserved.

### 1. Introduction

Bio-based packaging must serve a number of important functions, including containment and protection of food, maintaining its sensory quality and safety, and communicating information to consumers. A big effort to extend the shelf life and enhance food quality while reducing packaging waste has encouraged the exploration of new bio-based packaging materials, such as edible and biodegradable films from renewable resources. Biodegradable films can be used as a vehicle for the incorporation of food additives such as antioxidants and antimicrobial agents delivering them to the food surfaces where deterioration by microbial growth or oxidation often begins. The demands for high quality foods and opportunities to create new market outlets have contributed to increase the interest in the development of biodegradable packaging. In particular, the application of biodegradable edible films as effective barriers against gas, moisture and liquid migration has appeared to be the appropriate way for prolongation of the shelf-life of ready-to-eat food and for the increase of its quality. Films can be produced from natural polymers, such as polysaccharides, lipids and/or proteins, and are perfectly biodegradable and safe to the environment (Sorrentino et al., 2007; Ciesla et al., 2006; Silva et al., 2009; Zactiti and Kieckbusch, 2006).

Alginate is widely used in food, pharmaceutical and bioengineering industries for its gel- and film-forming properties. Alginate, a linear heteropolysaccharide of D-mannuronic and L-guluronic acid, is found in the cell walls and intercellular spaces of brown algae. Alginate is made up of arranged regions composed solely of D-mannuronic acid and L-guluronic acid, referred to as M-blocks and G-blocks, and regions where the two units alternate. Both the ratio of mannuronic/guluronic acid and the structure of the polymer determine the solution properties of the alginate (Lee et al., 2003; Khan et al., 2010; Simpson et al., 2004; Prakash and Jones, 2005). Alginate forms a thermally stable and biocompatible hydrogel in the presence of di- or trivalent cations. In addition, alginate beads can be easily produced by dropping an alginate solution in a calcium chloride bath (Chana et al., 2010).

Gamma irradiation has been found to be effective for degradation of carbohydrates such as alginate, cellulose, starch, chitosan and pectin. Cleavage of the molecular chain is ascribed to decaying processes of free radicals generated at the primary stage of gamma irradiation. Due to macro-radical formation and their further reactions, degradation methods are accompanied of various extents with changes in chemical composition and primary structure of the polysaccharides (Kim et al., 2008; Choi et al., 2002).

Gamma irradiation is also used for the biological sterilization of materials that can be subsequently used for manufacturing biomedical products. In addition, ionizing radiation leads to the degradation of polysaccharides such as alginate by the cleavage of the glycosidic bonds. The basic advantages of degradation of

\* Corresponding author. Tel.: +1 450 687 5010; fax: +1 450 686 5501.

E-mail address: [monique.lacroix@iaf.inrs.ca](mailto:monique.lacroix@iaf.inrs.ca) (M. Lacroix).

polymers by radiation include the ability to promote changes reproducibly and quantitatively, without the introduction of chemical reagents and without the need for special equipments/setup to control for temperature, environment and additives. Therefore, this technology is simpler and more environment-friendly than conventional methods (Byun et al., 2008). The objective of this experiment was to determine the effect of gamma radiation on the physico-chemical properties of alginate-based films and beads.

## 2. Materials and methods

### 2.1. Materials

Sodium alginate (guluronic acid content ~65–70% and manuronic acid content ~5–35%) and calcium chloride (granules) were purchased from Sigma-Aldrich Canada Ltd. (Oakville, ON, Canada).

### 2.2. Irradiation

An aqueous suspension containing 3% alginate (w/v) was prepared and then irradiated from 0.1 to 25 kGy. Irradiation of the 3% alginate solution (w/v) was conducted with  $\gamma$ -rays generated from  $^{60}\text{Co}$  source at room temperature, at a dose rate of 17.878 kGy/h (0.3578 kGy/min) in an Underwater Calibrator-15A Research Irradiator (Nordion Inc., Kanata, ON, Canada).

### 2.3. Preparation of alginate-based beads and films

The alginate-based films and beads were prepared from unirradiated and irradiated alginate suspension. Films were cast by applying 10 mL of the film-forming suspension onto petri dishes ( $100 \times 15 \text{ mm}^2$ ; VWR International, Ville Mont-Royal, QC, Canada) and allowed to dry for 24 h at room temperature and 35% relative humidity (RH). Dried water-soluble films were peeled off manually using a spatula and stored in polyethylene bags prior to characterization. The beads were produced by dropping through a 20-gage needle (0.9 mm in diameter and 1.5 in. in length) from a 10 mL plastic syringe into a beaker containing  $\text{CaCl}_2$  solution (5% w/v), under gentle stirring at room temperature. The formed beads were then allowed to harden for 30 min and then rinsed with distilled water (Salmieri and Lacroix, 2006).

### 2.4. Film and bead thickness

Thickness of the films (thickness ~25  $\mu\text{m}$ ) and 10 beads (2–3.5 mm in wet condition and 0.6–2 mm in dry condition) was measured using a Mitutoyo digimatic Indicator (Type ID-110E; Mitutoyo Manufacturing Co. Ltd., Tokyo, Japan) with a resolution of 0.001 mm, at five random positions around the film and bead, by slowly reducing the micrometer gap until the first indication of contact.

### 2.5. Puncture strength (PS) and puncture deformation (PD)

Mechanical properties were carried out according to an ASTM (1991) D882-91 procedure. Puncture strength (PS) and puncture deformation (PD) measurements were carried out using a Stevens-LFRA texture analyzer (model TA-1000; Texture Technologies Corp., Scarsdale, NY). The film samples were equilibrated in a dessicator containing a saturated sodium bromide solution ensuring 56% RH at room temperature (21 °C) for at least 24 h. Films were then fixed between two perforated Plexiglass<sup>®</sup> plates (3.2 cm in diameter), and the holder was held tightly with two

screws. A cylindrical probe (2 mm in diameter) was moved perpendicularly to the film surface at a constant speed (1 mm/s) until it passed through the film. Strength and deformation values at the puncture point were used to calculate the hardness and deformation capacity of the film. To avoid any variation related to the film thickness, the PS values were divided by the thickness of the films. PS was calculated using the equation  $\text{PS (N/mm)} = (9.81 \times F)/x$  where  $F$  is the force,  $x$  is the film thickness and 9.81 is the gravitational acceleration. The PD of the films was calculated from the PS curve, using the distance recorded between the time of first probe/film contact and the time of puncture point.

### 2.6. Viscoelasticity coefficient ( $Y$ )

Viscoelastic properties were evaluated using relaxation curves. The same puncture test procedure described above was used, but the probe is stopped to 3 mm after film contact and maintained for 1 min. The relaxation coefficient  $Y$  is calculated using the equation  $Y (\%) = [(F_i - F_f)/F_i] \times 100$  where  $F_i$  is the initial recorded value and  $F_f$  the second value measured after 1 min of relaxation. A low relaxation coefficient ( $Y \rightarrow 0\%$ ) indicates high film elasticity, whereas a high coefficient ( $Y \rightarrow 100\%$ ) indicates high film plasticity related to a more rigid and easily distorted material.

### 2.7. Rate of gel swelling

A water uptake apparatus was designed to study the water absorption properties of beads and consequently to determine the rate of gel swelling. Beads were dried at 40 °C for 24 h in a drying oven and placed in a 5 mL graduated cylinder (0.2 mL subdivision). Water penetration into beads was measured as a function of time (Han et al., 2008). The water uptake is expressed in the rate of gel swelling (percent weight increase).

### 2.8. Statistical analysis

To validate the results obtained during different experimental procedures, each analysis was carried out in triplicate in a completely randomized experimental design. An analysis of variance (ANOVA) and multiple comparison tests of Duncan's were used to compare all the results. Differences between means are considered significant when the confidence interval is smaller than 5% ( $p \leq 0.05$ ). The analysis was performed by the PASW Statistics 18 software (IBM Corporation, Somers, NY, USA).

## 3. Results and discussion

### 3.1. Effect of gamma irradiation on the PS and PD of films

The PS and PD results of the un-irradiated and irradiated alginate-based films are presented in Figs. 1 and 2. The PS and PD values of the un-irradiated alginate-based films (control) were found to be 333 N/mm and 3.2 mm, respectively. It was found that from 0.1 to 0.5 kGy, the PS values increased with the increase in gamma radiation dose. At doses of 0.1 and 0.5 kGy, the PS values of the irradiated films were 365 and 375 N/mm, which were about 10% and 13% higher, respectively, compared to un-irradiated alginate-based films. At doses higher than 0.5 kGy, the increase in irradiation dose decreased the PS values of the films significantly ( $p \leq 0.05$ ). At 1 and 5 kGy, the PS values of the films were 356 and 313 N/mm, respectively. The PD values increased with the increase in the dose of gamma radiation and results are shown in Fig. 2. At doses of 0.1 and 0.5 kGy, the PD values were 4.6 and 4.8 mm, respectively, which represented an increase in PD of about 44% and 50%, respectively, compared to un-irradiated

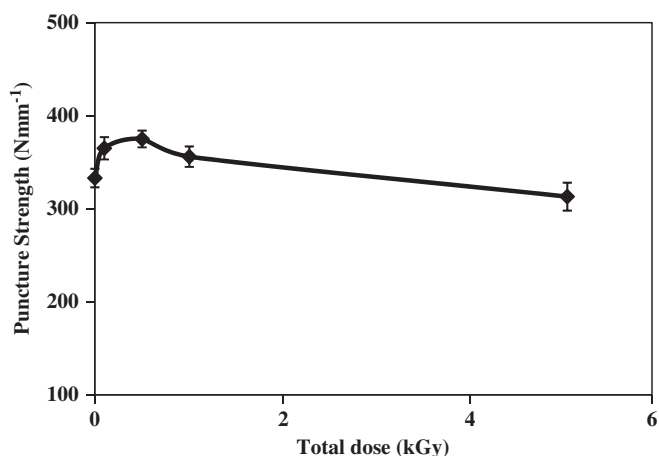


Fig. 1. Effect of gamma irradiation on PS of alginate-based films.

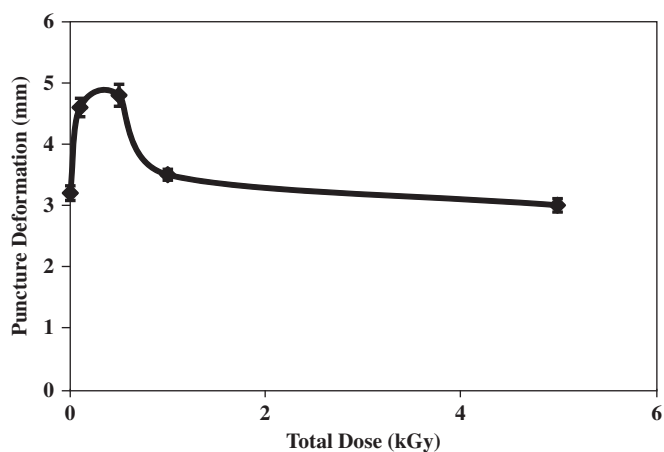


Fig. 2. Effect of gamma irradiation on PD of alginate-based films.

alginate films. At doses higher than 1 kGy, the PD values decreased significantly ( $p \leq 0.05$ ). On the other hand, viscoelasticity ( $Y$  coefficient) of irradiated films was found to be almost similar to the un-irradiated alginate-based films. So, it was found that at lower irradiation doses (0.1–0.5 kGy), the PS and the PD values increased significantly ( $p \leq 0.05$ ). The increase in mechanical properties of alginate-based films at low irradiation doses (0.1–0.5 kGy) may be attributed to the generation of free radicals and cross-linking of alginate molecules. However, at doses higher than 1 kGy, both PS and PD values decreased significantly ( $p \leq 0.05$ ). The decrease in PS and PD values may be due to the chain scission when alginate is exposed to gamma irradiation. Alginate, which is a polysaccharide, generally undergoes degradation by the breaking of the glycosidic linkage under higher dose of gamma irradiation. It is also reported in the literature that cellulose and alginate molecules also form free radicals in a similar nature when exposed to gamma radiation (Gul-E-Noor et al., 2009).

### 3.2. Effect of gamma irradiation on the rate of gel swelling

Effect of gamma irradiation on the rate of gel swelling of alginate-based beads prepared from irradiated alginate solution is presented in Fig. 3. The values of rate of gel swelling improved in irradiated alginate-based beads at doses up to 0.5 kGy. At 0.1 and 0.5 kGy, the rate of gel swelling decreased 18% and 21%, respectively, as compared to the un-irradiated alginate-based beads. At doses higher than 0.5 kGy, the rate of gel swelling increased. At 1 and 5 kGy, the rate

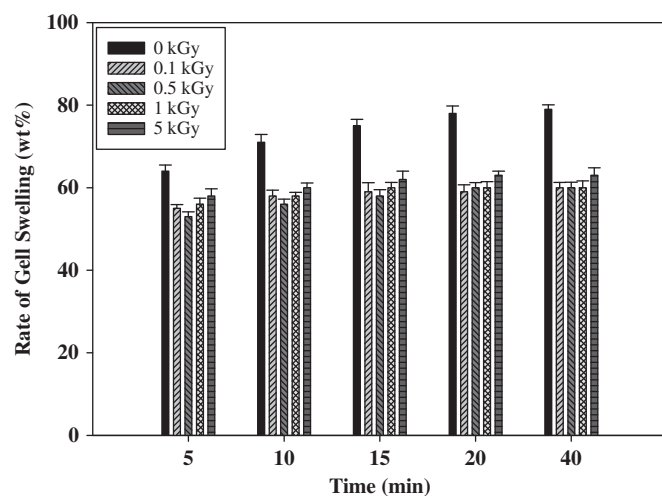
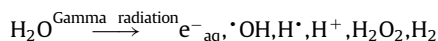


Fig. 3. Effect of gamma irradiation on rate of gel swelling properties of alginate-based beads.

of gel swelling found 58% and 60%, respectively, which was significantly ( $p \leq 0.05$ ) lower than the un-irradiated alginate-based bead.

### 3.3. Mechanism of radiolysis of alginate in aqueous solution

It is mentioned above that gamma radiation has a strong effect on alginate solution. At low doses, mechanical strength of the prepared films improved but after 5 kGy dose, the strength started to decrease. Here, 3% alginate solution was used. So, water has a great influence on the radiolysis of alginate. The mechanism of alginate radiolysis in aqueous solution is discussed below. Due to exposure of gamma radiation, firstly hydroxyl radicals have been generated by radiolysis of water (Von Sonntag, 1987). The radicals generated by water molecules under the effect of gamma radiation are as follows:



Thus the alginate-derived radicals would be formed almost solely by attack of OH radicals resulting from radiolysis of water. The  $\text{H}\cdot$  and  $\cdot\text{OH}$  radicals formed by radiolysis of water accelerated the molecular chain scission of alginate. Reaction between the above free radicals and alginate molecules leads to rapid degradation of alginate in aqueous solution. The free radicals formed by radiolysis of water are effective even in enhancing crosslinking. Then, H-atoms abstraction from various C-atoms by OH radicals might be occurred. Thus, in fact radicals located at all carbon atoms (except the carboxylic carbon) will be formed. Since, oxygen was present in the system; the initially formed alkyl radicals would rapidly react with oxygen to form peroxy radicals. Their transformations could lead to chain scission, oxidation with the formation of carbonyl groups, etc. (Von Sonntag et al., 1999). According to Nagasawa et al. (2000), probably hydrogen abstracted indirectly by hydroxyl radical or surrounding macroradical and as a result, a double bond formation could lead to stabilization of alginate radicals. It is reported (Wasikiewicz et al., 2005) that water radiolysis is the main effect of g-irradiation of diluted aqueous solutions. It results in the formation of transient products, which then react with the solute. In the case of diluted aqueous solutions of polycarbohydrates, formed hydroxyl radical and hydrogen atoms are able to abstract hydrogen atoms from the polymer. Thus, macroradicals are formed. Subsequent reactions of macroradicals can be chain scission, hydrogen transfer, inter- and intramolecular recombination and finally disproportionation of macroradicals. Effect of chain scission can be followed by a

decrease in the molecular weight of the polymer. Degradation rate increases with the decrease in the polymer concentration. Mainly, it is caused by the enhanced OH radical mobility rising with dilution of the solution, due to reduced viscosity. Moreover, in diluted solutions the distance between two radicals located on neighboring polymer chains becomes larger. This significantly decreases their recombination possibility, which could give an effect opposite to degradation, i.e., the crosslinking reaction. In the presence of oxygen, the alginate derived radicals are converted into the corresponding peroxy radicals. Due to their long lifetimes, these peroxy radicals can also undergo H-abstraction reactions. This induces chain reaction in this system. According to other researchers (Charlesby, 1958; Mollah et al., 2009; Charlesby and Swallow, 1959; Dole et al., 1959) when natural polymeric materials are subjected to high-energy radiation (gamma), radicals are produced on the main chain by hydrogen and hydroxyl abstraction. Gamma radiation also ruptures some carbon–carbon bonds and produces radicals. Chain scission may also take place to form other radicals. The ionizing radiation produces three types of reactive species in polymer. These are ionic, radical and peroxide. The peroxide species are produced when polymers are irradiated in the presence of oxygen (Charlesby, 1958; Charlesby and Swallow, 1959; Dole et al., 1959). Peroxide reacts with polymers and produces polymer diperoxides (POOP) and hydroperoxides (POOH) by a radical chain reaction process. The reactions occurs in three steps: activation, propagation and termination. The effect of high-energy radiation on polymers (such alginate) produced ionization and excitation; as a result some free radicals are produced. The polymers may undergo cleavage or scission (i.e., the polymer molecules may be broken into smaller fragment). Subsequent rupture of chemical bonds yields fragments of the large polymer molecules. The free radicals thus produced may react to change the structure of the polymer and also the physical properties of the materials. It also may undergo cross-linking (i.e., the molecules may be linked together into large molecules) (Saheb and Jog, 1999; Valdez-Gonzalez et al., 1999). Gamma irradiation also affects the polymeric structure and can produce active site. Gamma irradiation of alginate may result in cross-linking, which produces higher mechanical properties up to a certain dose. Active sites inside the polymer might be produced by the application of gamma radiation. This may be the reason behind the variation (increase and decrease) in the mechanical properties of the prepared alginate films at the exposure of gamma radiation (low and high doses).

#### 4. Conclusion

This study was carried out in order to investigate the effect of gamma irradiation on the physico-chemical and swelling properties of alginate-based films and beads. From this study, it is clear that low gamma irradiation doses (0.1–0.5 kGy) allowed the improvement not only in the mechanical properties but also in the swelling properties of alginate-based films and beads. However, at doses higher than 0.5 kGy, the mechanical properties decreased. The optimum gamma irradiation dose was found to be 0.5 kGy. Hence, low doses of gamma irradiation can conveniently improve the mechanical and swelling properties of alginate-based films and beads.

#### Acknowledgment

The authors are grateful to the Natural Sciences and Engineering Research Council of Canada (NSERC). They would also like to

thank Nordion Inc. for the irradiation procedures. Tanzina Huq is the recipient of a scholarship from Fondation Armand-Frappier.

#### References

- ASTM, 1991. Standard test method for tensile properties of thin plastic sheeting D882-91. Annual Book of ASTM Standards. American Society for Testing and Materials, Philadelphia, PA.
- Byun, E.H., Kim, J.H., Sung, N.K., Choi, J.L., Lim, S.T., Kim, K.H., Yook, H.S., Byun, M.W., Lee, J.W., 2008. Effects of gamma irradiation on the physical and structural properties of  $\beta$ -glucan. *Rad. Phys. Chem.* 77, 781–786.
- Chana, E.S., Wonga, S.L., Lee, P.P., Lee, J.S., Ti, T.B., Zhang, Z., Poncelete, D., Ravindraa, P., Phana, S.H., Yima, Z.H., 2010. Effects of starch filler on the physical properties of lyophilized calcium–alginate beads and the viability of encapsulated cells. *Carbohydr. Polym.* 83, 225–232.
- Choi, W.S., Ahn, K.J., Lee, D.W., Byun, M.W., Park, H.J., 2002. Preparation of chitosan oligomers by irradiation. *Polym. Degrad. Stab.* 78, 533–538.
- Charlesby, A., Swallow, A.J., 1959. Effects of starch filler on the physical properties of lyophilized calcium–alginate beads and the viability of encapsulated cells. *Radiat. Chem. Annu. Rev. Phys. Chem.* 10, 289–296.
- Charlesby, A., 1958. *Effects of Radiation on Materials*. Reinhold Publishing Corporation, New York, pp. 261–265.
- Ciesla, K., Salmieri, S., Lacroix, M., 2006.  $\gamma$ -irradiation influence on the structure and properties of calcium caseinate–whey protein isolate based films. Part 1: Radiation effect on the structure of proteins gels and films. *J. Agric. Food Chem.* 54, 6374–6384.
- Dole, M., Williams, T.F., Arvia, A.J., 1959. *Proceedings of the Second International Conference on the Peaceful Uses of Atomic Energy Geneva*, vol. 29, United Nations, New York, pp. 171–172.
- Gul-E-Noor, F., Khan, A.M., Ghoshal, S., Mazid, A.R., Chowdhury, S.M.A., Khan, A.R., 2009. Grafting of 2-ethylhexyl acrylate with urea on to gelatin film by gamma radiation. *J. Macromol. Sci., Pure Appl. Chem.* 46, 615–624.
- Han, J., Guenier, A.S., Salmieri, S., Lacroix, M., 2008. Alginate and chitosan functionalization for micronutrient encapsulation. *J. Agric. Food Chem.* 56, 2528–2535.
- Khan, A., Huq, T., Saha, M., Khan, R.A., Khan, M.A., 2010. Surface modification of calcium alginate fibers with silane and methyl methacrylate monomers. *J. Reinf. Plast. Comp.* 29 (20), 3125–3132.
- Kim, J.K., Srinivasan, P., Kim, J.H., Choi, J., Park, H.J., Byun, M.W., Lee, J.W., 2008. Structural and antioxidant properties of gamma irradiated hyaluronic acid. *Food Chem.* 109, 763–770.
- Lee, W.D., Choi, S.W., Byun, W.M., Park, J.H., Yu, Y.M., Lee, M.C., 2003. Effect of  $\gamma$ -irradiation on degradation of alginate. *J. Agric. Food Chem.* 51, 4819–4823.
- Mollah, M.Z.I., Khan, M.A., Khan, R.A., 2009. Effect of gamma irradiated sodium alginate on red amaranth (*Amaranthus cruentus* L.) as growth promoter. *Radiat. Phys. Chem.* 78, 61–64.
- Nagasawa, Naotsugu, Mitomo, Hiroshi, Yoshii, Fumio, Kume, Tamikazu, 2000. Radiation-induced degradation of sodium alginate. *Polym. Degradation Stab.* 69, 279–285.
- Prakash, S., Jones, M.L., 2005. Artificial cell therapy: new strategies for the therapeutic delivery of live bacteria. *J. Biomed. Biotechnol.* 1, 44–56.
- Salmieri, S., Lacroix, M., 2006. Physicochemical properties of alginate/polycaprolactone-based films containing essential oils. *J. Agric. Food Chem.* 54, 10205–10214.
- Saheb, D.N., Jog, J.P., 1999. Natural fiber polymer composites: a review. *Adv. Polym. Technol.* 18 (4), 351–363.
- Silva, D.A.M., Bierhalz, K.C.A., Kieckbusch, G.T., 2009. Alginate and pectin composite films crosslinked with  $\text{Ca}^{2+}$  ions: effect of the plasticizer concentration. *Carbohydr. Polym.* 77, 736–742.
- Simpson, N.E., Stabler, C.L., Simpson, C.P., Sambanis, A., Constantinidis, I., 2004. The role of the  $\text{CaCl}_2$ –guluronic acid interaction on alginate encapsulated bTC3 cells. *Biomaterials* 25, 2603–2610.
- Sorrentino, A., Gorrasi, G., Vittoria, V., 2007. Potential perspectives of bio-nanocomposites for food packaging applications. *Trends Food Sci. Technol.* 18, 84–95.
- Valdez-Gonzalez, A., Cervantes-Uea, J.M., Oleyob, R., Herrera-Franco, P.J., 1999. Effect of fiber-surface treatment on the fiber–matrix bond strength of natural fiber reinforced composites. *Composites: Part B* 3, 309–320.
- Von Sonntag, C., Bothe, Eberhard, Ulanski, Piotr, Adhikary, Amitava, 1999. Radical transfer reactions in polymers. *Radiat. Phys. Chem.* 55, 599–603.
- Von Sonntag, C., 1987. *The Chemical Basis of Radiation Biology*. Taylor & Francis, London.
- Wasikiewicz, J.M., Yoshii, Fumio, Nagasawa, Naotsugu, Wach, Radoslaw A., Mitomo, Hiroshi, 2005. Degradation of chitosan and sodium alginate by gamma radiation, sonochemical and ultraviolet methods. *Radiat. Phys. Chem.* 73, 287–295.
- Zactiti, E.M., Kieckbusch, T.G., 2006. Potassium sorbate permeability in biodegradable alginate films: effect of the antimicrobial agent concentration and cross-linking degree. *J. Food Eng.* 77, 462–467.